

# An Investigation into the role of Deubiquitinating Enzymes in Plant Disease Resistance

Thesis submitted for the degree of Doctor of Philosophy

Richard A. Ewan

Division of Molecular and Cellular Biology,  
Faculty of Biomedical and Life Sciences,  
University of Glasgow

November 2008

## Acknowledgments

I would like to acknowledge my supervisor Dr. Ari Sadanandom for providing me with the opportunity to study at Glasgow University and for his continual support and encouragement during my studies. I thank my colleagues Joelle Mesmar, Ros Taylor, Dr. Lucio Conti, Liz O'Donnell and Craig Carr for their help, ideas and stimulating company. I also thank members of the Arnott lab past and present for their technical assistance. Specific thanks goes to Dr. Andrew Love for his advice on pathology methods, donation of cDNA samples and training to conduct realtime PCR and Dr. John Christie and Dr. Matt Jones for their assistance with insect cell expression for *in vitro* DUB assays. Beyond Glasgow University, I extend my gratitude to Prof. Jonathan Jones and Dr. John Rathjen (Sainsbury Laboratory, Norwich) for the provision of VIGS plasmids, *Cf-9* tobacco and 35S *Pto N. Benthamiana* materials. I also thank our collaborators Dr. Misha Taliansky, Dr. Sang-Hyon Kim and Jane Shaw (SCRI, Dundee) for their advice and permission to report their findings related to my work. Finally I thank my family and long suffering wife for their support.

## Declaration

The work presented in this thesis was completed by the author Richard Ewan unless otherwise stated and has not been submitted for a degree at any other institution.

# Table of Contents

	Page
Title	i
Acknowledgments	ii
Declaration	ii
Table of Contents	iii
List of Figures	xi
List of Tables	xv
Abbreviations	xvi
Abstract	xvii
<b>Chapter 1 - Introduction</b>	<b>1</b>
<b>1.1 Plant defence against pathogen attack</b>	<b>1</b>
1.1.1 Plant immunity	1
1.1.2 PAMP triggered immunity	3
1.1.3 Effector triggered immunity	5
<b>1.2 Signal transduction during plant defence</b>	<b>9</b>
1.2.1 Signal transduction during PTI	10
1.2.2 Signal transduction during ETI	10
<b>1.3 The ubiquitin 26S proteasome system</b>	<b>13</b>
1.3.1 Discovery and background	13
1.3.2 The ubiquitin protein	15
1.3.3 The ubiquitin conjugation cascade	16
1.3.4 The 26S proteasome	22
1.3.5 Deubiquitinating enzymes	24
<b>1.4 Ubiquitination in plant defence signalling</b>	<b>28</b>
1.4.1 Involvement of E3 ubiquitin ligases in plant defence	28
1.4.2 <i>RAR1/SGT1</i> mediated R gene resistance	30
1.4.3 Targets of ubiquitination linked to plant defence	31
<b>1.5 Study objectives</b>	<b>34</b>

<b>Chapter 2 - Materials and methods</b>	<b>35</b>
<b>2.1 Materials</b>	<b>35</b>
2.1.1 Enzymes and Reagents	35
2.1.2 Antibiotics	36
2.1.3 Bacterial Strains	36
2.1.4 Antibodies	37
2.1.5 Plasmid Vectors	37
<b>2.2 General Laboratory Procedures</b>	<b>38</b>
2.2.1 pH Measurement	38
2.2.2 Autoclaving	38
2.2.3 Filter sterilisation	38
<b>2.3 Plant materials</b>	<b>38</b>
2.3.1 <i>Arabidopsis</i> seed stocks	38
2.3.2 Growth of <i>Arabidopsis</i> plants on soil	38
2.3.3 Surface sterilisation of <i>Arabidopsis</i> seeds	38
2.3.4 Growth of <i>Arabidopsis</i> plants on agar plates	39
2.3.5 Cross-Pollination of <i>Arabidopsis</i>	39
2.3.6 <i>Nicotiana tabacum</i> and <i>Nicotiana benthamiana</i> seed stocks	39
2.3.7 Growth of <i>Nicotiana tabacum</i> and <i>Nicotiana benthamiana</i> on soil	39
<b>2.4 DNA and RNA methods</b>	<b>40</b>
2.4.1 Preparation of competent <i>E. coli</i> cells for heat-shock transformation.	40
2.4.2 Transformation of <i>E. coli</i> competent cells	41
2.4.3 Isolation of plasmid DNA	41
2.4.4 Agarose gel electrophoresis of DNA	41
2.4.5 DNA extraction and purification from agarose gel	41
2.4.6 DNA ligation	41
2.4.7 Restriction Endonuclease digest of plasmid DNA	42
2.4.8 Quantification of DNA	42
2.4.9 Polyadenylation of PCR products	42
2.4.10 pENTR D-TOPO based DNA ligation	43
2.4.11 Gateway recombination based cloning	43

2.4.12	DNA sequencing	43
2.4.13	Isolation of genomic DNA from <i>Arabidopsis</i> plants	44
2.4.14	Isolation of plant RNA	44
2.4.15	Quantification of RNA	44
2.4.16	DNase treatment of RNA	44
2.4.17	cDNA synthesis	45
2.4.18	cDNA synthesis for Realtime PCR	45
<b>2.5</b>	<b>PCR methods</b>	<b>46</b>
2.5.1	Oligonucleotide primer design	46
2.5.2	Amplification of DNA by Polymerase Chain Reaction	46
2.5.3	Semi-Quantitative Reverse Transcriptase PCR	47
2.5.4	Quantitative Real-Time RT PCR	47
2.5.5	Site-directed mutagenesis of plasmid DNA	48
2.5.6	RACE PCR	48
<b>2.6</b>	<b>Generation of stable <i>Arabidopsis</i> transgenics</b>	<b>49</b>
2.6.1	Preparation of competent <i>Agrobacterium</i> cells for electroporation	49
2.6.2	Transformation of competent <i>Agrobacterium</i> cells by electroporation	49
2.6.3	<i>Agrobacterium</i> mediated transformation of <i>Arabidopsis</i> by floral dip	50
2.6.4	Screen for homozygous <i>Arabidopsis</i> lines	50
<b>2.7</b>	<b>Virus Induced Gene Silencing in <i>Nicotiana benthamiana</i></b>	<b>50</b>
2.7.1	Plasmid and <i>Agrobacterium</i> materials for VIGS	50
2.7.2	Inoculation of VIGS constructs on <i>N. benthamiana</i>	51
<b>2.8</b>	<b>Plant pathology methods</b>	<b>52</b>
2.8.1	Inoculation of <i>Pseudomonas syringae</i> on <i>Arabidopsis</i>	52
2.8.2	Bacterial growth assay of <i>Pseudomonas syringae</i> on <i>Arabidopsis</i>	52
2.8.3	HR cell death assay elicited by transient expression of <i>Cf-9/Avr9</i>	52
2.8.4	HR cell death assay triggered by Avr9 elicitor infiltration	53
2.8.5	HR cell death assay triggered by avrPto	53
2.8.6	Bacterial growth assay of <i>Pseudomonas syringae</i> on <i>N. benthamiana</i>	53

2.8.7	TMV U1 virus inoculation on <i>N. benthamiana</i>	54
2.8.9	TMV-GFP virus inoculation on <i>N. benthamiana</i>	54
<b>2.9</b>	<b>Protein expression and purification from <i>E. coli</i></b>	<b>54</b>
2.9.1	Protein expression using <i>E. coli</i>	55
2.9.2	Protein purification from <i>E. coli</i>	55
<b>2.10</b>	<b>Protein expression and purification from <i>S. frugiperda</i></b>	<b>55</b>
2.10.1	Protein expression in <i>S. frugiperda</i>	55
2.10.2	Protein purification from <i>S. frugiperda</i>	56
<b>2.11</b>	<b>Protein methods</b>	<b>56</b>
2.11.1	SDS-polyacrylamide gel electrophoresis (SDS-PAGE)	56
2.11.2	Western blotting	57
2.11.3	Staining of SDS-PAGE gels and PVDF membranes	57
<b>2.12</b>	<b><i>in Vitro</i> Deubiquitination activity assays</b>	<b>58</b>
2.12.1	<i>in vitro</i> Deubiquitination assays using Ubiquitin chains substrate	58
2.12.2	<i>in vitro</i> Deubiquitination assays using Diubiquitin substrate	58
<b>2.13</b>	<b>Transient expression of gene constructs in <i>Nicotiana</i> species</b>	<b>58</b>
<b>2.14</b>	<b>Plant protein methods</b>	<b>59</b>
2.14.1	Total protein extraction from <i>Nicotiana</i> species	59
2.14.2	Quantification of protein concentration	59
2.14.3	Protein precipitation with Trichloroacetic acid	59
<b>2.15</b>	<b>Confocal Microscopy</b>	<b>60</b>
<b>2.16</b>	<b>Computational methods</b>	<b>60</b>
2.16.1	Sequence Alignment analysis	60
2.16.2	Protein sequence domain analysis using Pfam	60
2.16.3	Protein structure modelling	61
2.16.4	Protein localisation prediction	61
2.16.5	Phylogenetic analysis using MEGA	61
2.16.6	Densitometry analysis using Scion Image	61

<b>Chapter 3 - <i>Arabidopsis</i> Deubiquitinating Enzymes</b>	<b>62</b>
<b>3.1 Introduction</b>	<b>62</b>
<b>3.2 Identification of <i>Arabidopsis</i> Deubiquitinating enzymes</b>	<b>63</b>
<b>3.3 Gene Expression analysis of <i>AtUBP12</i> and <i>AtUBP13</i></b>	<b>72</b>
3.3.1 Analysis of <i>AtUBP12</i> and <i>AtUBP13</i> gene expression during disease resistance signalling	72
3.3.2 Analysis of <i>AtUBP12</i> and <i>AtUBP13</i> gene expression following exogenous application of Salicylic Acid	77
3.3.3 Tissue distribution of <i>AtUBP12</i> and <i>AtUBP13</i> expression	81
3.3.4 Promoter analysis of <i>AtUBP12</i> and <i>AtUBP13</i>	81
<b>3.4 Characterisation of <i>ubp12</i> and <i>ubp13</i> mutant alleles during <i>Pseudomonas syringae</i> infection</b>	<b>85</b>
3.4.1 Isolation of homozygous UBP gene T-DNA insertion lines	85
3.4.2 <i>Pseudomonas syringae</i> growth assays in <i>ubp12</i> and <i>ubp13</i> null mutants	99
<b>3.5 <i>ubp12</i> mutants exhibit an early flowering phenotype</b>	<b>104</b>
<b>3.6 RNAi based silencing of <i>AtUBP12</i> and <i>AtUBP13</i></b>	<b>111</b>
3.6.1 RNAi in <i>Arabidopsis</i> using pHELLSGATE	111
3.6.2 RNAi based silencing of <i>AtUBP12</i> and <i>AtUBP13</i>	112
<b>3.7 Generation of <i>ubp12-1 ubp13-1</i> double mutant lines</b>	<b>125</b>
<b>3.8 Discussion</b>	<b>135</b>
3.8.1 The <i>Arabidopsis</i> deubiquitinating enzymes	135
3.8.2 Potential involvement of UBPs <i>AtUBP12</i> and <i>AtUBP13</i> in disease resistance signalling	136
3.8.3 Functional redundancy between <i>AtUBP12</i> and <i>AtUBP13</i>	138
3.8.4 <i>AtUBP12</i> regulates the floral transition signal	140
3.8.5 Potential targets of <i>AtUBP12</i> and <i>AtUBP13</i>	143
<b>Chapter 4 - Solanaceous UBP12 orthologs</b>	<b>145</b>
<b>4.1 Introduction</b>	<b>145</b>

<b>4.2</b>	<b>Identification of solanaceous UBP12 orthologs</b>	146
4.2.1	Solanaceous EST analysis	146
4.2.2	RACE PCR to determine <i>NtUBP12</i> 5' terminus sequence	149
<b>4.3</b>	<b><i>NtUBP12</i> transcript analysis during <i>Cf-9/Avr9</i> elicited HR</b>	154
<b>4.4</b>	<b>VIGS based silencing of <i>NbUbp12</i></b>	156
<b>4.5</b>	<b>Avr9 elicited cell death assay during VIGS silencing of <i>NbUbp12</i></b>	164
<b>4.6</b>	<b>AvrPto/Pto mediated HR cell death assay during <i>NbUbp12</i> silencing</b>	175
<b>4.7</b>	<b>Induction of basal disease resistance during <i>NbUBP12</i> silencing</b>	180
<b>4.8</b>	<b><i>NbUBP12</i> silencing increases resistance against TMV</b>	182
<b>4.9</b>	<b>Discussion</b>	188
4.9.1	<i>NbUBP12</i> - links to known resistance signalling pathways	191
4.9.2	Does <i>NbUBP12</i> regulate the HR and disease resistance?	194
<b>Chapter 5 - <i>In vitro</i> DUB activity assays of plant UBP12 proteins</b>		195
<b>5.1</b>	<b>Introduction</b>	195
<b>5.2</b>	<b><i>In vitro</i> activity assay of <i>E. coli</i> expressed AtUBP12</b>	197
5.2.1	Generation of Histidine tagged AtUBP12 proteins for <i>E. coli</i> based expression	197
5.2.2	Expression and purification of AtUBP12 proteins from <i>E. coli</i>	198
5.2.3	<i>In vitro</i> Ub-chain cleavage assay of <i>E. coli</i> expressed AtUBP12 proteins	201
<b>5.3</b>	<b><i>In vitro</i> activity assay of <i>S. frugiperda</i> expressed AtUBP12</b>	202
5.3.1	Generation of Histidine tagged AtUBP12 proteins for <i>S. frugiperda</i> based expression	202
5.3.2	Expression and purification of AtUBP12 proteins from <i>S. frugiperda</i>	205

5.3.3	<i>In vitro</i> diubiquitin cleavage assay of <i>S. frugiperda</i> expressed AtUBP12 proteins	209
5.4	<b><i>In vitro</i> activity assay of <i>S. frugiperda</i> expressed NtUBP12</b>	210
5.4.1	Generation of Histidine tagged NtUBP12 proteins for <i>S. frugiperda</i> based expression	210
5.4.2	Expression and purification of NtUBP12 proteins from <i>S. frugiperda</i>	210
5.4.3	<i>In vitro</i> diubiquitin cleavage assay of <i>S. frugiperda</i> expressed NtUBP12 proteins	211
5.5	<b>Phylogenetic analysis of eukaryotic UBP12 proteins</b>	216
5.6	<b>Discussion</b>	219
5.6.1	<i>In vitro</i> activity assay of AtUBP12 and NtUBP12 proteins	219
5.6.2	UBP12 linkage specificity	220
5.6.3	Structural aspects of HAUSP and plant UBP12 function	222
	<b>Chapter 6 - Transient overexpression of AtUBP12 proteins</b>	224
6.1	<b>Introduction</b>	224
6.2	<b>Transient overexpression of AtUBP12 proteins in tobacco</b>	225
6.2.1	Generation and expression of GFP-AtUBP12 fusion proteins	225
6.2.2	Cf-9/Avr9 triggered HR assay during transient overexpression of AtUBP12 proteins	229
6.3	<b>Transient overexpression of AtUBP12 proteins in <i>N. benthamiana</i> during Pto/avrPto triggered HR</b>	241
6.3.1	Transient overexpression of AtUBP12 proteins in <i>N. benthamiana</i>	241
6.3.2	avrPto/Pto triggered HR during overexpression of AtUBP12 proteins in <i>N. benthamiana</i>	245
6.4	<b>Analysis of GFP-AtUBP12 localisation during transient expression by confocal microscopy</b>	260
6.5	<b>Discussion</b>	265
6.5.1	Overexpression of AtUBP12 suppresses the Cf-9 triggered HR in tobacco	265

6.5.2	Overexpression of AtUBP12 does not alter Pto triggered HR development	266
6.5.3	AtUBP12 overexpression approaches prove that solanaceous UBP12 functions as a negative HR regulator	268
<b>Chapter 7 - Final Discussion</b>		<b>269</b>
7.1	<b>Introduction</b>	<b>269</b>
7.2	<b>AtUBP12 and AtUBP13 regulate multiple pathways</b>	<b>270</b>
7.3	<b>AtUBP12 regulates the floral transition</b>	<b>272</b>
7.4	<b>Solanaceous UBP12 proteins regulate the Cf-9 triggered HR and TMV infection</b>	<b>273</b>
7.5	<b>NbUBP12 orthologs and their substrates</b>	<b>275</b>
7.6	<b>Conclusions</b>	<b>281</b>
7.7	<b>Future work</b>	<b>282</b>
<b>References</b>		<b>284</b>
<b>Appendices</b>		<b>xix</b>

# List of Figures

Figure	Title	Page
<b>Chapter 1</b>		
1.1	Zigzag model to represent plant immune system output	4
1.2	Classes of plant disease resistance protein	7
1.3	Ubiquitin conjugation cascade	18
1.4	Functions of Deubiquitinating enzymes (DUBs) in ubiquitin metabolism	24
<b>Chapter 3</b>		
3.1	Analysis of the <i>Arabidopsis</i> JAMM domain ubiquitin proteases	67
3.2	Domains and phylogeny of <i>Arabidopsis</i> UBP enzymes	70
3.3	Transcript analysis of <i>AtUbp12</i> and <i>AtUbp13</i> during infection with virulent and avirulent <i>Pseudomonas</i>	76
3.4	Expression pattern of <i>AtUbp12</i> and <i>AtUbp13</i> following salicylic acid treatment	79
3.5	Expression pattern of <i>AtUbp12</i> and <i>AtUbp13</i> in plant tissues	82
3.6	Alignment of 5' UTR promoter regions from <i>AtUbp12</i> and <i>AtUbp13</i>	84
3.7	Genotyping <i>ubp8-1</i> , <i>ubp11-1</i> and <i>ubp25-1</i> alleles	88
3.8	Genotyping and <i>AtUBP12</i> transcript analysis of the <i>ubp12-1</i> allele	92
3.9	Genotyping and <i>AtUBP12</i> transcript analysis of the <i>ubp12-2</i> allele	94
3.10	Genotyping and <i>AtUBP13</i> transcript analysis of the <i>ubp13-1</i> allele	96
3.11	Genotyping and <i>AtUBP13</i> transcript analysis of the <i>ubp13-2</i> allele	98
3.12	Bacterial growth assay of <i>Pst</i> DC3000 and <i>Pst</i> DC3000 <i>avrB</i> on <i>ubp12</i> and <i>ubp13</i> mutant lines	101
3.13	Bacterial growth assay of <i>Pst</i> DC3000 and <i>Pst</i> DC3000 <i>avrRpt2</i> in <i>ubp12</i> and <i>ubp13</i> mutant lines	103
3.14	Early flowering of <i>ubp12</i> mutants under short days	107

3.15	Flowering time of <i>ubp12</i> and <i>ubp13</i> mutants under long and short days	110
3.16	Selection of a cDNA fragment to initiate hpRNAi gene silencing of <i>AtUbp12</i> and <i>AtUbp13</i>	115
3.17	<i>Arabidopsis</i> UBP_RNAi T <sub>1</sub> transgenics demonstrate reduced growth and increased anthocyanin accumulation relative to pHG12 controls	118
3.18	Expression analysis of <i>AtUbp12</i> and <i>AtUbp13</i> in <i>Arabidopsis</i> UBP_RNAi T <sub>2</sub> generation	120
3.19	Expression analysis of <i>AtUbp12</i> and <i>AtUbp13</i> in <i>Arabidopsis</i> UBP_RNAi T <sub>3</sub> generation	124
3.20	Genotype confirmation of <i>ubp12-1 ubp13-1</i> genetic cross lines in the F <sub>1</sub> and F <sub>2</sub> generation	127
3.21	Genotype confirmation of F <sub>3</sub> <i>ubp12-1 ubp13-1</i> genetic cross lines	130
3.22	Segregation analysis of <i>ubp12-1 ubp13-1</i> F <sub>4</sub> plants on sulfadiazene selective plates	134

#### Chapter 4

4.1	<i>NtUBP12</i> EST summary and full length cDNA determination	151
4.2	RACE PCR strategy to establish 5' region of <i>NtUBP12</i>	153
4.3	<i>NtUBP12</i> is suppressed during Avr9 HR elicitation	155
4.4	Development of photobleaching in <i>PDS</i> silenced <i>N. benthamiana</i>	158
4.5	VIGS based silencing of <i>NbUBP12</i> using TRV:U12_562	161
4.6	VIGS based silencing of <i>NbUBP12</i> using TRV:U12_742	163
4.7	Cf-9/Avr9 elicited HR is increased during <i>NbUBP12</i> silencing by TRV:U12_562	167
4.8	Scoring of the increased Cf-9/Avr9 elicited HR during <i>NbUBP12</i> silencing by TRV:U12_562	169
4.9	Cf-9/Avr9 elicited HR is increased during <i>NbUBP12</i> silencing by TRV:U12_742	171
4.10	Scoring of the increased Cf-9/Avr9 elicited HR during <i>NbUBP12</i> silencing by TRV:U12_742	173

4.11	<i>avrPto/Pto</i> elicited HR is unchanged during <i>NbUBP12</i> silencing by TRV:U12_562	177
4.12	<i>avrPto/Pto</i> elicited HR is unchanged during <i>NbUBP12</i> silencing by TRV:U12_562	179
4.13	Growth of virulent <i>P. s. pv. tabaci</i> is unaltered in <i>NbUBP12</i> silenced <i>N. benthamiana</i>	181
4.14	Silencing of <i>NbUBP12</i> reduces TMV induced HR symptoms in A310 <i>N</i> transgenic <i>N. benthamiana</i>	184
4.15	Silencing <i>NbUBP12</i> reduces TMV:GFP virus accumulation independent of <i>N</i> triggered TMV resistance	187

## Chapter 5

5.1	Active site cysteine conservation in UBP enzymes	196
5.2	Expression and purification of His-AtUBP12 WT and His-AtUBP12 C208S proteins from <i>E. coli</i> .	200
5.3	DUB activity assay of AtUBP12 WT and AtUBP12 C208S proteins	204
5.4	Expression and purification of His-AtUBP12 WT and His-AtUBP12 C208S proteins from <i>S. frugiperda</i>	207
5.5	AtUBP12 is a deubiquitinating enzyme and mutations in its active site abolish its activity	209
5.6	Expression and purification of His-NtUBP12 WT and His-NtUBP12 C206S proteins from <i>S. frugiperda</i>	213
5.7	NtUBP12 is a deubiquitinating enzyme and mutations in its active site abolish its activity	215
5.8	Plant UBP12 proteins cluster with their eukaryotic orthologs	217

## Chapter 6

6.1	GFP-AtUBP12 fusion protein accumulation peaks on day 2 during transient overexpression in tobacco	228
6.2	Expression GFP-AtUBP12 WT and GFP-AtUBP12 C208S in tobacco	231
6.3	Transient overexpression of AtUBP12 in <i>Cf-9</i> tobacco suppresses Avr9 elicited HR	234

6.4	Transient overexpression of the non-catalytic mutant AtUBP12 C208S in <i>Cf-9</i> tobacco fails to suppress Avr9 elicited HR	236
6.5	Transient overexpression of AtUBP12 C208S in <i>Cf-9</i> tobacco promotes Avr9 elicited HR through a dominant negative effect	239
6.6	Coinfiltration of the P19 silencing suppressor enhances transient overexpression of GFP-AtUBP12 in <i>N. benthamiana</i>	244
6.7	Transient overexpression GFP-AtUBP12 and GFP-AtUBP12 C208S in <i>N. benthamiana</i>	248
6.8	Overexpression of AtUBP12 in <i>N. benthamiana</i> does not effect <i>avrPto/Pto</i> elicited HR	250
6.9	Overexpression of AtUBP12 C208S in 35S <i>Pto N. benthamiana</i> does not effect <i>avrPto/Pto</i> elicited HR	252
6.10	Transient overexpression GFP-AtUBP12 and GFP-AtUBP12 C208S with P19 coinfiltration in <i>N. benthamiana</i>	255
6.11	P19 enhanced transient overexpression of AtUBP12 in 35S <i>Pto N. benthamiana</i> does not effect <i>avrPto/Pto</i> elicited HR	257
6.12	P19 enhanced transient overexpression of AtUBP12 C208S in 35S <i>Pto N. benthamiana</i> does not effect <i>avrPto/Pto</i> elicited HR	259
6.13	GFP-AtUBP12 and GFP-AtUBP12 C208S fusion proteins are localised in the cytoplasm and nucleus during transient overexpression in <i>N. benthamiana</i>	262

## Chapter 7

7.1	Substrate interaction determinants in the TRAF-like domain of HAUSP are conserved in its eukaryotic orthologs	280
-----	---	-----

## Appendix

A1	Alignment of <i>AtUBP12</i> , <i>AtUBP13</i> and <i>NtUBP12</i> cDNA sequences	xxi
----	--	-----

# List of Tables

Table	Title	Page
<b>Chapter 2</b>		
2.1	Antibiotics used for plasmid and bacterial selection	36
2.2	Antibodies used for Western blots in this study	37
2.3	Plasmid DNA vectors used in this study	37
<b>Chapter 3</b>		
3.1	Deubiquitinating enzymes identified in the <i>Arabidopsis</i> genome	71
3.2	Primers for RT-PCR transcript analysis in <i>ubp12</i> and <i>ubp13</i> alleles	90
3.3	Segregation analysis of <i>ubp12-1 ubp13-1</i> F <sub>4</sub> seedlings 20 days after germination on sulfadiazine plates	131
<b>Chapter 4</b>		
4.1	Solanaceous <i>UBP12</i> ESTs recovered from TIGR gene indices	148
<b>Appendix</b>		
A1	Initial DUB protein sequences used to query the <i>Arabidopsis</i> proteome	xix
A2	PCR primers used for RT-PCR and cloning	xix
A3	<i>Arabidopsis</i> T-DNA lines isolated in this study	xxiv

## Abbreviations

ACIF1, Avr9/Cf-9-INDUCED F-BOX 1; ACRE, Avr9/Cf9 Rapidly Elicited; ADP, adenosine diphosphate; AMSH, Associated Molecule with the SH3 domain of STAM; APC, Anaphase Promoting Complex; ATP, adenosine triphosphate; cDNA, complementary DNA; CC, Coiled Coil; Col-0, Columbia-0; CP, Core protease; COI1, CORONATINE INSENSITIVE; CSN, COP9 signalosome; Cys, Cysteine; dNTP, deoxynucleotide triphosphate; DUB, Deubiquitinating enzyme; EBF1, EIN3 binding F-box; EDS1, ENHANCED DISEASE SUSCEPTIBILITY; eIF3, elongation Initiation Factor 3; EIN3, ETHYLENE INSENSITIVE 3; EST, Expressed Sequence Tag; ETI, Effector Triggered Immunity; ET, Ethylene; GFP, Green Fluorescent Protein; HAUSP, Herpesvirus Associated Ubiquitin Specific Protease; HECT, Homology to E6AP C-Terminus; His, Histidine; HR, Hypersensitive Response; HSP90, Heat Shock Protein 90; ISR, Induced Systemic Resistance; JAMM, JAB1/MPN/Mov34; JA, Jasmonic Acid; *L. er*, Landsberg *erecta*; LRR, Leucine Rich Repeat; MAPK, Mitogen Activated Protein Kinase; mRNA, messenger RNA; NB, Nucleotide Binding; NDR1 NON-RACE SPECIFIC DISEASE RESISTANCE; NES, Nuclear Export Signal; NPR1, NON-EXPRESSOR OF PR GENES 1; NLS, Nuclear Localisation Signal; NES, Nuclear Export Signal; OD, Optical Density; OTU, ovarian tumour; PAMP, Pathogen Associated Molecular Pattern; PAD4, PHYTOALEXIN DEFICIENT4; PCD, Programmed Cell Death; PCR, Polymerase Chain Reaction; PR, Pathogenesis Related; PTI, PAMP Triggered Immunity; PUB, PLANT U-BOX; RACE, Rapid Amplification of cDNA Ends; ROI, Reactive Oxygen Intermediate; RLP, Receptor Like Protein; RP, Regulatory particle; RPK, Receptor Protein Kinase; RIN, RPM1-INTERACTING PROTEIN; RING, Really Interesting New Gene; RNAi, RNA interference; SA, Salicylic acid; SAR, Systemic Acquired Resistance; SCF, Skp1/Cullin/F-box; Ser, Serine; SGT1, SUPPRESSOR OF G-2 ALLELE OF SKP1; SON1, SUPPRESSOR OF NIM1-1; SPL11, Spotted Leaf 11; STAM, Signal Transducing Adaptor Molecule; STK, Serine/Threonine Kinase; T-DNA, Transfer DNA; Thr, Threonine; TIR, Toll Interleukin Receptor; TMV, Tobacco Mosaic Virus; TRV, Tobacco Rattle Virus; Ub, Ubiquitin; Ubl, Ubiquitin like; UBP, Ubiquitin Specific Protease; UCH, Ubiquitin Carboxy Hydrolase; VIGS, Virus Induced Gene Silencing; WT, Wild type.

## Abstract

The importance of the ubiquitin-proteasome pathway in eukaryotic cellular regulation has become increasingly apparent during the last decade. In plants, regulated degradation by the ubiquitin/26S proteasome has been implicated in diverse signalling events including embryogenesis, hormone signalling and disease resistance. Ubiquitin moieties are ligated to target proteins through the sequential activities of E1, E2 and E3 enzymes leading either to proteasomal degradation or other regulatory outcomes in the cell. It is now established that ubiquitination is a reversible process and that removal of ubiquitin from target proteins by deubiquitinating enzymes (also termed ubiquitin proteases) can also serve a regulatory function. Deubiquitinating enzymes are proteases with specificity for the isopeptide linkages formed during ubiquitin ligation events.

Current understanding of deubiquitinating enzyme function in plants is relatively limited and the aim of this project was to establish novel findings in this emerging field. This study reports an extensive analysis of the deubiquitinating enzymes in the *Arabidopsis thaliana* genome and functional characterisation of two closely related *Arabidopsis* Ubiquitin Specific Proteases: AtUBP12 and AtUBP13 and their respective orthologs in the solanaceous plants tobacco (*Nicotiana tabacum*) and *Nicotiana benthamiana*.

Previous work suggested the potential involvement of *NbUBP12* in disease resistance, in this study, established methodologies in *Arabidopsis*, tobacco and *Nicotiana benthamiana* were applied to investigate this possibility. Transcript induction studies in *Arabidopsis* reported the induction of both *AtUBP12* and *AtUBP13* by avirulent *Pseudomonas* and exogenously applied Salicylic acid (SA). Pathology assays in single allele *Arabidopsis ubp12* and *ubp13* mutants reported no alteration in resistance against virulent and avirulent strains of *Pseudomonas*, raising the possibility that *AtUBP12* and *AtUBP13* are functionally redundant. Investigations into redundancy between *AtUBP12* and *AtUBP13* were conducted using transgenic RNAi based cosuppression and the isolation of

genetic crosses between *ubp12* and *ubp13* mutant alleles. Collectively these approaches provide the first report that AtUBP12 and AtUBP13 are functionally redundant and are required for normal plant development with homozygous *ubp12 ubp13* double mutants exhibiting a seedling lethal phenotype. Phenotypic analysis of *ubp12* and *ubp13* mutants indicated that functional redundancy between these genes was not complete with the novel observation of early flowering in *ubp12* alleles under both long and short day photoperiods. Short day early flowering in *ubp12* mutants was accompanied by the development aerial rosettes and suggests the crucial involvement of deubiquitination in the floral transition.

The cDNA sequence of the tobacco *AtUBP12* ortholog *NtUBP12* was determined and utilised for VIGS based *NbUBP12* gene silencing studies during disease resistance signalling in *N. benthamiana*. Loss of function studies indicated that NbUBP12 functions as a negative regulator of hypersensitive cell death (HR) induced by the *Cladisporium fulvum* elicitor Avr9 and *R* gene independent viral resistance against TMV. These findings represent the first reported link between deubiquitination and plant disease resistance. Respective cDNAs for *AtUBP12* and *NtUBP12* were cloned and expressed to demonstrate the function of their gene products by *in vitro* ubiquitin protease activity assays. Ubiquitin protease activity of UBP12 was directly implicated in *C.fulvum* Avr9 elicited cell death during tobacco transient overexpression assays. This experimental approach confirmed that UBP12 activity negatively regulates the Avr9 elicited HR with overexpression of AtUBP12 causing HR suppression and the corresponding AtUBP12 C208S active site mutant conferring a dominant negative HR promotion effect.

Overall the presented data reports several novel insights which implicate *Arabidopsis* UBPs: AtUBP12 and AtUBP13 in plant development and suggests they also may stabilise common substrates which regulate disease resistance. AtUBP12 is also specifically implicated as a floral suppressor and *in vitro* assays have demonstrated that AtUBP12 and NtUBP12 encode functional ubiquitin proteases. In solanaceous plants, UBP12 activity negatively regulates the defence associated HR and virus resistance.

# Chapter 1 - Introduction

## 1.1 Plant defence against pathogen attack

### 1.1.1 Plant immunity

Plants are subject to attack by a diverse range of microbial pathogens and insect herbivores. Disease resulting from pathogen infection results in large crop losses and contributes to worldwide hunger and malnutrition. Consequently, the control of plant diseases is of fundamental importance and is the principle objective of plant-breeding and pathology programs with relevance to the agriculture industry. Plants resist pathogen attacks both with preformed defences such as 'waxy' cuticular layers and anti-microbial compounds and by inducing multilayered defence responses (Martin et al., 2003). Plant pathogens fall into two categories which either derive nutrients from dead or dying cells (necrotrophs) or living host tissues (biotrophs). Biotrophic plant pathogens use diverse life strategies. Pathogenic bacteria proliferate in the plant apoplast after entering through existing wounds, stomata or hydathodes (Glazebrook, 2005). From the apoplast, bacterial pathogens access the plant cell through a type III secretion pilus (Glazebrook, 2005). Pathogenic and symbiotic fungi and oomycetes can invaginate feeding structures (haustoria) into the host cell plasma membrane (Glazebrook, 2005). Aphids and nematodes feed from stylets directly inserted into host plant cells (Dangl and McDowell, 2006). Early pathogen perception events occur at the extracellular matrix and host cell plasma membrane where the outcome of the interaction is determined (Jones and Dangl, 2006). To influence host defence responses and enhance microbial fitness, these diverse pathogen classes all deliver effector molecules (avirulence factors) into the plant cell (Dangl and McDowell, 2006).

Plants lack the mobile defender cells and adaptive immune system found in mammals, relying instead on cellular innate immunity and the induction of systemic signals emanating from sites of infection (Jones and Dangl, 2006). Current research suggests that the inducible plant immune system can be broadly divided into two branches (Jones and Dangl, 2006). One of

these mediates the perception of microbial- or pathogen-associated molecular patterns (MAMPS or PAMPs respectively) such as flagellin through transmembrane pattern recognition receptors (PRRs) (Schwessinger and Zipfel, 2008). Defence responses activated by PAMPs are collectively termed PAMP triggered immunity (PTI) or basal resistance (Schwessinger and Zipfel, 2008). The second branch acts primarily inside the cell using disease resistance (R) proteins which recognise pathogen delivered effectors or their effects on host proteins. R protein mediated defenses are termed effector triggered immunity (ETI) or gene-for-gene resistance (Jones and Dangl, 2006).

Activation of PTI by PAMP recognition is proposed to be the plant's first inducible response to microbial perception (Schwessinger and Zipfel, 2008). In the majority of cases, PTI halts pathogen growth at an early infection stage due to the induction of pathogen-responsive genes, production of reactive oxygen species and deposition of callose to reinforce the cell wall at sites of infection (Schwessinger and Zipfel, 2008).

Biotrophic pathogens deploy effector proteins which disrupt plant immune responses and promote successful infection. Direct or indirect recognition of effectors by R proteins initiates ETI which is an amplified and accelerated PTI response resulting in disease resistance (Jones and Dangl, 2006). ETI is usually accompanied by a localised hypersensitive cell death response (HR) at the infection site (Jones and Dangl, 2006). R proteins have been classified into five distinct classes (as discussed below), most of which contain characteristic leucine rich repeat (LRR) domains. LRR domains are detected in diverse proteins and function as sites of protein-protein interaction, peptide-ligand binding and protein-carbohydrate interaction (Kajava, 1998). The majority of plant R proteins contain LRR domains and comparative sequence analysis indicates that R gene specificity results primarily from hypervariability in this region (Dangl and Jones, 2001). R proteins mediate perception of effectors from diverse kingdoms and integrate recognition of bacterial, viral, fungal and oomycete pathogens to activate similar downstream defence responses which result in disease resistance (Dangl and Jones, 2001).

In the majority of cases, ETI triggered during gene-for-gene resistance is proposed to be most accurately described by the ‘guard hypothesis’ (Dangl and Jones, 2001). In the guard hypothesis, R proteins are proposed to monitor the integrity of host effector targets (Dangl and Jones, 2001). Alteration of host targets by pathogen derived effectors is perceived by specific R proteins leading to the activation of ETI (Jones and Dangl, 2006). This current view of plant immunity depicts the relationship between biotrophic pathogens and their hosts as a molecular ‘arms race’ which was recently described by Jones and Dangl using a four phased ‘zig zag’ model to illustrate the relationship between PTI and ETI (Figure 1.1) (Jones and Dangl, 2006). During phase 1, early PAMP based perception of pathogen components causes PTI that can stop further infection. In phase 2, successful pathogens promote virulence by releasing effectors into the plant cell which suppress PTI resulting in effector-triggered susceptibility (ETS). In phase 3, direct or indirect perception of pathogen effectors by R proteins leads to the activation of ETI resulting in disease resistance. Phase 4 depicts the ongoing natural selection that drives pathogens to avoid ETI either by discarding or diversifying the recognised effector gene, or by lateral acquisition of additional ETI suppressors. Ultimately, selection favours the generation of new R gene alleles that recognize novel effectors allowing the restoration of ETI (Jones and Dangl, 2006).

### **1.1.2 PAMP triggered immunity**

As previously discussed, perception of conserved microbe structural components termed PAMPs leads to the prompt activation of plant defences through PTI. PTI signaling in plants has been most extensively characterised in the case of the flagellin which is an archetypal PAMP and triggers defence responses in various plants (Schwessinger and Zipfel, 2008). Flagellin subunits collectively form the bacterial flagellum required for motility and virulence and distinct conserved flagellin domains are recognised by mammalian and plant receptors TLR5 and FLS2 respectively (Zipfel and Felix, 2005). *Arabidopsis* FLS2 (FLAGELLIN-SENSING2) is a LRR receptor kinase which directly binds the 22 amino acid flagellin epitope flg22 (Zipfel and Felix, 2005) and *fls2* mutants exhibit enhanced susceptibility to bacterial infection (Zipfel et al., 2004). Characterisation

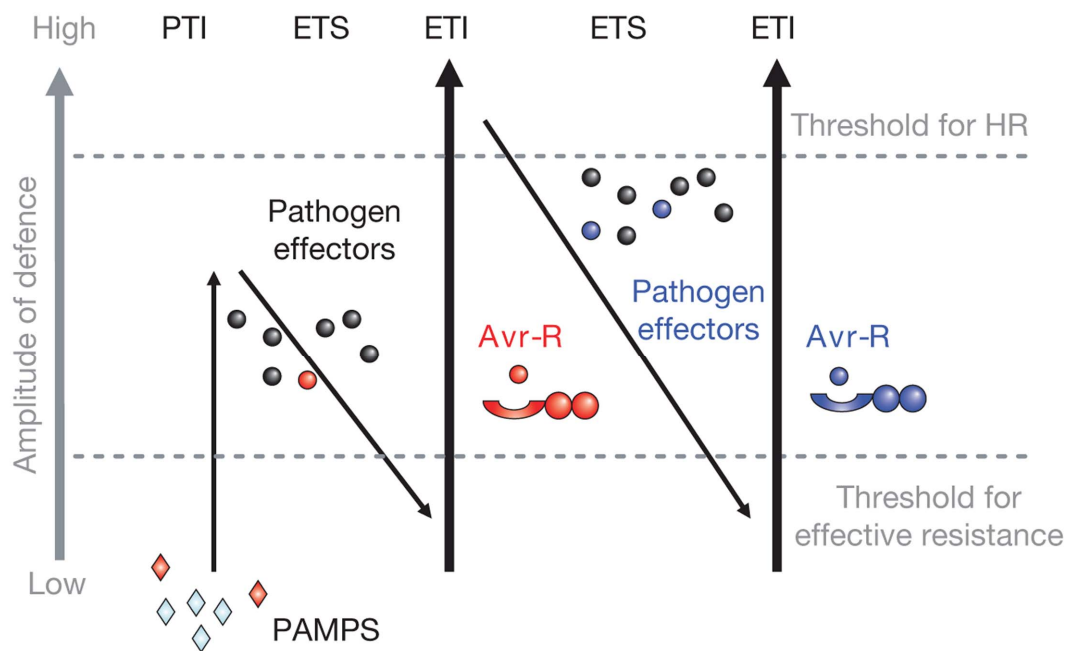


**Figure 1.1** Zigzag model to represent plant immune system output.

In this model, the ultimate amplitude of disease resistance or susceptibility is proportional to  $[PTI - ETS + ETI]$ . In phase 1, plants detect microbial / pathogen-associated molecular patterns (MAMPs/PAMPs, red diamonds) via PRRs to trigger PAMP-triggered immunity (PTI). In phase 2, successful pathogens deliver effectors that interfere with PTI, or otherwise enable pathogen nutrition and dispersal, resulting in effector-triggered susceptibility (ETS). In phase 3, one effector (indicated in red) is recognized by an NB-LRR protein, activating effector-triggered immunity (ETI), an amplified version of PTI that often passes a threshold for induction of hypersensitive cell death (HR). In phase 4, pathogen isolates are selected that have lost the red effector, and perhaps gained new effectors through horizontal gene flow (in blue) — these can help pathogens to suppress ETI. Selection favours new plant NB-LRR alleles that can recognize one of the newly acquired effectors, resulting again in ETI. Taken from Jones and Dangl (Jones and Dangl, 2006).

of other flg22 insensitive mutants led to the elucidation of downstream MAP kinase cascade and WRKY signaling pathways that function downstream of flagellin perception (Asai et al., 2002). Similar signaling responses have been reported during the perception of bacterial elongation factor Tu (EF-Tu) by the LRR receptor kinase EFR and the elicitation of PTI in *fls2 efr-1* double mutants indicates the existence of other PAMP receptors in *Arabidopsis* (Zipfel et al., 2006). Molecules with PAMP activity have also been identified in fungal and oomycete plant pathogens.

PAMP response activators have also been identified in fungal and oomycete pathogens. Characteristic PAMP molecules include the cell wall components ergosterol and chitin from fungi and heptagluco-side from oomycetes (Nurnberger et al., 2004).

### **1.1.3 Effector triggered immunity**

Beyond the amplified induction of PTI responses, activation of ETI by pathogen effectors results in rapid production of reactive oxygen intermediates (ROI) termed the oxidative burst and development of localised programmed cell death known as the hypersensitive response (HR) (Nimchuk et al., 2003). ETI activation causes elevated salicylic acid (SA) accumulation which induces transcription of various pathogenesis-related (PR) genes and the activation of systemic acquired resistance (SAR) (Durrant and Dong, 2004). The oxidative burst is proposed to serve a direct antimicrobial effect and also initiates signal activation for other downstream defence responses (discussed below) whilst the HR is thought to act to suppress biotroph infection by restricting pathogen access to water and nutrients (Nimchuk et al., 2003). The activation of common disease resistance signaling pathways results from the perception of bacterial, viral, fungal, oomycete, and nematode pathogen effectors by their associated R proteins (Dangl and Jones, 2001). Despite the broad taxonomic origins of known plant pathogens and the presumed diversity in their effector molecules, only five structural classes of R protein have been reported (Figure 1.2) with the presence of LRR domains being a recurring theme in the majority of cases (Dangl and Jones, 2001).

## NB-LRR R proteins

In the model plant *Arabidopsis thaliana*, the largest group of R proteins is the cytoplasmic ‘Nucleotide Binding Site plus Leucine Rich Repeat’ (NB-LRR) encoded by ~150 distinct *R* genes (Dangl and Jones, 2001). Within the NB-LRR R protein structure, the NB domain is part of a larger region (NB-ARC) which shares sequence similarity with the apoptosis regulators CED4 from *Caenorhabditis elegans* and Apaf-1 from animals (van der Biezen and Jones, 1998). Nucleotide binding and hydrolysis by the NB domain has been reported in a number of cases and nucleotide exchange from ADP to ATP is proposed to be regulated by conformational changes induced by recognition of pathogen effectors or effector targets through the LRR domain (Takken et al., 2006). In the NB-LRR R proteins, the C-terminal LRR domain is highly variable in terms of repeat number and sequence diversity (Dangl and Jones, 2001). The LRR are under diversifying selection and play a central role to generate specificity for different effectors or effector targets within the conserved structure of the R protein (Dangl and Jones, 2001).

The NB-LRR proteins can be subdivided into two classes on the basis of TIR or CC domains present in the N-terminus. The TIR domain is implicated in signaling by its similarity to *Drosophila* Toll mammalian interleukin (IL)-1 receptors and is detected in 40% of the *Arabidopsis* NB-LRR proteins (Dangl and Jones, 2001). Numerous TIR-NB-LRR proteins have been characterised including the N from tobacco and RPS4 from *Arabidopsis* which mediate resistance against Tobacco Mosaic Virus and *Pseudomonas syringae* respectively (Whitham et al., 1994) (Gassmann et al., 1999). The remaining *Arabidopsis* NB-LRR proteins contain a CC (coiled coil) domain which is a repeated heptad sequence with interspersed hydrophobic amino acids (Martin et al., 2003). The CC domain consists of two or more alpha helices which interact to form a supercoil, it is found in diverse proteins and is implicated in protein-protein interactions (Martin et al., 2003). CC-NB-LRR proteins mediate resistance against diverse pathogen classes and examples include potato Rx and *Arabidopsis* RPM1 which enable resistance against Potato Virus X and *Pseudomonas syringae* (Martin et al., 2003).

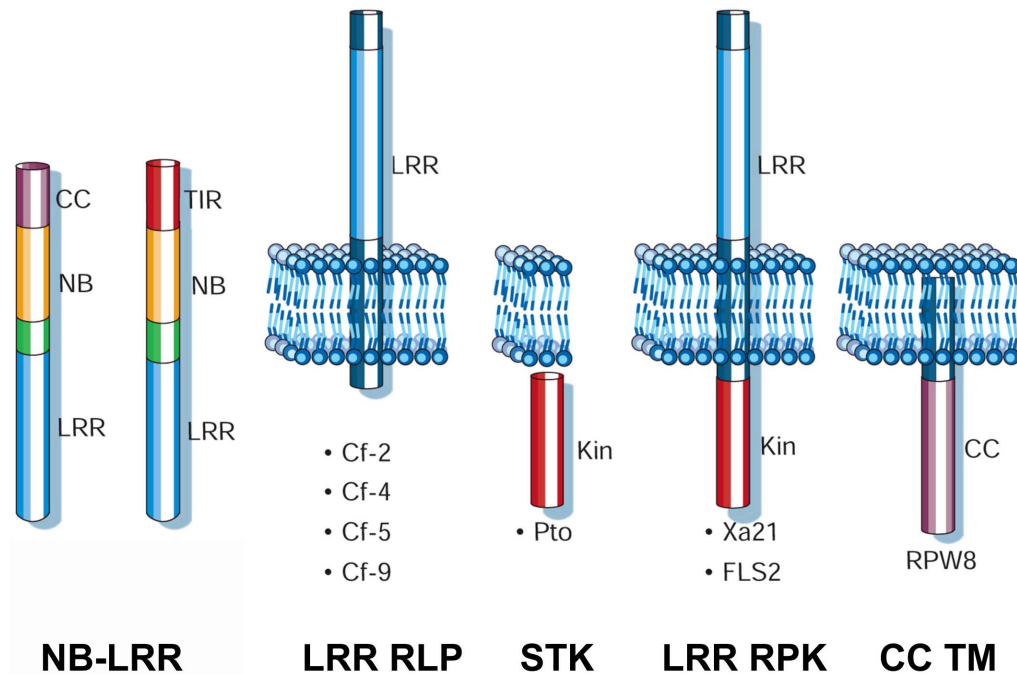


**Figure 1.2** Classes of plant disease resistance protein.

Schematic models of structure and location of the five main classes of plant disease resistance (R) proteins. The proposed cytoplasmic NB-LRR R proteins can be subdivided on the basis of distinct Coiled Coil (CC - purple) or Toll Interlukin Receptor (TIR - red) domains present in the N-terminus. The LRR RLP Cf R proteins carry transmembrane domains and extracellular LRRs. The *Pto* gene encodes a cytoplasmic Ser/Thr kinase (STK) and forms a single member R protein class. The LRR RLK proteins FLS2 and Xa21 have a similar organisation to RLP proteins but carry an additional cytoplasmic Ser/Thr kinase in their C-terminus. The *RPW8* genes encode a distinct class of transmembrane R proteins that carry a proposed Coiled Coil domain in their N-terminus. Adapted from Dangl and Jones (Dangl and Jones, 2001).

## **LRR receptor-like proteins**

LRR Receptor-like Proteins (RLP) are distinct R proteins comprised of extracytoplasmic LRR domains, a transmembrane region and a short cytoplasmic domain (Figure 1.1) with no obvious signaling function (Rivas and Thomas, 2005). The LRR RLP family is highly elaborated plants relative to their mammalian orthologs and is implicated in the regulation of development as well as disease resistance (Shiu and Bleecker, 2003). Two subfamilies of tomato LRR RLP *R* genes have been reported which mediate resistance against the fungal pathogens *Cladisporium fulvum* (*Cf* genes) and *Verticillium dahliae* (*Ve* genes) (Rivas and Thomas, 2005) (Kawchuk et al., 2001).

The tomato *Cf* genes (*Cf-2*, *Cf-4*, *Cf-5* and *Cf-9*) encode the best characterised LRR RLP R proteins (Rivas and Thomas, 2005). *Cf* proteins indirectly perceive the apoplastic presence of effectors (*Avr2*, *Avr4*, *Avr5* and *Avr9*) from different races of the tomato fungal pathogen *Cladisporium fulvum* (Rivas and Thomas, 2005). As seen in the NB-LRR proteins, recognition specificity in the *Cf* proteins resides in variations between the number of repeats and solvent exposed amino acid composition within the LRR domain (Rivas and Thomas, 2005). *Cf* R proteins are proposed to conform to the guard hypothesis of effector target surveillance (Rivas and Thomas, 2005) and current research efforts are aimed at establishing their interacting partners and how they transduce extracellular effector perception signals to inside the cell.

## **LRR Receptor-like kinases**

LRR receptor-like kinases (RLK) are structurally related to LRR receptor-like proteins but contain an additional cytoplasmic serine/threonine protein kinase in the C-terminal region (Jones and Takemoto, 2004). LRR RLK proteins from *Arabidopsis* have been implicated plant development where the LRR RLK CLV1 forms part of the CLAVATA complex and PAMP perception through FLS2 which senses flagellin (as previously discussed)(Shiu and Bleecker, 2003). The only currently known LRR RLK gene with a role in disease resistance is the *Xa21* gene from rice which

confers resistance to the *Xanthomonas oryzae* pv. *oryzae* through specific perception of the avirulence factor avrXa21 (Lee et al., 2006).

### **Ser/Thr kinases**

Identification and characterisation of the tomato *R* gene *Pto* as a cytosolic Ser/Thr kinase established an atypical class of R protein which lacks any LRR domains or transmembrane region (Figure 1.2) (Pedley and Martin, 2003). *Pto* is reported to directly interact with the *Pseudomonas syringae* pv. *tomato* effector avrPto to enable resistance against bacterial speck disease (Pedley and Martin, 2003). Whilst *Pto* does not contain LRR domains, it does require interaction with the NB-LRR protein Prf to initiate resistance against avrPto and Prf is proposed to 'guard' *Pto* against the avrPto effector (Pedley and Martin, 2003).

### **Membrane bound coiled-coil**

Another atypical *R* gene class was established by the identification of the *RPW8* genes in *Arabidopsis* (*RPW8.1* and *RPW8.2*) which confer broad spectrum resistance to powdery mildew pathogens (Xiao et al., 2001). The *RPW8* proteins are small basic proteins with a putative N-terminal transmembrane region and a coiled-coil domain (Figure 1.2) (Xiao et al., 2001). *RPW8* R proteins have been shown induce resistance through established disease resistance signaling pathways but are atypical as they do not appear to exhibit a gene-for-gene interaction with specific fungal effectors (Xiao et al., 2005).

## **1.2 Signal transduction during plant defence**

Plant defence mechanisms have been characterised as a multilayered system consisting of preformed physical barriers and inducible defences (Dangl and Jones, 2001). Inducible defences can be activated by the extracellular recognition of general PAMP elicitors such as bacterial flagellin during PTI or intracellular recognition events resulting from perception of pathogen delivered effectors by their cognate R proteins (Martin et al., 2003).

### 1.2.1 Signal transduction during PTI

Basal resistance (PTI) triggered by PAMP perception represents the frontline of inducible defense and triggers diverse signaling responses. These include the rapid changes in intracellular  $\text{Ca}^{2+}$  flux, induction of an oxidative burst, transcriptional reprogramming, cell wall reinforcement and receptor endocytosis (Schwessinger and Zipfel, 2008) (Altenbach and Robatzek, 2007). PAMP perception results in SA accumulation and recent reports indicate that disruption SA biosynthesis in the *Arabidopsis sid2* mutant results in compromised PTI defences against virulent *Pseudomonas syringae* (Tsuda et al., 2008). PAMP triggered PTI induction also results in the activation of MAPK kinase cascades and the *Arabidopsis* MKK1 - MPK3/MPK6 kinase module has been shown to act downstream of the flagellin receptor FLS2 leading to the activation of WRKY22/29 transcriptional targets (Asai et al., 2002). Microarray analysis indicates that PAMP perception induces rapid changes in gene expression with a significant expression overlap during PTI induced by fungal or bacterial PAMPs (Zipfel et al., 2006). Significant overlap has also been reported between PTI and ETI transcriptomes underscoring the fact that ETI includes amplified aspects of the PTI response (Zipfel et al., 2006).

### 1.2.2 Signal transduction during ETI

Gene-for-gene resistance (ETI) is superimposed onto basal resistance mechanisms and is characterised by a sustained burst of reactive oxygen intermediates (ROI), induction of localised cell death (HR) with activation of defence gene expression and resistance in systemic tissues (systemic acquired resistance) (Jones and Dangl, 2006). Key proteins that regulate ETI have been identified in *Arabidopsis* with isolated mutants indicating that R protein activation leads to activation of the oxidative burst, causing a change in cellular redox status which induces HR and SA accumulation (Nimchuk et al., 2003). Elevated SA levels potentiate the HR and lead to the induction of defense genes and the subsequent development of SAR (Nimchuk et al., 2003). Signal transduction events which cause disease resistance following R protein activation during ETI occur through multiple interacting pathways which are regulated by increased transmembrane ion

flux ( $\text{Ca}^{2+}$ ,  $\text{K}^{+}$  and  $\text{H}^{+}$ ), nitric oxide production and increased salicylic acid (SA) accumulation amongst many other factors (Hofius et al., 2007).

Genetic screens for loss of resistance to *Peronospora parasitica* and *Pseudomonas syringae* identified NDR1 (NON-RACE SPECIFIC DISEASE RESISTANCE) and EDS1 (ENHANCED DISEASE SUSCEPTIBILITY) as components required to mediate signaling by distinct R genes (Aarts et al., 1998). It is now established that NDR1 is required for resistance mediated by most CC-NB-LRR R genes whilst EDS1 mediates resistance signaling through the TIR-NB-LRR R gene class (Dangl and Jones, 2001).

Numerous components of the SA linked disease signaling pathway have been identified including EDS1 and its interacting partner PAD4 (Wiermer et al., 2005). EDS1 and PAD4 (PHYTOALEXIN DEFICIENT4) function as key regulators of biotic and oxidative stress which exert an early activity in TIR-NB-LRR resistance acting upstream of the oxidative burst and HR (Wiermer et al., 2005). EDS1 and PAD4, together, are required for SA accumulation and defence signal propagation involving the processing of ROI signals around the infection site (Wiermer et al., 2005).

Following activation of ETI, local SA levels are dramatically increased through the isochorismate synthesis pathway and regulate HR development and downstream signaling events which induce defence gene expression leading to SAR (Durrant and Dong, 2004). SA is proposed to function through feedback loops both upstream and downstream of the HR establishing an SA dependent gradient which restricts cell death development to the initial infection site (Hofius et al., 2007).

HR development is also subject to positive and negative feedback regulation through the interacting effects between SA, ROI, ET (ethylene) and JA (jasmonate). Together, SA and ROI are proposed to trigger cell death initiation causing an increase in ET which stimulates further ROS production and SA synthesis in surrounding cells to effect cell death propagation (Hofius et al., 2007). JA has been reported to exert both inhibitory and pro-cell death regulation through perception of distinct ROI

species but is proposed to function primarily through antagonistic effects on ET signaling to promote lesion containment (Hofius et al., 2007).

Regulation by phosphorylation through MAPK (mitogen-activate protein kinase) cascades has also been implicated in the development HR and SAR and a central role of MAPKs in the onset of pathogen defense is firmly established (Pedley and Martin, 2005). In tobacco two parallel MAPK cascades have been found that are activated downstream of TMV perception by the R protein N, One pathway consists of NtNPK1, NtMEK1, and Ntf6 whilst the other consists of an unknown MAPKKK, NtMEK2, and NtSIPK and NtWIPK (Pedley and Martin, 2005). Orthologous pathways have also been detected in tomato which regulate Pto mediated resistance (Pedley and Martin, 2005) .

Avirulent pathogen perception typically leads to increased SA accumulation in local infected and systemic non-infected tissue which results in the expression of defence associated *PR* (*PATHOGENESIS-RELATED*) genes which are collectively implicated in SAR development (Durrant and Dong, 2004). Transduction of the SA signal to activate *PR* gene expression and SAR requires the function of NPR1 (*NON-EXPRESSOR OF PR GENES 1*). Several *Arabidopsis npr1* alleles have been isolated in genetic screens for non-expression of *PR* genes after SAR induction (Durrant and Dong, 2004). Analysis of the *npr1* mutant indicates its role in multiple disease signaling pathways including Induced Systemic Resistance (ISR) and the regulation of crosstalk between SA and JA mediated pathways (Durrant and Dong, 2004).

The function of NPR1 in *PR* gene expression has been extensively characterised and it is now established that cytosolic NPR1 oligomers are conformationally sensitive to a change in cellular redox status resulting from pathogen induced SA accumulation (Durrant and Dong, 2004). SAR induction causes redox sensitive reduction of inactive NPR1 oligomers to active NPR1 monomers (Pieterse and Van Loon, 2004). Monomeric NPR1 is translocated to the nucleus where it interacts with numerous TGA transcription factors to activate the expression of *PR-1* and several other defense associated genes (Pieterse and Van Loon, 2004).

Regulatory feedback and cross-regulation between signaling pathways are recurring themes in plant disease resistance signaling. Current analysis suggests that defence responses are highly regulated in timing and amplitude against specific pathogens or general elicitors by the interaction of many discrete pathways including hormone signaling, redox control and transcriptional reprogramming (Hofius et al., 2007).

### **1.3 The ubiquitin 26S proteasome system**

#### **1.3.1 Discovery and background**

All aspects of plant physiology and development are controlled by regulated synthesis of new polypeptides and degradation of existing proteins. Within this ‘protein cycle’ the intricate transcriptional and translational events leading to protein synthesis are relatively well characterised (Vierstra, 2004). Studies conducted in the last decade have greatly improved our appreciation of the corresponding catabolic processes that regulate protein degradation. Protein degradation serves key housekeeping functions by removing misfolded proteins and in the maintenance of free amino acids during growth and starvation (Vierstra, 1996). It is also essential for the many aspects of cellular regulation by removing rate-limiting enzymes and suppressing regulatory networks to fine-tune homeostasis and adapt to new environments (Vierstra, 2004).

Current research indicates that the ubiquitin (Ub)/26S proteasome pathway functions as the principle proteolytic system in eukaryotes and is extensively involved in plant cellular signaling (Vierstra, 2003). In this pathway, the 76 amino acid protein ubiquitin serves as a reusable tag which serves to direct target proteins for selective turnover (Hershko and Ciechanover, 1998). Polymeric chains of ubiquitin are covalently attached to protein targets through the iterative action of a three step (E1 ► E2 ► E3) enzyme conjugation cascade (Figure 1.3) (Hershko and Ciechanover, 1998). Resulting ubiquitinated target proteins are directed to the 26S proteasome for degradation with the concomitant release of ubiquitin moieties for reuse (Hershko and Ciechanover, 1998)

In the 1970s, initial work aimed at understanding protein turnover indicated that different proteins had widely varying cellular half-lives, which were, in some cases, altered by exogenous stimuli (Schimke, 1973). Subsequent development of a cell free lysate from rabbit reticulocyte capable of selective protein degradation in the presence of ATP allowed dissection of the process, as described in studies by Hershko and colleagues (Hershko and Ciechanover, 1998). This work led to the identification of ubiquitin and the discovery that covalent modification of substrates by ubiquitin was critical for their degradation. The subsequent purification of a protease capable of degrading poly-ubiquitinated targets, the 26S proteasome, established the mechanistic framework for ubiquitin dependant proteolysis via the ubiquitin - 26S proteasome pathway (Hough et al., 1987). The fundamental role of the ubiquitin - 26S proteasome pathway in various cellular processes was first made clear by Varshavsky and coworkers in mammalian cells and yeast (Finley and Varshavsky, 1985). Using molecular genetics, numerous aspects of the ubiquitin system and the diverse processes it affects have since been extensively investigated (primarily in yeast) (Hershko and Ciechanover, 1998).

The implication of the ubiquitin - 26S proteasome system in a wide range of cellular contexts reflects the advantages conferred by selective protein degradation over other types of regulatory mechanism. The main advantages relate to the speed and commitment of ubiquitin based signaling. Ubiquitin tagged substrates can have their half-lives swiftly reduced (to the order of minutes) with rapid changes in steady state level induced by specific stimuli (Vierstra, 2004). The irreversible removal of substrates also prevents the effects of inappropriate reactivation and correlate with the frequent involvement of selective protein degradation in signaling processes requiring explicit timing control such as: cell cycle progression, embryogenesis and cell lineage specification (Gottesman and Maurizi, 1992).

The cost to the cell of maintaining such a rapid and sensitive system to regulate protein levels is the large overall energy consumption required to continually degrade and resynthesise proteins (Gottesman and Maurizi, 1992). This is offset however, by the relatively small fraction of proteins

(most of which are key regulatory proteins) that normally undergo continuous turnover in the cell (Vierstra, 2004).

### 1.3.2 The ubiquitin protein

Ubiquitin is a 76 amino acid globular protein found in all eukaryotes, its sequence is highly conserved and only three residues differ between yeast and human species (Callis et al., 1995). It is the prototypical member of the ubiquitin like (Ubl) protein family which covalently modify target proteins to alter various aspects of their regulation (Jentsch and Pyrowolakis, 2000). Ubiquitin assumes a compact structure with a five-strand mixed  $\beta$  sheet forming a cavity into which a single  $\alpha$  helix fits diagonally to form a characteristic 'Ub fold' (Vierstra, 1996). Numerous intramolecular hydrogen bonds impart ubiquitin with high stability, presumably to encourage recycling rather than proteolysis during the conjugation/ degradation process (Vierstra, 2004). The flexible C-terminus of ubiquitin protrudes from the Ub fold and terminates with an essential glycine residue. The carboxy group of this glycine functions as an initiation site for the covalent attachment of ubiquitin to substrates (Vierstra, 2004).

Ubiquitin gene family members (*UBQs*) are detected either as Ub polymers in which multiples (typically 4-6 in *Arabidopsis*) of the 228 bp coding region are concatenated head-to-tail or as one of three different fusion proteins (Callis et al., 1995). The Ub-fusion genes encode either one of two different ribosomal subunits or the Ubl RUB-1 (Related to Ubiquitin) protein fused to the C-terminus of ubiquitin (Callis et al., 1990). In all cases ubiquitin-fusion precursors are cleaved at the terminal glycine by deubiquitinating enzymes (DUBs) to release active monomers (Amerik and Hochstrasser, 2004).

Ubiquitin contains seven lysines (K6, K11, K27, K29, K31, K48 and K63). To target substrates for degradation by the proteasome, covalent inter-ubiquitin linkages are made from the C-terminal glycine to the K48 of the previous ubiquitin moiety (i.e. G76-K48 isopeptide bond) to form ubiquitin chains (poly-Ub) (Fushman and Pickart, 2004). Poly-Ub chains of at least

four ubiquitin moieties (tetra-ubiquitin) are required to provide an efficient proteasome delivery signal (Thrower et al., 2000).

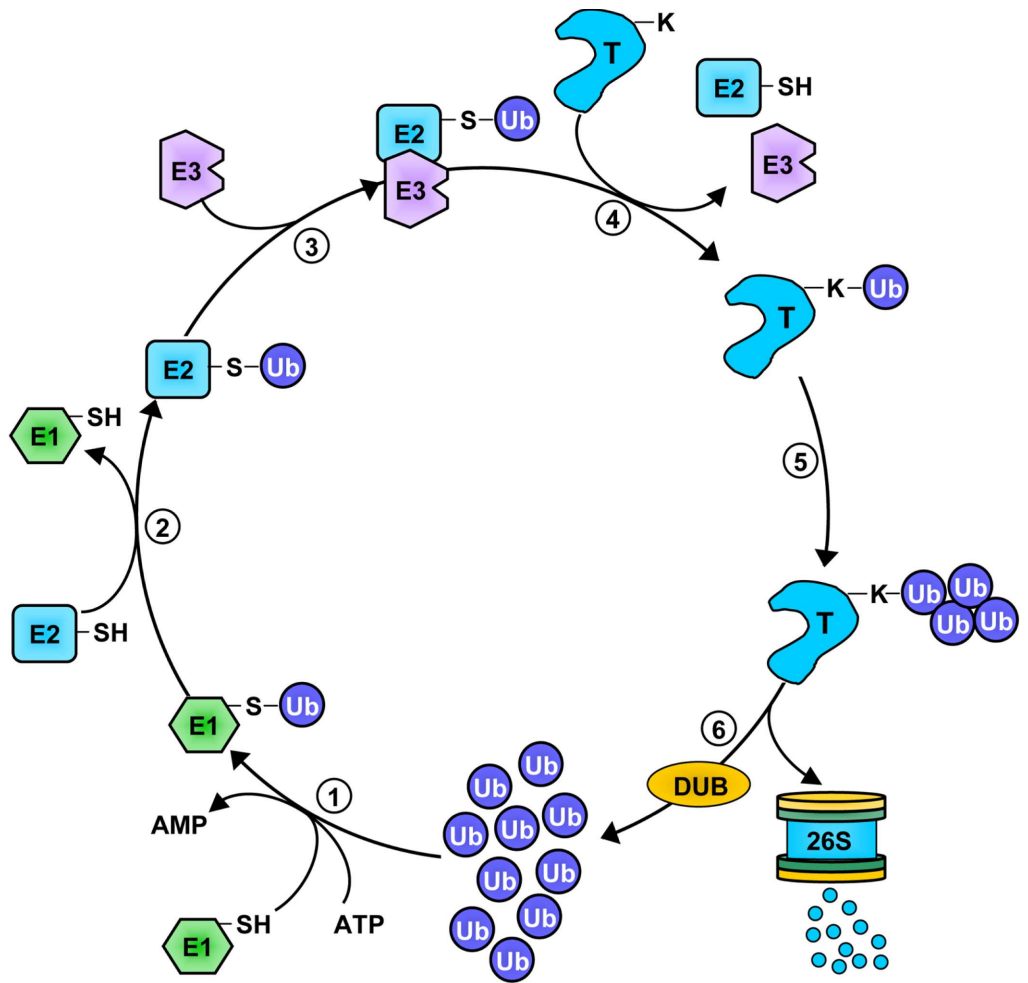
### 1.3.3 The ubiquitin conjugation cascade

Attachment of free ubiquitin moieties to appropriate substrates proceeds by an ATP dependent E1 ► E2 ► E3 enzyme conjugation cascade (Figure 1.3). The cascade starts with E1 ubiquitin activating enzyme. The E1 enzyme catalyses the formation of an acyl phosphoanhydride bond between the ATP adenosine monophosphate (AMP) of ATP and the C-terminal glycine carboxy group of ubiquitin (Hershko and Ciechanover, 1998). Activated ubiquitin then forms a stable intermediate by binding directly to an E1 cysteine via a thiolester linkage (Hershko and Ciechanover, 1998). This activated ubiquitin is transferred from E1 to E2 ubiquitin conjugating enzyme by transesterification. The E2-ubiquitin intermediate delivers ubiquitin onto a substrate acceptor lysine using an E3 ubiquitin ligase (Hershko and Ciechanover, 1998). E3 enzymes impart substrate recognition to the process and either promote direct transfer of Ub to substrates from E2 or form a final E3-Ub intermediate prior to transfer (Vierstra, 2004). The end product is a ubiquitin-protein conjugate containing an isopeptide bond between the C-terminal glycine of ubiquitin and lysyl  $\epsilon$ -amino group in the substrate (Hershko and Ciechanover, 1998).

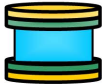
After attachment of an initial ubiquitin moiety to a substrate, additional Ubs are ligated to specific internal lysine residues on the first Ub to form poly-Ub chains. Whether ubiquitin chains are extended by ligation of pre-assembled poly-Ub or by iterative rounds of E3 based ligation is currently unclear (Vierstra, 2004). Whilst linkages through all seven Ub lysines have been detected *in vivo*, poly-Ub chains linked through lysine 48 (K48) predominate in the cell and present a proteasome targeting/recognition signal (Fushman and Pickart, 2004). Upon delivery to the proteasome, ubiquitinated substrates have poly-Ub chains removed by deubiquitinating enzymes prior to unfolding, import and proteolysis (Hartmann-Petersen et al., 2003).

**Figure 1.3** Ubiquitin conjugation cascade.

**(1)** ATP dependent activation of Ub by E1. Activated Ub binds to a conserved cysteine in E1 via a thiolester linkage from a carboxy group in its terminal glycine. **(2)** Transfer of Ub to Ubiquitin conjugating enzyme (E2) forming an E2-Ub thiolester linkage. **(3)** The E2 carries the activated ubiquitin to the ubiquitin ligase (E3), which facilitates the transfer of the ubiquitin from the E2 to a lysine residue in the target protein, often by forming an intermediate complex with the E3 and the target. **(4)** Initial ubiquitination of target forming a Ub-protein conjugate linked by a isopeptide bond. **(5)** Additional Ubs are ligated to form poly-Ub chains. Proteins tagged with K48 linked poly-Ub chains are targeted to the proteasome. **(6)** Poly-Ub chains are disassembled by a proteasome associated deubiquitinating activity (DUB) and free Ub moieties are released. Proteasome localised substrates are then unfolded, imported and degraded into peptide fragments.



**Key:**

- |   |                                   |   |                               |
|---|-----------------------------------|---|-------------------------------|
|  | Ubiquitin activating Enzyme (E1)  |  | Ubiquitin moiety              |
|  | Ubiquitin conjugating Enzyme (E2) |   | 26S Proteasome                |
|  | Ubiquitin ligase (E3)             |   | Deubiquitinating Enzyme (DUB) |
|  | Target protein                    |  | Degradation products          |

Although ubiquitin was first identified in the context of proteolysis (Hershko and Ciechanover, 1998), it has become increasingly clear that the addition of single Ub moieties (mono-ubiquitination) (Hicke, 2001b) or alternative Ub chain linkage configurations can impart diverse consequences on substrates (Fushman and Pickart, 2004). Other than the archetypal K48 linkage, non-proteolytic signaling by K63 linked poly-Ub chains has been shown to mediate DNA repair, trafficking and kinase activation (Fushman and Pickart, 2004). Whilst ubiquitin chains linked through K29 have been shown to function in lysosomal targeting and protein degradation (Chastagner et al., 2006).

### **E1 Ubiquitin activating enzyme**

E1 enzymes initiate the Ub conjugation cascade but have a negligible effect on its regulation. The enzyme is a single polypeptide of ~1100 residues that contains a positionally conserved cysteine to bind activated Ub and a nucleotide binding motif that interacts with either ATP or AMP-Ub intermediates (Hatfield et al., 1997). There are two E1 isoforms in *Arabidopsis*, one of which may be nuclear localised (Hatfield et al., 1997).

### **E2 Ubiquitin conjugating enzyme**

The E2 enzymes contain a diagnostic 150 residue catalytic core that surrounds the active site cysteine. Using this conserved region, 37 E2 isoforms (UBCs) have been identified in the *Arabidopsis* genome (Vierstra, 1996). Outwith the core E2 domain, many detected isoforms contain various N and C-terminal extensions that are proposed to influence target recognition and localisation (Hamilton et al., 2001). The elaboration of E2s is presumed to ensure equality in the distribution of activated Ub to the vast array of E3s. Individual E2 isoforms in yeast and animals have distinct functions including: cell cycle regulation, DNA repair and degradation of ER translocated proteins (Pickart, 2001). Sequence analysis has clustered *Arabidopsis* E2s into 12 distinct subfamilies (Vierstra, 1996) but the majority of subtypes currently await functional classification.

## E3 Ubiquitin ligases

There are currently five types of known E3 ubiquitin ligase: VBC-Cul2, HECT, RING/U-box, SCF and APC, the latter four of which have been identified in the *Arabidopsis* genome (Vierstra, 2004). The E3s all share a common requirement for a specific E2 interaction domain and a substrate recognition domain (Vierstra, 2004). In order to confer substrate selectivity for an extensive range of substrates, the E3s are the most diverse proteins in the ubiquitination cascade (Vierstra, 2004). A specialised case of substrate recognition relates to degradation by the 'N-end Rule' where the half-life of a protein is influenced by the identity of its N-terminal residue (Varshavsky, 1996). N-terminal residues cluster by their capacity to reduce protein half-life and are termed N-degrons (Varshavsky, 1996). Specific ubiquitin ligases have been linked to the N-end rule, the best characterised of which in *Arabidopsis* is PRT1 (Potuschak et al., 1998). The *Arabidopsis* genome contains over 1300 genes that encode putative E3 subunits equating to approximately 5% of the proteome .

E3 ubiquitin ligase subclasses can be broadly defined by subunit composition and mechanism of action. HECT E3s are monomeric enzymes with a diagnostic 350 residue region termed the HECT (Homology to E6AP C-Terminus) domain first detected in the founding member, human E6AP (Huibregtse et al., 1995). HECT E3s are unique as they form an thiol-ester intermediate E3-Ub on a conserved cysteine during Ub transfer. The N-terminal region of the HECT domain forms a stable binding pocket for the E2-Ub intermediate and the C-terminal region contains the active site cysteine (Huibregtse et al., 1995). A variety of protein-protein interaction domains upstream of the HECT domain are thought to participate in substrate recognition and localisation (Vierstra, 2004). Genome analysis has identified 7 HECT E3s in *Arabidopsis*, 5 in yeast and over 50 in humans (Downes et al., 2003).

The remaining E3s interact with E2-Ub intermediates using variants of a zinc-finger structure termed the RING (Really Interesting New Gene) domain (Kosarev et al., 2002). The RING finger motif consists of four ligand pairs (either histidine or cysteine) which coordinate two zinc ions in

a spatially conserved arrangement (Freemont, 2000). The RING finger assumes a cross braced structure formed by the octet of zinc binding histidines and cysteines in either a  $C_3H_2C_3$  (RING-H2) or  $C_3H_1C_4$  (RING-HC) configuration. RING finger proteins have been implicated in a broad range of cellular processes with an expanding subset of these being assigned ubiquitin ligase activity (Kosarev et al., 2002).

RING/U-box E3s are single subunit ubiquitin ligases that interact with E2-Ub via the RING finger domain (RING E3s) or a structurally analogous motif, the U-box (U-box E3s). The U-box motif lacks the specific zinc coordinating residues of the RING finger and has been shown to instead stabilise a RING finger type structure through conserved electrostatic interactions (Ohi et al., 2003). Numerous RING/U-box proteins have been detected in the *Arabidopsis* proteome with around 500 RING and 130 U-box proteins currently identified (Mudgil et al., 2004). Genetic analysis of several indicate their diverse roles in plant physiology, including photomorphogenesis (Osterlund et al., 2000), self incompatibility (Stone et al., 2003) and the removal of misfolded peptides (Yan et al., 2003).

SCF E3s are heterotetrameric ubiquitin ligases with subunits named after those of the founding member: SKP1, CUL1/Cullin and an F-box protein (Deshaies, 1999). A fourth subunit, RBX was subsequently discovered and found to contain a RING H2-type domain. The architecture of the SCF complex divides E2-Ub interaction, substrate recognition and complex assembly between its different subunits. The RBX subunit interacts with E2-Ub via its RING domain and as part of the Cullin-RBX-SKP1 subcomplex confers Ub transferase activity (Deshaies, 1999). Substrate specificity is provided by the F-box subunit which is anchored to SKP1 via an N-terminal F-box motif and targets proteins through C-terminal protein-protein interactions motifs (Gagne et al., 2002).

F-box proteins constitute the largest single protein family in *Arabidopsis* containing almost 700 members (Gagne et al., 2002) with wide target specificity conferred by various C-terminal substrate recognition domains including: leucine-rich repeats, Arm repeats, and tetratricopeptide repeats (Gagne et al., 2002). In many cases, substrate phosphorylation is known to

be a prerequisite for recognition by F-box proteins, potentially implicating many plant kinases in the regulation of proteolysis (Deshaies, 1999). Plant SCF components show a greater degree of divergence than their mammalian counterparts (Vierstra, 2003), in *Arabidopsis* the diversity of F-box proteins coupled with 2 RBX1 subunits, five Cullins (CUL1, 2, 3a, 3b and 4) and 21 possible SKPs (termed ASKs in *Arabidopsis*) could potentially assort in over 100,000 distinct SCF complexes (Vierstra, 2004). SCF E3s are implicated in numerous plant signaling pathways including responses to the plant hormones, cell cycle progression and photomorphogenesis (Schwechheimer and Villalobos, 2004).

The APC (Anaphase Promoting Complex) is the most elaborate known E3 ligase, consisting of 11 subunits (APC1-11). The APC was first identified in a yeast screen for mutants unable to degrade the mitotic cyclin Clb2 (Wasch and Cross, 2002). Subsequently, the role of APC in degrading other crucial cell cycle regulators was discovered (Capron et al., 2003) and the name cyclosome was assigned to the complex. *Arabidopsis* orthologs have been detected for most APC subunits (Capron et al., 2003) which are predominantly present in single copy suggesting a limited number of APC isoforms are assembled. APC subunits APC2 and APC11 are related to SCF subunits CUL1 and RBX1 respectively (Capron et al., 2003). These subunits are presumed to have analogous structural (CUL1) and E2-Ub transferase (RBX1) roles in APC complex. The function of the remaining subunits is largely unknown although two proteins, CDC20 and CDH1, that are crucial for substrate recognition have been identified (Vodermaier, 2001).

#### **1.3.4 The 26S proteasome**

The 26S proteasome is a 2 MDa ATP dependent proteolysis complex which degrades ubiquitin tagged substrates. Whilst initial characterisation of the complex was derived from studies of yeast and mammalian proteasomes, subsequent studies in rice and *Arabidopsis* indicate a similar design (Hu et al., 1998). The 26S proteasome is comprised of 31 subunits divided into two subcomplexes, the 20S core protease (CP) and 19S regulatory particle (RP) (Hu et al., 1998). The CP functions as a non-specific ATP and Ub-independent protease which assumes a cylindrical structure by the

assembly of four heptameric rings (Wolf and Hilt, 2004). The peripheral rings are composed of seven related  $\alpha$  subunits and the central rings are composed of seven related  $\beta$  subunits in a  $\alpha_{1-7} \beta_{1-7} \beta_{1-7} \alpha_{1-7}$  configuration (Wolf and Hilt, 2004). Initial crystallography studies of the CP in yeast reported a large central chamber into which face protease active sites contributed by the  $\beta_1$   $\beta_2$  and  $\beta_5$  subunits (Wolf and Hilt, 2004).

These three proteases generate peptidylglutamyl, trypsin-like and chymotrypsin-like activities, imparting the capacity to cleave most peptide bonds (Wolf and Hilt, 2004). Entry into the CP chamber is restricted by a pore formed at the periphery by the seven  $\alpha$ -subunits (Hartmann-Petersen et al., 2003). The narrow pore requires entering proteins to be unfolded and flexible extensions in each  $\alpha$ -subunit provide a channel gating function to control substrate entry (Hartmann-Petersen et al., 2003). CP entry channel gating and the requisite unfolding of substrates provides a demarcation between protease activity and the cellular milieu, meaning that degradation of proteins is limited to those unfolded and imported into the proteasome (Hartmann-Petersen et al., 2003).

The RP associates with either end of the CP and confers ATP dependence and poly-Ub recognition to the proteasome (Hartmann-Petersen and Gordon, 2004). The RP is composed of seventeen subunits which form two subcomplexes termed Lid and Base (Fu et al., 2001). The Base sits directly over the CP  $\alpha$ -ring channel and comprises a ring of six related AAA-ATPases (RPT1-6) and three non-ATPase subunits (RPN1, 2 and 10). The Lid interacts with the Base via RPN10 and contains the remaining non-ATPase subunits (RPN 3, 5-9 and 11-12) (Fu et al., 2001). The overall structure function relationships between RP subunits remain to be clarified, but key functions have been ascribed to individual subunits (Hartmann-Petersen and Gordon, 2004).

Cooperatively the RP Base and Lid mediate recognition of K48 linked poly-Ub chains, removal of covalently bound Ub moieties, unfolding of targeted substrates, pore gating and substrate import to the proteasome (Hartmann-Petersen and Gordon, 2004). K48 poly-Ub recognition by RPN10

has been observed but is non-essential in yeast and *Arabidopsis* suggesting is not the sole poly-Ub binding determinant (Hartmann-Petersen and Gordon, 2004). RPN11 is a zinc metalloprotease with deubiquitinating activity that disassembles/recycles Ub chains during target degradation (Verma et al., 2002b). ATPase subunits in the Base (RPT1-6) contact the CP pore gating  $\alpha$ -subunits and are presumed to facilitate substrate unfolding and pore opening (Vierstra, 2004).

Two evolutionary relatives of the lid complex in the proteasome RP have been identified in plants and animals. These complexes (COP9 and eIF3) contain eight subunits synonymous to those in the proteasome lid. COP9, termed the signalosome (CSN) assists in numerous eukaryotic signaling pathways (Wei et al., 1998) whereas eIF3 is involved in translational control (Dunand-Sauthier et al., 2002). Experimental evidence indicates that both COP9 and eIF3 can associate with the proteasome CP to create functionally distinct particles (Dunand-Sauthier et al., 2002).

### **1.3.5 Deubiquitinating enzymes**

The ligation of ubiquitin to substrates is a reversible process and all known peptide linkages made from ubiquitin moieties are efficiently cleaved by deubiquitinating enzymes (DUBs) (Amerik and Hochstrasser, 2004). Following the identification of various classes of DUBs it is thought that ubiquitin removal is a dynamic process with proposed constitutive and regulated DUB activates in the cell (Amerik and Hochstrasser, 2004). DUB enzymes perform several important functions in the ubiquitin - 26S proteasome pathway (Figure 1.4) (Amerik and Hochstrasser, 2004).

To ensure normal rates of targeted proteolysis DUB enzymes maintain a sufficient pool free of ubiquitin in the cell. To achieve this, DUBs function to process precursor ubiquitin fusions from translation products and release poly-Ub chains bound to proteasome RP (Amerik and Hochstrasser, 2004). In processing ubiquitin fusion proteins and ubiquitin tagged targets, DUB activities that cleave either peptide or isopeptide bonds (or both) have been reported (Amerik and Hochstrasser, 2004). Following activation, ubiquitin is susceptible to attack by abundant intracellular

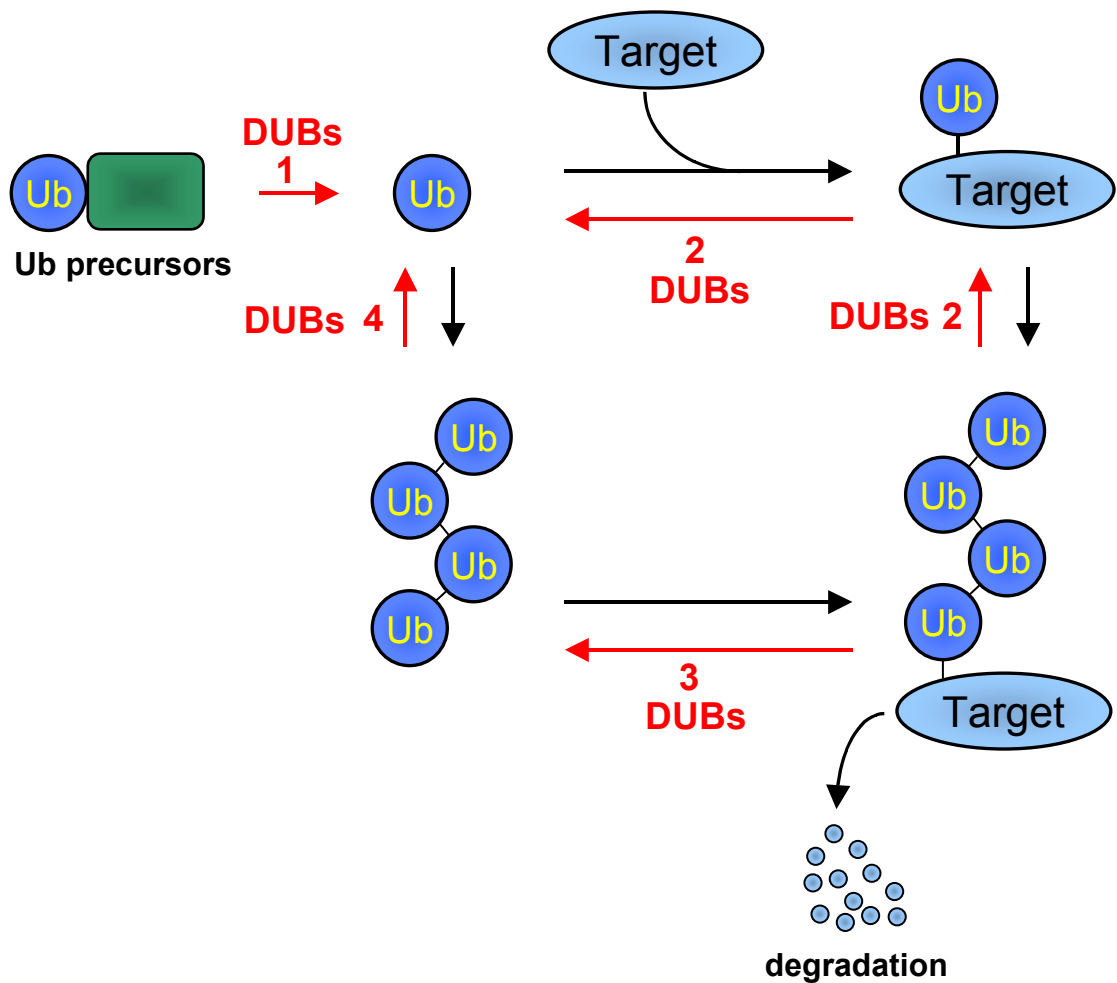


**Figure 1.4** Functions of Deubiquitinating enzymes (DUBs) in ubiquitin metabolism.

**(1)** Processing of ubiquitin precursors. **(2)** Editing or rescue of ubiquitin conjugates, which are generally linked to other proteins in the cell but may also be ligated to abundant small nucleophiles such as glutathione. **(3)** Recycling of ubiquitin or poly-Ub chains from ubiquitin-protein conjugates targeted for degradation. **(4)** Disassembly of unanchored poly-Ub chains. Adapted from (Amerik and Hochstrasser, 2004).

nucleophiles such as glutathione and polyamine. To prevent loss of activated ubiquitin through such pathways DUBs function to prevent titration by these compounds (Amerik and Hochstrasser, 2004).

Beyond roles in basic ubiquitin metabolism, DUBs also serve to negatively regulate protein degradation. The commitment of substrates to proteasomal degradation by ubiquitination can be reversed by DUBs, altering the half-life of specific targets in response to signaling events (Amerik and Hochstrasser, 2004). More generally, DUB enzymes have been proposed to function as a final proof reading mechanism for degradation, rescuing proteins that are inappropriately targeted to the proteasome (Lam et al., 1997). The distinct metabolic and substrate specific roles performed by different DUBs remains to be clarified and the known DUB target repertoire is a focus of current research.

### **DUB enzyme families**

The DUBs are broadly classified into five subfamilies on the basis of sequence homology and catalytic mechanism. Four of the families represent specialised cysteine proteases adopting a classic 'papain type' fold (Makarova et al., 2000), whilst the final subfamily represents a novel zinc metalloprotease specific for protein linked ubiquitin. The cysteine protease DUBs consist of two well established subgroups: UCH (ubiquitin carboxy hydrolase) and UBP (ubiquitin specific protease) and two more recently identified subgroups: OTU (ovarian tumour) related proteases and Ataxin-3 (Amerik and Hochstrasser, 2004).

For the UCH family, crystal structures have been determined for two family members (human UCH-L3 and yeast Yuh1) allowing the diagnosis of catalytic residues and structurally conserved motifs (Amerik and Hochstrasser, 2004). From such analysis, it is known that UCH enzymes contain four conserved motifs usually spanning around 200 amino acids. Two of these motifs contain catalytic cysteine and histidine/aspartate residues respectively termed His and Cys boxes (Amerik and Hochstrasser, 2004). In the case of the UBP family, equivalent catalytic residues to UCH enzymes are seen in different configuration within a 400 residue catalytic

'core region' (Hu et al., 2002a). UBPs bear key histidine and cysteine boxes and four less stringently conserved regions (Q, G, L and F motifs), one of which includes the remaining catalytic aspartic acid residue (Hu et al., 2002a). From structure determination of human UBP proteins, clear fold and active site homology with papain and UCH enzymes is apparent (despite limited sequence identity) (Hu et al., 2002a). The UBP enzymes are greater in size and sequence diversity than the UCHs with 27 versus 3 known examples in *Arabidopsis* (Yan et al., 2000b). Steric restrictions within the active site of most UCHs are proposed to limit their substrates to unfolded peptides or small adducts to the C-terminus of ubiquitin (Amerik and Hochstrasser, 2004).

Recently identified from a bioinformatics analysis, the ovarian tumour related (OTU) proteases have emerged as an additional class of DUB enzyme (Makarova et al., 2000). Following the structure determination of a human OTU, Otubain2, limited structural homology to other cysteine protease DUBs was observed in the catalytic core of the enzyme (Nanao et al., 2004). Five OTU type proteins have been detected in the human genome, of which three have experimentally confirmed DUB activity against poly-Ub chains (Balakirev et al., 2003).

Ataxin-3 currently represents a single member DUB family in mammals, plants and yeast (Scheel et al., 2003). Originally identified as a causative factor in the human polyglutamine expansion disease spinocerebellar ataxia type 3, Ataxin-3 exhibits typical DUB enzyme properties and is characterised by a region termed the Josephin domain (Burnett et al., 2003). Over thirty examples of Josephin domain proteins are known in mammals many of which contain regions of weak similarity to the Cys and His boxes of UCH and UBP enzymes (Amerik and Hochstrasser, 2004).

The JAMM proteases represent a recently identified class of novel zinc metalloprotease DUBs (Amerik and Hochstrasser, 2004). Classified within the established JAB1/MPN/Mov34 domain a putative metal ion binding site motif: EX<sub>n</sub>HS/THX<sub>7</sub>SXXD, termed the JAMM domain is now recognised as the determinant of isopeptidase activity (Ambroggio et al., 2004a). JAMM domain subunits have been identified as key components of the

proteasome regulatory particle (RPN11) (Verma et al., 2002b), COP9 signalosome (CSN5) (Cope et al., 2002), eIF3 translation initiation complex (Glickman et al., 1998) and STAM endocytotic regulatory complex (McCullough et al., 2004b). In the above cases JAMM domain proteins have been proven to facilitate hydrolysis of ubiquitin or Ubiquitin-like moieties (e.g. RUB-1) with RPN11 proving to be essential for viability in yeast (Verma et al., 2002b).

#### **1.4 Ubiquitination in plant defence signalling**

The ubiquitin - 26S proteasome system has been broadly implicated in plant cell signaling pathways linked to hormone signaling, growth and development (Vierstra, 2003). In accordance with these findings, current research also indicates the regulatory involvement of ubiquitination at multiple levels of plant defence signaling (Dreher and Callis, 2007).

##### **1.4.1 Involvement of E3 ubiquitin ligases in plant defence**

Regulation of defence gene expression by signaling hormones ethylene (ET) and jasmonate (JA) has been linked to ubiquitination. The EIN3 (ETHYLENE INSENSITIVE 3) transcription factor family are key components of ethylene signaling and have been reported to control transcription of numerous defence related genes including oxidative burst regulators and a subset of *PR* genes (Dreher and Callis, 2007). The stability of EIN3 type transcription factors is regulated by ubiquitin SCF E3 ligase complexes containing the F-box subunits EBF1 or EBF2 (EIN3 binding F-box) (Delauré et al., 2008). JA signaling has also been linked to ubiquitination through the identification of the *coi1* mutant in *Arabidopsis*. COI1 is an SCF F-box subunit which is implicated in most JA mediated signaling responses including defence against herbivores and biotrophic pathogens (Turner et al., 2002).

Positive and negative regulators of plant defence signaling pathways have been identified in multiple E3 ubiquitin ligase classes resulting from elicitor/avirulence induction studies and genetic screens for pathogenesis-related phenotypes (Dreher and Callis, 2007).

Reported F-box defense regulators include SON1 (SUPPRESSOR OF NIM1-1). The *Arabidopsis son1* mutant was identified in the *npr1/nim1* background as negative defence regulator which is implicated in SAR independent resistance against virulent *Peronospora parasitica* and *Pseudomonas syringae* strains (Kim and Delaney, 2002). Tobacco transcript profiling experiments during ETI elicited by the *Cladisporium fulvum* effector Avr9 led to the identification of numerous upregulated ACRE (Avr9/Cf9 Rapidly Elicited) genes several of which encode ubiquitin E3 ligases (Durrant et al., 2000). One such gene is *ACIF1* (Avr9/Cf-9-INDUCED F-BOX 1) which encodes an F-box protein that has been implicated as a positive regulator of HR and resistance mediated by the *R* genes *Cf-9*, *Pto* and *N* against their associated fungal, bacterial and viral pathogens (van den Burg et al., 2008).

Despite the large number of RING domain E3 ligases identified in plants, few have been implicated in defence signaling to date. The RING domain E3 ubiquitin ligase ACRE132 was identified in the ACRE screen reported by Durrant *et al.* (Durrant et al., 2000). *ACRE132* is the proposed tobacco ortholog of the *Arabidopsis ATL2* gene, which is transcriptionally induced by fungal chitins during basal resistance suggesting a possible conservation in function for these proteins in plant fungal response pathways (Delauré et al., 2008).

Several studies have indicated a prominent role for U-box E3 ubiquitin ligases during plant defence both in PTI and ETI. Trujillo *et al.* recently reported the cumulative involvement of *Arabidopsis* U-box proteins PUB22, PUB23 and PUB24 (PLANT U-BOX 22-24) as negative regulators of basal resistance (Trujillo et al., 2008). In this study single, double and triple *ubp22 ubp23 ubp24* mutants exhibited progressive loss of suppression in the flg22 induced ROI burst, MPK3 MAPK kinase activation and downstream PTI marker gene expression (Trujillo et al., 2008).

U-box E3 ubiquitin ligases were also identified in the previously discussed ACRE screen resulting in the implication of ACRE276/PUB17 and ACRE74/CMPG1 as positive regulators of ETI (Yang et al., 2006) (Gonzalez-Lamothe et al., 2006). Gene silencing approaches demonstrated that

tobacco ACRE276 is required for efficient HR development mediated by the R proteins Cf-9 and N and that the tomato ACRE276 ortholog is required for full resistance against *Cladisporium fulvum* (Yang et al., 2006). PUB17, the *Arabidopsis* ortholog of ACRE276, was also implicated in defense with *pub17* mutants demonstrating increased susceptibility against avirulent strains of *Pseudomonas syringae* (Yang et al., 2006). Similar experimental approaches have also demonstrated that the tobacco U-box protein CMPG1 mediates Cf-9 triggered HR and resistance (Gonzalez-Lamothe et al., 2006). Mutant screening programs in rice led to the identification of lesion mimic mutant *spl11* which negatively regulates basal resistance against rice pathogens *Magnaporthe grisea* and *Xanthomonas oryzae* (Yin et al., 2000). Subsequent studies led to the characterisation of SPL11 and demonstration of its *in vitro* activity as a functional U-box E3 ubiquitin ligase (Zeng et al., 2004).

#### **1.4.2 RAR1/SGT1 mediated R gene resistance**

The finding that several defense associated E3 ubiquitin ligases regulate disease resistance against distinct pathogen species supports the idea that multiple pathogen perception systems converge on common ubiquitination based signaling pathways (Devoto et al., 2003). The identification of *RAR1* and *SGT1* has defined one such convergence point between ubiquitination and resistance mediated by multiple R genes in monocot and dicot plant species (Muskett and Parker, 2003). *RAR1* encodes a predicted cytosolic protein of unknown function which contains two similar cysteine and histidine-rich (CHORD) Zn<sup>2+</sup> binding domains (Shirasu et al., 1999). *RAR1* is conserved in all eukaryotes except yeast and was initially implicated in disease resistance against powdery mildew in barley mediated by the R genes *Mla6* and *Mla12* (Shirasu et al., 1999). Plant *RAR1* proteins were found to interact through their C-terminal CS motif with *SGT1* (SUPPRESSOR OF THE G2 ALLELE OF *SKP1*) which has multiple functions in yeast by association with several distinct protein complexes (Schadick et al., 2002).

One function of *SGT1* in yeast is to regulate SCF ubiquitin E3 ligase complexes with which it associates through the *SKP1* subunit (Kitagawa et al., 1999). Similar interactions have been reported in *Arabidopsis*, barley

and *N. benthamiana* (Azevedo et al., 2002). Association of SGT1 with the SCF complex in plants is supported by the finding that F-box mediated Auxin and JA dependent signaling is disrupted in *Arabidopsis sgt1b* mutants suggesting that SGT1b is a key component of multiple SCF-regulated pathways (Gray et al., 2003). Mutant analyses in *Arabidopsis* and silencing experiments in barley and *N. benthamiana* have demonstrated that SGT1 is required for responses that are mediated by diverse R gene structural types to induce resistance against a variety of pathogens (Azevedo et al., 2002) (Liu et al., 2002b) (Peart et al., 2002b).

Additional evidence which supports the role of ubiquitin mediated degradation in defence signaling has come from silencing genes encoding SKP1 and subunits of the COP9 signalosome (CSN) in *N. benthamiana*, resulting in the loss of N mediated TMV resistance (Liu et al., 2002b). As discussed previously, the CSN is an evolutionarily conserved multiprotein complex which is closely related to the lid subcomplex of the 26S proteasome, interacts with RAR1 and SGT1 and regulates ubiquitination by SCF E3 ubiquitin ligases (Muskett and Parker, 2003).

SGT1 has also been shown to interact with HSP90 (HEAT SHOCK PROTEIN 90) which has been implicated in resistance mediated by several *R* genes (Takahashi et al., 2003). Current research suggests that SGT1 and RAR1 associate as cochaperones with HSP90 and are proposed to function in close proximity to R proteins, possibly to assist in the maintenance of conformation sensitive signaling states during R protein activation (Shirasu and Schulze-Lefert, 2003). Collectively, SGT1 and RAR1 are thought to function in disease resistance through participation in multiple protein complexes where they are proposed to influence the conformation of R gene complexes and regulate ubiquitination by several classes of E3 ligase (Shirasu and Schulze-Lefert, 2003).

### **1.4.3 Target of ubiquitination linked to plant defence**

Beyond the reported interactions of RAR1 and SGT1 discussed above, relatively few defence associated ubiquitination targets have been identified in plants. A potential link between ubiquitination and defence

has been established in the case of the *Arabidopsis* R protein RPM1 which is degraded coincident with the onset of the HR elicited by *Pseudomonas syringae* carrying the *avrRpm1*, *avrB*, *avrRps4* or *avrRpt2* avirulence genes (Boyes et al., 1998). RPM1 has been found to interact with the proteins RIN2 and RIN3 (RPM1-interacting proteins) which both demonstrate *in vitro* E3 ubiquitin ligase activity and collectively contribute to pathogen elicited RPM1-dependent ion leakage (Kawasaki et al., 2005). HR associated degradation of RPM1 is not altered in *rin2 rin3* double mutants suggesting that whilst RIN2 and RIN3 are linked to defence signaling, they may not directly control RPM1 stability (Kawasaki et al., 2005).

Manipulation of host ubiquitination signaling by several viral and bacterial plant pathogens which mimic host proteins to suppress defense and promote their own survival have been reported (Dreher and Callis, 2007). The *Pseudomonas syringae* pv. *tomato* (*Pst*) effector protein *avrPtoB* represents one such example which functions to suppress immunity by inhibiting the plant HR.

The *Pst* effectors *avrPto* and *avrPtoB* are delivered into the plant cell through the type III secretion system and are both recognised by the tomato resistance protein Pto to initiate HR and resistance (Pedley and Martin, 2003). In *N. benthamiana*, *avrPtoB* has been shown to be a SUPPRESSOR of HR induced by *avrPto*/Pto recognition as well as HR induced by fungal elicitors and other bacterial effectors (Abramovitch et al., 2003). *AvrPtoB* is a modular protein for which deletion and structural analysis has established that the C-terminal domain triggers HR whilst the N-terminal domain controls hypersensitive cell death suppression and possesses the structural features of a U-box E3 ubiquitin ligase (Janjusevic et al., 2006). The *avrPtoB* C-terminal domain exhibits *in vitro* E3 ubiquitin ligase activity and structural or catalytic mutations within this domain result in reduced HR suppression and virulence of *Pseudomonas syringae* *in vivo* (Janjusevic et al., 2006).

*AvrPtoB* uses its E3 ligase activity to ubiquitinate and degrade the host R protein Fen, a Ser/Thr kinase that is able to physically interact with the N-terminal region of *AvrPtoB* that is lacking its C-terminal domain (Rosebrock

et al., 2007). The proposed relationship between avrPtoB, Fen and Pto illustrates the evolving relationship between plant effectors and R proteins and how host ubiquitination can be exploited to benefit pathogen virulence (Rosebrock et al., 2007). Firstly, the pathogen encoded avrPtoB (N-terminal domain only) evolved to suppress plant basal defences. Next, the plant Fen kinase evolved to bind avrPtoB (N-terminal domain only), leading to activation of R gene mediated resistance. Subsequently, the pathogen responded by incorporating an E3 ubiquitin ligase domain into avrPtoB (forming full length avrPtoB) that targets the Fen kinase for degradation. Finally, the plant kinase Pto, which is not susceptible to avrPtoB mediated ubiquitination, evolved to bind avrPtoB, thus restoring host immunity through R gene mediated resistance (Rosebrock et al., 2007).

Opportunistic acquisition of host genetic material by pathogens such as *Agrobacterium tumefaciens* represents an alternative virulence strategy to the U-box structural mimicry demonstrated by avrPtoB which was generated through convergent evolution.

*Agrobacterium tumefaciens* uses a type IV secretion system to translocate effectors and single-stranded DNA (T-DNA) into eukaryotic cells, resulting in genetic colonization of the host (Tzfira et al., 2004). During infection, *Agrobacterium tumefaciens* translocates the F-box protein VirF into host cells and utilizes host components to form a functional SCF complex required for degradation of VirE2 and host VIP1 (Schrammeijer et al., 2001). VirE2 and VIP1 proteins must be eliminated to allow integration of the *Agrobacterium* T-DNA into the host genome (Tzfira et al., 2004). VirF was the first prokaryotic protein reported to contain a conserved F-box domain (Schrammeijer et al., 2001) and demonstrates the utilisation of host functional domains obtained by lateral gene transfer to improve pathogen virulence.

## 1.5 Study objectives

Many previous studies have implicated ubiquitination in diverse plant signalling pathways, establishing its role as a fundamental regulatory mechanism. Knowledge of plant deubiquitinating enzymes and their function is comparatively limited with prior studies limited primarily to the UBP subclass as described by Yan *et al.* (Yan *et al.*, 2000b). This study aims to identify the full complement of *Arabidopsis* deubiquitinating enzymes based on current knowledge of other eukaryotic DUBs and establish novel data on their function using established reverse genetic approaches.

As there is accumulating evidence which implicates ubiquitination at various levels of plant defence and disease resistance signalling, the primary aim of this study is to establish the potential involvement of deubiquitinating enzymes in plant defence. Model plant-pathogen systems in *Arabidopsis*, tobacco and *N. benthamiana* will be utilised to examine the role of candidate DUB genes in defence signalling during gain and loss of function assays.

## Chapter 2 – Materials and Methods

### 2.1 Materials

#### 2.1.1 Enzymes and Reagents

All chemicals were provided by Sigma-Aldrich Ltd (Poole, UK), Fisher Scientific UK (Southampton, UK) or VWR International Ltd. (Poole, UK) unless otherwise stated. Agarose MP (cat# 11388983001), Restriction endonucleases, 2<sup>nd</sup> generation RACE kit (cat# 03353621001), Expand HiFidelity polymerase (cat# 04738250001 ) and Complete® protease inhibitor cocktail Tablets (EDTA-free, cat# 11836170001) were supplied by Roche. Phusion™ High-Fidelity polymerase (cat# F530S) Thermopol Taq polymerase (cat# M0267S), PCR marker (cat# N343S) and Protein molecular weight markers (cat# P7708S) were provided by New England Biolabs Ltd. (Hitchin UK). Ponceau S powder (cat# P3504), Coomassie Brilliant Blue stain (cat# B8647), His-Select affinity purification columns (cat# H7787), GenElute plant genomic DNA miniprep kit (cat# NA1111), Triton X-100 (cat# T8787), Tween20 (cat# P5927), Murashige and Skoog Basal Medium (cat# M5519) and Rifampicin (cat# R3501) were provided by Sigma-Aldrich. QIAprep plasmid miniprep kit (cat# 27104) and QIAquick gel extraction kit (cat# 28704) were provided by Qiagen Ltd. (Crawley, UK). 29:1 acrylamide:bis-acrylamide solution (cat# 161-0156) and Polyvinylidene fluoride PVDF membrane (cat# 162-0177) were provided by BioRad Laboratories. Chemiluminescent HRP substrate (cat# WBKLS0500) was provided by Millipore Ltd. SuperscriptII reverse transcriptase (cat# 18064022), TRIzol RNA extraction (cat# 15596026), RnaseOut inhibitor (cat# 10777019), Insect cell media (cat# 10902088), LR Clonase (cat# 11791100) and PENTR D-TOPO kit (cat# K240020) were provided by Invitrogen Ltd. (Paisley, UK). T4 DNA ligase (cat# M1801), dNTPs (cat# U1330), AMV reverse transcriptase (cat# M510A) and RNasin Ribonuclease Inhibitor (cat# N2111) were provided by Promega (Southampton, UK). DNA-free DNase (cat# 1906) and Nuclease-free H<sub>2</sub>O (cat# 9930) were provided by Ambion. Brilliant SYBR Green QPCR Master Mix (cat# 600548) was provided by Stratagene Ltd. Proteose Peptone salts (cat# LP0085) was

provided by Oxoid Ltd. BD BaculoGold™ baculovirus transfection kit (cat# 554740) was supplied by BD Biosciences (CA, USA). Cell culture flasks (cat# 43072) provided by Corning (NY, USA). His-Bind affinity purification resin (cat# 69670), Alkali-soluble Casein (cat# 70955) and BugBuster cell lysis reagent (cat# 70584) were provided by Novagen (Nottingham, UK). Isopeptidase T (cat# UW8560), Ubiquitin chains (cat# UW8860) and Diubiquitin (cat# UW9800) were supplied by Affiniti Research (Exeter, UK).

### 2.1.2 Antibiotics

Antibiotic	Solvent	Stock Concentration	Working Concentration
Kanamycin	H <sub>2</sub> O	50 mg/ml	50 µg/ml
Rifampicin	Methanol	10 mg/ml	100 µg/ml
Carbenicillin	H <sub>2</sub> O	100 mg/ml	100 µg/ml
Hygromycin B	PBS	50 mg/ml	50 µg/ml
Chloramphenicol	H <sub>2</sub> O	100 mg/ml	100 µg/ml
Tetracycline	Ethanol	5 mg/ml	5 µg/ml
Spectinomycin	H <sub>2</sub> O	100 mg/ml	100 µg/ml

**Table 2.1** Antibiotics used for plasmid and bacterial selection.

### 2.1.3 Bacterial Strains

*E. coli* strains DH5α and BL21(DE3) Star (Invitrogen) were transformed with various plasmid constructs for sub-cloning, expression and amplification. *Agrobacterium* strains GV3101 and LBA440 were used for plant transformation and transient expression. *Pseudomonas syringae* pv. *tomato* DC3000, DC3000 *avrB* and DC3000 *avrRpt2* were used to infect *Arabidopsis*. *Pseudomonas syringae* pv. *tabaci* and *Pseudomonas syringae* pv. *tabaci avrPto* were used for *Nicotiana benthamiana* infections.

## 2.1.4 Antibodies.

Antibody	Dilution	Source	Incubation	Supplier
Anti-Ubiquitin	1:10000	Mouse	60 min	Covance P4D1
Anti-Histidine	1:4000	Rabbit	90 min	Santa Cruz sc-803
Anti-Mouse HRP	1:20000	Goat	60 min	Sigma A5278
Anti-Rabbit HRP	1:10000	Goat	60 min	Sigma A6154
Anti-GFP	1:4000	Rabbit	90 min	AbCam ab6556

**Table 2.2** Antibodies used for Western blots in this study.

## 2.1.5 Plasmid Vectors

Plasmid Vector	Description	Source
pGEM-T Easy	Sequencing & Sub-cloning	Promega
pENTR D-TOPO	Gateway entry cloning	Invitrogen
pENTR4	Gateway entry cloning	Invitrogen
pHellsgate12	Gateway RNAi	Dr P. Waterhouse
pTV00	VIGS RNA2	Prof D. Baulcombe
pBINTRA6	VIGS RNA1	Prof D. Baulcombe
pSA-rep	VIGS helper plasmid	Prof D. Baulcombe
pCf9	<i>Cf-9 R</i> gene	Prof J. D. Jones
pAvr9	<i>Avr9</i> avirulence gene	Prof J. D. Jones
pDEST17	Gateway Histidine tag	Invitrogen
pACHLT	Baculovirus transfer	BD Biosciences
pGWB6	Gateway GFP tag	Prof T. Kimura
pCR BLUNT II TOPO	Sub-cloning	Invitrogen
p19	Gene silencing SUPPRESSOR	Prof P. Birch

**Table 2.3** Plasmid DNA vectors used in this study.

## 2.2 General Laboratory Procedures

### 2.2.1 pH Measurement

The pH of solutions and media were measured using a Metler Toledo MP220 pH meter and glass electrode.

## **2.2.2 Autoclaving**

Solutions and equipment were sterilised in a benchtop (Prestige Medical, Model 220140) or free-standing (Laboratory Thermal Equipment Autoclave 225E) autoclaves.

## **2.2.3 Filter sterilisation**

Solutions that were heat sensitive or of small volume were sterilised by filtration using a Sartorius Minisart disc filters (0.2  $\mu\text{M}$ ).

## **2.3 Plant materials**

### **2.3.1 *Arabidopsis* seed stocks**

Wild-type *Arabidopsis thaliana* ecotype Columbia-0 (Col-0) seeds were obtained from The National Arabidopsis Stock Centre (NASC, Nottingham, UK). T-DNA insertional mutant lines in the Col-0 genetic background were obtained from NASC (Nottingham, UK) and GABI-Kat (Cologne, Germany).

### **2.3.2 Growth of *Arabidopsis* plants on soil**

*Arabidopsis* seeds were vernalised in water and dark conditions at 4°C for 3 days prior to sowing. Seeds were sown onto pots or trays containing compost soaked in a 0.15 g/l solution of the insecticide Intercept (Scotts UK). Plants were grown in growth chambers at 22°C and were kept under clingfilm for 1 week after germination. Plants were grown under white light (80  $\mu\text{mol}/\text{m}^2/\text{s}$ ) on either a long day photoperiod (16 hours light/8 hours dark) or short day photoperiod (8 hours light/16 hours dark) at 60% relative humidity.

### **2.3.3 Surface sterilisation of *Arabidopsis* seeds**

*Arabidopsis* seeds were surface sterilised using an ethanol solution (70% (v/v) ethanol, 0.05% (v/v) Triton X-100). Seed was shaken for 5 minutes in this solution, then washed twice for 3 minutes in 100% ethanol. Seed was resuspended in 100% ethanol and pipetted onto sterile filter paper. After

sufficient drying time, seeds were deposited onto agar plates by gentle tapping.

#### **2.3.4 Growth of *Arabidopsis* plants on agar plates**

For segregation studies of transgenic or genetically crossed *Arabidopsis* plants, surface sterilised seeds were sown on 0.8% agar plates containing 7.5 g/l sucrose and 2.2 g/l Murashige and Skoog salts with appropriate antibiotics. Seeds were vernalised on the plates for 3 days at 4°C and grown under long day conditions.

#### **2.3.5 Cross-Pollination of *Arabidopsis***

For genetic crosses, parent lines of *Arabidopsis* were grown under long day conditions for 3 - 4 weeks until the initiation of flowering. Fine forceps were used to emasculate female parent plants and open or budding flowers not selected for crossing were removed. Unopened buds selected for crossing were dissected using fine forceps and a stereo microscope where all organs were removed except the pistil. Female parents were fertilised with pollen from an open male flower and returned to long day growth conditions. F<sub>1</sub> seed from successful crosses was harvested after elongated siliques had begun to brown.

#### **2.3.6 *Nicotiana tabacum* and *Nicotiana benthamiana* seed stocks**

Transgenic *N. tabacum* seeds carrying either the *L. esculentum* resistance gene *Cf-9* or *C. fulvum* avirulence gene *Avr9* were provided by Prof J. D. Jones (Sainsbury Laboratory, Norwich). Transgenic *N. benthamiana* seeds carrying the *L. esculentum* resistance gene *Pto* were provided by Dr J. P. Rathjen (Sainsbury Laboratory, Norwich).

#### **2.3.7 Growth of *Nicotiana tabacum* and *Nicotiana benthamiana* on soil**

*N. tabacum* and *N. benthamiana* seeds (~50) were sown on a single pot of compost soaked with a 0.15 g/l solution of the insecticide Intercept (Scotts UK) and covered in clingfilm. Plants were grown at 24°C under long day

conditions ( $48 \mu\text{mol}/\text{m}^2/\text{s}$ ) at 60% relative humidity, and 1 week after germination seedlings were transferred to individual pots and covered with a humidifier. For transient gene expression assays, *N. tabacum* plants were grown for 5-6 weeks. For Virus Induced Gene Silencing (VIGS), *N. benthamiana* plants were grown for 3-4 weeks prior to *Agrobacterium* inoculation, then a further 3 weeks whilst gene silencing developed.

## **2.4 DNA and RNA methods**

### **2.4.1 Preparation of competent *E. coli* cells for heat-shock transformation.**

A 50  $\mu\text{l}$  aliquot of *E. coli* DH5 $\alpha$  cells were inoculated into 10 ml LB media and grown overnight at 37°C. Following overnight growth, 1 ml of culture was used to inoculate 250 ml of SOB media (20 g/L bacto-tryptone, 5 g/L yeast-extract, 8.5 mM NaCl, 2.5 mM KCl, 10 mM MgCl<sub>2</sub>, 10 mM MgSO<sub>4</sub>) which was grown at 18°C to an OD<sub>600</sub> of 0.6. Cell culture was cooled on ice for 15 minutes then pelleted by centrifugation at 2500 g for 10 minutes at 4°C. Pelleted cells were gently resuspended in 80 mls of ice cold TB buffer (10 mM HEPES pH 6.7, 15 mM CaCl<sub>2</sub>, 55 mM MnCl<sub>2</sub>, 250 mM KCl) and chilled on ice for 10 minutes. Cells were pelleted by centrifugation at 2500 g for 10 minutes at 4°C and gently resuspended in 20 mls of ice cold TB buffer. Filter sterilised DMSO was added to a final concentration of 7% and cells were incubated on ice for 10 minutes. Cells were aliquotted in 200  $\mu\text{l}$  volumes into pre-chilled eppendorfs on dry ice and stored at -80°C.

### **2.4.2 Transformation of *E. coli* competent cells**

Competent *E. coli* cells were placed on ice to thaw for ten minutes. Approximately 5  $\mu\text{l}$  of plasmid DNA or DNA ligation reaction was added to the competent cells which were then incubated on ice for 20 minutes. The cells and DNA were heat-shocked in a waterbath at 42°C for 35 seconds then immediately placed on ice. After a 2 minute incubation on ice, 700  $\mu\text{l}$  of LB media was added to the cells and DNA which were then incubated at 37°C for 1 hour with shaking at 200 rpm. Transformations were plated out

on LB agar plates with appropriate antibiotic and incubated overnight at 37°C until colonies developed.

### **2.4.3 Isolation of plasmid DNA**

Plasmid DNA purification from *E. coli* was performed using Qiagen Plasmid MiniPrep kits. Cells from a single bacterial colony were inoculated into a 10 ml overnight LB medium culture with appropriate antibiotics and grown at 37°C with shaking at 200 rpm. Bacterial culture (3 ml) was pelleted by centrifugation at 2500 g for 1 minute and supernatant was discarded. Cell lysis and DNA purification was carried out according to the manufacturer's instructions. The purified plasmid DNA was eluted with dH<sub>2</sub>O in a final volume of 50 µl. Plasmid DNA was stored at -20°C.

### **2.4.4 Agarose gel electrophoresis of DNA**

All DNA agarose gels contained 0.8 % - 1.0 % (w/v) agarose melted in TAE buffer (40 mM Tris-acetate, 1 mM EDTA). SYBR Safe (Invitrogen) was added to the agarose solution at 1:10,000 dilution for DNA labelling. DNA samples were mixed with 5 x loading buffer (0.25 % (w/v) bromophenol blue, 0.25 % (w/v) xylene cyanol FF, 30 % (w/v) glycerol) and separated by agarose gel electrophoresis in TAE buffer at 100 V.

### **2.4.5 DNA extraction and purification from agarose gel**

DNA bands were separated by electrophoresis in agarose gels and bands of the expected size were excised on a UV illuminator. DNA was extracted and purified using the Qiaquick Gel Extraction Kit in accordance with the manufacturer's instructions. Purified DNA was eluted in 50 µl dH<sub>2</sub>O.

### **2.4.6 DNA ligation**

DNA obtained from PCR amplification or restriction digest was ligated in a final volume of 10 µl. Aliquots of plasmid and insert DNA were examined on an agarose gel to establish their relative concentrations. Typically insert and vector fragments were mixed in a 5:1 ratio (500 ng: 100 ng) with

1 x ligation buffer (Promega), 1 unit of T4 DNA ligase (Promega) and sterile water to a final volume of 10  $\mu$ l. The ligation mix was incubated at 22 °C for 20 hours. Typically, 5  $\mu$ l of ligation reaction was used for transformation of *E. coli* cells.

#### **2.4.7 Restriction Endonuclease digest of plasmid DNA**

Plasmid DNA was digested with restriction enzymes either for analysis (20  $\mu$ l reaction) or in preparation for cloning (50  $\mu$ l reaction). Analytical restriction digests were performed on 7  $\mu$ l of plasmid DNA in a 20  $\mu$ l reaction volume with 5 - 8 units of each enzyme. Preparative restriction digests were performed on 20  $\mu$ l of plasmid DNA in a 50  $\mu$ l reaction volume with 10-15 units of each enzyme. When sequential preparative digests were performed, initial 50  $\mu$ l digests were diluted 2 fold into secondary digest reactions (i.e. 25  $\mu$ l initial digest into 50  $\mu$ l secondary digest). All enzymes and 10 x buffers were supplied by Roche and digest reactions were incubated at the appropriate temperature for 4 hours.

#### **2.4.8 Quantification of DNA**

Purified plasmid DNA concentration was assessed by absorbance measurement at 260 and 280 nm. DNA samples were diluted 50 fold in dH<sub>2</sub>O (2  $\mu$ l in 100  $\mu$ l), transferred to a quartz cuvette and absorbance at 260 and 280 nm were measured against a dH<sub>2</sub>O blank sample. Plasmid DNA concentration in ng/ $\mu$ l was calculated by the following formula:

$$\text{Plasmid DNA (ng/\mu l)} = (\text{OD}_{260} \times 50) \times \text{Dilution Factor}$$

The ratio of 260/280 nm absorbance values indicated the purity of the samples (optimal purity being 260/280 =1.8) (Sambrook and Russel, 2001).

#### **2.4.9 Polyadenylation of PCR products**

Blunt ended PCR products produced by Phusion polymerase were polyadenylated to allow ligation into pGEM-T Easy vector. Polyadenylation reactions contained 8  $\mu$ l of PCR product, 2 mM dATP, 1 x Thermopol Taq

polymerase buffer (NEB) and 0.5 units Thermopol Taq polymerase (NEB) in final volume of 10  $\mu$ l. Reactions were incubated at 72 °C for 30 minutes, chilled on ice then transferred directly to DNA ligation (typically 7  $\mu$ l polyadenylation reaction in a 10  $\mu$ l ligation).

#### **2.4.10 pENTR D-TOPO based DNA ligation**

PCR products destined for ligation into pENTR D-TOPO (Invitrogen) were amplified with appropriate primers containing CACC in the 5' primer termini. Purified PCR products (typically 500 ng DNA) were ligated into pENTR D-TOPO using TOPO directional cloning based on the manufacturer's instructions. Ligation reactions contained upto 4  $\mu$ l PCR product, 1  $\mu$ l salt solution (Invitrogen), 1  $\mu$ l D-TOPO vector (Invitrogen) and dH<sub>2</sub>O to a final volume of 6  $\mu$ l. D-TOPO ligation reactions were incubated at 22 °C for 30 minutes then transformed (typically 3  $\mu$ l ligation) into *E. coli* (Section 2.4.2).

#### **2.4.11 Gateway recombination based cloning**

DNA fragments were cloned into pENTR D-TOPO or pENTR4 entry vectors to facilitate Gateway® recombination based cloning into a variety of destination vectors. Recombination reactions contained 5  $\mu$ l (500 ng) entry plasmid, 1  $\mu$ l destination vector, 2  $\mu$ l LR clonase enzyme mix (Invitrogen) and 2  $\mu$ l dH<sub>2</sub>O. Reactions were incubated at 22 °C for 1 hour then inactivated by the addition of 1 unit Proteinase K (Invitrogen) for 10 minutes at 37 °C. Recombination reactions (typically 5  $\mu$ l) were transformed into *E. coli* (Section 2.4.2).

#### **2.4.12 DNA sequencing**

Sequencing of DNA was carried out by Dundee Sequencing Service (University of Dundee) in accordance with their instructions. Sequencing was carried out on plasmid DNA to verify sequence insert integrity of all experimental constructs generated for this study.

#### **2.4.13 Isolation of genomic DNA from *Arabidopsis* plants**

Genomic DNA was extracted from *Arabidopsis* plant tissue using GenElute Plant Genomic DNA Miniprep kits (Sigma) according to the manufacturer's instructions. Approximately 200 mg of *Arabidopsis* tissue was powdered under liquid N<sub>2</sub> and transferred to an eppendorf tube. Cell lysis and genomic DNA purification were carried out in accordance with the manufacturer's protocol. Purified genomic DNA was eluted in a final volume of 100 µl and stored at -20°C.

#### **2.4.14 Isolation of plant RNA**

Total RNA was extracted from plant tissue using TRIzol RNA extraction reagent (Invitrogen) in accordance with the manufacturer's instructions. Approximately 200 mg of plant tissue was powdered under liquid N<sub>2</sub> and transferred to an eppendorf tube. Cell lysis and total RNA extraction were carried out in accordance with the manufacturer's protocol. RNA pellets were gently resuspended in 30 µl of autoclaved dH<sub>2</sub>O and stored at -80°C.

#### **2.4.15 Quantification of RNA**

RNA concentration and purity was assessed by absorbance measurement at 260 and 280 nm. DNA samples were diluted 50 fold in dH<sub>2</sub>O (2 µl in 100 µl), transferred to a quartz cuvette and absorbance at 260 and 280 nm were measured against a dH<sub>2</sub>O blank sample. RNA sample concentration in ng/µl was calculated by the following formula:

$$\text{RNA ng/}\mu\text{l} = ((\text{OD}_{260} \times 0.33) \times \text{Dilution factor}) / 1000$$

The ratio of 260/280 absorbance values indicated the purity of the samples (optimal purity being 260/280 =2.0) (Sambrook and Russel, 2001).

#### **2.4.16 DNase treatment of RNA**

To abolish possible genomic DNA contamination, RNA extracts (Section 2.4.14) were treated with DNAFree (Ambion) in accordance with the manufacturer's instructions. Recovered RNA fractions were incubated with

2 units of DNase I (Ambion) in 1 x DNase buffer (Ambion) at 37°C for 30 minutes. DNase I was inactivated by the addition of 0.1 volumes DNase inactivation reagent (Ambion) which was mixed for 2 minutes at room temperature. Treated RNA samples were centrifuged at 10,000 g for 1 minute and supernatants were transferred to a fresh eppendorf tube.

#### **2.4.17 cDNA synthesis**

cDNA synthesis for cloning (Section 2.4.6) and semi-quantitative RT-PCR (Section 2.5.3) was completed using Superscript II Reverse Transcriptase (Invitrogen) in accordance with the manufacturer's instructions. DNase treated RNA (1.5 µg) was prepared for cDNA synthesis by incubation with 1 µM oligo dT (dTTP<sub>15</sub>) in a 10 µl volume at 70°C for 10 minutes. Samples were then cooled on ice for 1 minute before the addition of a 9 µl master mix containing 1 x RT buffer (Invitrogen), 10 mM DTT, 1 mM dNTPs (Promega) and 40 units RnaseOut (Invitrogen). Following a 2 minute incubation at 42°C, 100 units of Superscript II reverse transcriptase was added to each cDNA synthesis reaction to a final volume of 20 µl. Reactions were incubated at 42°C for 90 minutes and then 70°C for 10 minutes to deactivate the reverse transcriptase enzyme. After cDNA synthesis, 30 µl of autoclaved dH<sub>2</sub>O was added to each reaction which was stored in 15 µl aliquots at -20°C.

#### **2.4.18 cDNA synthesis for Realtime PCR**

cDNA synthesis for Realtime PCR was completed using AMV Reverse Transcriptase (Promega) in accordance with the manufacturer's instructions. DNase treated RNA (2.5 µg) was prepared for cDNA synthesis by incubation with 5 µM oligo dT (dTTP<sub>15</sub>) in a 15.9 µl volume at 70°C for 10 minutes. Samples were then cooled on ice for 1 minute before the addition of a 9.1 µl master mix containing 1 x AMV Reverse Transcriptase buffer (Promega), 1 mM dNTPs (Promega), 25 units of RNase inhibitor (Promega) and 10 units of AMV Reverse Transcriptase (Promega). Samples were incubated for 45 minutes at 48°C followed by 5 minutes at 95°C to inactivate the reverse transcriptase enzyme. All volumes were completed

with nuclease free water (Ambion). Synthesised cDNA was diluted 4 fold for Realtime PCR analysis and stored at -20 °C.

## 2.5 PCR methods

### 2.5.1 Oligonucleotide primer design

Primer oligonucleotides were either designed *de novo* or using Primer3 software (Rozen and Skaletsky, 2000) as appropriate. Typically, Primer3 designed oligonucleotides were 21 bp in length with a melting temperature ( $T_M$ ) of 60 °C and GC content  $\geq 40\%$ . Primers were synthesised by MWG and supplied as 100  $\mu$ M stocks. Primers used in this study are listed in appendix Table A2.

### 2.5.2 Amplification of DNA by Polymerase Chain Reaction

Polymerase chain reactions (PCR) were completed using a MJ Research DNA Engine PTC-200 Peltier Thermal Cycler (Genetic Research Instrumentation, Essex, UK). Typical PCR reactions were completed in a final volume of 20  $\mu$ l. Template DNA (0.2-0.01 ng) was added to 1 x Thermopol buffer (NEB) with 0.5  $\mu$ M of each primer, 250  $\mu$ M dNTPs and 1 unit of *Taq* DNA polymerase (NEB).

PCR Annealing temperature ( $T_A$ ) was calculated using the following formula:

$$T_A = (2 \times (A + T) + 4 \times (G + C)) - 5$$

Amplification was performed using a suitable number of cycles after an initial denaturation step of 2 minutes at 94 °C. A typical cycle consisted of denaturation at 94 °C for 30 seconds, annealing at 55 °C for 30 seconds and extension at 72 °C for 1 minute per Kb of DNA in the target amplicon. This basic program was modified as required to use specific DNA templates or primers. PCR for cloning applications was completed using proofreading Phusion DNA polymerase (NEB) in accordance with the manufacturers instructions. Amplification was performed using a suitable number of

cycles following an initial denaturation for 30 seconds at 98°C. A typical cycle consisted of denaturation at 98°C for 15 seconds, annealing at 58°C for 20 seconds and extension at 72°C for 30 seconds per Kb of DNA in the target amplicon.

### **2.5.3 Semi-Quantitative Reverse Transcriptase PCR**

cDNA for semi-quantitative RT-PCR was prepared using Superscript II reverse transcriptase (Section 2.4.17). PCR amplification of cDNA for semi-quantitative RT-PCR measurement of mRNA was completed in a final volume of 20 µl using *Taq* DNA polymerase (Section 2.5.2). cDNA samples were checked by PCR using appropriate *Actin2* primers with 2 µl cDNA and sufficient cycles (typically 24) to achieve product amplification in the linear range (Sambrook and Russel, 2001). PCR reactions (16 µl) were resolved on TAE agarose gels (Section 2.4.4) and cDNA content in each PCR reaction was then normalised by comparative analysis based on *Actin2* amplification. cDNA volumes were adjusted based on initial *Actin2* analysis and the *Actin2* PCR was repeated to check the normalisation of cDNA content in each reaction. cDNA normalisation PCRs using *Actin2* primers were repeated until all samples were suitably equalised. RT-PCR to investigate a particular gene of interest was completed on normalised cDNA samples with an appropriate number of cycles. *Actin2* primers for *Arabidopsis*, Tobacco and all other RT-PCR primers used in this study are listed in Appendix Table A2.

### **2.5.4 Quantitative Real-Time RT PCR**

cDNA for quantitative real-time RT-PCR was prepared using AMV reverse transcriptase (Section 2.4.18). mRNA levels were assessed by quantitative PCR using a Stratagene MX4000 real-time PCR machine (Stratagene). Reactions were carried out in a final volume of 25 µl using Stratagene Brilliant SYBR Green QPCR master mix in accordance with the manufacturer's protocol. Each 25 µl reaction contained 2 µl of cDNA and primer concentrations were 0.2 µM. PCR conditions were 10 minute denaturation at 95°C followed by 40 cycles of 30 seconds at 95°C, 30 seconds at 55°C and 1 minute at 72°C. Reactions were carried out in

duplicate for each biological sample and 2 biological samples were analysed for each data point. The *Arabidopsis* gene *Actin2* was used as an internal reference to normalise cDNA samples. Regression lines were generated from external standards using template plasmid DNA containing cDNA encoding *Actin2* or the amplicon from the gene of interest. The concentration of amplified cDNA amplicons was calculated by normalising the recorded data values against recorded *Actin2* concentrations. Primers used for real-time PCR in this study are listed in appendix Table A2.

### 2.5.5 Site-directed mutagenesis of plasmid DNA

Site-directed mutagenesis was completed using the QuikChange (Stratagene) method using specific primers bearing a mutagenic codon. Proof reading PCR was completed with Phusion DNA polymerase using appropriate template DNA and mutagenic primers. Primers were designed to contain ~10 - 15 base pairs either side of the mutated codon with allowances made such that the GC content was at least 40%. The melting temperature ( $T_M$ ) of each primer was  $\geq 78^\circ\text{C}$  according to the following formula:

$$T_M = 81.5 + 0.41(\%GC) - 675/N - \%mismatch$$

where %GC and %mismatch are expressed as whole numbers and N is the primer length (in bases). Primers used for site-directed mutagenesis reactions are listed in appendix Table A2. Following PCR the template DNA was removed by restriction digest with DpnI (10 units) for 1 hour at  $37^\circ\text{C}$ . Undigested mutated plasmid was transformed into *E. coli* and resultant clones were completely sequenced to confirm introduction of the desired mutation and sequence integrity.

### 2.5.6 RACE PCR

5' Rapid Amplification of cDNA Ends (RACE) was performed using RACE 2<sup>nd</sup> Generation Kit (Roche) and Expand HiFi DNA polymerase (Roche) in accordance with manufacturers instructions. Total RNA from tobacco (2  $\mu\text{g}$ ) was used as source material for RACE PCR reactions with primers:

NtUBP12\_942RC, NtUBP12\_762RC and NtUBP12\_554RC in SP1, SP2 and SP3 reactions respectively (appendix Table A2). RACE PCR products were cloned into pGEM T-Easy vector and 2 independent clones were sequenced.

## **2.6 Generation of stable *Arabidopsis* transgenics**

### **2.6.1 Preparation of competent *Agrobacterium* cells for electroporation**

Cells from a single colony of *Agrobacterium tumifaciens* strain GV3101 were inoculated into a 10 ml overnight culture of LB media containing rifampicin (100 µg/ml). Following overnight growth at 28°C, the 10 ml culture was inoculated into 1000 ml of LB media containing rifampicin (100 µg/ml) and grown at 28°C for 4-5 hours to OD<sub>600</sub> 0.5. Cells were pelleted by centrifugation at 2500 g for 10 minutes at 4°C. Cells were resuspended on ice in 100 mls of 10% (v/v) glycerol then pelleted by centrifugation at 2500 g for 10 minutes at 4°C. Cells were resuspended on ice in 10 mls of 10% (v/v) glycerol then pelleted and resuspended as above in a final volume of 1 ml 10% (v/v) glycerol. Resuspended cells were then divided into 50 µl aliquots in pre-chilled eppendorfs and frozen on dry ice prior to storage at -80°C.

### **2.6.2 Transformation of competent *Agrobacterium* cells by electroporation**

Competent cells of *Agrobacterium* strain GV3101 (as prepared in 2.6.1) were thawed on ice. 1 µl (100-200 ng) of plasmid DNA was added to the cells and incubated on ice for 5 minutes. The cells containing DNA were transferred to an electroporation cuvette and pulsed with 1800 V using an electroporator. 1 ml of LB medium was added immediately to the cells which were then transferred to an eppendorf and incubated for 2 hours at 28°C with shaking (200 rpm). Transformed cells were plated out on LB agar containing rifampicin (100 µg/ml) and antibiotics appropriate for the transformed plasmid. Plates were incubated at 28°C for two days until colonies developed.

### **2.6.3 *Agrobacterium* mediated transformation of *Arabidopsis* by floral dip**

*Arabidopsis* transgenic lines were generated in the Col-0 ecotype by means of *Agrobacterium* mediated transformation. Col-0 *Arabidopsis* plants were grown under long day conditions (Section 2.3.2) for 4-5 weeks until flowers developed. Cells from a single colony of *Agrobacterium* GV3101 containing the plasmid of interest were inoculated into a 10 ml overnight culture of LB media with rifampicin (100 µg/ml) and plasmid specific antibiotic. Following overnight growth at 28°C, 5 mls of culture was used to inoculate 500 mls of LB media containing rifampicin (100 µg/ml) and plasmid specific antibiotic. This culture was grown overnight at 28°C to a final OD<sub>600</sub> ~0.6-0.8. Cells were pelleted by centrifugation at 2500 g for 10 minutes and resuspended in Infiltration medium (5% w/v sucrose, 0.03% v/v Silwet L-77). Plants were immersed in the *Agrobacterium* solution for 1 minute and then placed in a sealed bag for 24 hours. Plants were then returned to standard growth conditions and allowed to set seed (2-3 weeks growth).

### **2.6.4 Screen for homozygous *Arabidopsis* lines**

T<sub>1</sub> seed from transformed *Arabidopsis* plants was selected on 0.8% agar MS plates (Section 2.3.3) containing appropriate antibiotics. T<sub>2</sub> generation plants demonstrating 3:1 (75%) segregation on antibiotic selection were selected. Multiple independent homozygous T<sub>3</sub> plant lines were selected from plants demonstrating 100% antibiotic resistance. Homozygous T<sub>3</sub> plant lines were used in all experiments unless otherwise stated.

## **2.7 Virus Induced Gene Silencing (VIGS) in *Nicotiana benthamiana***

### **2.7.1 Plasmid and *Agrobacterium* materials for VIGS**

VIGS based gene silencing in *N. benthamiana* plants was achieved using the pTV00 tobnavirus vector based on RNA2 of Tobacco Rattle Virus (TRV) strain PPK20 (Ratcliff et al., 2001). VIGS infection requires proteins encoded by TRV PPK20 RNA1 which has been cloned under a 35S promoter in the vector pBINTRA6 (Ratcliff et al., 2001). Replication of pTV00 in

*Agrobacterium* also requires the helper plasmid pSA-rep (Hellens et al., 2000). VIGS vectors were kindly provided by Prof D. Baulcombe. pBINTRA6 was transformed into *Agrobacterium* strain LBA440 by electroporation (Section 2.6.2) and transformants selected on kanamycin (50 µg/ml) LB agar plates. pSA-rep was transformed into *Agrobacterium* strain GV3101 by electroporation and transformants were selected on rifampicin (100 µg/ml) and tetracycline (5 µg/ml) LB agar plates. Electrocompetent *Agrobacterium* stocks were prepared from pSA-rep GV3101 (section 2.6.1) and transformed with respective individual pTV00 plasmids by electroporation to generate *Agrobacterium* stocks resistant to rifampicin (100 µg/ml), tetracycline (5 µg/ml) and kanamycin (50µg/ml) containing pSA-rep and pTV00 vectors.

### **2.7.2 Inoculation of VIGS constructs on *N. benthamiana***

All *Agrobacterium* stocks for VIGS experiments were maintained on fresh LB agar plates and used for no more than 10 days. Overnight 10 ml LB cultures of pBINTRA6 and various pTV00 constructs were grown at 28°C (shaking at 200 rpm). Following overnight growth, 1 ml of *Agrobacterium* culture was used to inoculate three 10 ml LB cultures which were subsequently grown for 4-5 hours at 28°C to an OD<sub>600</sub> 1.0. Cultures were pooled and cells pelleted by centrifugation at 2500 g for 10 minutes. Pelleted *Agrobacterium* were resuspended in 10 mM MgCl<sub>2</sub> and culture OD<sub>600</sub> was adjusted to 1.0. Resuspended cultures of pTV00 and pBINTRA6 were mixed in a 1:1 ratio and acetosyringone was added to a final concentration of 150 µM. Mixed *Agrobacterium* cultures were incubated at room temperature for 2 hours prior to plant inoculation. *N. benthamiana* plants were grown for 3-4 weeks (Section 2.3.7) prior to inoculation of VIGS cultures which were infiltrated using a blunt syringe on the abaxial surface on the 2<sup>nd</sup> and 3<sup>rd</sup> emerging leaf. Following culture inoculation, *N. benthamiana* plants were grown for a further 21 - 24 days to allow the development of gene silencing.

## 2.8 Plant pathology methods

### 2.8.1 Pressure inoculation of *Pseudomonas syringae* on *Arabidopsis*

For timecourse transcript analysis during pathogen infection, virulent and avirulent strains of *Pseudomonas syringae* pv. *tomato* (*Pst*) were used to infect 5 - 6 week old *Arabidopsis* plants grown under short day conditions. Bacterial strains *P. s.* pv. *tomato* DC3000, *P. s.* pv. *tomato* DC3000 *avrB* and *P. s.* pv. *tomato* DC3000 *avrRpt2* were grown in overnight cultures of Kings media with rifampicin (100 µg/ml) and kanamycin (50 µg/ml) as described by Katagiri *et al.* (Katagiri *et al.*, 2002). Bacterial cultures were resuspended in 10 mM MgCl<sub>2</sub> and adjusted to a density of 1 x 10<sup>6</sup> colony forming units (cfu)/ml then infiltrated into the abaxial leaf surface using a blunt syringe.

### 2.8.2 Bacterial growth assay of *Pseudomonas syringae* on *Arabidopsis*

Bacterial growth assays were performed on 5 - 6 week old *Arabidopsis* plants following spray inoculation of virulent and avirulent *Pseudomonas syringae* pv. *tomato* (*Pst*) strains described in section 2.1.3. Overnight *Pst* cultures were resuspended in 10 mM MgCl<sub>2</sub> supplemented with 0.05% (v/v) Silwet L77 and adjusted to a density of 1 x 10<sup>8</sup> cfu/ml then sprayed using a fine aerosol pump onto the adaxial leaf surface as described by Zipfel *et al.* (Zipfel *et al.*, 2004). Plants were kept under high humidity and short day growth conditions prior to bacterial growth measurement at 72 hours post inoculation. Bacterial growth was measured from 1 cm<sup>2</sup> leaf discs by maceration in 10 mM MgCl<sub>2</sub> followed by serial dilution and plating on Kings media with appropriate antibiotic selection. Plates were incubated at 28°C for 36 hours and bacterial growth was calculated from colony counts based on 6 independent replicates.

### 2.8.3 HR cell death assay elicited by transient expression of *Cf-9/Avr9*

For analysis of *Cf-9*-mediated HR development, *Agrobacterium* carrying binary constructs containing either *Cf-9* or *Avr9* genes as described by Van

der Hoorn *et al.* (Van der Hoorn *et al.*, 2000) were mixed equally and inoculated in 5 - 6 week old *N. benthamiana* leaves. *Agrobacterium* cultures were prepared as described in Section 2.7.2 and adjusted to a final OD<sub>600</sub> of either 0.4 or 0.2 prior to patch infiltration in *N. benthamiana* leaves using a blunt syringe. HR development was scored at 4 - 5 days after infiltration.

#### **2.8.4 HR cell death assay triggered by Avr9 elicitor infiltration**

For analysis of *Cf-9*-mediated HR development in tobacco, various dilutions of Avr9 peptide solution were infiltrated into leaves of 7 week old transgenic tobacco expressing the *Cf-9* gene as described by Hammond-Kossack *et al.* (Hammond-Kosack *et al.*, 1998).

#### **2.8.5 HR cell death assay triggered by avrPto**

To analyse *Pto*-mediated HR development, *Pseudomonas syringae* pv. *tabaci* *avrPto* was inoculated into leaves of 5 - 6 week old transgenic *N. benthamiana* plants expressing the *Pto* gene as described by Rommens *et al.* (Rommens *et al.*, 1995). Following overnight growth at 28°C, bacterial cultures were resuspended in 10 mM MgCl<sub>2</sub> at various optical densities between 3 x 10<sup>6</sup> cfu/ml and 1 x 10<sup>7</sup> cfu/ml. *Pseudomonas* cultures were patch infiltrated into transgenic 35S *Pto* *N. benthamiana* leaves using a blunt syringe. HR development was scored at 4 - 5 days after bacteria infiltration.

#### **2.8.6 Bacterial growth assay of *Pseudomonas syringae* on *N. benthamiana***

Bacterial growth assays were performed on 5 - 6 week old *N. benthamiana* plants following infection with *Pseudomonas syringae* pv. *tabaci*. Following overnight growth at 28°C, bacterial cultures were resuspended in 10 mM MgCl<sub>2</sub> at 1 x10<sup>4</sup> cfu/ml and were patch infiltrated into *N. benthamiana* leaves with a blunt syringe. Infected plants were kept at 22°C and bacterial growth was measured at 24 and 72 hours after inoculation. Bacterial growth was measured from 1 cm<sup>2</sup> leaf discs by

maceration in 10 mM MgCl<sub>2</sub> followed by serial dilution and plating on Kings media with appropriate antibiotic selection. Plates were incubated at 28°C for 36 hours and bacterial growth was calculated from colony counts based on 8 independent replicates.

### **2.8.7 TMV U1 virus inoculation on *N. benthamiana***

Twelve days after inoculation of VIGS silencing cultures, *N. benthamiana* plants were dusted with carborundum and rub inoculated with TMV U1 virion preparation. TMV virion preparation from TMV U1 infected *N. benthamiana* was conducted as described by Gooding and Herbert (Gooding and Herbert, 1967) and final preparations were adjusted to 20 mg/ml. Diluted TMV virion preparations (5 µl at 0.2 mg/ml) were rub inoculated onto silenced *N. benthamiana* leaves.

### **2.8.8 TMV-GFP virus inoculation on *N. benthamiana***

Transcript RNA corresponding to TMV carrying an inserted GFP coding was transcribed from a template vector TMV(30B)-GFP described by Ryabov et al. (Ryabov et al., 1999) using the mMESAGE mMACHINE T7 kit (Ambion). TMV-GFP transcription reactions (5ul) were combined with sodium phosphate diluted TMV U1 virion preparation (60 µl, 1.5 mg/ml) overnight at 25°C. Following incubation, 5 µl of virion/transcript preparation was rub inoculated onto *N. benthamiana* as previously described (2.8.8).

## **2.9 Protein expression and purification from *E. coli***

### **2.9.1 Protein expression using *E. coli***

Expression of UBP12 fusion proteins with an N-terminal histidine tag was carried out using BL21 Star (DE3) *E. coli* cells. DNA fragments were cloned by Gateway recombination from pENTR4 entry clones to the pDEST17 destination vector and transformed into BL21 Star (DE3) *E. coli* for expression studies. Bacterial cells from a single colony were inoculated into a 10 ml LB overnight initial culture which was grown at 37°C with shaking (200 rpm). A 50 ml expression culture was inoculated with 1 ml of

initial culture and grown at 37°C for approximately 2 hours until it reached OD<sub>600</sub> 0.6. Protein expression was induced by the addition of isopropyl β-D-galactopyranoside (IPTG) to a final concentration of 1 mM. Culture aliquots (1 ml) were taken prior to, then at 1, 2 and 3 hours post induction for fusion protein expression analysis. Following induction, expression cultures were grown for 3 hours at 37°C then *E. coli* cells were pelleted by centrifugation at 2500 g for 10 minutes.

### **2.9.2 Protein purification from *E. coli***

Recovered *E. coli* cell pellets were lysed using BugBuster (Novagen) in accordance with the manufacturer's instructions to yield the soluble fraction in a 2.5 ml volume. Soluble expressed proteins were purified using His-Bind nickel affinity resin (Novagen) using a bed volume of 500 µl. His-Bind resin was loaded on Poly-prep chromatography column (BioRad) then charged and equilibrated by washing in 3 volumes dH<sub>2</sub>O, 5 volumes of Charge buffer (50 mM NiSO<sub>4</sub>) and 3 volumes of Binding buffer (20 mM Tris-HCl pH 7.9, 500 mM NaCl, 5 mM imidazole). Soluble protein extract was loaded onto the column which was then washed with 10 volumes of Binding buffer and 6 volumes of Wash buffer (20 mM Tris-HCl pH 7.9, 500 mM NaCl, 20 mM imidazole). Proteins were eluted with 6 volumes of Elution buffer (20 mM Tris-HCl pH 7.9, 500 mM NaCl, 1 M imidazole) in 500 µl aliquots. Column flow-through, wash and elution fractions were kept and protein elution was checked by SDS-PAGE (Section 2.11.1). Purified protein fractions were pooled and dialysed into HEPES deubiquitination assay buffer (Section 2.12.1) using Slydalyzer cassettes (30 kDa MWC).

## **2.10 Protein expression and purification from *S. frugiperda***

### **2.10.1 Protein expression in *S. frugiperda***

*Spodoptera frugiperda* (Sf9 cells, Invitrogen) were used for the expression of UBP12 proteins. Recombinant baculovirus encoding N-terminal histidine tagged UBP12 fusion proteins were generated using the BaculoGold™ Transfection Kit (BD Biosciences) in accordance with the manufacturer's instructions. Recombinant baculovirus was titred by end point dilution and

used to infect additional Sf9 cells. Infected cells were grown in serum free medium (Invitrogen) supplemented with 10% (v/v) fetal bovine serum (Biosera) at 27°C for three days in cell culture flasks (Corning, UK). Cells were harvested through gentle washing of the flask floor. Harvested cells were centrifuged (1000 g, 1 minute) and the supernatant removed before pelleted cells were resuspended in 100 µl Lysis Buffer (37.5 mM Tris-HCl, 5.3 mM MgSO<sub>4</sub>, 150 mM NaCl, 1 mM EGTA, 1 mM DTT, pH 7.5). Cells were lysed by sonication (using a MSE Soniprep) and cell debris removed by centrifugation (16 000 g) for 3 minutes. The crude soluble fraction was removed to a fresh tube and stored on ice before use.

### **2.10.2 Protein purification from *S. frugiperda***

Histidine tagged UBP12 fusion proteins were purified directly from crude Sf9 cell lysate using His-Select affinity columns (Sigma). Cell lysates were diluted to a final volume of 600 µl in Lysis buffer and purified in accordance with manufacturer's instructions. His-Select columns were equilibrated with Equilibration buffer (50 mM NaH<sub>2</sub>PO<sub>4</sub>, 300 mM NaCl, pH 8.0), loaded with Sf9 cell lysate, washed twice with Wash buffer (50 mM NaH<sub>2</sub>PO<sub>4</sub>, 300 mM NaCl, 5 mM imidazole pH 8.0) and proteins eluted in 200 µl Elution buffer (50 mM NaH<sub>2</sub>PO<sub>4</sub>, 300 mM NaCl, 250 mM imidazole pH 8.0). All centrifugation steps were performed at 325 g for 2 minutes. Purification fractions were analysed by SDS-PAGE (Section 2.11.1) and purified UBP12 proteins were immediately tested for activity *in vitro* (Section 2.12.2).

## **2.11 Protein methods**

### **2.11.1 SDS-polyacrylamide gel electrophoresis (SDS-PAGE)**

Protein samples were denatured by boiling at 100°C for 10 minutes following resuspension in 1 x SDS Loading Buffer (25 mM Tris-HCl pH 6.8, 10% (v/v) glycerol, 2% (w/v) SDS, 5% (v/v) B-mercaptoethanol, 0.001% bromophenol blue). Denatured proteins were electrophoresed at 100 V according to the method initially outlined by Laemmli (Sambrook and Russel, 2001) using SDS-PAGE gels containing separating gels ranging from

8% - 15% polyacrylamide and a 5% polyacrylamide stacking gel. Protein molecular weights estimated by loading 'Broad Range Pre-stained Molecular Weight' marker (New England Biolabs) alongside the samples.

### **2.11.2 Western blotting**

Antibodies were sourced as indicated in Table 2.2. SDS-PAGE resolved proteins were electro-transferred at either 100 V for 1 hour or 30 V for 16 hours onto PVDF membrane in Transfer Buffer (25 mM Tris-HCl, 190 mM glycine, 20% (v/v) methanol). Following electro-transfer, membranes were blocked for 1 hour in either 5% milk powder or 1% casein dissolved in TBST (15 mM Tris-HCl pH 7.6, 150 mM NaCl, 0.1% (v/v) Tween 20). After blocking, primary antibodies were incubated with the membrane at the dilutions and durations indicated in Table 2.2. The membrane was then washed 5 times for 5 minutes in TBST before secondary antibodies were added at the dilutions indicated in Table 2.2 for 1 hour. The membrane was then washed 5 times for 5 minutes in TBST prior to treatment with chemiluminescent substrate. All secondary antibodies used in this study were horseradish peroxidase (HRP) conjugates and were developed using Millipore chemiluminescent substrate in accordance with the manufacturer's instructions.

### **2.11.3 Staining of SDS-PAGE gels and PVDF membranes**

Coomassie staining of SDS-PAGE gels was completed after removal of the stacking gel. The resolved gel was stained in Coomassie Stain Solution (0.1% (w/v) Coomassie Brilliant Blue R-250, 50% (v/v) methanol, 10% (v/v) acetic acid) for 30 minutes. The stained gel was then destained in several changes of Destain Solution (50% (v/v) methanol, 10% (v/v) acetic acid). Electro-transferred PVDF membranes were stained in Ponceau Solution (0.1% (w/v) Ponceau S, 1% (v/v) acetic acid) for 30 minutes then washed in dH<sub>2</sub>O for 10 minutes.

## **2.12 *in Vitro* Deubiquitination activity assays**

### **2.12.1 *in vitro* Deubiquitination assays using Ubiquitin chains substrate**

Partially purified UBP12 proteins (10 µl of extract) were incubated with 1 µg of a mixture of oligo-ubiquitin chains (Affiniti UW8860) in 30 µl buffer (150 mM KCl, 50 mM Hepes, 10 mM DTT, 5% glycerol, pH 7.4) for 20 hours at 37°C. Recombinant human Isopeptidase T (Affiniti UW8560) was used as a positive experimental control, where 0.8 µg was incubated with oligo-ubiquitin chains under standard assay conditions. Assay reactions were stopped by the addition of 4 x SDS buffer and aliquots were analysed by western blotting using anti-ubiquitin and anti-Histidine antibodies

### **2.12.2 *in vitro* Deubiquitination assays using Diubiquitin substrate**

Purified UBP proteins (0.2 - 3 µg) were incubated with 2 µg of diubiquitin (Affiniti UW9800) in 30 µl buffer (25 mM Tris HCl, 100 mM NaCl, 2 mM DTT, BSA 100 µg/ml, pH 8.0) for 20 hours at 37°C. Recombinant human Isopeptidase T (Affiniti UW8560) was used as a positive experimental control, where 0.8 µg was incubated with diubiquitin under standard assay conditions. Assay reactions were stopped by the addition of 4 x SDS buffer and aliquots were analysed by western blotting using anti-ubiquitin and anti-Histidine antibodies.

## **2.13 Transient expression of gene constructs in *Nicotiana* species**

Gene constructs were transiently expressed in *N. tabacum* and *N. benthamiana* plants using *Agrobacterium* mediated transformation. Cells from a single colony of recently transformed *Agrobacterium* were inoculated into an overnight 10 ml culture of LB media with rifampicin (100 µg/ml) and kanamycin (50 µg/ml) which was grown at 28°C with shaking at 200 rpm. Following overnight growth, cells were pelleted by centrifugation at 2500 g for 10 minutes then resuspended in 10 mM MgCl<sub>2</sub>. Cultures were adjusted to OD<sub>600</sub> 0.5 unless otherwise stated and acetosyringone was added to a final concentration of 150 µM prior to a 2 hour incubation at 22°C. Cultures were infiltrated into the abaxial leaf

surface by pressure inoculation using a blunt 1 ml syringe. Following culture inoculation, plants were incubated at 22°C for 2 or 3 days before experimental analysis.

## **2.14 Plant protein methods**

### **2.14.1 Total protein extraction from *Nicotiana* species**

Plant tissue samples (approx 1 g) were frozen under liquid N<sub>2</sub> prior to grinding with 100 mg PVPP (Sigma). Ground tissue (100 mg) was transferred into eppendorf tubes and vortexed with chilled protein extraction buffer (25 mM Tris-HCl pH 7.5, 1 mM EDTA, 150 mM NaCl, 10% (v/v) Glycerol, 5 mM DTT) containing a protease inhibitor tablet (Roche) for 30 seconds. Homogenised plant tissue samples were centrifuged at 12,000 g and 4°C for 20 minutes and supernatants was transferred to a new eppendorf tube.

### **2.14.2 Quantification of protein concentration**

Protein content of samples was determined using Bradford reagent as described in Sambrook *et al.* (Sambrook and Russel, 2001). Extracted protein samples were diluted 25 and 50 fold in 100 µl dH<sub>2</sub>O then mixed in an eppendorf tube with 900 µl Bradford reagent by vortexing. Protein standards for assay calibration were diluted from stock bovine serum albumin (2 mg/ml) and prepared at 0.04, 0.08, 0.16 and 0.2 mg/ml. The absorbance at 550 nm of a blank sample (no protein added) was recorded and protein concentrations were estimated based on the curve gradient calculated from protein standards.

### **2.14.3 Protein precipitation with Trichloroacetic acid**

Protein samples were concentrated prior to SDS-PAGE separation using Trichloroacetic acid precipitation. Required volumes of extracted protein solution were mixed by pipetting in an eppendorf tube with 20 µl of 2% sodium deoxycholate (w/v), followed by the addition of 700 µl dH<sub>2</sub>O with mixing then 250 µl of 24% trichloroacetic acid (w/v) with mixing. Protein

precipitation was performed on ice for 1 hour prior to centrifugation at 12,000 g and 4°C for 20 minutes. After centrifugation, the supernatant was discarded and precipitated proteins were resuspended in 20 µl of 1 x SDS PAGE loading buffer (Section 2.11.1) and 2 µl 2M Tris-HCl.

## **2.15 Confocal Microscopy**

The subcellular localisation of GFP was visualised using a confocal laser scanning microscope (Zeiss LSM 510) under water with a 10 x objective lens. GFP tags were excited using an argon laser at 488 nm. GFP emission was collected between 505-530 nm to avoid cross-talk with chloroplast autofluorescence.

## **2.16 Computational methods**

### **2.16.1 Sequence Alignment analysis**

Alignment based analysis and sequence database interrogation was performed using the BLAST algorithm as described by Altschul et al (Altschul et al., 1997). Protein and nucleotide sequence queries were performed against genome and EST sequence repositories at the TAIR (<http://www.arabidopsis.org>) and TIGR (<http://www.tigr.org>) websites using BLASTP and BLASTN programs with default search parameters. Protein sequence alignments for phylogenetic analysis were generated with the ClustalW program using default parameters as described by Chenna et al (Chenna et al., 2003).

### **2.16.2 Protein sequence domain analysis using Pfam**

Protein sequences were analysed for the presence of known domains and motifs against the Pfam database (<http://pfam.sanger.ac.uk>) using default search parameters as described by Finn *et al.* (Finn et al., 2006).

### **2.16.3 Protein structure modelling**

Three-dimensional protein structures were obtained from the RCSB Protein Data Bank (<http://www.rcsb.org>) and rendered using Pymol (<http://pymol.org>) (Hodis et al., 2007).

### **2.16.4 Protein localisation prediction**

Proteins were analysed for potential nuclear localisation signals using NLSpredict (<http://cubic.bioc.columbia.edu/predictNLS>) with default settings (Cokol et al., 2000). Proteins were analysed for potential targeting signals using TargetP (<http://www.cbs.dtu.dk/services/TargetP>) with default settings and the plant specific database (Emanuelsson et al., 2007).

### **2.16.5 Phylogenetic analysis using MEGA**

Phylogenetic relationships were inferred from protein sequence alignments using the MEGA program suite (Tamura et al., 2007). Phylogenetic trees were constructed using the neighbor-joining method and inferred relationships were tested with 10,000 bootstrap replicates.

### **2.16.6 Densitometry analysis using Scion Image**

Image data from semi-quantitative RT-PCR experiments was analysed using Scion Image software (<http://www.scioncorp.com>).

## Chapter 3 – *Arabidopsis* Deubiquitinating Enzymes

### 3.1 Introduction

The most complete analysis of plant deubiquitinating (DUB) enzymes was reported by Yan *et al.* (Yan *et al.*, 2000a) and was based on analysis of the near complete genome sequence in the model plant *Arabidopsis thaliana* (referred to hereafter as *Arabidopsis*). Subsequent studies have characterised a limited number of DUBs from *Arabidopsis* but the majority still await function assignment. Whilst additional classes of DUB enzyme have recently been identified in other model eukaryotes (Amerik and Hochstrasser, 2004), equivalent orthologous plant classes remain to be established. As a starting point in this study, knowledge of mammalian DUB enzymes was utilised to comprehensively identify all currently known classes of DUB enzyme in the *Arabidopsis* genome.

This chapter reports a preliminary characterisation of the two paralogous *Arabidopsis* UBP enzymes: AtUBP12 and AtUBP13. On the basis of recently reported microarray data examining pathogen associated signalling in *Nicotiana benthamiana* (Kim *et al.*, 2006), the potential role of *Arabidopsis* genes *AtUBP12* and *AtUBP13* in disease resistance signalling was investigated.

The *Arabidopsis-Pseudomonas* interaction was utilised to examine the transcriptional response of *AtUBP12* and *AtUBP13* during pathogen infection. Transcriptional responses of *AtUBP12* and *AtUBP13* to the disease resistance signalling hormone salicylic acid were also examined. Homozygous mutant alleles of *ubp12* and *ubp13* were isolated and alterations in their resistance to virulent and avirulent strains of *Pseudomonas* were assessed.

Potential functional redundancy between AtUBP12 and AtUBP13 was investigated using approaches based on transgenic RNA interference and the generation of genetic crosses between *ubp12* and *ubp13* mutant alleles.

The principal findings in this chapter support three main conclusions. Both *AtUBP12* and *AtUBP13* are transcriptionally responsive to avirulent *Pseudomonas syringae* expressing *avrB* and exogenously applied salicylic acid. That *AtUBP12* and *AtUBP13* proteins share functional redundancy in the regulation of development with *ubp12 ubp13* double homozygotes exhibiting a seedling lethal phenotype. Finally, that mutant *ubp12* alleles demonstrate a significant reduction in flowering time when grown under a short day photoperiod.

### **3.2 Identification of *Arabidopsis* Deubiquitinating enzymes**

The complete sequencing and publication of the *Arabidopsis* genome has facilitated identification and classification of many new genes based on existing knowledge of conserved protein domains and motifs. Sequence analysis of the *Arabidopsis* genome has identified different ubiquitin metabolism enzyme classes and established the elaboration of different E3 ubiquitin ligase classes relative to sequenced animal genomes (Vierstra, 2003). Plant deubiquitinating enzymes (DUBS) were initially identified on the basis of biochemical activity in tissue extracts (Sullivan et al., 1990) but the first extensive genetic analysis of these enzymes was reported by Yan *et al.* and was based on screening of the near complete *Arabidopsis* genome (Yan et al., 2000a). In the initial *Arabidopsis* study Yan *et al.* queried available sequence data using the yeast *UBP4* cDNA sequence to report 27 distinct Ubiquitin Specific Protease (UBP) genes. Having implicated *AtUBP1* and *AtUBP2* in canavanine resistance, Yan *et al.* acknowledged the presence of Ubiquitin C-terminal Hydrolases (UCH) in *Arabidopsis* but concluded that the UBPs were likely to be the most functionally diverse DUB enzymes based on the extensive divergence of UBPs sequences outside their catalytic regions (Yan et al., 2000a).

Subsequent studies, focussed primarily on yeast and human genomes, have identified other DUB classes and current research indicates the existence of five distinct DUB enzyme families: UCH, UBPs, Otubain, Ataxin and JAMM (Amerik and Hochstrasser, 2004). As has been previously discussed, UCH, UBPs, Otubain and Ataxin DUBS are all variant cysteine proteases (Nijman

et al., 2005) whilst the JAMM family are zinc metalloproteases (Ambroggio et al., 2004b).

At the initiation of this study, the *Arabidopsis* UBP enzyme analysis published by Yan *et al.* represented the most extensive analysis of plant DUBs but only reported the existence of UBP and UCH enzymes. As a starting point in this study, the *Arabidopsis* genome was screened for potential DUBS using sequence data from each currently defined class of DUB enzyme.

The *Arabidopsis* genome database at TAIR (Swarbreck et al., 2008) was queried using yeast, human and *Arabidopsis* protein sequences retrieved from Swiss-Prot (Bairoch et al., 2005) that represented each class of DUB enzyme (listed in appendix Table A1) and high scoring sequences were rescreened to obtain any further matches. All significant hits were checked for the presence of the appropriate ubiquitin protease domain using the Pfam database (Finn et al., 2006) and detected DUB genes from each subfamily are reported in Table 3.1.

This analysis of *Arabidopsis* DUBS confirmed that the UBP family represent the largest subclass with 27 members (Figure 3.2). The UCH class of DUBs comprises 3 closely related members two of which (AtUCH1 and AtUCH2) have recently been implicated in the regulation of shoot development and architecture (Yang et al., 2007). Based on studies of animal orthologs, the plant UCH DUBs are also proposed to have housekeeping functions related to ubiquitin metabolism (Larsen et al., 1998). In *Arabidopsis*, the Otubain and Ataxin DUB classes have 1 and 2 members respectively. There is currently no published data relating to the potential function of the Otubain or Ataxin DUBs in plants but comparative genome analysis using InParanoid (Remm et al., 2001) indicates they have orthologs in other model eukaryotes suggesting a fundamental role for these proteins.

The recently identified JAMM class of DUBS has 10 members in *Arabidopsis* (Figure 3.1). The JAB1/MPN/Mov34 (JAMM) domain DUBs were initially characterised with the identification of RPN11 as a key deubiquitinating subunit of the 26S proteasome lid complex and two homologous JAMM

subunits that cleave the ubiquitin-like protein RUB (Related to Ubiquitin) were also identified in the COP9 signalosome (Ambroggio et al., 2004b).

The remaining detected *Arabidopsis* JAMM DUBs exhibit conservation in most or all of the JAMM active site residues (Figure 3.1 A) but have yet to be experimentally characterised as deubiquitinating enzymes. Phylogenetic analysis of the detected JAMM enzymes was conducted based on an alignment of the full JAMM domain (as detected by Pfam - PF01398) (Figure 3.1 B). The resulting phylogeny reported four distinct clades within the *Arabidopsis* JAMM proteins (Figure 3.1 B). The proteasome /signalosome associated subunits RPN11, CSN5A and CSN5B form a distinct clade with high bootstrap support. Proteins encoded by AT1G80210 and AT3G06820 cluster within the same overall clade as proteasome /signalosome JAMM enzymes but are not closely related to them (Figure 3.1 B). AT1G80210 and AT3G06820 lack annotation and do not contain other domains to suggest their possible functions, however the high scoring Pfam JAMM domain match indicates that they are putative deubiquitinating enzymes.

Proteins encoded by AT1G80070 and AT4G38780 form a distinct clade (Figure 3.1 B) within which the former has been characterised and is annotated as SUS2. The *sus2* mutant is one of three reported suspensor mutants (*sus1*, *sus2* and *sus3*) which cause early embryo arrest due to improper suspensor development (Zhang and Somerville, 1997). AT1G80070 and AT4G38780 are located on chromosomes 1 and 4 respectively and exhibit 100% sequence identity, Pfam analysis indicates the presence of JAMM ubiquitin protease and several nuclear RNA spliceosome interaction domains. JAMM domain DUBs AT4G16144, AT1G48790 and AT1G10600 form a distinct clade (Figure 3.1 B) and are most closely related to the recently characterised yeast AMSH protein which regulates receptor sorting at endosomes through deubiquitination (McCullough et al., 2004a).

Having identified the UBP enzymes as the largest subfamily of DUBs, their phylogenetic relationships were inferred (Figure 3.2). The phylogeny was based on an alignment of conserved catalytic His and Cys box regions and

**Figure 3.1** Analysis of the *Arabidopsis* JAMM domain ubiquitin proteases.

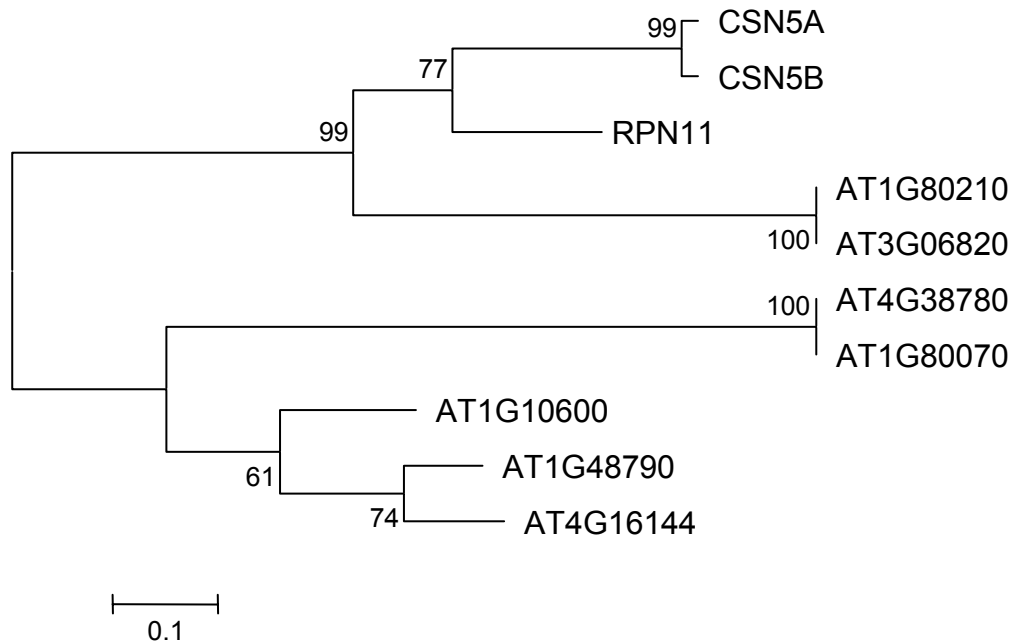
(A) Alignment of JAMM domain active site region in detected *Arabidopsis* JAMM domain proteins. Pfam analysis of *Arabidopsis* matches to known JAMM domain ubiquitin proteases detected 10 high scoring JAMM domain proteins: RPN11, CSN5A, CSN5B, AT1G80210, AT3G06820, AT1G80070, AT4G38780, AT4G16144, AT1G48790 and AT1G10600. JAMM domain catalytic active site residues are highlighted in green. (B) Phylogeny of *Arabidopsis* JAMM ubiquitin proteases inferred from an alignment of the JAMM domain of detected JAMM proteins. The phylogeny was inferred by neighbor joining using MEGA from an alignment of the catalytic JAMM domain from recovered *Arabidopsis* JAMM proteins. Node values represent percentage support values estimated from 10,000 bootstrap replicates and scale bar represents evolutionary distance as amino acid substitutions per site.

**A**

RPN11	DMLKQTGRPEMVVGWY	<b>H</b>	<b>S</b>	<b>H</b>	<b>P</b>	<b>G</b>	<b>F</b>	<b>G</b>	<b>C</b>	<b>W</b>	<b>L</b>	<b>S</b>	SGVDINTQQSFEALNQR
CSN5A	QTNKLAGRLENVVGWY	<b>H</b>	<b>S</b>	<b>H</b>	<b>P</b>	<b>G</b>	<b>Y</b>	<b>G</b>	<b>C</b>	<b>W</b>	<b>L</b>	<b>S</b>	SGIDVSTQRLNQQHQEP
CSN5B	QTSKLAGRLENVVGWY	<b>H</b>	<b>S</b>	<b>H</b>	<b>P</b>	<b>G</b>	<b>Y</b>	<b>G</b>	<b>C</b>	<b>W</b>	<b>L</b>	<b>S</b>	SGIDVSTQMLNQQYQEP
AT1G48790	-FEVQDKQSLFPLGWI	<b>H</b>	<b>T</b>	<b>H</b>	<b>P</b>	<b>T</b>	<b>Q</b>	<b>S</b>	<b>C</b>	<b>F</b>	<b>M</b>	<b>S</b>	SSIDVHTHYSYQIMLPE
AT1G10600	-FSIQNERELYPVGWI	<b>H</b>	<b>T</b>	<b>H</b>	<b>P</b>	<b>S</b>	<b>Q</b>	<b>G</b>	<b>C</b>	<b>F</b>	<b>M</b>	<b>S</b>	SSVDLHTHYSYQVMVPE
AT1G80210	RMTISTGRTRRVIGWY	<b>H</b>	<b>S</b>	<b>H</b>	<b>P</b>	<b>H</b>	<b>I</b>	<b>T</b>	<b>V</b>	<b>L</b>	<b>P</b>	<b>S</b>	SHVDVRTQAMYQLLDSG
AT3G06820	-MTISTGRTRRVIGWY	<b>H</b>	<b>S</b>	<b>H</b>	<b>P</b>	<b>H</b>	<b>I</b>	<b>T</b>	<b>V</b>	<b>L</b>	<b>P</b>	<b>S</b>	SHVDVRTQAMYQLLDSG
AT4G38780	---HQFLDDLEPLGWI	<b>H</b>	<b>T</b>	<b>Q</b>	<b>P</b>	<b>N</b>	<b>E</b>	<b>L</b>	<b>P</b>	<b>Q</b>	<b>L</b>	<b>S</b>	SPQDVTFHTR-----
AT1G80070	---HQFLDDLEPLGWI	<b>H</b>	<b>T</b>	<b>Q</b>	<b>P</b>	<b>N</b>	<b>E</b>	<b>L</b>	<b>P</b>	<b>Q</b>	<b>L</b>	<b>S</b>	SPQDVTFHTR-----
AT4G16144	--FVQDRLSLFPLGWI	<b>H</b>	<b>T</b>	<b>H</b>	<b>P</b>	<b>T</b>	<b>Q</b>	<b>T</b>	<b>C</b>	<b>F</b>	<b>M</b>	<b>S</b>	SSVDLHTHYSYQIMLPE

**JAMM active site**

**B**



for clarity, only clade relationships with significant bootstrap support values over 70% (Soltis and Soltis, 2003) were reported (Figure 3.2). In the phylogeny of all 27 *Arabidopsis* UBP enzymes, five closely related pairs corresponding to AtUBP1 and AtUBP2, AtUBP3 and AtUBP4, AtUBP6 and AtUBP7, AtUBP12 and AtUBP13 and AtUBP20 and AtUBP21 were inferred. Two five member UBP subfamilies were reported one of which contained AtUBP5, AtUBP8, AtUBP9, AtUBP10 and AtUBP11 where the other contained of AtUBP15, AtUBP16, AtUBP17, AtUBP18 and AtUBP19. All remaining UBP enzymes were present as singletons demonstrating no significant clustering with other family members (Figure 3.2).

Outside the conserved UBP enzyme core functional motifs (Figure 3.2 - Cys, His, Q, G, L and F boxes) described by Yan *et al.* (Yan et al., 2000a), additional domains were detected by Pfam analysis. A zinc finger domain (PF01753) was found in all members of the UBP subfamily containing AtUBP15, AtUBP16, AtUBP17, AtUBP18 and AtUBP19 which was identified as belonging to the MYND subclass (Masselink and Bernards, 2000). A MATH/TRAF domain (PF00917) was detected in the paired AtUBP12 and AtUBP13 subfamily which is predicted to mediate protein-ligand interactions (Uren and Vaux, 1996). Ubiquitin-like domains (UBL) and ubiquitin associated domains (UBA) which are associated with targeting and recognition of ubiquitinated proteins (Welchman et al., 2005) were detected in AtUBP6, AtUBP7, AtUBP14 and AtUBP26 (Figure 3.2).

In the first analysis of *Arabidopsis* UBP enzymes, Yan *et al.* reported the involvement of AtUBP1 and AtUBP2 in resistance to the synthetic arginine analog canavanine (Yan et al., 2000a). The absolute requirement of AtUBP14 for embryogenesis has been established with studies of *ubp14* aborted embryos indicating accumulation of uncleaved ubiquitin chains (Doelling et al., 2001). *Arabidopsis* UBP enzymes AtUBP3 and AtUBP4 have been found to regulate pollen development where the loss of AtUBP3/AtUBP4 activity in *ubp3 upb4* double mutants abrogates mitosis progression during male gametogenesis (Doelling et al., 2007). In a more recent analysis of *Arabidopsis* UBP enzymes, Liu *et al.* reported the involvement of AtUBP15 and AtUBP16 in cell proliferation and leaf development (Liu et al., 2008).

**Figure 3.2** Domains and phylogeny of *Arabidopsis* UBP enzymes.

Domain structure of the *Arabidopsis* Ubiquitin Specific Protease (UBP) family. Locations of functional Cys, Q, G, L, F and His motifs are indicated. Phylogeny was inferred by neighbour joining using MEGA to define UBP subfamilies. Phylogeny was inferred from an alignment of catalytic His and Cys boxes where node values represent percentage support values estimated from 10,000 bootstrap replicates. Scale represents evolutionary distance as amino acid substitutions per site. Putative zinc fingers are denoted by black diamonds, Ubiquitin-like domains are denoted by black circles, Ubiquitin associated domains are denoted by white triangles and MATH/TRAF domains are denoted by white circles. UBP domain figures adapted from Yan *et al.* (Yan *et al.*, 2000a).



Protein	TAIR gene code	DUB Class	Pfam domain	Pfam E-value
AtUBP1	AT2G32780	UBP	PF00443	$4.3 \times 10^{-63}$
AtUBP2	AT1G04860	UBP	PF00443	$1.8 \times 10^{-63}$
AtUBP3	AT4G39910	UBP	PF00443	$1.1 \times 10^{-98}$
AtUBP4	AT2G22310	UBP	PF00443	$5.9 \times 10^{-105}$
AtUBP5	AT2G40930	UBP	PF00443	$3.2 \times 10^{-125}$
AtUBP6	AT1G51710	UBP	PF00443	$7.5 \times 10^{-74}$
AtUBP7	AT3G21280	UBP	PF00443	$1.2 \times 10^{-75}$
AtUBP8	AT5G22030	UBP	PF00443	$3.5 \times 10^{-114}$
AtUBP9	AT4G10590	UBP	PF00443	$1.7 \times 10^{-121}$
AtUBP10	AT4G10570	UBP	PF00443	$8.8 \times 10^{-122}$
AtUBP11	AT1G32850	UBP	PF00443	$8 \times 10^{-117}$
AtUBP12	AT5G06600	UBP	PF00443	$1.9 \times 10^{-77}$
AtUBP13	AT3G11910	UBP	PF00443	$1.1 \times 10^{-77}$
AtUBP14	AT3G20630	UBP	PF00443	$2.3 \times 10^{-59}$
AtUBP15	AT1G17110	UBP	PF00443	$9.1 \times 10^{-54}$
AtUBP16	AT4G24560	UBP	PF00443	$2.3 \times 10^{-54}$
AtUBP17	AT5G65450	UBP	PF00443	$8.1 \times 10^{-49}$
AtUBP18	AT4G31670	UBP	PF00443	$2.5 \times 10^{-46}$
AtUBP19	AT2G24640	UBP	PF00443	$2.3 \times 10^{-43}$
AtUBP20	AT4G17895	UBP	PF00443	$2.8 \times 10^{-78}$
AtUBP21	AT5G46740	UBP	PF00443	$5.1 \times 10^{-66}$
AtUBP22	AT5G10790	UBP	PF00443	$5.2 \times 10^{-62}$
AtUBP23	AT5G57990	UBP	PF00443	$7.6 \times 10^{-61}$
AtUBP24	AT4G30890	UBP	PF00443	$1 \times 10^{-56}$
AtUBP25	AT3G14400	UBP	PF00443	$1.1 \times 10^{-66}$
AtUBP26	AT3G49600	UBP	PF00443	$4.9 \times 10^{-55}$
AtUBP27	AT4G39370	UBP	PF00443	$9.8 \times 10^{-38}$
AtUCH1	AT4G17510	UCH	PF01088	$1.2 \times 10^{-92}$
AtUCH2	AT5G16310	UCH	PF01088	$1.8 \times 10^{-90}$
AtUCH3	AT1G65650	UCH	PF01088	$2.7 \times 10^{-102}$
Q8LG98	AT1G28120	Otubain	PF02338	0.036
Q9M391	AT3G54130	Ataxin	PF02099	$2.2 \times 10^{-34}$
O82391	AT2G29640	Ataxin	PF02099	$5.4 \times 10^{-148}$
RPN11	AT5G23540	JAMM	PF01398	$1.6 \times 10^{-51}$
CSN5A	AT1G22920	JAMM	PF01398	$3.9 \times 10^{-52}$
CSN5B	AT1G71230	JAMM	PF01398	$3.2 \times 10^{-51}$
Q8VYB5	AT1G48790	JAMM	PF01398	$8.2 \times 10^{-22}$
Q6NKP9	AT1G10600	JAMM	PF01398	$3.2 \times 10^{-19}$
Q8RW94	AT1G80210	JAMM	PF01398	$1.6 \times 10^{-14}$
Q8RY58	AT3G06820	JAMM	PF01398	$5 \times 10^{-16}$
Q5PNU3	AT4G16144	JAMM	PF01398	$1.3 \times 10^{-24}$
Q9T016	AT4G38780	JAMM	PF01398	$1 \times 10^{-14}$
Q9SSD2	AT1G80070	JAMM	PF01398	$4.1 \times 10^{-13}$

**Table 3.1** Deubiquitinating enzymes identified in the *Arabidopsis* genome.

DUB enzymes of each respective subclass (UBP, UCH, Otubain, Ataxin and JAMM) were identified in the *Arabidopsis* genome by screening with known DUB sequences listed in appendix Table A1. Uniprot ID numbers are reported in cases where a given match has no designated protein name. Entries were screened against the Pfam database and corresponding ubiquitin protease domain E-value scores are reported.

### 3.3 Gene Expression analysis of *AtUBP12* and *AtUBP13*

The activation of the plant defence response requires coordination of multiple signalling pathways to alter changes in hormone balance, ion flux, redox status and gene expression (Katagiri, 2004). A recent study by Kim *et al.* described a microarray study comparing programmed cell death (HR) elicited by *Pseudomonas* infection and induced proteasome malfunction in the model solanaceous plant *N. benthamiana* (Kim *et al.*, 2006).

The results published by Kim *et al.* highlighted genes showing HR specific induction behaviour including established marker genes such as pathogenesis related 1 (*PR-1*) and several genes encoding ubiquitination enzymes (Kim *et al.*, 2006). Of particular relevance to this study was the reported suppression of a DUB gene specifically during *Pseudomonas* elicited HR corresponding to the *N. benthamiana* ortholog of *Arabidopsis AtUBP12*. In the *Arabidopsis* genome, *AtUBP12* is paired with a close evolutionary relative *AtUBP13* (Figure 3.2). These two UBP genes share 86% nucleotide identity and form a distinct clade within the *Arabidopsis* UBP enzymes (Figure 3.2).

#### 3.3.1 Analysis of *AtUBP12* and *AtUBP13* gene expression during disease resistance signalling

In this study, the established model plant-pathogen interaction between *Arabidopsis* and *Pseudomonas syringae* was used to investigate plant disease resistance signalling (Katagiri *et al.*, 2002). *Pseudomonas syringae* pv. *tomato* (*Pst*) strain DC3000 is virulent on tomato and *Arabidopsis* and infection causes bacterial speck disease (Alfano and Collmer, 1996). The introduction of cloned avirulence genes into *Pst* DC3000 has also facilitated its application to the study of gene-for-gene disease resistance mechanisms in *Arabidopsis* (Dong *et al.*, 1991). Following their delivery into the plant cell via a type-III secretion system (TTSS) (Dangl and Jones, 2001), bacterial effector proteins can trigger gene-for-gene resistance. In this study, disease resistance was triggered by *Arabidopsis R* genes *RPM1* (Grant *et al.*, 1995) and *RPS2* (Bent *et al.*, 1994) upon specific recognition

of *Pst* strains expressing the cognate avirulence genes *avrB* and *avrRpt2* (Katagiri et al., 2002).

Virulent and avirulent *Pst* DC3000 strains were used to investigate the transcriptional induction of *Arabidopsis* UBPs *AtUBP12* and *AtUBP13* during disease resistance signalling. Defence responses were induced by the high titre ( $1 \times 10^6$  cfu/ml) inoculation (Katagiri et al., 2002) of either *Pst* DC3000, *Pst* DC3000 *avrB* or *Pst* DC3000 *avrRpt2* onto 5 week old *Arabidopsis* plants. Leaf samples were taken at various timepoints then *AtUBP12* and *AtUBP13* gene expression was analysed by RT-PCR (Figure 3.3). The cDNA content of timecourse samples corresponding to four treatments with either  $MgCl_2$  (wounding control), *Pst* DC3000 (virulent), *Pst* DC3000 *avrB* or *Pst* DC3000 *avrRpt2* were normalised by PCR analysis of the constitutively expressed *Actin2* gene (Laval et al., 2002). The Pathogenesis Related 1 (*PR-1*) defence marker gene demonstrated the expected induction (Volko et al., 1998) in each treatment condition and provided a positive experimental control (Figure 3.3).

RT-PCR was conducted on the respective normalised cDNA samples with primers specific for *AtUBP12* (*AtUBP12RT\_5* and *AtUBP12RT\_3*) and *AtUBP13* (*AtUBP13RT\_5* and *AtUBP13\_RT3*) (Figure 3.3). Densitometry analysis indicated that both genes were induced by wounding. In the wounding control, *AtUBP12* and *AtUBP13* gene induction peaked 6 hours after  $MgCl_2$  infiltration (Figure 3.3) with *AtUBP12* demonstrating a greater fold induction from initial levels (3.2 fold increase versus 1.3 fold increase for *AtUBP13*). Both genes demonstrated increased expression during *avrB* elicited HR relative to the wounding control. From initial to peak expression (at 6 hours post infiltration), *AtUBP12* expression was increased 15.6 fold whilst *AtUBP13* expression increased 2.4 fold (Figure 3.3 B).

During *avrRpt2* elicited HR, early fold changes in *AtUBP12* and *AtUBP13* expression (1-6 hours) were similar to those observed during wounding (Figure 3.3 C) and didn't indicate a clear pathogen associated induction. The initiation of HR by *avrRpt2/RPS2* is slower (14-18 hours) than by *avrB/RPM1* (4-6 hours) (Mackey et al., 2003) (as confirmed by *PR-1* induction) and this may explain the wounding associated level of gene

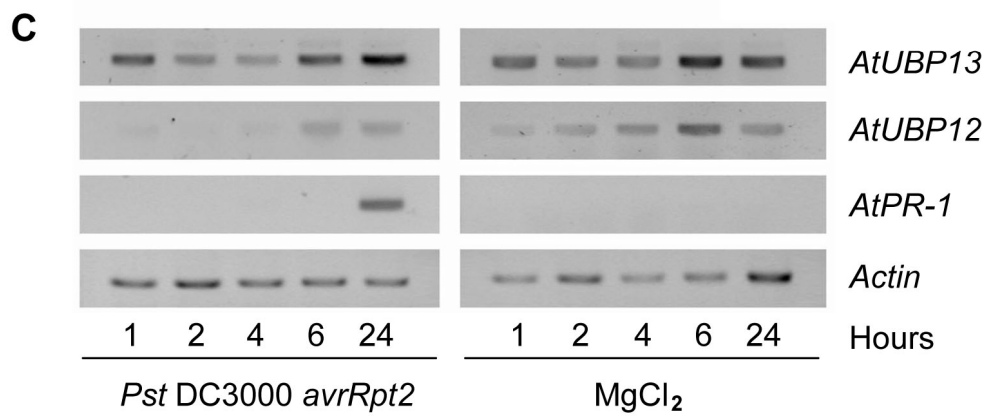
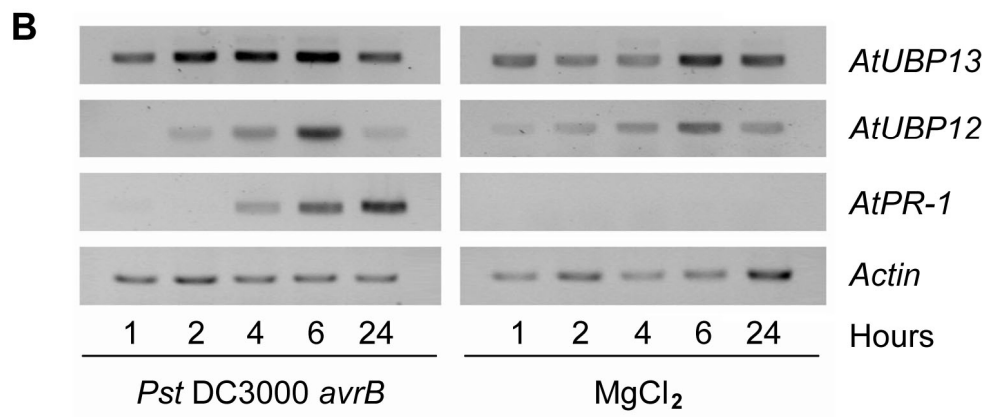
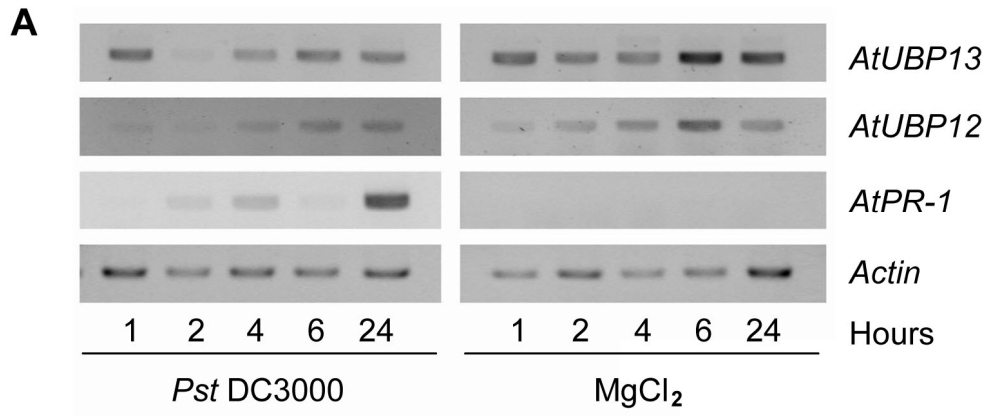
induction compared to *Pst* DC3000 *avrB* treatment between 1 and 6 hours. *PR-1* gene expression is induced at 24 hours post *Pst* DC3000 *avrRpt2* infiltration, at this timepoint *AtUBP12* and *AtUBP13* both show a minor induction with a 1.4 and 1.8 fold increase in expression respectively.

Infiltration of virulent *Pst* DC3000 was used to trigger PAMP associated basal defence signalling responses. Following *Pst* DC3000 treatment, gene expression profiles of *AtUBP12* and *AtUBP13* exhibited mild induction that was similar in magnitude and timing to that seen during wounding (Figure 3.3 A).

The observed transcriptional induction of *AtUBP12* and *AtUBP13* following avirulent *Pseudomonas syringae* pv. *tomato avrB* infection is at odds with the suppression of their *N. benthamiana* ortholog during pathogen *Pseudomonas* induced HR reported by Kim *et al.* (Kim *et al.*, 2006). The reported suppression of *NbUBP12* was relatively low (1.6 fold) but was detected in a high stringency microarray analysis of transcript alterations ( $p$  value  $\leq 0.01$ ) at 24 hours post inoculation of avirulent *Pseudomonas syringae* pv. *syringae* 61 (Kim *et al.*, 2006). The respective difference between timecourse experiments reported in this study and the single timepoint analysis reported by Kim *et al.* limits further comparison but both studies demonstrate the transcriptional alteration of plant UBPs genes during pathogen associated defence responses.

**Figure 3.3** Transcript analysis of *AtUbp12* and *AtUbp13* during infection with virulent and avirulent *Pseudomonas*.

*Arabidopsis* Col-0 plants were inoculated with *Pst* DC3000 (**A**), *Pst* DC3000 *avrB* (**B**) or *Pst* DC3000 *avrRpt2* (**C**) at  $1 \times 10^6$  cfu/ml, and leaves sampled at time points indicated. Total RNA was isolated and used for RT-PCR with specific primers for *AtUbp12* (27 cycles), *AtUbp13* (27 cycles), *PR-1* (27 cycles) and *Actin* (24 cycles).



### 3.3.2 Analysis of *AtUBP12* and *AtUBP13* gene expression following exogenous application of Salicylic Acid

Following the observed transcriptional induction of *AtUBP12* and *AtUBP13* during *Pst* DC3000 *avrB* stimulated HR, their induction by exogenous Salicylic Acid (SA) treatment was investigated using quantitative realtime RT-PCR.

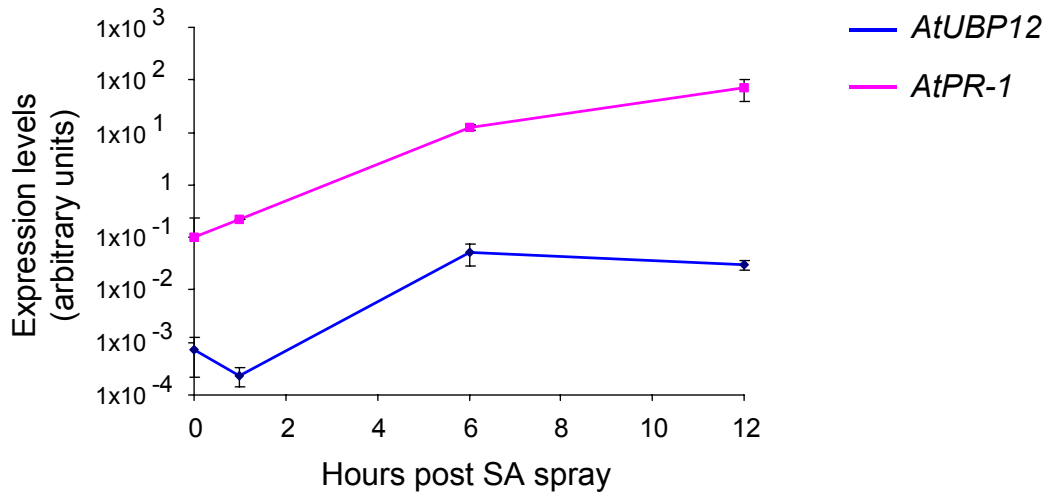
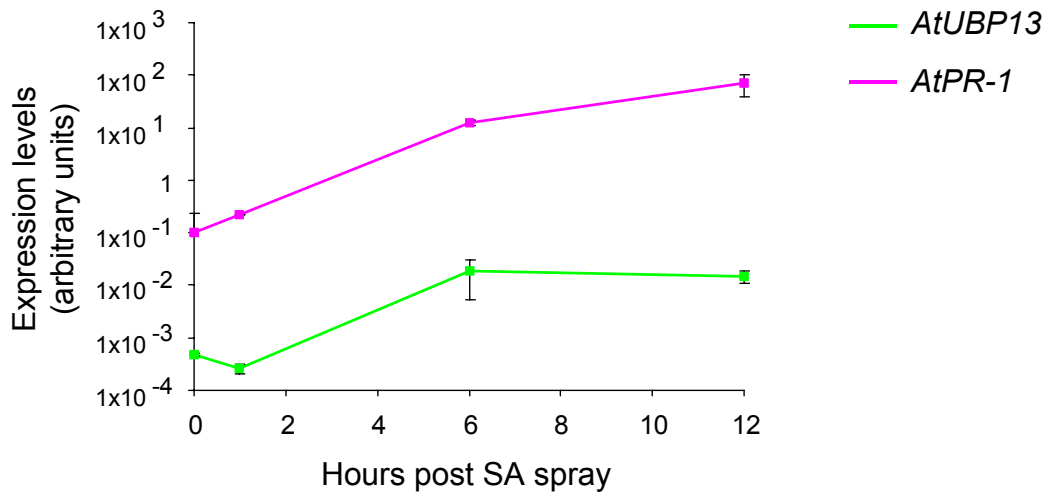
A key signal during the induction of plant disease resistance is the accumulation of SA in both local and systemic tissues. SA has been implicated in the potentiation of localised pathogen induced HR (Alvarez, 2000) and the induction of systemic acquired resistance (SAR) in response to a broad range of pathogens (Durrant and Dong, 2004). The perception of elevated SA levels leads to redox status changes in the cell which causes induction of pathogenesis-related (*PR*) genes leading to the activation of SAR (Durrant and Dong, 2004).

The activation of *PR* gene expression and SAR can be induced by the exogenous application of SA instead of pathogen inoculation (Dong, 2004). In this study, cDNA prepared from *Arabidopsis Landsberg erecta* (*L. er*) leaf tissue at various timepoints after spraying with 1mM SA (kindly donated by Dr A. Love) was analysed by realtime RT-PCR to investigate the transcriptional induction of *AtUBP12* and *AtUBP13* following SA treatment (Figure 3.4). Samples were normalised by analysis of the constitutively expressed *Actin2* gene (*Actin2\_REAL5* and *Actin2\_REAL3*) and increased expression of the SA responsive *PR-1* defence marker gene (Volko et al., 1998) was analysed as a positive control in this experiment using specific primers (*AtPR1\_REAL5* and *AtPR1\_REAL3*). At 6 hours after SA treatment, *PR-1* demonstrated a 200 fold increase in expression confirming the expected induction of a defence response.

The transcriptional response of *AtUBP12* and *AtUBP13* to SA treatment was analysed using specific primers for *AtUBP12* (*UBP12\_REAL5* and *UBP12\_REAL3*) and *AtUBP13* (*UBP13\_REAL5* and *UBP13\_REAL3*). Realtime PCR data indicated a similar, strong induction of both genes with an expression peak at 6 hours post SA treatment corresponding to an

**Figure 3.4** Expression pattern of *AtUbp12* and *AtUbp13* following salicylic acid treatment.

*Arabidopsis* Ler plants aged 4 weeks were sprayed with 1mM salicylic acid and leaves were sampled at timepoints indicated. Total RNA was isolated and used for quantitative real-time RT-PCR. Expression of *AtUbp12* (**A**) and *AtUbp13* (**B**) was normalised against *Actin2*. Each data point represents the mean of two biological replicates each analysed in duplicate, error bars represent one standard deviation. The *PR-1* defence marker gene was analysed as a positive experimental control.

**A****B**

approximate 70 fold and 40 fold change in expression level for *AtUBP12* and *AtUBP13* respectively (Figure 3.4). Measurement of transcript levels at 1 hour after SA spraying indicated a consistent, approximately 2 fold 'dip' in expression from initial levels for both *AtUBP12* and *AtUBP13* prior to the significant induction of both genes after 6 hours. Following the peak of induction, both *AtUBP12* and *AtUBP13* exhibited a limited reduction in expression by 12 hours post treatment (approximately 1.7 and 1.3 fold change respectively) (Figure 3.4).

The relatively heightened induction of *AtUBP12* and *AtUBP13* by exogenous SA application compared to avirulent *Pseudomonas syringae* infection may reflect the artificial nature of plant defence stimulation by exogenous hormone application. That expression of both *AtUBP12* and *AtUBP13* are highly induced following SA treatment suggests that they may be involved in disease resistance signalling. The timing of *AtUBP12* and *AtUBP13* expression corresponds to the 'late' class (4-8 hours) of SA responsive gene induction typically seen in the case of *PR* gene induction (Blanco et al., 2005). This data indicates that *AtUBP12* and *AtUBP13* may function together or redundantly to perceive the SA signal during disease resistance.

Key components of the SA signalling machinery including EDS1, PAD4 and NPR1 have been extensively characterised to establish the role of lipid signalling, redox status and reactive oxygen species in disease resistance signalling (Dong, 2004). That *AtUBP12* and *AtUBP13* are responsive to SA indicate that they may function downstream of signalling events that stimulate SA accumulation. The use of mutant *Arabidopsis* lines for further gene induction studies may provide further insight into the function of *AtUBP12* and *AtUBP13*. Using mutants of known SAR signalling components such as *sabp2* and *npr1* (Dong, 2004) for similar SA spraying experiments would allow assessment of *AtUBP12* and *AtUBP13* induction and their possible placement within specific disease signalling pathways.

### 3.3.3 Tissue distribution of *AtUBP12* and *AtUBP13* expression

RT-PCR analysis was performed on cDNA derived from different *Arabidopsis* tissues to examine expression of *AtUBP12* and *AtUBP13*. Gene expression was analysed in rosette leaf, cauline leaf, stem and unopened bud tissue from 4 week old wildtype Col-0 *Arabidopsis* grown under long days. Root tissue from plate grown Col-0 *Arabidopsis* seedlings was harvested three weeks after germination on vertical plates grown under long days. Gene expression was analysed using primers specific for *AtUBP12* (*AtUBP12\_RT5* and *AtUBP12\_RT3*) and *AtUBP13* (*AtUBP13\_RT5* and *AtUBP13\_RT3*). RT-PCR analysis detected expression of *AtUBP12* and *AtUBP13* in all tissues and indicated that expression of both genes was markedly higher in bud derived cDNA than any other tissue (Figure 3.5).

The reported RT-PCR data indicates a similar trend of expression for *AtUBP12* and *AtUBP13* in each respective tissue but suggests that *AtUBP13* is more highly expressed than *AtUBP12* (Figure 3.5). This relative difference in expression was not observed in rosette leaves where measurements conducted during realtime PCR analysis (Figure 3.4) indicated comparable expression levels of *AtUBP12* and *AtUBP13*. Differences in primer efficiency are a plausible explanation for the apparent difference in expression levels between *AtUBP12* and *AtUBP13* which could be more accurately assessed by northern blot or realtime PCR.

### 3.3.4 Promoter analysis of *AtUBP12* and *AtUBP13*

An analysis of *Arabidopsis* segmental genome duplication reported at The Institute for Genome Research (TIGR) confirmed the historic pairing of chromosomal regions containing *AtUBP12* and *AtUBP13* (Haas et al., 2004). The segmental duplication between their respective locations on chromosomes 5 and 3 was assigned to a larger polyploidy event occurring at some point between the *Arabidopsis-Brassica* split and *Arabidopsis-cotton* split estimated at 92 Mya (Blanc et al., 2003). The plant specific duplication of an ancestral UBP gene generating *AtUBP12* and *AtUBP13* is supported by the detection of single copy orthologs of *AtUBP12* in other

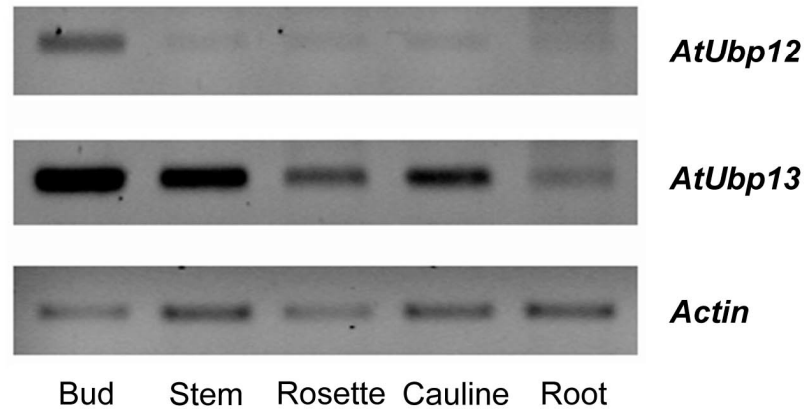


**Figure 3.5** Expression pattern of *AtUbp12* and *AtUbp13* in plant tissues.

RT-PCR analysis of total RNA extracted from various *Arabidopsis* tissues (bud, stem, rosette leaf, cauline leaf and root). Gene expression in tissue specific cDNA was analysed by PCR using specific primers for *AtUbp12* (27 cycles), *AtUbp13* (27 cycles) and *Actin* (25 cycles).

model eukaryotes. Gene annotation for *AtUBP12* and *AtUBP13* entries at TAIR based on InParanoid orthology genome analysis (Remm et al., 2001) reports the detection of single copy gene orthologs in model eukaryotes including *S. cerevisiae*, *C. elegans*, *D. melanogaster* and *H. sapiens*.

Analysis of upstream genomic regions for *AtUBP12* and *AtUBP13* indicates the presence of neighbouring genes within approximately 2000 base pairs. Alignment of upstream genomic DNA detected a putative common promoter region of approximately 300 bp demonstrating numerous regions of conservation between *AtUBP12* and *AtUBP13* (Figure 3.6). Data reported in this chapter indicates that *AtUBP12* and *AtUBP13* are differentially expressed in various untreated plant tissues but that both demonstrate induction in response to *Pst* DC3000 *avrB* and SA spraying. *AtUBP12* appears to be more responsive to tested stimuli than *AtUBP13*. These results indicate that transcriptional control of *AtUBP12* and *AtUBP13* may be a determinant in discriminating between cellular functions that are distinct, collaborative or redundant.

The promoter regions of *AtUBP12* and *AtUBP13* were screened for known pathogen associated W-box (TTGAC) and TGA-bZIP (TGACG) binding elements (Rowland and Jones, 2001) and also using the *Arabidopsis* promoter analysis tool Athena (O'Connor et al., 2005). Alignment approaches detected no TGA-bZIP or W-box binding sites in either promoter. Analysis using Athena indicated no significant enrichment of known promoter elements in the 1000 bp upstream of either *AtUBP12* or *AtUBP13*. There was also no significant conservation of any known promoter elements between *AtUBP12* and *AtUBP13*.

Despite the demonstration of coordinated transcriptional responses and regions of upstream conservation between *AtUBP12* and *AtUBP13*, this analysis failed to detect promoter sequence based evidence of their association. The association of *AtUBP12/AtUBP13* induction with established pathogen signalling may be easier to clarify by performing gene induction experiments in known disease resistance signalling mutants as previously discussed (Section 3.3.2).

```

AtUBP12  AGTTTTTGTATGACAGTAGCATCGTAAGTCTTATACGTGCCGCTT
AtUBP13  AGTTTTAAT-TGGTGACAGCATCTGAAGAGTCGTATATGTCGCAT

AtUBP12  TCTCATTGGTCTGTCTCGCTTGATAGACCCAACCTCGGAGAAA-T
AtUBP13  TCTCATTAGCCTGTCACGTTTCTCAGACGAACACTCAGGGAAACA

AtUBP12  TATAAATCTGAGCCCGTATACTG--TGAAATTACATTAATGACCC
AtUBP13  TATAAATCTGAATCCAATAGTAATTGGAATTACAATAGAAACCC

AtUBP12  TTTAAATTCTCGAAAATATCAGAATAATCAATATATCGAAGC-CG
AtUBP13  TT-AATTTAGTGAAAATATCGTAATTATCC---TATCGAAAAGTG

AtUBP12  AGAAAGAGTAAG-----AATGAGCGATTGTATTTCTCC--CTAA
AtUBP13  AGAAAGAGTAAGCAGAGAAATAAGCGATTG-ATCTCTCCTTCTGC

AtUBP12  GAGT-----CACTTTGCCTTTGTCTT-----
AtUBP13  AAGTTCTCTATTTCTTCCCTCACTTCTTCTTCTTCTTCTCCCCTT

AtUBP12  TGATTTTCTCTGTAT-CGTCGGTCTCTCTTTTGCCTTCTCTCGAT
AtUBP13  TCATTGTTCTCTCTGTTTCGGCG--CTCTCTTCTACTTCTCTCGAT

AtUBP12  CCACCGTCTAATCCTTCTCCGGCCAATG
AtUBP13  CCGACCGT-GAATCACTATCGGAGCAATG

```

**Figure 3.6** Alignment of 5' UTR promoter regions from *AtUbp12* and *AtUbp13*.

Alignment of genomic DNA region 300 bp upstream of *AtUbp12* and *AtUbp13* start codons (ATG boxed grey). Alignment colours indicate conservation (red), non-conservation (blue) or insertion (black).

### **3.4 Characterisation of *ubp12* and *ubp13* mutants alleles during *Pseudomonas syringae* infection**

The potential function of the *Arabidopsis* UBPs *AtUBP12* and *AtUBP13* in disease resistance signalling was analysed using a loss of function reverse genetics approach. In *Arabidopsis*, the principle reverse genetics approach is based on *Agrobacterium tumefaciens* transformation to insert T-DNA into the plant genome causing disruption of gene function (Krysan et al., 1999). The availability of large populations of T-DNA transformed *Arabidopsis* lines enables reverse genetic analysis of most genes. Multiple T-DNA insertion alleles for *AtUBP12* and *AtUBP13* were isolated and alterations in their response to virulent and avirulent strains of *Pseudomonas* were investigated.

#### **3.4.1 Isolation of homozygous UBP gene T-DNA insertion lines**

T-DNA insertional mutant lines for *AtUBP12* and *AtUBP13* were part of a larger collection of *Arabidopsis* DUB T-DNA insertion lines isolated during the initial stages of this study. *Arabidopsis* T-DNA insertion lines corresponding to 18 UBP genes were obtained from either the European Arabidopsis Stock Centre (NASC - Nottingham, UK) or GABI-Kat (Cologne, Germany) repositories and genotyped by PCR. From the obtained T-DNA insertion lines, 7 homozygous lines were isolated corresponding to insertions in *AtUBP8* (*ubp8-1*), *AtUBP11* (*ubp11-1*), *AtUBP12* (*ubp12-1* and *ubp12-2*), *AtUBP13* (*ubp13-1* and *ubp13-2*) and *AtUBP25* (*ubp25-1*) (Respective gene polymorphism identifiers from SALK and GABI-Kat are reported in appendix Table A3).

The zygosity of T-DNA insertion mutants was confirmed by PCR using internal T-DNA left border and gene specific primers. For genotyping purposes, gene specific primers were designed to flank the genomic T-DNA insertion site using protocols specified by SALK and GABI-Kat. To confirm the presence of T-DNA insertions, products were PCR amplified using a gene specific primer in combination with a T-DNA left border primer (SALK\_Lba1 or GK\_T-DNA). Zygosity status was confirmed using T-DNA

insertion flanking primers and PCR conditions that prevented product amplification in homozygous lines.

T-DNA insertion lines and genotyping primers are reported in appendix Tables A3 and A2 and genotyping results for *ubp8-1*, *ubp11-1*, *ubp12-1*, *ubp12-2*, *ubp13-1*, *ubp13-2* and *ubp-25* are presented in Figures 3.7 - 3.11.

The single allele mutants *ubp8-1*, *ubp11-1* and *ubp25-1* contain T-DNA insertions in their 6<sup>th</sup>, 8<sup>th</sup> and 4<sup>th</sup> introns respectively (Figure 3.7), disruption in expression of each corresponding gene remains to be established. The *ubp12-1* and *ubp12-2* alleles contain a T-DNA insertion within the 15<sup>th</sup> intron (Figure 3.8 A) and 28<sup>th</sup> exon (Figure 3.9 A) respectively. The *ubp13-1* and *ubp13-2* alleles contain a T-DNA insertion within the 5<sup>th</sup> exon (Figure 3.10 A) and 21<sup>st</sup> exon (Figure 3.11 A) respectively. For each *ubp12* and *ubp13* allele, insertion bands were cloned and sequenced to verify the location of the T-DNA insertion.

Disruption of mRNA expression was checked in *ubp12* and *ubp13* alleles by RT-PCR. Primers were designed from respective cDNAs to amplify products corresponding to full length transcript (FL) or upstream (5') and downstream (3') regions relative to the T-DNA insertion site (Figures 3.8 - 3.11). Given the high level of nucleotide identity between *AtUBP12* and *AtUBP13* cDNAs (86%), a primary consideration in RT-PCR primer design was the possibility of cross hybridisation of *AtUBP12* primers to *AtUBP13* mRNA and vice versa.

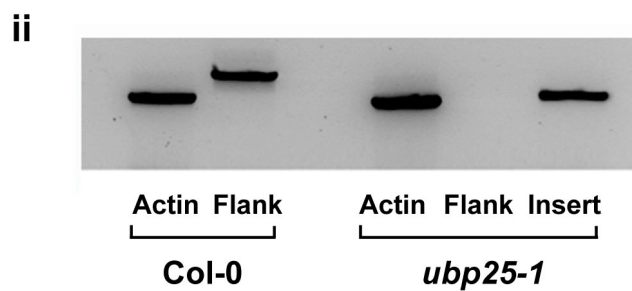
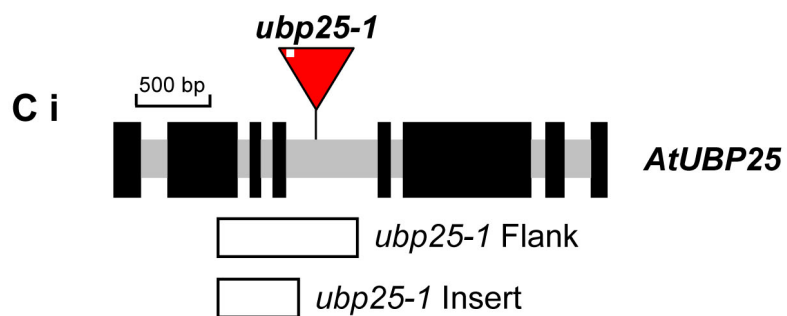
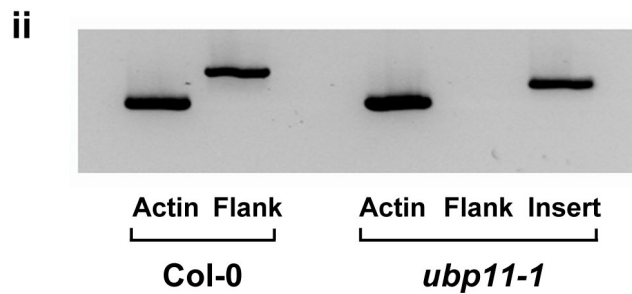
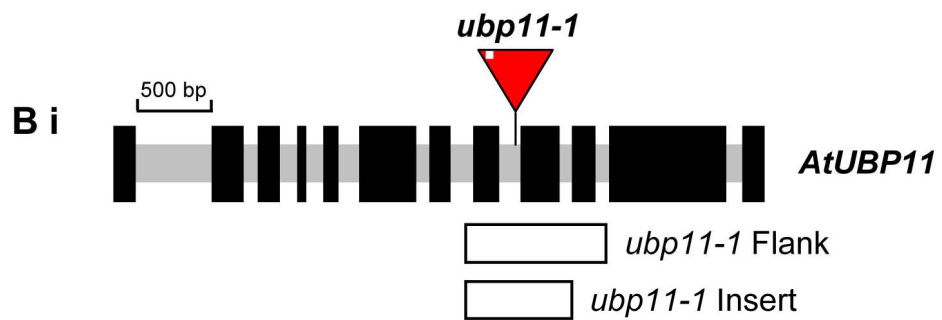
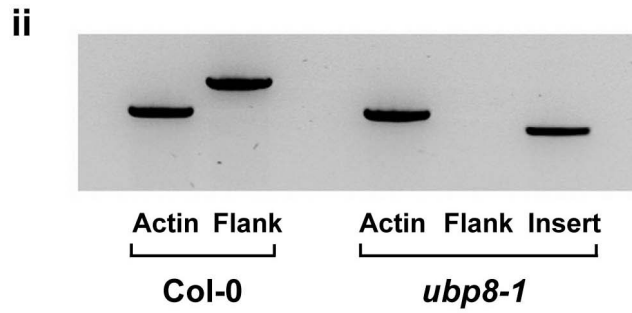
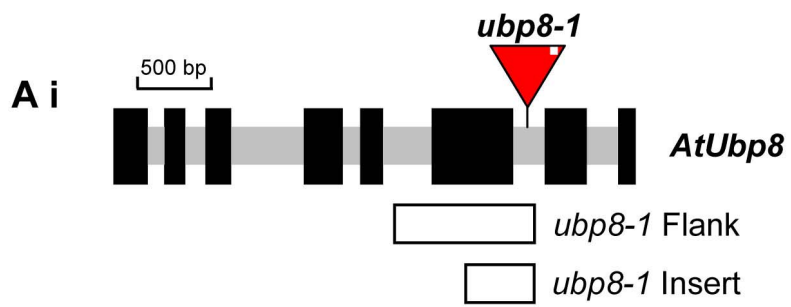
To avoid this scenario, regions of insertion and maximum degeneracy between *AtUBP12* and *AtUBP13* cDNAs were selected for primer design and maximum primer annealing temperatures were established by gradient PCR. There were typically at least 5 base pair mismatches between *AtUBP12* and *AtUBP13* cDNAs in each RT-PCR primer designed for transcript analysis. Primer details and a full length alignment between *AtUBP12* and *AtUBP13* cDNAs are reported in appendix Table A2 and Figure A1.

**Figure 3.7** Genotyping *ubp8-1*, *ubp11-1* and *ubp25-1* alleles.

**(Ai)** Gene structure of *AtUBP8* where exons and introns are represented as black and grey boxes respectively. Location of *ubp8-1* T-DNA insertion is indicated by a red triangle within which a white box indicates the position of the T-DNA left border. PCR genotyping amplicons for *ubp8-1* insert flanking primers (*ubp8-1* Flank) and *ubp8-1* insert specific primers (*ubp8-1* Insert) are indicated by white boxes. **(Aii)** PCR genotyping results for *ubp8-1* allele. Appropriate PCR reactions were completed using Col-0 and *ubp8-1* genomic DNA with primers for *Actin* (30 cycles), *ubp8-1* Flank (30 cycles) or *ubp8-1* Insert (30 cycles).

**(Bi)** Gene structure of *AtUBP11* where exons and introns are represented as black and grey boxes respectively. Location of *ubp11-1* T-DNA insertion is indicated by a red triangle within which a white box indicates the position of the T-DNA left border. PCR genotyping amplicons for *ubp11-1* insert flanking primers (*ubp11-1* Flank) and *ubp11-1* insert specific primers (*ubp11-1* Insert) are indicated by white boxes. **(Bii)** PCR genotyping results for *ubp11-1* allele. Appropriate PCR reactions were completed using Col-0 and *ubp11-1* genomic DNA with primers for *Actin* (30 cycles), *ubp11-1* Flank (30 cycles) or *ubp11-1* Insert (30 cycles).

**(Ci)** Gene structure of *AtUBP25* where exons and introns are represented as black and grey boxes respectively. Location of *ubp25-1* T-DNA insertion is indicated by a red triangle within which a white box indicates the position of the T-DNA left border. PCR genotyping amplicons for *ubp25-1* insert flanking primers (*ubp25-1* Flank) and *ubp25-1* insert specific primers (*ubp25-1* Insert) are indicated by white boxes. **(Cii)** PCR genotyping results for *ubp25-1* allele. Appropriate PCR reactions were completed using Col-0 and *ubp25-1* genomic DNA with primers for *Actin* (30 cycles), *ubp25-1* Flank (30 cycles) or *ubp25-1* Insert (30 cycles).



RT-PCR analysis failed to detect near full length *AtUBP12* mRNA species in both *ubp12-1* and *ubp12-2* alleles relative to wildtype control cDNA (Figure 3.8 B and Figure 3.9 B). PCR products corresponding to upstream and downstream *AtUBP12* mRNA regions were not detected in the *ubp12-1* allele (Figure 3.8 B). In the case of the *ubp12-2* allele, PCR products corresponding to upstream and downstream mRNA regions were amplified (Figure 3.8 B), but their accumulation was strongly reduced in comparison to wild type cDNA (cDNA content was considered comparable based on *Actin2* PCR product amplification). Examination of *AtUBP13* mRNA expression in *ubp13-1* and *ubp13-2* alleles by RT-PCR failed to detect full length, upstream or downstream PCR products relative to wildtype control cDNA (Figures 3.10 B and 3.11 B).

Gene models of *AtUBP12* (AT5G06600.1) and *AtUBP13* (AT3G11910.1) reported at TAIR indicate the existence of 2 splice variants of *AtUBP12* (AT5G06600.2 and AT5G06600.3) but no splice variants of *AtUBP13*. Splice variants of *AtUBP12* correspond to a 3 bp deletion (AT5G06600.2) resulting in the loss of amino acid residue Q11 or the premature termination of transcription after exon 27 (AT5G06600.3) resulting in a truncated 2958 bp transcript compared to 3351 bp in full length *AtUBP12* (AT5G06600.1). The truncated mRNA produced from the *AtUBP12* (AT5G06600.3) splice variant produces a corresponding protein lacking 132 amino acids at the C-terminus relative to full length *AtUBP12*.

The T-DNA insertion in *ubp12-2* is located in exon 28 (Figure 3.9) and may potentially allow expression of the *AtUBP12* (AT5G06600.3) splice variant as opposed to the *ubp12-1* allele which has a T-DNA insertion in intron 15 and should consequently disrupt the expression of full length *AtUBP12* and both of its splice variants (Figure 3.8).

The 5' upstream amplicon detected in RT-PCR analysis of *AtUBP12* mRNA expression in *ubp12-2* (Figure 3.9 B) may correspond to the *AtUBP12* (AT5G06600.3) splice variant rather than reduced levels of full length *AtUBP12* (AT5G06600.1). In this case, RT-PCR analysis suggests that expression of the *AtUBP12* (AT5G06600.3) splice variant is significantly lower than full length *AtUBP12* although the relative expression levels of

full length and splice variant *AtUBP12* in a non-mutant background remain to be established.

Analysis of cDNA derived from *ubp12* and *ubp13* mutant lines indicated that all four alleles had disrupted gene expression resulting from T-DNA insertion. In all cases, full length mRNA was not detectable indicating that each line was suitable for loss of function studies for the respective gene. Based on the location of T-DNA inserts, the isolated *ubp12-2* allele may not alter expression of the *AtUBP12* (AT5G06600.3) splice variant whereas the *ubp12-1* allele abolishes full length and splice variants to equal effect. The possibility of additional, distal T-DNA insertion events in each allele was not investigated as the potential influence of additional insertions could be discounted based on the phenotypic assessment of multiple isolated alleles.

UBP allele	mRNA region	5' primer	3' primer	Amplicon size (bp)
ubp12-1	<i>ubp12-1</i> FL	U12-1_FL_5	U12-1_FL_3	3162
ubp12-1	<i>ubp12-1</i> 5'	U12-1_FL_5	U12-1_5P_3	1910
ubp12-1	<i>ubp12-1</i> 3'	U12-1_3P_5	U12-1_FL_3	505
ubp12-2	<i>ubp12-2</i> FL	U12-1_FL_5	U12-1_FL_3	3162
ubp12-2	<i>ubp12-2</i> 5'	U12-1_FL_5	U12-1_5P_3	1910
ubp12-2	<i>ubp12-2</i> 3'	U12-2_3P_5	U12-1_FL_3	126
ubp13-1	<i>ubp13-1</i> FL	U13-1_FL_5	U13-1_FL_3	3348
ubp13-1	<i>ubp13-1</i> 5'	U13-1_5P_5	U13-1_5P_3	401
ubp13-1	<i>ubp13-1</i> 3'	U13-1_3P_5	U13-1_3P_3	1207
ubp13-2	<i>ubp13-2</i> FL	U13-1_FL_5	U13-1_FL_3	3348
ubp13-2	<i>ubp13-2</i> 5'	U13-2_5P_5	U13-2_5P_3	1977
ubp13-2	<i>ubp13-2</i> 3'	U13-2_3P_5	U13-2_3P_3	803

**Table 3.2** Primers for RT-PCR transcript analysis in *ubp12* and *ubp13* alleles.

**Figure 3.8** Genotyping and *AtUBP12* transcript analysis of the *ubp12-1* allele.

**(Ai)** Gene structure of *AtUBP12* where exons and introns are represented as black and grey boxes respectively. Location of *ubp12-1* T-DNA insertion is indicated by a red triangle within which a white box indicates the position of the T-DNA left border. PCR genotyping amplicons for *ubp12-1* insert flanking primers (*ubp12-1* Flank) and *ubp12-1* insert specific primers (*ubp12-1* Insert) are indicated by white boxes. **(Aii)** PCR genotyping results for *ubp12-1* allele. Appropriate PCR reactions were completed using Col-0 and *ubp12-1* genomic DNA with primers for *Actin* (28 cycles), *ubp12-1* Flank (28 cycles) or *ubp12-1* Insert (28 cycles).

**(Bi)** *AtUBP12* mRNA diagram indicating position of amplicons analysed by RT-PCR to examine *AtUBP12* mRNA expression in the *ubp12-1* allele. *AtUBP12* mRNA and internal RT-PCR amplicons are represented as black and white boxes respectively. Amplicons corresponding to near full length mRNA (*ubp12-1* FL), upstream of the T-DNA insertion (*ubp12-1* 5') and downstream of the T-DNA insertion (*ubp12-1* 3') are indicated. **(Bii)** RT-PCR transcript analysis in *ubp12-1*. Appropriate PCR cycles were completed using Col-0 and *ubp12-1* cDNA with primers for *Actin* (25 cycles), *ubp12-1* FL (38 cycles), *ubp12-1* 5' (36 cycles) and *ubp12-1* 3' (31 cycles).

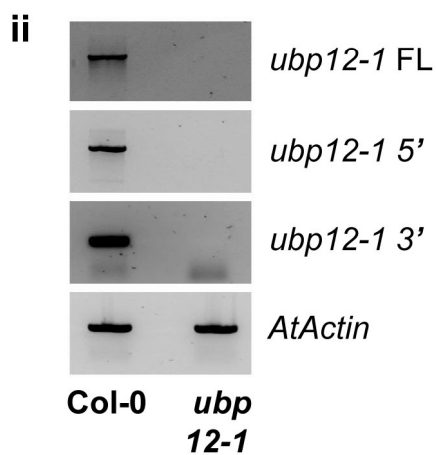
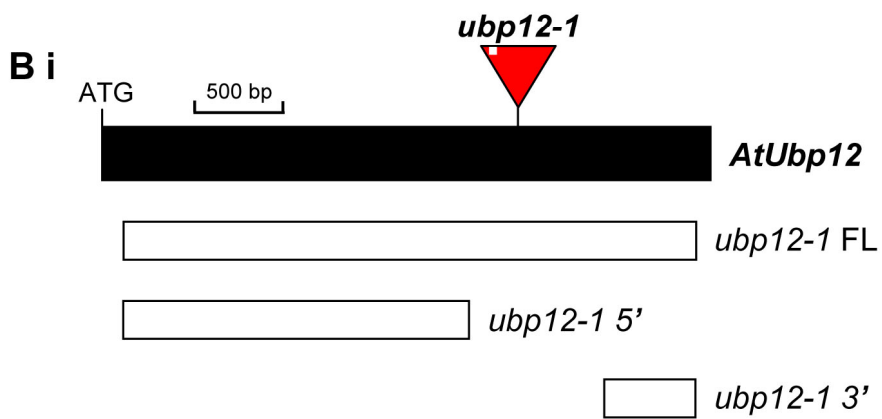
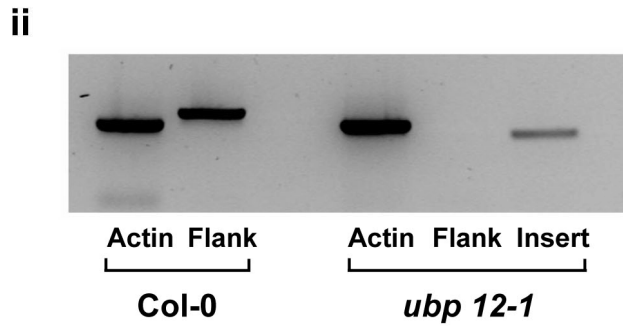
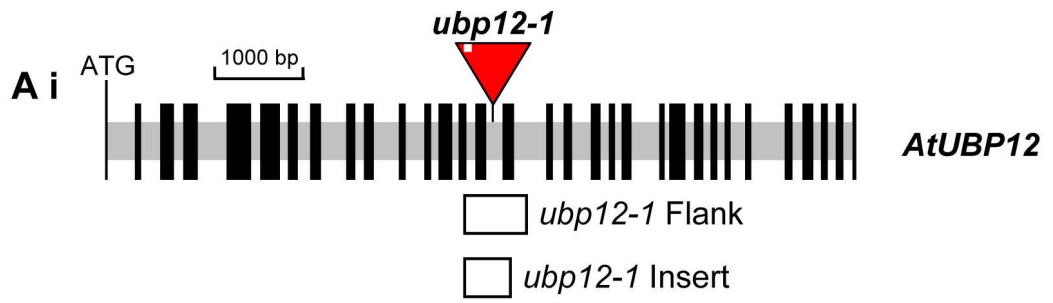


**Figure 3.9** Genotyping and *AtUBP12* transcript analysis of the *ubp12-2* allele.

**(Ai)** Gene structure of *AtUBP12* where exons and introns are represented as black and grey boxes respectively. Location of *ubp12-2* T-DNA insertion is indicated by a red triangle within which a white box indicates the position of the T-DNA left border. PCR genotyping amplicons for *ubp12-2* insert flanking primers (*ubp12-2* Flank) and *ubp12-2* insert specific primers (*ubp12-2* Insert) are indicated by white boxes. **(Aii)** PCR genotyping results for *ubp12-2* allele. Appropriate PCR reactions were completed using Col-0 and *ubp12-2* genomic DNA with primers for *Actin* (28 cycles), *ubp12-2* Flank (28 cycles) or *ubp12-2* Insert (28 cycles).

**(Bi)** *AtUBP12* mRNA diagram indicating position of amplicons analysed by RT-PCR to examine *AtUBP12* mRNA expression in the *ubp12-2* allele. *AtUBP12* mRNA and internal RT-PCR amplicons are represented as black and white boxes respectively. Amplicons corresponding to near full length mRNA (*ubp12-2* FL), upstream of the T-DNA insertion (*ubp12-2* 5') and downstream of the T-DNA insertion (*ubp12-2* 3') are indicated. **(Bii)** RT-PCR transcript analysis in *ubp12-2*. Appropriate PCR cycles were completed using Col-0 and *ubp12-2* cDNA with primers for *Actin* (25 cycles), *ubp12-2* FL (38 cycles), *ubp12-2* 5' (36 cycles) and *ubp12-2* 3' (35 cycles).

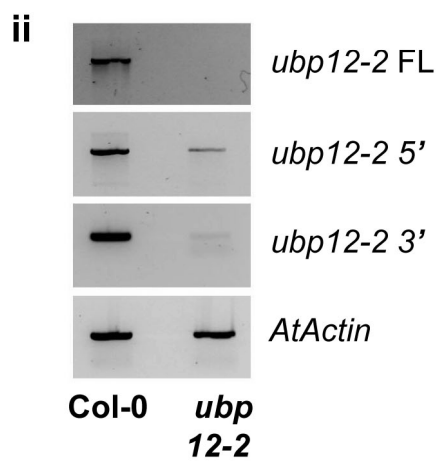
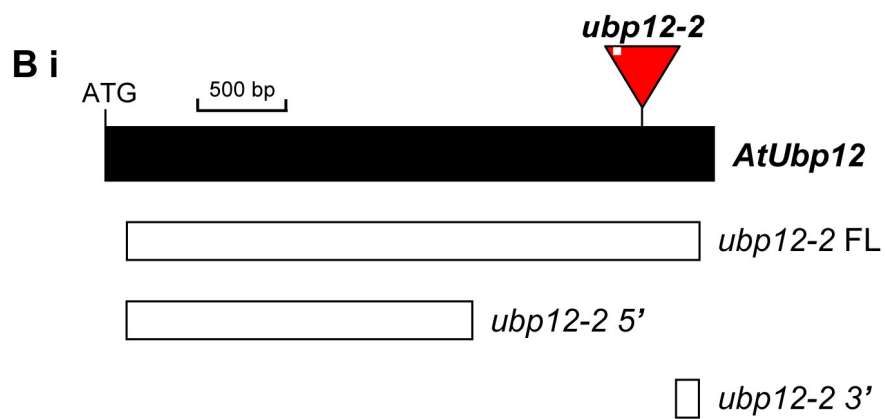
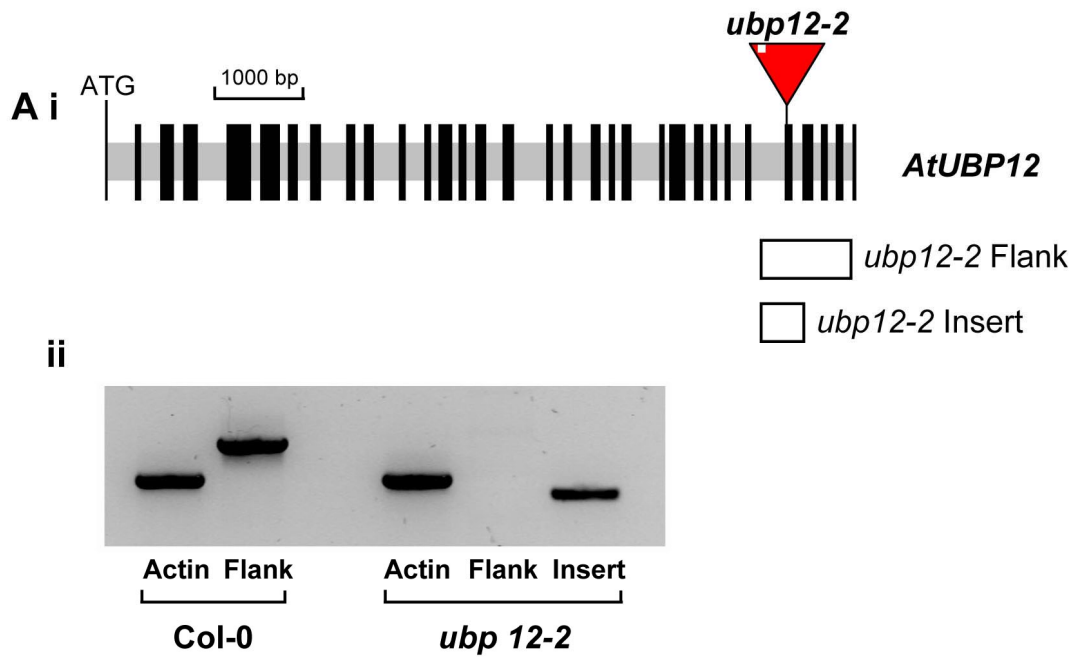


**Figure 3.10** Genotyping and *AtUBP13* transcript analysis of the *ubp13-1* allele.

(Ai) Gene structure of *AtUBP13* where exons and introns are represented as black and grey boxes respectively. Location of *ubp13-1* T-DNA insertion is indicated by a red triangle within which a white box indicates the position of the T-DNA left border. PCR genotyping amplicons for *ubp13-1* insert flanking primers (*ubp13-1* Flank) and *ubp13-1* insert specific primers (*ubp13-1* Insert) are indicated by white boxes. (Aii) PCR genotyping results for *ubp13-1* allele. Appropriate PCR reactions were completed using Col-0 and *ubp13-1* genomic DNA with primers for *Actin* (28 cycles), *ubp13-1* Flank (28 cycles) or *ubp13-1* Insert (28 cycles).

(Bi) *AtUBP13* mRNA diagram indicating position of amplicons analysed by RT-PCR to examine *AtUBP13* mRNA expression in the *ubp13-1* allele. *AtUBP13* mRNA and internal RT-PCR amplicons are represented as black and white boxes respectively. Amplicons corresponding to full length mRNA (*ubp13-1* FL), upstream of the T-DNA insertion (*ubp13-1* 5') and downstream of the T-DNA insertion (*ubp13-1* 3') are indicated. (Bii) RT-PCR transcript analysis in *ubp13-1*. Appropriate PCR cycles were completed using Col-0 and *ubp13-1* cDNA with primers for *Actin* (25 cycles), *ubp13-1* FL (45 cycles), *ubp13-1* 5' (33 cycles) and *ubp13-1* 3' (43 cycles).

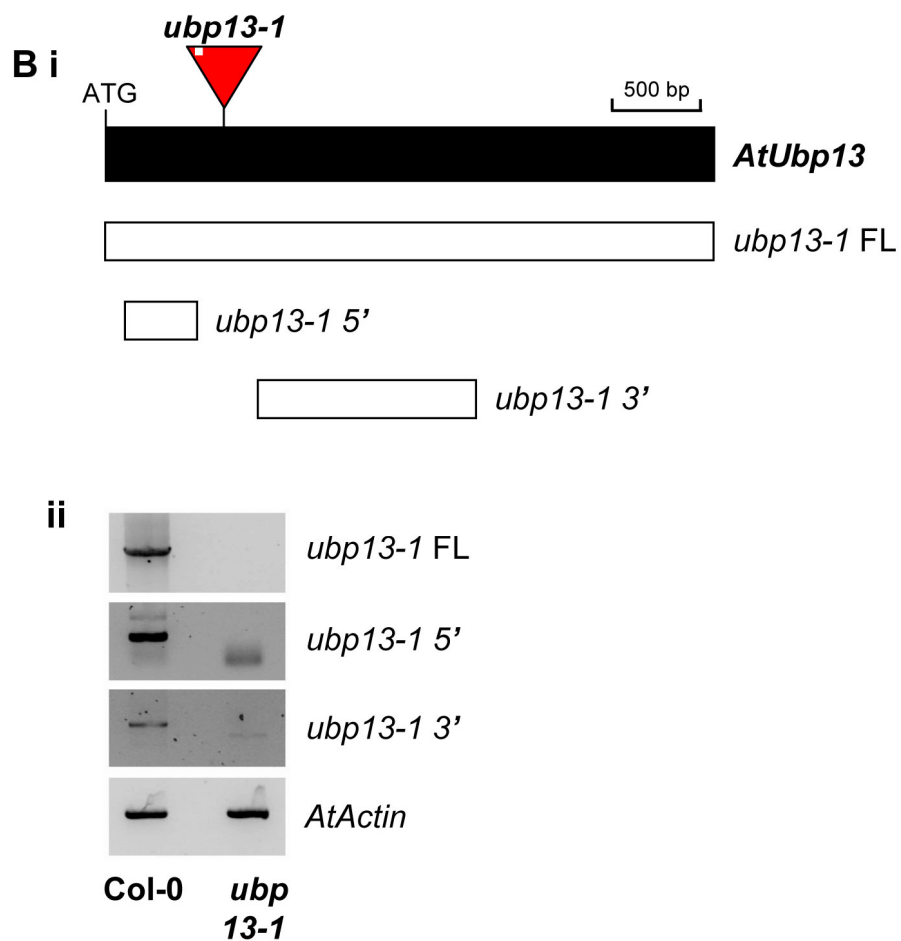
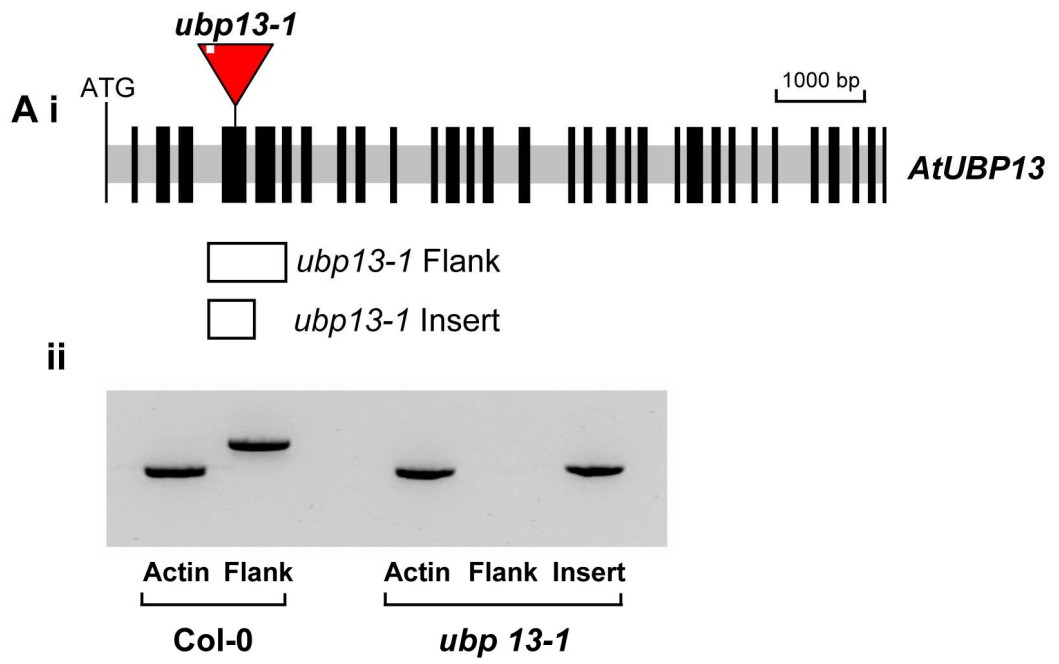
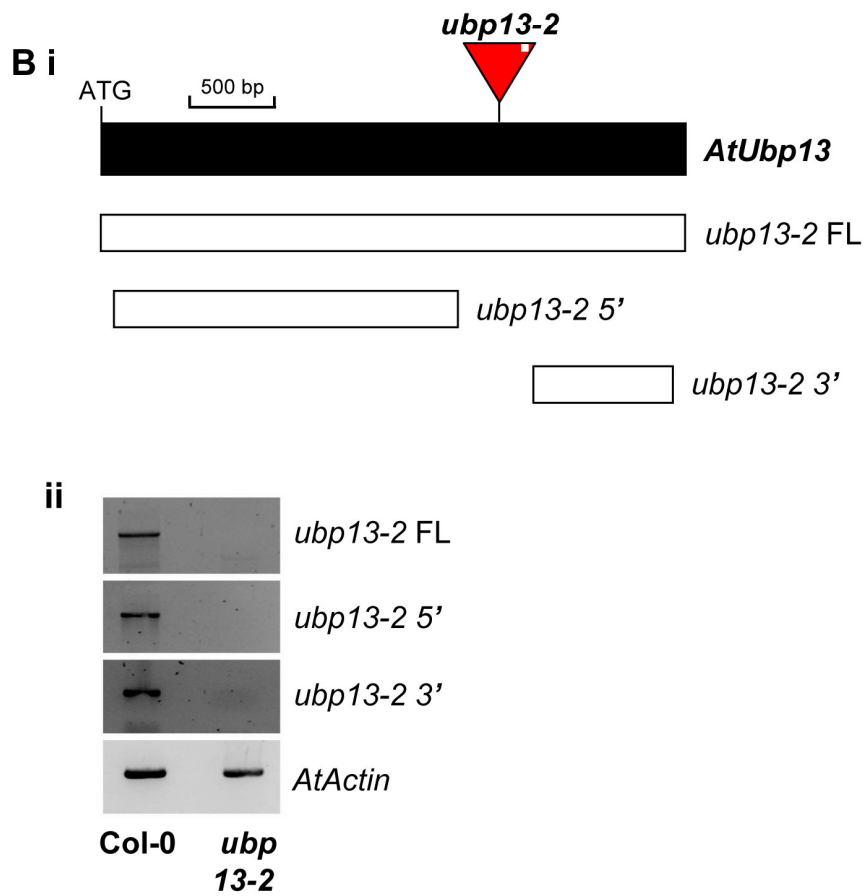
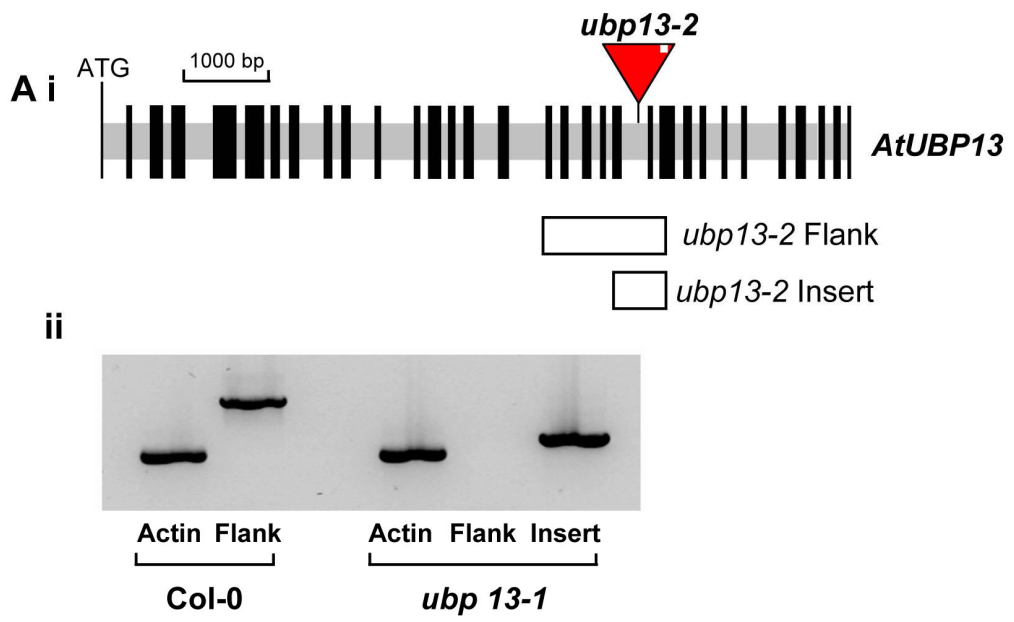


**Figure 3.11** Genotyping and *AtUBP13* transcript analysis of the *ubp13-2* allele.

(Ai) Gene structure of *AtUBP13* where exons and introns are represented as black and grey boxes respectively. Location of *ubp13-2* T-DNA insertion is indicated by a red triangle within which a white box indicates the position of the T-DNA left border. PCR genotyping amplicons for *ubp13-2* insert flanking primers (*ubp13-2* Flank) and *ubp13-2* insert specific primers (*ubp13-2* Insert) are indicated by white boxes. (Aii) PCR genotyping results for *ubp13-2* allele. Appropriate PCR reactions were completed using Col-0 and *ubp13-2* genomic DNA with primers for *Actin* (28 cycles), *ubp13-2* Flank (28 cycles) or *ubp13-2* Insert (28 cycles).

(Bi) *AtUBP13* mRNA diagram indicating position of amplicons analysed by RT-PCR to examine *AtUBP13* mRNA expression in the *ubp13-2* allele. *AtUBP13* mRNA and internal RT-PCR amplicons are represented as black and white boxes respectively. Amplicons corresponding to full length mRNA (*ubp13-2* FL), upstream of the T-DNA insertion (*ubp13-2* 5') and downstream of the T-DNA insertion (*ubp13-2* 3') are indicated. (Bii) RT-PCR transcript analysis in *ubp13-2*. Appropriate PCR cycles were completed using Col-0 and *ubp13-2* cDNA with primers for *Actin* (25 cycles), *ubp13-2* FL (45 cycles), *ubp13-2* 5' (34 cycles) and *ubp13-2* 3' (36 cycles).



### 3.4.2 *Pseudomonas syringae* growth assays in *ubp12* and *ubp13* null mutants

Isolated *ubp12* and *ubp13* mutant lines were infected with virulent and avirulent strains of *Pseudomonas syringae* pv. *tomato* DC3000 to assess perturbations in disease resistance. As previously discussed, to trigger HR through *RPM1* or *RPS2* *R* genes, plants were infected with *Pst* DC3000 expressing *avrB* and *avrRpt2* avirulence factors respectively.

Short day grown plants, aged 5 - 6 weeks were infected by spray inoculation of high titre *Pseudomonas* strains ( $1 \times 10^8$  cfu/ml) as described by Zipfel *et al.* (Zipfel *et al.*, 2004). Infected plants were returned to short day growth conditions under high humidity and bacterial growth was measured after 72 hours by colony counting (Figures 3.12 and 3.13). In each experiment, plants were infected with virulent *Pst* DC3000 to test for alterations in basal PAMP triggered defence and serve as an empty vector control for comparison against tested avirulent *Pst* strains.

Colony count data indicated no significant difference in resistance between Col-0 control and *ubp12* and *ubp13* mutant alleles during *Pseudomonas* infection. Virulent *Pst* DC3000 demonstrated approximately  $7.5 \log \text{ cfu/cm}^2$  growth on each plant line at 72 hours post infection in two independent experiments (Figures 3.12 and 3.13). Avirulent *Pst* DC3000 strains containing *avrB* or *avrRpt2* demonstrated 4 and  $5.5 \log \text{ cfu/cm}^2$  growth respectively on each plant line at 72 hours post infection (Figure 3.12 and Figure 3.13). Bacterial growth measurements were based on six independent replicates and t-tests confirmed that observed differences in mean growth were not significant (Figure 3.12 and Figure 3.13).

Bacterial growth assays were previously conducted on *ubp12-1* and *ubp13-1* mutant lines using pressure inoculation to deliver virulent and avirulent *Pseudomonas* strains into the apoplast. Bacterial growth measurements were recorded at two time points during infection (72 and 96 hours post infection), results obtained in these experiments indicated no significant difference in bacterial growth (data not shown) and were in agreement with results presented in Figures 3.12 and 3.13.

**Figure 3.12** Bacterial growth assay of *Pst* DC3000 and *Pst* DC3000 *avrB* on *ubp12* and *ubp13* mutant lines.

Growth of *Pst* DC3000 (**A**) and *Pst* DC3000 *avrB* (**B**) on *Arabidopsis* Col-0, *ubp12-1*, *ubp12-2*, *ubp13-1* and *ubp13-2* lines. Bacterial growth was measured three days after spray inoculation, each data point represents the mean and standard deviation of six replicates. Statistical significance of observed growth differences were assessed by two sided t-test where a p value equal to or less than 0.05 was considered significant.

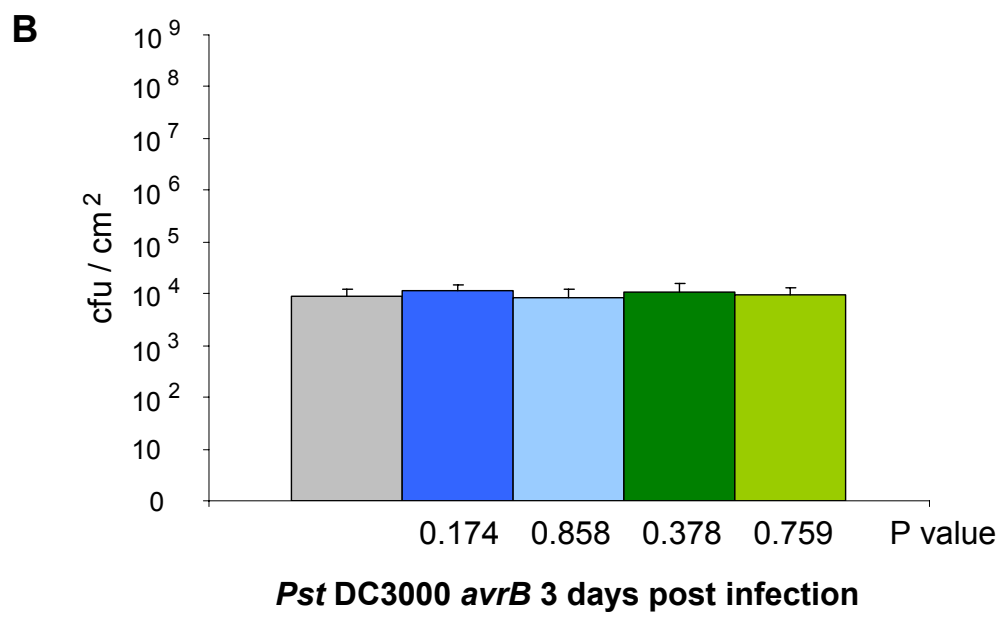
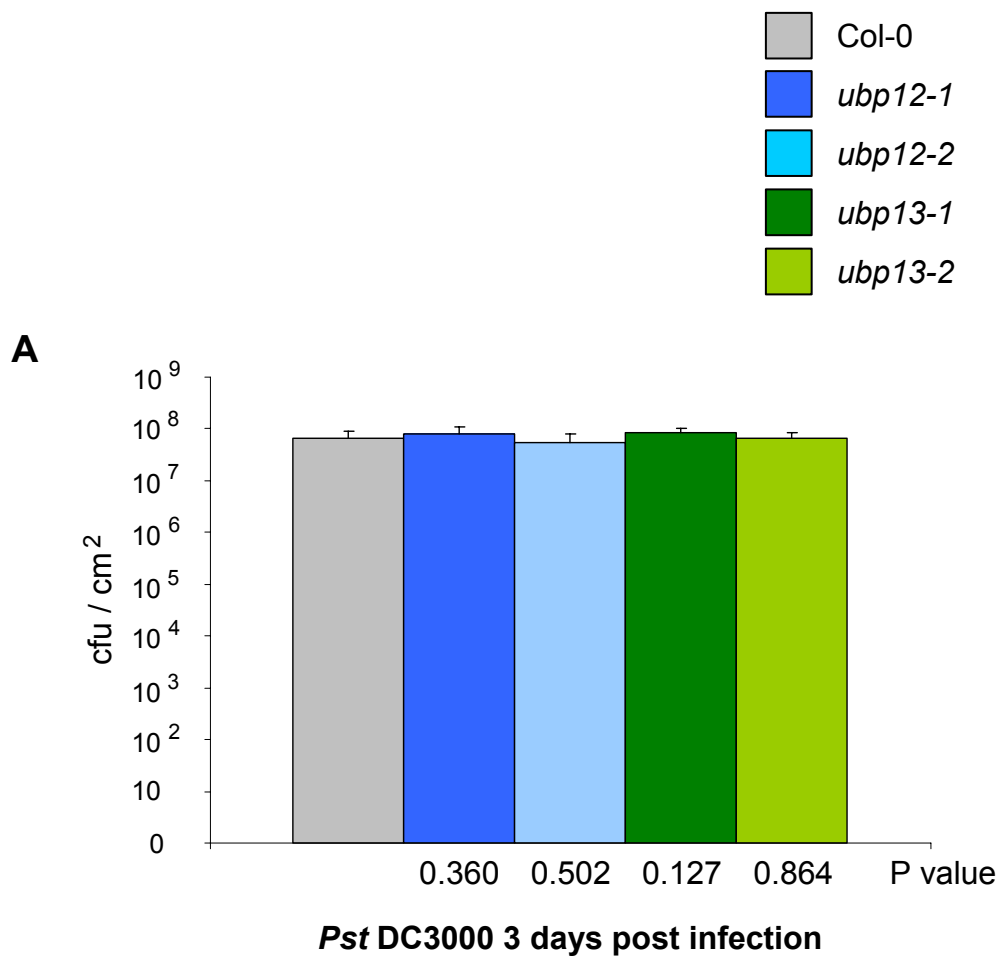
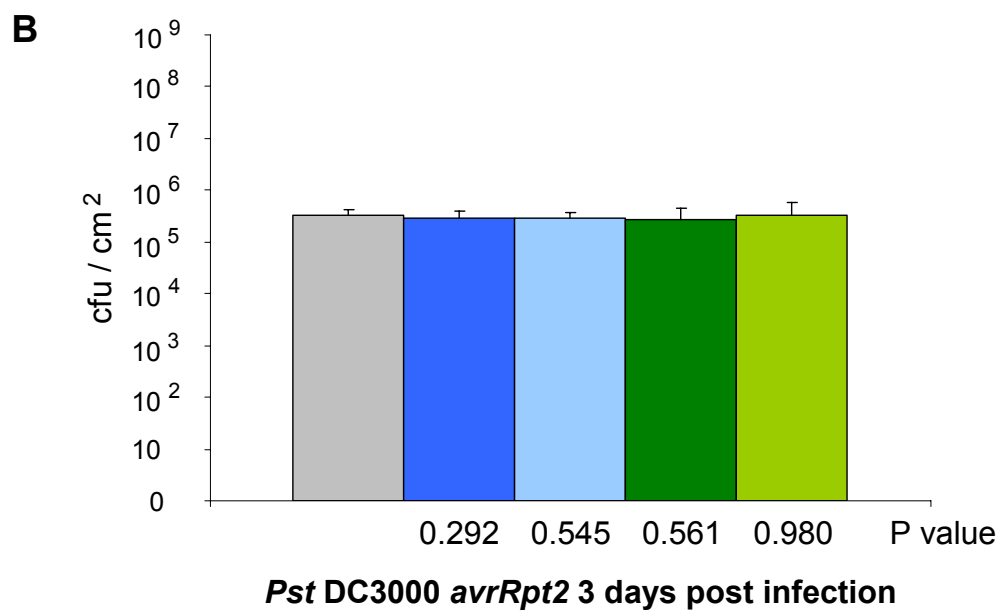
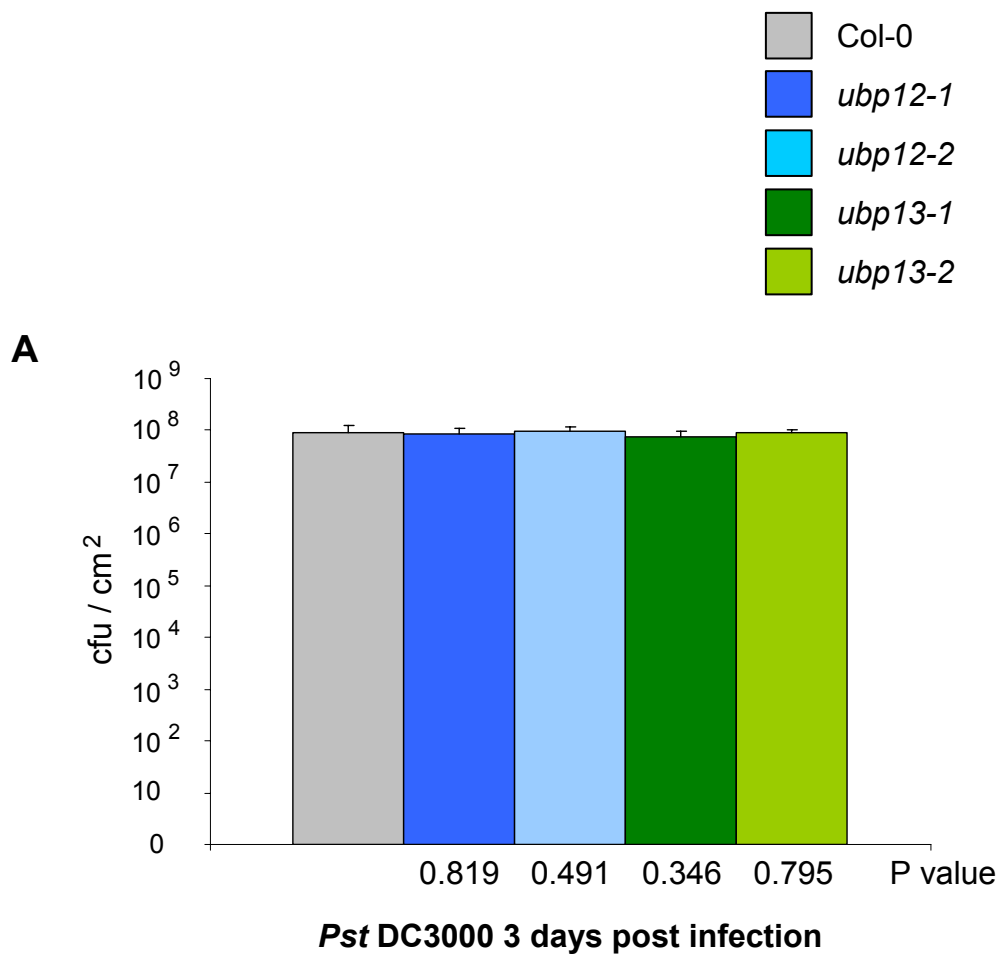


**Figure 3.13** Bacterial growth assay of *Pst* DC3000 and *Pst* DC3000 *avrRpt2* in *ubp12* and *ubp13* mutant lines.

Growth of *Pst* DC3000 (**A**) and *Pst* DC3000 *avrRpt2* (**B**) on *Arabidopsis* Col-0, *ubp12-1*, *ubp12-2*, *ubp13-1* and *ubp13-2* lines. Bacterial growth was measured three days after spray inoculation, each data point represents the mean and standard deviation of six replicates. Statistical significance of observed growth differences were assessed by two sided t-test where a p value equal to or less than 0.05 was considered significant.



### 3.5 *ubp12* mutants exhibit an early flowering phenotype

In the initial stages of this study, homozygous T-DNA insertion alleles of several UBP genes were isolated (Section 3.4). Growth of *ubp8-1*, *ubp11-1* and *ubp25-1* under long day conditions indicated no obvious morphological differences to Col-0 WT plants (data not shown). These findings were confirmed in a recent screen for *Arabidopsis* developmental phenotypes in a collection of 39 mutant alleles corresponding to 25 of the 27 UBP genes (Liu et al., 2008). Liu *et al.* reported no detectable phenotype in *ubp8*, *ubp11* and *ubp25* mutants (Liu et al., 2008) (where *ubp8* and *ubp11* mutant alleles were identical to SALK *ubp8-1* and *ubp11-1* alleles isolated in this study - appendix Table A3)

Mutant *ubp12* lines were not analysed by Liu *et al.* (Liu et al., 2008), but results obtained in this study demonstrate that *ubp12-1* and *ubp12-2* alleles exhibit an early flowering phenotype which is particularly prevalent under short day growth conditions (Figure 3.14).

The angiosperm shoot can be described as a series of repeating units termed phytomers that are formed sequentially by the shoot apical meristem (SAM). The basic phytomer structure consists of a node with the associated leaf, axillary meristem and internode region (Schultz and Haughn, 1991). In *Arabidopsis* the SAM undergoes phase change, first producing rosette phytomers consisting of a large vegetative leaves separated by short internodes. At the floral transition, several lateral shoot bearing phytomers are produced with smaller cauline leaves and elongated internodes followed by the determinate floral meristem (McSteen and Leyser, 2005).

The transition from the vegetative phase to flowering and reproductive growth is governed by the interplay of endogenous signalling pathways and environmental cues. Molecular characterisation of *Arabidopsis* mutants with altered flowering phenotypes has led to a current model of flowering control which is regulated by the interplay of physical, chemical and biological signals. Currently, four genetic flowering pathways have been defined termed: light dependent pathway, gibberellin pathway,

vernalisation pathway and the autonomous pathway (Komeda, 2004). Separate environmental signals are perceived by these distinct pathways but they eventually converge to initiate expression of common downstream floral morphogenesis genes (Komeda, 2004). *Arabidopsis* is a facultative long day plant which flowers in response to long days (16 hour photoperiod) but also eventually flowers under short days (8 hour photoperiod) after a prolonged vegetative growth phase (Mouradov et al., 2002).

The early flowering phenotype of *ubp12* mutants was scored as an index of the number of rosette leaves present at the initiation of flowering under long and short day photoperiods (Figure 3.15). Early flowering was apparent in both mutant alleles of *ubp12* under long day photoperiods but was far more conspicuous under short day conditions (Figure 3.15). Under short days, *ubp12-1* and *ubp12-2* alleles flowered with an average of 14 and 13 rosette leaves respectively compared to 67 rosette leaves in Col-0 WT controls (Figure 3.15 A). Under long days, *ubp12-1* and *ubp12-2* alleles both flowered with an average of 7 rosette leaves compared to 8 in Col-0 WT controls (Figure 3.15 B). T-test analysis confirmed that *ubp12* early flowering was significant under short days (average  $p = 0.0001$ ) and significant under long days (average  $p = 0.0158$ ).

The flowering of *ubp13* mutant alleles was also scored under short and long days (Figure 3.15). Under short days *ubp13-1* and *ubp13-2* alleles both flowered with an average of 70 rosette leaves compared to 67 in Col-0 WT controls (Figure 3.15 A). The significance of the observed difference in rosette leaf number between Col-0 and *ubp13* alleles by was assessed by t-test and found to be significant ( $p$  values: *ubp13-1* - 0.0539 and *ubp13-2* - 0.0637). The flowering phenotype of *ubp13* mutants under short days is clearly comparable to Col-0 controls rather than *ubp12* mutants (Figure 3.15 A) despite the paralogous relationship between *AtUBP12* and *AtUBP13*. Under long days *ubp13-1* and *ubp13-2* alleles both flowered with an average of 8.5 rosette leaves compared to 8.1 in Col-0 controls (Figure 3.15 B) although t-test analysis indicated this difference was not significant ( $p$  values: *ubp13-1* - 0.15 and *ubp13-2* - 0.23).

**Figure 3.14** Early flowering of *ubp12* mutants under short days.

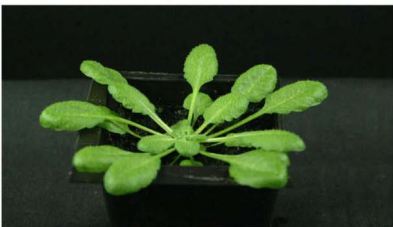
Representative examples of Col-0, *ubp12-1*, *ubp12-2*, *ubp13-1* and *ubp13-2* plants 5 weeks after germination following growth under a short day photoperiod (8 hours light/16 hours dark).



***ubp 12-1***



***ubp 12-2***



***ubp 13-1***



***ubp 13-2***



**Col-0**

Short day grown *ubp12* mutants also developed aerial rosette structures instead of a single subtending cauline leaf (Figure 3.14 C). Aerial rosettes were consistently observed at each node on the primary inflorescence in *ubp12* mutants. Axillary inflorescences of *ubp12* mutants exhibited wild type lateral shoot growth with aerial rosettes being restricted to the primary inflorescence (Figure 3.15 C). The observed transition to flowering under short days was far earlier in *ubp12* alleles than Col-0 plants with the corresponding early development of axillary and secondary inflorescences. Floral morphology in *ubp12* and *ubp13* mutants appeared normal.

As with many aspects of plant physiology, regulation by ubiquitin-26S proteasome mediated degradation has been heavily implicated in the control of flowering (Vierstra, 2003). In flowering, ubiquitin E3 ligases have been linked to the vernalisation pathway (Dong et al., 2006), gibberellin pathway (Swain and Singh, 2005), light dependent pathway (Turck et al., 2008) and maintenance of circadian rhythms (Fujiwara et al., 2008).

The clear early flowering of *ubp12* mutants under short days invites further scrutiny of disruption to established floral signalling pathways in these lines. Further characterisation of early flowering in *ubp12* mutants aims to examine altered behaviour of known floral signal integrators such as CO and FLC in the *ubp12* background (Turck et al., 2008). Linkage of the observed phenotype to known flowering pathways will also be investigated by making genetic crosses with established mutants that exhibit late flowering under short days.

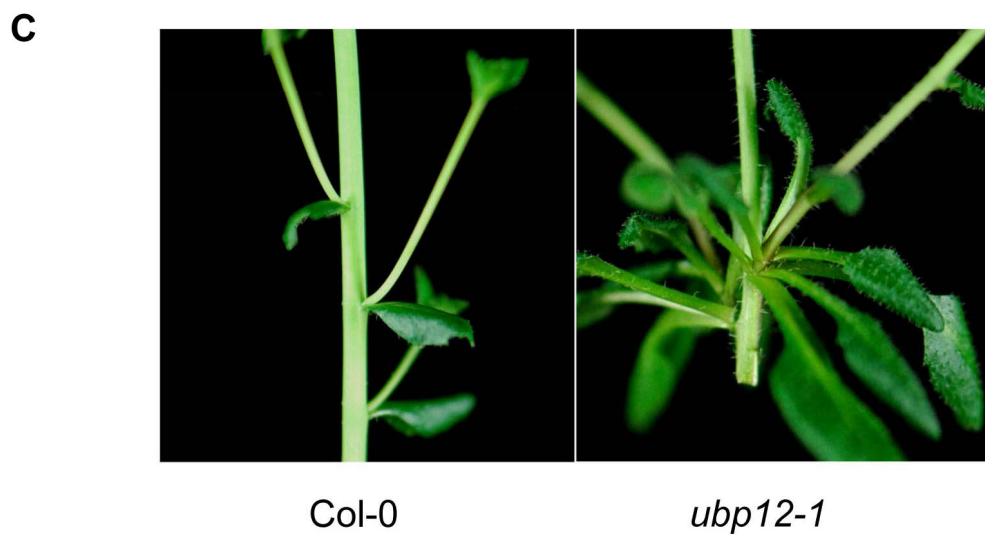
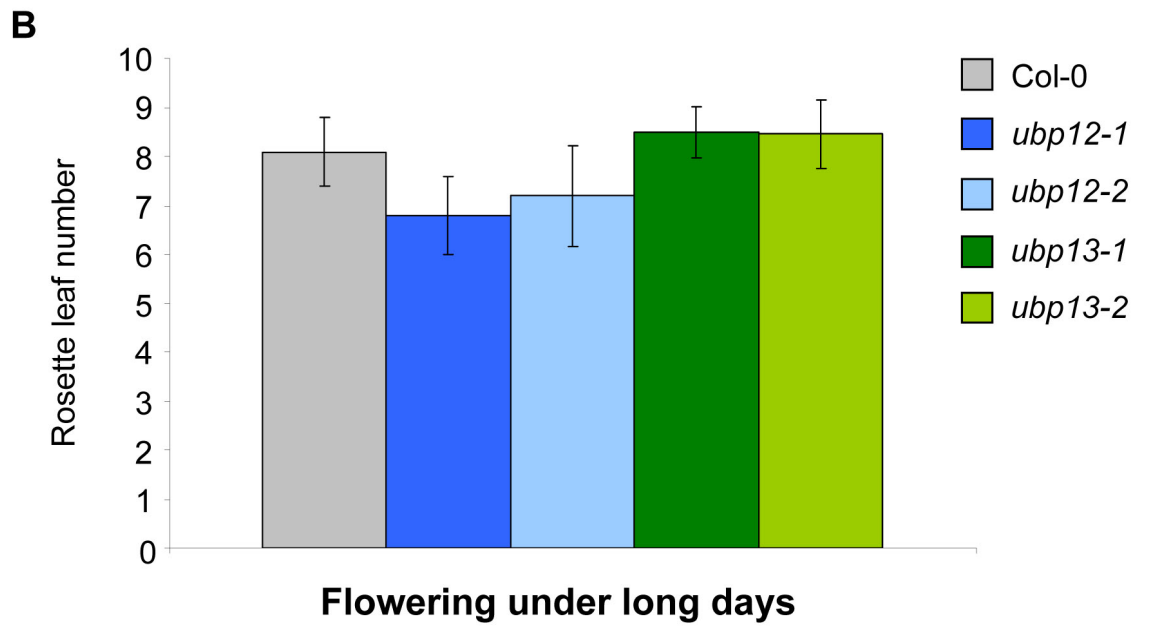
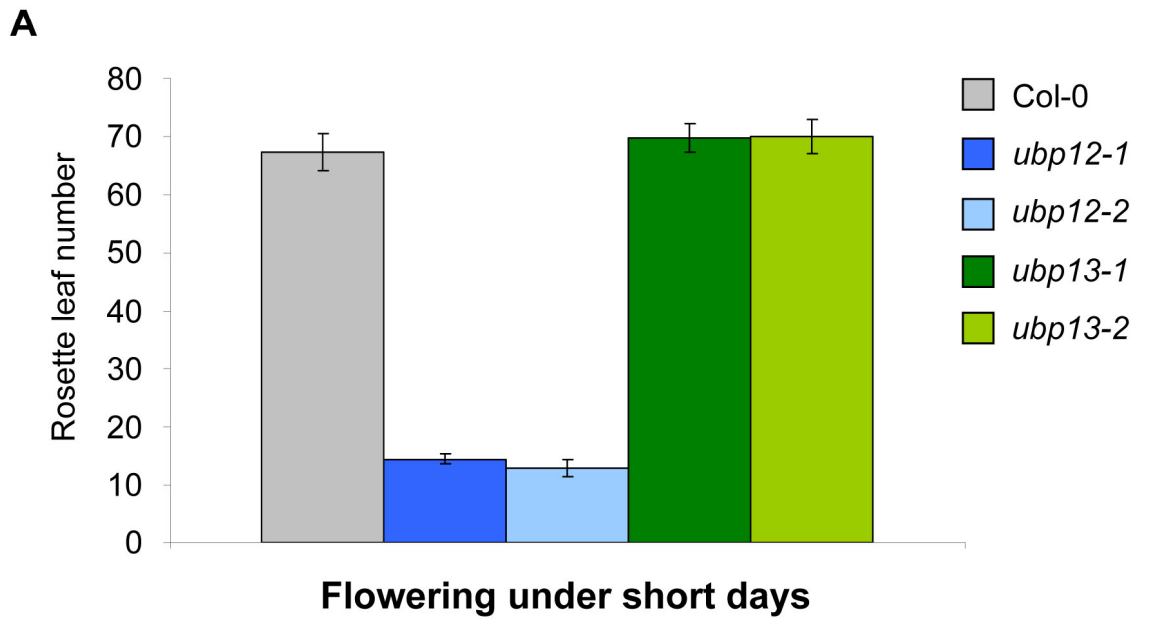
The reported early flowering phenotype of *ubp12* mutants should be amenable to transgenic complementation approaches to restore wild type function. *In vitro* DUB assay results reported in Chapter 5 have proven the ubiquitin protease activity of expressed full length AtUBP12 WT protein and that activity is abolished in a corresponding AtUBP12 C208S active site mutant. To facilitate complementation studies, transgenic *ubp12-1* lines overexpressing either *AtUBP12\_WT* or *AtUBP12\_C208S* cDNAs under a CaMV 35S promoter are currently being generated.

**Figure 3.15** Flowering time of *ubp12* and *ubp13* mutants under long and short days.

(A) Flowering time of Col-0, *ubp12-1*, *ubp12-2*, *ubp13-1* and *ubp13-2* under short days expressed as rosette leaf number counted after opening of the first flower. Plants were grown for approximately 5 weeks under a short day photoperiod (8 hours light/16 hours dark). Measurements represent the mean of 10 individuals and error bars indicate one standard deviation.

(B) Flowering time of Col-0, *ubp12-1*, *ubp12-2*, *ubp13-1* and *ubp13-2* under long days expressed as rosette leaf number counted after opening of the first flower. Plants were grown for approximately 4 weeks under a long day photoperiod (16 hours light/8 hours dark). Measurements represent the mean of 10 individuals and error bars indicate one standard deviation.

(C) Aerial rosette structures seen on the primary inflorescence of *ubp12* mutant alleles compared to Col-0 plants grown under a short day photoperiod (8 hours light/16 hours dark). Photographs taken following approximately 14 weeks of growth under short day conditions.



## 3.6 RNAi based silencing of *AtUBP12* and *AtUBP13*

### 3.6.1 RNAi in *Arabidopsis* using pHELLSGATE

As discussed previously, reverse genetic approaches to study gene function in *Arabidopsis* rely primarily on insertional mutagenesis approaches based on T-DNA insertion. Results presented in Section 3.5 demonstrate that T-DNA insertion mutants can effectively abolish mRNA accumulation for specific genes allowing the characterisation of novel phenotypes. However, the use of insertion mutants has associated limitations when studying duplicated genes. Duplicated genes often exhibit functional redundancy that invalidates the T-DNA approach as the potential phenotype of a null allele is obscured by the presence of a functional sibling (Gu et al., 2003).

One approach that can circumvent such limitations exploits the biological phenomenon of RNA induced gene silencing, variously termed RNA interference (RNAi) in animals or Post Transcriptional Gene Silencing (PTGS) in plants (Waterhouse and Helliwell, 2003). Initial studies established the mechanistic similarity between gene silencing and plant anti-viral defence (Ratcliff et al., 1997). Non-host double stranded RNA (dsRNA) produced during viral replication is recognised by the host and degraded into ~21 nucleotide fragments termed small interfering RNAs (siRNAs) (Baulcombe, 2005). The incorporation of siRNAs into a nuclease complex called RISC (RNAi silencing complex) guides the homology dependent degradation of the corresponding viral mRNA causing gene silencing (Baulcombe, 2005).

The mechanism of gene silencing has been applied to plant genomics using various approaches to deliver dsRNA into the plant cell (Helliwell and Waterhouse, 2005). Introduction of user defined exogenous dsRNA sequences has allowed recruitment of gene silencing machinery to efficiently silence specific host genes (Waterhouse and Helliwell, 2003).

Presentation of dsRNA in the plant cell can occur from naturally occurring viral RNA (the replication of which produces dsRNA). This principle is

commonly applied in Virus Induced Gene Silencing (VIGS) to initiate transient gene silencing in virus compatible host plant species (Ratcliff et al., 2001). To facilitate gene silencing in *Arabidopsis*, self-complementary single-stranded 'hairpin' RNA (hpRNA) corresponding to a target host gene can be stably introduced as a transgene to initiate heritable gene silencing (Helliwell and Waterhouse, 2005).

This hairpin RNAi approach was utilised to address potential functional redundancy between *AtUBP12* and *AtUBP13*. The generation of hairpin RNA expressing constructs has been simplified by the recent development of the Gateway compatible pHELLSGATE vector (Helliwell and Waterhouse, 2003). The pHELLSGATE vector allows recombination based transfer of DNA fragments from attL1-attL2 sites in a Gateway entry clone into pHELLSGATE12 which carries two attR1-attR2 cassettes under a CaMV 35S promoter (Helliwell and Waterhouse, 2003). The attR1-attR2 cassettes are separated by an intron and are in opposite sense orientations with respect to the promoter giving rise to inverted repeat constructs. Expression of gene fragments transferred to pHELLSGATE *in planta* produces a hairpin RNA with the intron spliced out. This hpRNA will present the requisite dsRNA signal to initiate gene silencing targeted against host gene (or genes) corresponding to the pHELLSGATE expressed cDNA fragment.

### **3.6.2 RNAi based silencing of *AtUBP12* and *AtUBP13***

Data presented in this chapter indicates that *AtUBP12* and *AtUBP13* are differentially expressed in various plant tissues and that both are transcriptionally activated by pathogen stimuli and exogenously applied SA. The high level of amino acid identity between *AtUBP12* and *AtUBP13* (86%) coupled with their coordinated induction suggests a potential redundancy in their function.

To investigate this possibility, a pHELLSGATE12 construct was generated using a cDNA fragment from *AtUBP13* which would generate siRNAs with homology to *AtUBP12* and initiate silencing of both genes (construct - UBP\_RNAi). The ability to silence multiple genes simultaneously is a key benefit of the gene silencing method but does require consideration of

potential 'off target' silencing effects. In the case of *AtUBP12* and *AtUBP13*, if siRNAs were generated from the conserved His and Cys box catalytic regions they could potentially initiate gene silencing of any of the 27 UBP enzymes.

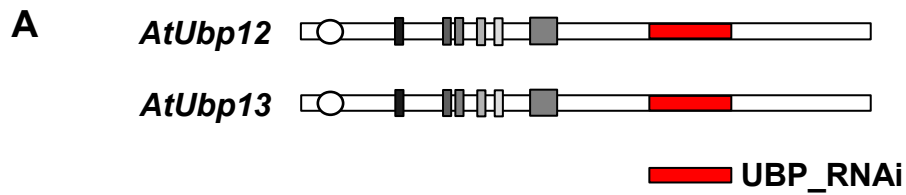
To avoid this outcome, a 420 bp region unique to *AtUBP12* and *AtUBP13* was selected from the cDNA sequence of *AtUBP13* (Figure 3.16 A). Alignment analysis of the selected *AtUBP13* cDNA fragment indicated multiple regions over 21 nucleotides in length with continuous identity to *AtUBP12* (Figure 3.16 B) indicating it could initiate silencing of both genes. To assess potential off target silencing effects, the selected UBP\_RNAi cDNA fragment was BLAST queried against the *Arabidopsis* genome and recovered *AtUBP13* and *AtUBP12* as top scoring matches (E-values of 0 and  $4e^{-84}$  respectively) followed by a low scoring third non-UBP match to *AtATMAP65-1* (E-value 0.023). There were no additional UBP genes recovered using this cDNA fragment and the extent of continuous sequence match to *AtATMAP65-1* was limited to a single region of 13 base pairs. This analysis indicated that the cDNA region selected for the UBP\_RNAi construct was unlikely to cause 'off target' cross silencing effects.

The UBP\_RNAi cDNA fragment was amplified from *Arabidopsis* cDNA using Gateway compatible primers (UBP\_RNAi\_5 and UBP\_RNAi\_3) and TOPO cloned into the appropriate Gateway entry vector (pENTR D-TOPO). Using Gateway recombination, the UBP\_RNAi fragment was transferred to pHELLSGATE12 and the resulting inverted repeat construct was confirmed by restriction digest and PCR using insert fragment and vector specific primers (HG12\_35S and HG12\_int). *Arabidopsis* UBP\_RNAi and empty pHELLSGATE12 (pHG12) control transgenic lines were made by floral dip transformation and T<sub>1</sub> transformants were identified on kanamycin selective plates (Figure 3.17).

The expression of hairpin RNA fragments from a 35S promoter in pHELLSGATE12 confers a genetically dominant effect therefore any phenotypic effects should be apparent in the T<sub>1</sub> generation (Helliwell and Waterhouse, 2003). Comparison of resistant UBP\_RNAi and pHG12 T<sub>1</sub> seedlings at 20 days post germination on kanamycin selection indicated a

**Figure 3.16** Selection of a cDNA fragment to initiate hpRNAi gene silencing of *AtUbp12* and *AtUbp13*.

Hairpin based RNAi silencing of *AtUbp12* and *AtUbp13*. **(A)** Domain diagrams of *AtUbp12* and *AtUbp13*, red box indicates *AtUbp13* cDNA region selected for UBP\_RNAi silencing construct. **(B)** Sequence alignment of RNAi\_UBP cDNA fragment from *AtUbp13* and corresponding region in *AtUbp12*. Nucleotide conservation is indicated in red.



**B**

<i>AtUbp12</i>	--CCTGGATT	TACGTCCTAT	TCCTCCTCCT	GAAAAATCAA	AAGAA
<i>AtUbp13</i>	GGACCGGATG	ACCTTCCTAT	TCCTCCCCCA	GAAAAACTTT	CTGAG
UBP_RNAi	GGACCGGATG	ACCTTCCTAT	TCCTCCCCCA	GAAAAACTTT	CTGAG
<i>AtUbp12</i>	GATATCTTC	TTTTCTTCAA	GCTTTATGAC	CCCGAGAAGG	CAGTA
<i>AtUbp13</i>	GATATCCTTC	TTTTCTTTAA	ACTCTATGAC	CCTGAGAACG	CAGTA
UBP_RNAi	GATATCCTTC	TTTTCTTTAA	ACTCTATGAC	CCTGAGAACG	CAGTA
<i>AtUbp12</i>	TTAAGCTATG	CTGGCAGGCT	GATGGTGAAA	AGTTCCAGTA	AGCCT
<i>AtUbp13</i>	CTAAGATATG	TTGGCAGGCT	AATGGTGAAA	AGTTCCAGTA	AGCCC
UBP_RNAi	CTAAGATATG	TTGGCAGGCT	AATGGTGAAA	AGTTCCAGTA	AGCCC
<i>AtUbp12</i>	ATGGATATAA	CTGGAAAACT	GAATGAAATG	GTTGGCTTTG	CTCCT
<i>AtUbp13</i>	ATGGATATAG	TAGGGCAATT	GAATAAAATG	GCTGGTTTTG	CTCCT
UBP_RNAi	ATGGATATAG	TAGGGCAATT	GAATAAAATG	GCTGGTTTTG	CTCCT
<i>AtUbp12</i>	GATGAAGAAA	TAGAACTTTT	TGAGGAAATC	AAGTTTGAAC	CTTGT
<i>AtUbp13</i>	GATGAGGAAA	TAGAACTTTT	TGAGGAAATA	AAGTTTGAAC	CTTGC
UBP_RNAi	GATGAGGAAA	TAGAACTTTT	TGAGGAAATA	AAGTTTGAAC	CTTGC
<i>AtUbp12</i>	GTTATGTGCG	AACACTTGGG	TAAGAAAACT	TCATTCAGAT	TGTGT
<i>AtUbp13</i>	GTAATGTGTG	AACAGATTGA	TAAGAAAGACT	TCTTTCAGGC	TGTGT
UBP_RNAi	GTAATGTGTG	AACAGATTGA	TAAGAAAGACT	TCTTTCAGGC	TGTGT
<i>AtUbp12</i>	CAAATTGAAG	ATGGAGATAT	CATTTGCTTT	CAGAAACCTC	TTGTT
<i>AtUbp13</i>	CAAATTGAAG	ATGGAGATAT	CATTTGTTAT	CAGAAACCTC	TTTCT
UBP_RNAi	CAAATTGAAG	ATGGAGATAT	CATTTGTTAT	CAGAAACCTC	TTTCT
<i>AtUbp12</i>	AACAAGGAGA	TTGAATGCCT	CTACCCAGCT	GTGCCATCAT	TTCTT
<i>AtUbp13</i>	ATCGAGGAGA	GTGAATTTTCG	ATACCCAGAT	GTGCCATCAT	TTTTG
UBP_RNAi	ATCGAGGAGA	GTGAATTTTCG	ATACCCAGAT	GTGCCATCAT	TTTTG
<i>AtUbp12</i>	GAATATGTCC	AGAATAGACA	GCTGGTCCGG	TTTCGTGCTC	TGGAA
<i>AtUbp13</i>	GAGTATGTAC	AGAATCGAGA	GCTGGTGCGT	TTTCGCACAC	TGGAA
UBP_RNAi	GAGTATGTAC	AGAATCGAGA	GCTGGTGCGT	TTTCGCACAC	TGGAA
<i>AtUbp12</i>	AAACCTAAAG	AAGATGAGTT	TGTTCTGGAG	TTGTCAAGC	AGCAC
<i>AtUbp13</i>	AAACCAAAAG	AGGATGAGTT	TACTATGGAG	CTGTCAAAGC	TGCAC
UBP_RNAi	AAACCAAAAG	AGGATGAGTT	TACTATGGAG	CTGTCAAAGC	TGCAC
<i>AtUbp12</i>	ACTTATGACG	ATGTTGTGGA	GAAAGTGGCT	GA	
<i>AtUbp13</i>	ACTTATGATG	ATGTAGTGGA	AAGGGTGGCT	GA	
UBP_RNAi	ACTTATGATG	ATGTAGTGGA	AAGGGTGGCT	GA	

clear inhibition of growth and accumulation of anthocyanin in UBP\_RNAi silencing lines (Figure 3.17). Control transgenic T<sub>1</sub> lines carrying empty pHELLSGATE12 appeared healthy and developmentally unaffected (Figure 3.17) suggesting the observed phenotype was due to the specific co-silencing of *AtUBP12* and *AtUBP13*.

From the recovered T<sub>1</sub> transgenic seedlings, 30 UBP\_RNAi plants and 10 pHG12 plants were transferred to soil and grown to harvest seeds. After transfer to soil, growth of T<sub>1</sub> UBP\_RNAi plants was initially slower than pHG12 controls but they ultimately grew to equivalent size, without further obvious morphological differences then flowered and set seed.

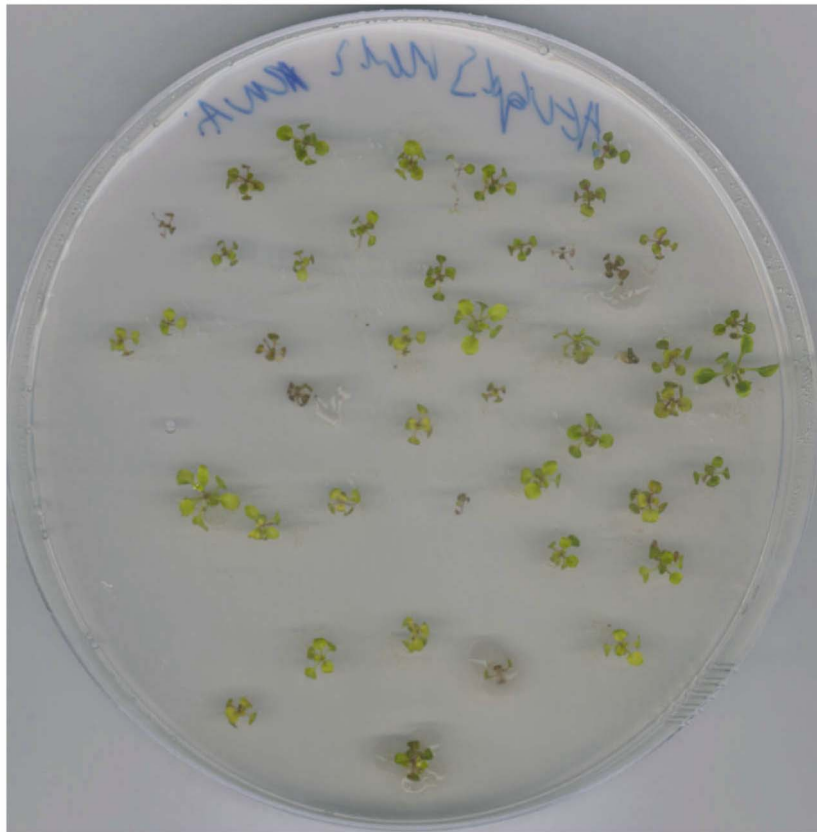
Independent lines of T<sub>2</sub> UBP\_RNAi (10 lines) and pHG12 (2 lines) seed were grown on selective plates. In kanamycin resistant seedlings of the T<sub>2</sub> generation, no clear difference in growth or anthocyanin accumulation was seen between the UBP\_RNAi and pHG12 seedlings (data not shown) and individual plants from each line were transferred to soil and grown to harvest seeds.

Co-silencing of *AtUBP12* and *AtUBP13* genes was assessed in isolated T<sub>2</sub> plants by RT-PCR (Figure 3.18). Total RNA was extracted from rosette leaves of 4 week old T<sub>2</sub> UBP\_RNAi and pHG12 plants then the relative expression of *AtUBP12* and *AtUBP13* mRNA was assessed by RT-PCR using primers specific for *AtUBP12* (AtUBP12\_KD5 and AtUBP12\_KD3) or *AtUBP13* (AtUBP13\_KD5 and AtUBP13\_KD3). *AtUBP12* KD and *AtUBP13* KD RT-PCR amplicons were selected from cDNA regions outside the UBP\_RNAi fragment to ensure amplification from endogenous mRNAs rather than the overexpressed transgenic UBP\_RNAi fragment (Figure 3.18 A).

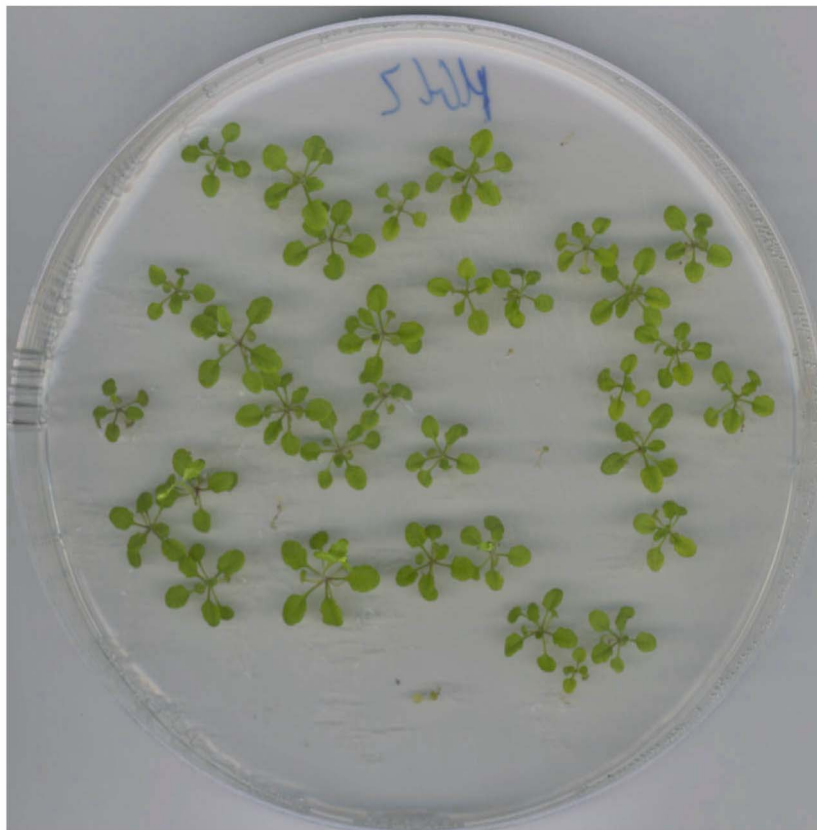
Ten independent T<sub>2</sub> UBP\_RNAi lines were analysed as the efficiency of hpRNAi has been reported to vary significantly between different transgenics (Helliwell and Waterhouse, 2003). RT-PCR analysis of the 10 independent UBP\_RNAi lines demonstrated a clear reduction in mRNA levels of both *AtUBP12* and *AtUBP13* relative to pHG12 controls in at least 5 of the selected UBP\_RNAi individuals (Figure 3.18 B, UBP\_RNAi #1, #2, #6, #9 and #10). In UBP\_RNAi lines #2 and #6, densitometry analysis

**Figure 3.17** *Arabidopsis* UBP\_RNAi T<sub>1</sub> transgenics demonstrate reduced growth and increased anthocyanin accumulation relative to pHG12 controls.

*Arabidopsis* T<sub>1</sub> UBP\_RNAi transformants (upper panel) and pHG12 vector transformants 21 days post germination on kanamycin selective plates (kanamycin resistant seedlings were transferred to fresh selective plates 14 days post germination).



UBP<sup>-</sup>RNAi  
T<sub>1</sub>

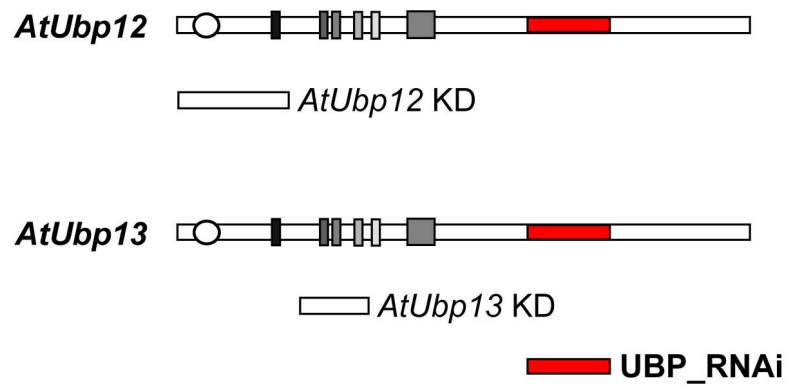


pHG12  
T<sub>1</sub>

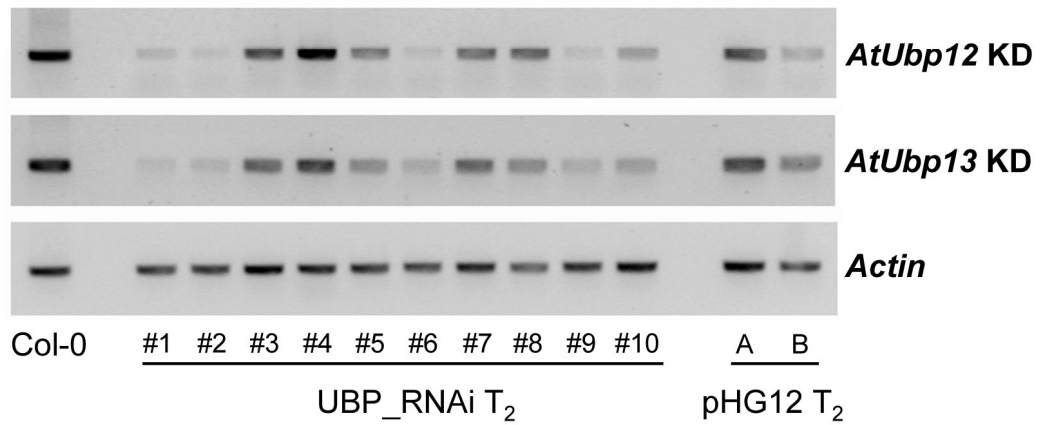
**Figure 3.18** Expression analysis of *AtUbp12* and *AtUbp13* in *Arabidopsis* UBP\_RNAi T<sub>2</sub> generation.

RT-PCR analysis of *Arabidopsis* UBP\_RNAi T<sub>2</sub> plants. **(A)** Domain diagrams of *AtUbp12* and *AtUbp13* indicating the respective locations of RT-PCR amplicons (white boxes - *AtUbp12* KD and *AtUbp13* KD) amplified to analyse gene silencing and cDNA fragment (red box) selected for UBP\_RNAi silencing construct. Total RNA was extracted from T<sub>2</sub> kanamycin selected, 5 week old *Arabidopsis* plants: UBP\_RNAi (ten independent lines) and HG Vector (two independent lines). RNA was used for RT-PCR and gene expression was analysed **(B)** using specific primers for *AtUbp12* (30 cycles), *AtUbp13* (30 cycles) and *Actin* (25 cycles).

**A**



**B**



indicated mRNA level reductions of 69% and 65% for *AtUBP12* and 83% and 81% for *AtUBP13* respectively (Figure 3.18 B). Having identified transgenic plants with efficient co-silencing of *AtUBP12* and *AtUBP13* in the T<sub>2</sub> generation, 10 individual T<sub>2</sub> seedlings from UBP\_RNAi lines #2 and #6 and pHG12 control lines were transferred to soil and grown to set T<sub>3</sub> seed. Homozygous T<sub>3</sub> lines of UBP\_RNAi and pHG12 were identified on kanamycin selective plates and confirmed homozygous lines were grown for further characterisation.

Selected homozygous T<sub>3</sub> lines of UBP\_RNAi #2 and #6 and pHG12 were genotyped by PCR and the efficiency of *AtUBP12* and *AtUBP13* co-silencing was assessed by RT-PCR as before (Figure 3.19 A). RT-PCR analysis of selected T<sub>3</sub> lines indicated a large reduction in silencing efficiency of both *AtUBP12* and *AtUBP13* genes relative to pHG12 controls (Figure 3.19 B). Densitometry analysis indicated that in the T<sub>3</sub> generation mRNA levels were reduced in UBP\_RNAi lines #2 and #6 by 7% and 0% for *AtUBP12* and 43% and 13% for *AtUBP13* respectively (Figure 3.19 B). The marked reduction in silencing efficiency indicated *AtUBP12* expression levels were effectively the same as wildtype and suggested that the expression of the HELLSGATE12 transgene was affected in the later T<sub>3</sub> generation.

Previous reports indicate that transgene expression in transformed *Arabidopsis* lines is highly variable due to the effect of gene silencing targeted against the transformed vector (Matzke et al., 1996). This possibility could have been investigated using PCR with pHELLSGATE12 vector specific primers to compare transgene expression in each respective transgenic generation. An alternative northern blotting strategy could also have been employed to investigate pHELLSGATE12 efficiency by examining the accumulation of *AtUBP12*/*AtUBP13* specific siRNAs in each generation of UBP\_RNAi transformants. The efficiency of *AtUBP12* and *AtUBP13* silencing in the T<sub>1</sub> generation was not assessed by RT-PCR but the reduced growth/anthocyanin accumulation phenotype of T<sub>1</sub> UBP\_RNAi transformants was not observed in the T<sub>2</sub> and T<sub>3</sub> generations. These results suggests the possibility that co-silencing efficiency of *AtUBP12* and *AtUBP13* was maximal in the T<sub>1</sub> generation and then reduced in the subsequent generations to a level that was less deleterious to the plant.

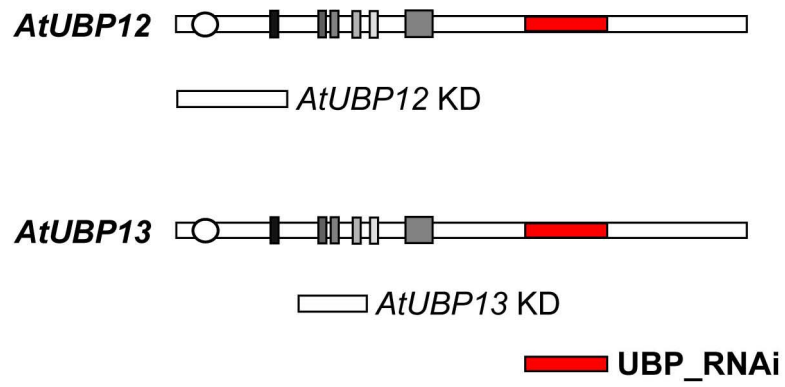
This possibility may explain why no reduced growth/anthocyanin accumulation phenotype was seen in T<sub>2</sub> UBP\_RNAi transgenic lines.

The overall reduction in co-silencing efficiency observed between T<sub>2</sub> and T<sub>3</sub> UBP\_RNAi lines may reflect the fundamental requirement for either *AtUBP12* or *AtUBP13* to allow normal plant development. If the introduction of a silencing vector to reduce levels of endogenous *AtUBP12* and *AtUBP13* is deleterious to the plant then the transgene maybe silenced in a shorter number of plant generations than is typically reported (Matzke et al., 1996). The observed phenotype of the T<sub>1</sub> UBP\_RNAi transgenics suggests that *AtUBP12* and *AtUBP13* are functionally redundant particularly as no such phenotype was observed in the single gene T-DNA knockout lines of either gene. No further studies were undertaken using the selected UBP\_RNAi lines on the basis of their weak co-silencing of *AtUBP12* and *AtUBP13* in the T<sub>3</sub> generation.

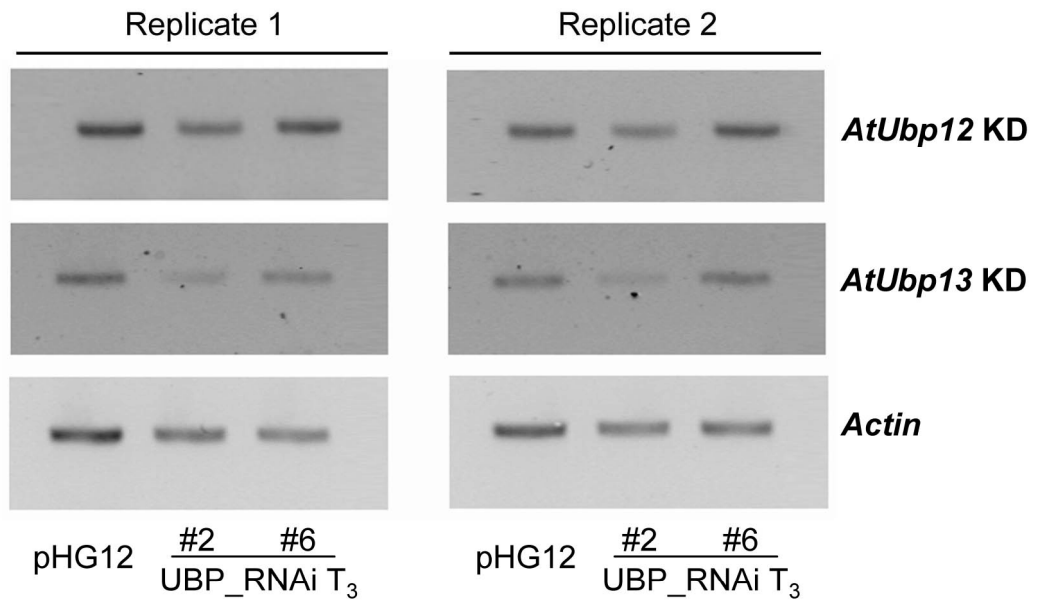
**Figure 3.19** Expression analysis of *AtUbp12* and *AtUbp13* in *Arabidopsis* UBP\_RNAi T<sub>3</sub> generation.

RT-PCR analysis of *Arabidopsis* UBP\_RNAi T<sub>3</sub> plants. Domain diagrams of *AtUbp12* and *AtUbp13* (**A**) indicating the respective locations of RT-PCR amplicons (white boxes - *AtUbp12* KD and *AtUbp13* KD) amplified to analyse gene silencing and cDNA fragment (red box) selected for UBP\_RNAi silencing construct. Total RNA was extracted from T<sub>3</sub> kanamycin selected, 5 week old *Arabidopsis* plants: UBP\_RNAi #2, UBP\_RNAi #6 and pHG12. This RNA was used for RT-PCR and gene expression was analysed in duplicate (**B**) using specific primers for *AtUbp12* (27 cycles), *AtUbp13* (27 cycles) and *Actin* (24 cycles).

**A**



**B**



### 3.7 Generation of *ubp12-1 ubp13-1* double mutant lines

To circumvent the issues of weak co-silencing identified in T<sub>3</sub> UBP\_RNAi lines, a double mutant line was created by cross-fertilising *ubp12-1* and *ubp13-1* plants.

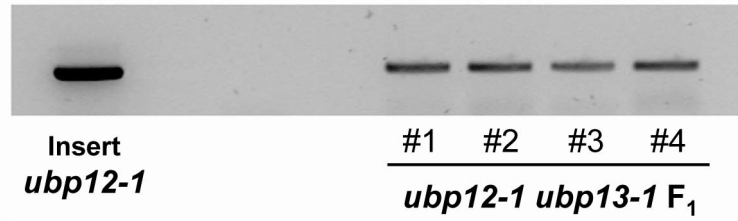
*Arabidopsis ubp12-1* and *ubp13-1* plants were grown to the appropriate developmental stage and cross-fertilisation was performed between female *ubp12-1* and male *ubp13-1* parents. Seeds were harvested from four successful crosses and the presence of respective T-DNA insertions in F<sub>1</sub> *ubp12-1 ubp13-1* plants was confirmed by PCR using genotyping primers as previously described (Figure 3.20 A). Having established the presence of both T-DNA insertions in four independent *ubp12-1 ubp13-1* F<sub>1</sub> plants, the zygosity of F<sub>2</sub> seedlings from an individual F<sub>1</sub> parent (line #1 Figure 3.20 A) was assessed by PCR (Figure 3.20 B).

Homozygous *ubp12-1 ubp13-1* double mutants should segregate 1:16 in the F<sub>2</sub> generation. Thirty F<sub>2</sub> progeny of a single F<sub>1</sub> *ubp12-1 ubp13-1* parent were genotyped by PCR to isolate homozygous *ubp13-1* lines (data not shown). From this analysis, a single homozygous *ubp13-1* line was recovered (*ubp12-1 ubp13-1* F<sub>2</sub> #24) which was found to be heterozygous for *ubp12-1* (Figure 3.20 B). The identification of a single *ubp13-1* homozygote in the F<sub>2</sub> generation was lower than expected from the 1:4 segregation ratio (which would predict at least 7 individual homozygotes in 30 plants). This outcome was assumed to result from variability in genomic DNA recovery which led to failed amplification in some genotyping reactions (data not shown). Rather than screen more F<sub>2</sub> progeny, seeds from the isolated cross line #24 were grown to characterise the F<sub>3</sub> population.

**Figure 3.20** Genotype confirmation of *ubp12-1 ubp13-1* genetic cross lines in the F<sub>1</sub> and F<sub>2</sub> generation.

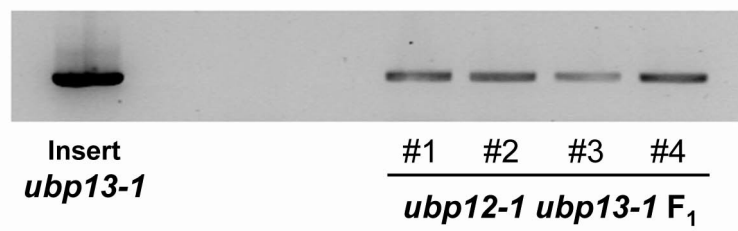
(A) Genomic DNA was isolated from F<sub>1</sub> progeny of four independent *ubp12-1 ubp13-1* genetic crosses and checked by PCR for the presence of *ubp12-1* T-DNA (Ai) and *ubp13-1* T-DNA (Aii) T-DNA insert amplicons. (B) Genomic DNA was isolated from the F<sub>2</sub> progeny (F<sub>2</sub> plant #24) of the *ubp12-1 ubp13-1* (F<sub>1</sub> plant #1) genetic cross and checked by PCR to confirm *ubp12-1* (Bi) and *ubp13-1* (Bii) zygosity.

**Ai**



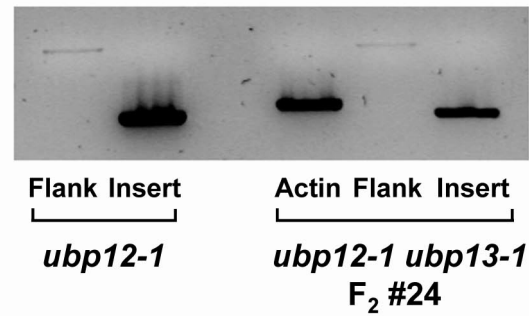
*ubp12-1*  
Insert

**ii**

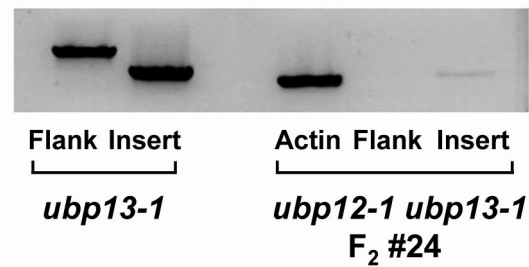


*ubp13-1*  
Insert

**Bi**



**ii**



During the isolation of *ubp12-1* mutants, the suitability of sulfadiazene resistance segregation as an indicator of zygosity was confirmed. During growth on selective sulfadiazene plates, PCR confirmed *ubp12-1* homozygotes exhibited 100% resistance whereas *ubp12-1* heterozygotes exhibited 75% resistance (data not shown). This data confirmed the Mendelian co-segregation of sulfadiazene resistance with the *ubp12-1* T-DNA insertion rather than an unlinked T-DNA insertion effect.

In the F<sub>3</sub> generation, progeny of *ubp12-1 ubp13-1* F<sub>2</sub> #24 were expected to be segregating for the *ubp12-1* allele and homozygous for the *ubp13-1* allele. F<sub>3</sub> progeny of *ubp12-1 ubp13-1* F<sub>2</sub> #24 were grown on sulfadiazene selection and twelve resistant seedlings were transferred to soil.

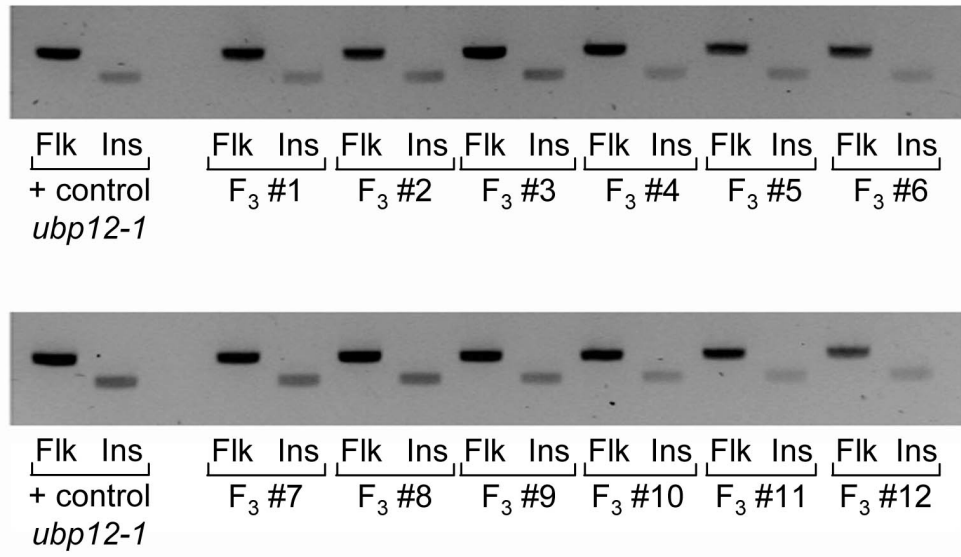
The selected seedlings were expected to be segregating for the *ubp12-1* homozygotes:heterozygotes in a 1:2 ratio after the removal of sulfadiazene sensitive WT plants. PCR genotyping of selected F<sub>3</sub> *ubp12-1 ubp13-1* lines indicated the expected homozygosity of *ubp13-1* (Figure 3.21 A) but that all twelve lines were heterozygous for *ubp12-1* (Figure 3.21 B). Based on the removal of WT plants by sulfadiazene selection, 1 in 3 resistant F<sub>3</sub> plants should be homozygous for *ubp12-1*. With an allele segregation ratio of 1:2, the probability of finding a homozygous *ubp12-1* individual in twelve F<sub>3</sub> progeny is over 99%. This finding indicated that double mutant lines of *ubp12-1 ubp13-1* were not viable and were probably embryo lethal.

To confirm the PCR genotyping of F<sub>3</sub> *ubp12-1 ubp13-1* lines and examine potential embryo lethality, F<sub>4</sub> progeny of each selected F<sub>3</sub> line were examined on selective sulfadiazene plates. Segregation of sulfadiazene resistance and thus *ubp12-1* zygosity was observed in progeny of all twelve F<sub>3</sub> lines (Table 3.3). This result confirmed that all 12 selected F<sub>3</sub> lines were heterozygous for *ubp12-1* and indicated that homozygous double mutant *ubp12-1 ubp13-1* lines are not viable. For each selected *ubp12-1 ubp13-1* F<sub>3</sub> line, 100 F<sub>4</sub> individuals were germinated on sulfadiazene plates. Within each population of F<sub>4</sub> individuals, *ubp12-1* homozygotes, heterozygotes and WT were expected to segregate in 1:2:1 ratio with the according resistance or susceptibility to sulfadiazene (Figure 3.22).

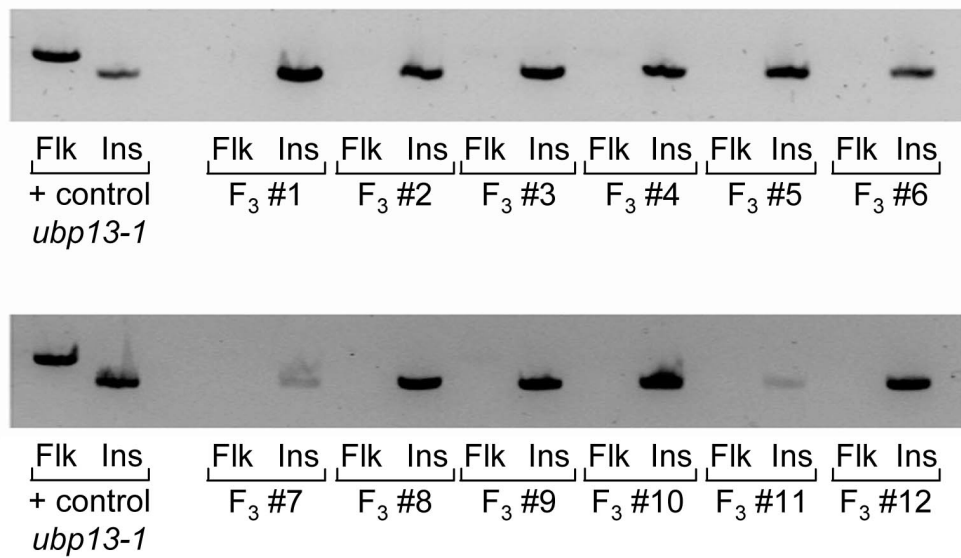
**Figure 3.21** Genotype confirmation of F<sub>3</sub> *ubp12-1 ubp13-1* genetic cross lines.

Genomic DNA was isolated from the F<sub>3</sub> progeny of *ubp12-1 ubp13-1* #24 F<sub>2</sub> genetic cross (twelve independent lines) and checked by PCR to confirm *ubp12-1* (**A**) and *ubp13-1* (**B**) zygosity. Flk denotes mutant allele specific T-DNA flanking amplicon, Ins denotes mutant allele specific T-DNA insert amplicon.

**A**



**B**



Plant line	Resistant Sulf <sup>20</sup>	Sensitive Sulf <sup>20</sup>	Non germinants	Aborted seedlings	Non-germinants + Aborted seedlings (%)
<i>ubp12-1</i>	91	0	3	0	3
Col-0	0	53	12	0	18
F4 #1	49	35	12	4	16
F4 #2	52	29	10	9	19
F4 #3	59	24	13	4	17
F4 #4	51	32	11	6	17
F4 #5	46	36	15	3	18
F4 #6	50	26	12	12	24
F4 #7	33	41	20	6	26
F4 #8	46	34	18	2	20
F4 #9	38	28	29	5	34
F4 #10	47	28	21	4	25
F4 #11	39	33	25	3	28
F4 #12	48	29	22	1	23

**Table 3.3** Segregation analysis of *ubp12-1 ubp13-1* F<sub>4</sub> seedlings 20 days after germination on sulfadiazine plates.

A subset of F<sub>4</sub> seedlings on each plate were phenotypically distinct from resistant and susceptible individuals (Figure 3.22 A and B) and were instead classified as aborted seedlings (Table 3.3 and Figure 3.22 C). In the majority of cases, aborted seedlings developed green cotyledons of reduced size and limited root tissue but failed to grow beyond this stage (Figure 3.22 C). Other individuals demonstrated even more severe developmental arrest, failing to progress beyond limited radicle emergence (Figure 3.22 C).

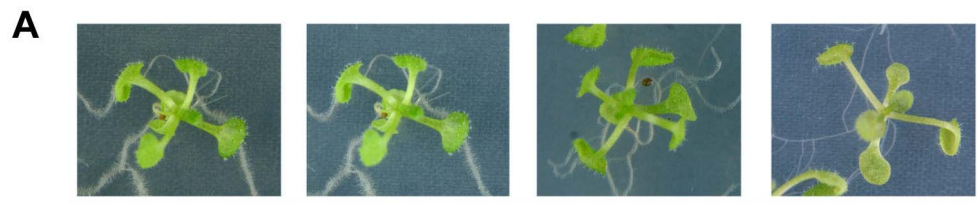
The observed aborted seedling phenotypes did not resemble the chlorotic phenotype of sulfadiazene sensitive plants (Figure 3.22 B), indicating resistance was due to the presence of *ubp12-1* and that aborted seedlings were double mutants of *ubp12-1* and *ubp13-1*. Sulfadiazene segregation data of the F<sub>4</sub> progeny supported the proposition that aborted seedlings were homozygous *ubp12-1 ubp13-1* double mutants.

In this analysis, a segregating population of *ubp12-1* alleles in a homozygous *ubp13-1* background exhibited distinct phenotypes corresponding to the 1:2:1 WT:heterozygote:homozygote ratio. As reported in Table 3.3, from each parental F<sub>3</sub> line approximately 25% of F<sub>4</sub> progeny were sulfadiazene sensitive, 50% were sulfadiazene resistant and the remaining 25% were either non-germinants or aborted seedlings. The segregation data indicates that collectively, non-germinants and aborted seedlings account for the expected number of *ubp12-1 ubp13-1* homozygotes in the F<sub>4</sub> population and that double mutants have a range of developmental arrest phenotypes ranging from non-germination to seedling lethality.

The observed differences in seedling abortion phenotype may reflect incomplete genetic penetrance in one or both of the T-DNA mutants. Variations in penetrance may allow sufficient *AtUBP12* or *AtUBP13* gene expression to facilitate the limited development of the seedling seen in F<sub>4</sub> progeny. The variable number of aborted seedlings seen in different F<sub>4</sub> populations (Table 3.3) suggests that homozygous *ubp12-1 ubp13-1* double mutants may actually be embryo lethal and fail to germinate with aborted

**Figure 3.22** Segregation analysis of *ubp12-1 ubp13-1* F<sub>4</sub> plants on sulfadiazine selective plates.

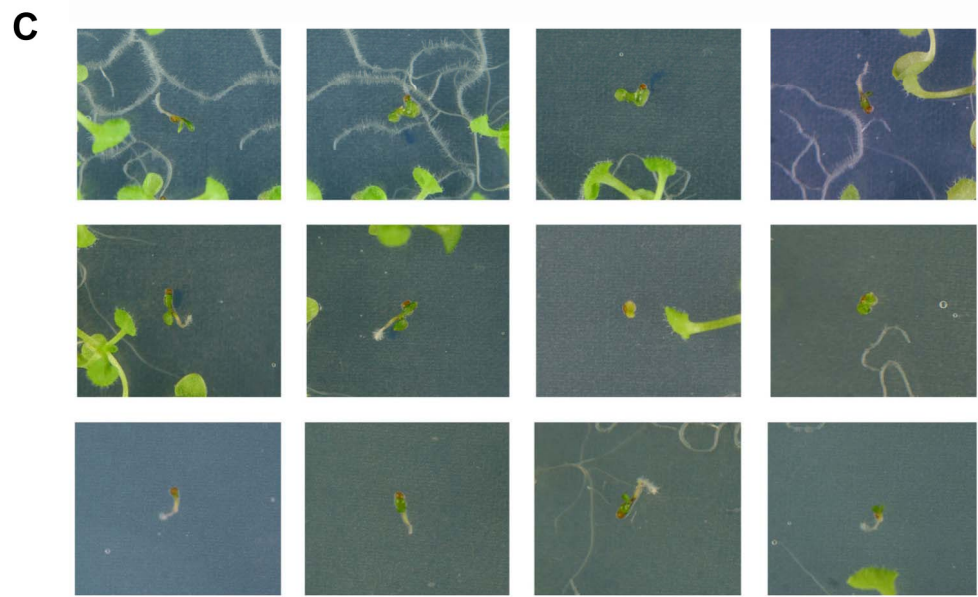
F<sub>4</sub> generation seedlings of *ubp12-1 ubp13-1* genetic cross twenty days after germination on sulfadiazine selective agar plates. (A) *ubp12-1*, (B) Col-0 and (C) *ubp12-1 ubp13-1* F<sub>4</sub>.



*ubp12-1*



Col-0



*ubp12-1 ubp13-1 F<sub>4</sub>*

seedlings representing partial escapes from this phenotype. Visual inspection of T<sub>4</sub> seed harvested directly from drying T<sub>3</sub> siliques indicated no morphological differences to suggest embryo lethality (data not shown). The reported data indicates that *ubp12-1 ubp13-1* double mutants are not viable, an equivalent genetic cross between *ubp12-2* and *ubp13-2* alleles was subsequently made and F<sub>2</sub> generation plants are currently being grown for analysis (data not shown).

### **3.8 Discussion**

#### **3.8.1 The *Arabidopsis* deubiquitinating enzymes**

*Arabidopsis*, like other eukaryotes, contains a large number of deubiquitinating enzymes which function to hydrolyse the various peptide and isopeptide bonds formed by ubiquitin in the cell. Current research indicates that five distinct subclasses of deubiquitinating enzyme exist, four of which are variant cysteine proteases whilst the fifth class are zinc metalloproteases (Amerik and Hochstrasser, 2004).

Using the sequences of various eukaryotic members of the UBP, UCH, Ataxin, Otubain and JAMM DUB families, a comprehensive analysis of DUBs present in the *Arabidopsis* genome was completed. This analysis detected 45 distinct *Arabidopsis* genes that encode DUB enzymes including newly discovered members of the Ataxin and JAMM classes that lack annotation to indicate their function as putative ubiquitin proteases.

The characterised *Arabidopsis* JAMM domain DUBs correspond to RPN11, a regulatory subunit of the 26S proteasome (Verma et al., 2002a) and the related paralogs CSN5a and CSN5b which function as de-rubylating enzymes in the COP9 signalosome (Gusmaroli et al., 2007). The crucial importance of RPN11 and CSN5a/CSN5b for *Arabidopsis* development has been established (Verma et al., 2002a) (Gusmaroli et al., 2007) and the homology of other *Arabidopsis* JAMM domain enzymes to known regulators of RNA splicing (Staub et al., 2004) and protein trafficking (McCullough et al., 2004a) also suggests a fundamental role for these enzymes.

This analysis confirmed that the *Arabidopsis* UBP family is the largest and most divergent class of DUB with 27 members many of which fall into distinct subfamilies of between 2 and 5 members. Previous studies have established that members of the UBP family regulate shoot development (Yang et al., 2007), male fertility (Doelling et al., 2007) and cell proliferation (Liu et al., 2008). Redundancy of function has also been demonstrated within several UBP subfamilies (Liu et al., 2008) and that mutation of *AtUBP14* confers an embryo lethal phenotype (Doelling et al., 2001). The remaining 20 UBP enzymes, of which 6 are single copy genes, are currently not functionally characterised.

### **3.8.2 Potential involvement of UBPs *AtUBP12* and *AtUBP13* in disease resistance signalling**

Following the reported transcriptional suppression of a solanaceous UBP gene during HR in *N. benthamiana* (Kim et al., 2006), experiments were conducted to investigate possible involvement of the orthologous *Arabidopsis* UBP enzymes *AtUBP12* and *AtUBP13* in disease resistance. A prior analysis of segmental chromosome duplication (Blanc et al., 2003) indicated that *AtUBP12* and *AtUBP13* arose from a gene duplication event and their recent evolutionary divergence was confirmed in a phylogenetic analysis of the *Arabidopsis* UBP enzymes.

Time course induction studies indicated a clear upregulation of both *AtUBP12* and *AtUBP13* in response to avirulent *Pseudomonas syringae* expressing *avrB* and following treatment with salicylic acid. The large transcriptional induction of both *AtUBP12* and *AtUBP13* in response to SA treatment suggests a more general role for these proteins in disease resistance signalling. The extent of *AtUBP12/AtUBP13* gene induction following SA treatment provides a clear molecular phenotype which could be further characterised using realtime PCR and mutant lines that are disrupted at different signalling nodes within SA responsive SAR activation pathways (Durrant and Dong, 2004). The induction of *AtUBP12* and *AtUBP13* in response to other established disease signalling hormones such as jasmonate and ethylene (Bostock, 2005) could also be investigated using this system.

The reported data suggests that transcriptional control of *AtUBP12* and *AtUBP13* expression may be relevant to their function and the identification of a shared promoter region between the two genes appeared to support this possibility. Despite detectable conservation of upstream regions between *AtUBP12* and *AtUBP13*, formal promoter analysis failed to detect conserved promoter elements between these genes.

Differences in the extent of induction between *AtUBP12* and *AtUBP13* indicate that whilst both genes respond to specific stimuli, their respective promoters may also confer specific regulation on each gene. Unconserved regions either within the reported 'minimal' promoter region or further upstream of each respective gene may confer such specific regulatory effects. Based on the induction of *AtUBP12* and *AtUBP13*, delineation of an approximate promoter region would aid future transgenic studies allowing the design of own-promoter or promoter-reporter constructs for each respective gene.

Characterisation of single gene *ubp12* and *ubp13* mutant alleles during infection with virulent and avirulent *Pseudomonas syringae* indicated no alteration in the disease resistance of either allele. This finding raises the possibility that either *AtUBP12* and *AtUBP13* are not involved in resistance against the *Pseudomonas syringae* strains used in this study or that they regulate a specific aspect of resistance which has a minimal consequences during *Pseudomonas syringae* infection.

The potential involvement of *AtUBP12* and *AtUBP13* in disease resistance was investigated by using *Pseudomonas syringae* expressing either *avrB* or *avrRpt2* avirulence genes to initiate resistance through *RPM1* or *RPS2* *R* genes respectively. As previously discussed, the NBS-LRR R-genes are broadly divided into two functional subclasses based on the N-terminal presence of either a Toll interleukin1 domain (TIR-NBS-LRR) or a coiled-coil domain (CC-NBS-LRR) (Dangl and Jones, 2001). Disease resistance signalling associated with TIR-NBS-LRR and CC-NBS-LRR R proteins is mediated by distinct pathways utilising either NDR1 or EDS1 respectively (Aarts et al., 1998). Both *RPM1* and *RPS2* belong to the CC-NB-LRR class of *R* genes which are associated with signalling through the NDR1. It is

possible that *AtUBP12* and *AtUBP13* are functioning specifically in the TIR-NBS-LRR signalling pathway although induction of both genes by *Pst* DC3000 *avrB* suggests otherwise. Using experimental gene induction and resistance assays described in this study, the role of *AtUBP12* and *AtUBP13* in EDS1 mediated signalling could be assessed using *Pseudomonas* expressing *avrRps4* which triggers disease resistance through the TIR-NBS-LRR class *R* gene *RPS4* (Gassmann et al., 1999).

The reported gene induction data warrants a broader investigation into the involvement *AtUBP12* and *AtUBP13* in resistance against different pathogen and *R* gene classes. Established pathogen systems are available to test defence against bacteria, fungi, oomycetes and viruses in *Arabidopsis* (Kunkel, 1996) allowing the further analysis of basal and gene-for-gene defence in *AtUBP12* and *AtUBP13* mutants.

The bacterial growth assays performed in this study specifically examined local resistance to *Pseudomonas* rather than perturbations to systemic acquired resistance (SAR). Given that both *AtUBP12* and *AtUBP13* are highly induced by SA treatment, their potential role in SAR development could be investigated further. Gene induction studies using *ubp12* and *ubp13* mutant lines and established SA responsive *PR* marker genes would be a suitable starting point for such studies.

### **3.8.3 Functional redundancy between *AtUBP12* and *AtUBP13***

The detection of altered downstream signalling or perturbations in pathogen resistance in *ubp12* and *ubp13* mutants may be obscured by functional redundancy between the two genes. Functional redundancy typically results from incomplete speciation between duplicated genes (Pickett and Meeks-Wagner, 1995) and has been previously reported between the *Arabidopsis* UBPs: *AtUBP15* and *AtUBP16* which regulate cell proliferation and leaf development (Liu et al., 2008). In this study, potential functional redundancy between *AtUBP12* and *AtUBP13* was investigated using approaches based on transgenic RNAi silencing and genetic crossing to obtain double mutants.

Results obtained using transgenic expression of a *AtUBP13* hpRNA fragment to induce co-silencing of *AtUBP13* and *AtUBP12* indicated a functional overlap between these genes. The reduced growth/anthocyanin accumulation phenotype seen specifically in T<sub>1</sub> UBP\_RNAi transformants indicated the requirement of either *AtUBP12* or *AtUBP13* for normal plant development. Careful consideration of the *AtUBP13* mRNA region selected to induce co-silencing of *AtUBP12* and *AtUBP13* makes off-target silencing an improbable explanation for the phenotype seen in UBP\_RNAi T<sub>1</sub> plants.

The UBP\_RNAi T<sub>1</sub> phenotype was observed in plants derived from different transformation events thus excluding the possibility that observed phenotypes were linked to the disruption of an existing gene by transgene insertion event. The loss of reduced growth phenotype seen in the T<sub>2</sub> and T<sub>3</sub> generations suggests a possible depletion in transgene expression leading to a decrease in co-silencing efficiency in latter transgenic generations. The silencing of inserted transgenes is frequently observed and represents an obstacle to the development of stable transgenic lines in many cases (Matzke et al., 1996).

RT-PCR analysis of different T<sub>2</sub> generation UBP\_RNAi lines demonstrated marked variability in the extent of co-silencing. Despite co-silencing levels of *AtUBP12* and *AtUBP13* of at least 70% in some UBP\_RNAi T<sub>2</sub> lines, there was no development of the growth reduction phenotype seen in the T<sub>1</sub> generation. This observation suggests that T<sub>1</sub> co-silencing efficiency of *AtUBP12* and *AtUBP13* was potentially higher than that seen in the most efficient T<sub>2</sub> lines to cause the resulting phenotype.

On the basis of these observations, it would seem that endogenous *AtUBP12* and *AtUBP13* mRNA levels need to be reduced beyond 70% to demonstrate the observed growth reduction phenotype and that markedly depleted levels of *AtUBP12* and *AtUBP13* in the cell are still sufficient to provide wild type signalling capacity. Further characterisation of UBP\_RNAi lines is being undertaken to establish if co-silencing effects vary within the life-cycle of the plant and to what extent transgene expression is affected in latter generations.

Attempts to isolate homozygous *ubp12-1 ubp13-1* double mutant lines indicated that simultaneous abolition of transcript from both genes conferred a seedling lethal phenotype and supported the conclusion from the UBP\_RNAi experiments that collectively, *AtUBP12* and *AtUBP13* serve a key function in development.

Analysis of the F<sub>4</sub> cross population where *ubp13-1* was homozygous and *ubp12-1* was segregating demonstrated a range abortion phenotypes in approximately 25% of plants suggesting that double homozygotes were developmentally impaired. Issues related to the genetic penetrance of the *ubp12-1* or *ubp13-1* mutations could be obscuring the fact that double mutant lines lacking *AtUBP12* and *AtUBP13* may actually be embryo lethal rather than seedling lethal.

The observed seedling lethal phenotype of proposed *ubp12-1 ubp13-1* double mutant plants is currently being confirmed in *ubp12-2 ubp13-2* cross plants (data not shown). The reported seedling lethal phenotype in the F<sub>4</sub> generation of *ubp12-1 ubp13-1* plants does suggest that reproductive events leading to the development of F<sub>3</sub> embryos of double homozygotes is intact and that observed lethality is not a sex-linked effect. Issues related to the potential sex linkage of the observed lethality phenotype will need to be examined in future reciprocal male and female crosses between each *ubp12* and *ubp13* mutant line.

The conservation of *AtUBP12/AtUBP13* orthologs in other sequenced eukaryotes implies that they may function to serve an essential signalling role in the cell. On this basis, lethality resulting from the disruption of both *AtUBP12* and *AtUBP13* genes is entirely plausible and has been previously reported for the *Arabidopsis* UBP enzyme *AtUBP14* which is also conserved in eukaryotes rather than plants (Doelling et al., 2001).

#### **3.8.4 AtUBP12 regulates the floral transition signal**

The observed early flowering phenotype of *ubp12* mutant lines indicates that functional redundancy between *AtUBP12* and *AtUBP13* is not complete. Early flowering in multiple *ubp12* null alleles was particularly

evident under short day growth conditions and future work aims to complement this phenotype with transgenic *AtUBP12* overexpressing lines.

The importance of ubiquitination in the maintenance of circadian rhythms and regulation of flowering pathways is well established (Turck et al., 2008) and *AtUBP12* represents the second reported DUB to be implicated in flowering regulation (Liu et al., 2008).

The phenotypic observations suggest that *AtUBP12* functions to stabilise a floral repressor which is presumably ubiquitinated appropriately under long day conditions as part of the floral signal. The loss of *AtUBP12* in *ubp12* mutant alleles presumably results in the increased ubiquitination of the target repressor causing its degradation and resulting in floral induction. The severe abolition of short day induced floral repression seen in *ubp12* mutants suggests that *AtUBP12* may function as a regulator of photoperiod perception. Future studies aim to investigate dysregulation of the light dependent pathway in *ubp12* mutants focussing initially on temporal *CONSTANS* accumulation (Turck et al., 2008).

The contributions of the autonomous and vernalisation pathways to the regulation of flowering are also well characterised (Komeda, 2004). A major point of integration between the autonomous and vernalisation pathways is at the *FLOWERING LOCUS C (FLC)* locus. *FLC* is a *MADS*-box transcription factor which functions as a key floral repressor (Rouse et al., 2002). Elevated levels of *FLC* are associated with late flowering and during the floral transition *FLC* expression is repressed by components of the autonomous and vernalisation pathways (Rouse et al., 2002). *FLC* repression is mediated by chromatin modification where changes in chromatin condensation status affect expression of *FLC* (He and Amasino, 2005). Previous studies have identified numerous signalling proteins that influence chromatin status through histone modification to induce *FLC* repression (Bastow et al., 2004) (He et al., 2003). A recent discovery reported the direct involvement of ubiquitination in chromatin based *FLC* activation implicating the E2 ubiquitin conjugating enzymes *AtUBC1* and *AtUBC2* as *FLC* transcriptional regulators which promote floral repression (Xu et al., 2008).

Future work aims to clarify if the early flowering phenotype of *ubp12* mutants can be linked to the established knowledge of FLC's role in floral signalling. Initial experiments to examine early suppression of FLC transcript levels in *ubp12* mutants under long and short days would be a start point for such studies.

Future studies may also investigate potential linkage of AtUBP12 to *FLC* chromatin status using chromatin immunoprecipitation (ChIP) assays. Chromatin is modified by a variety of post-translational modifications including acetylation, methylation, sumoylation and ubiquitination (Berger, 2001) to exert regulatory outcomes on gene expression. In ubiquitination, regulation of chromatin status of histones H2B and H2A by monoubiquitination is the most frequently detected mode of modification (Weake and Workman, 2008). Corresponding regulatory deubiquitination of histones has also been reported (Weake and Workman, 2008), and it is possible that AtUBP12 functions as regulator of chromatin architecture at the *FLC* locus to modify *FLC* expression.

The observation of aerial rosette structures on short day grown *ubp12* mutants also suggests linkage of AtUBP12 to FLC signalling. Previous studies in the *Arabidopsis* Sy-0 ecotype have established that *FLC* expression regulates late flowering and the formation of aerial rosettes is due to its synergistic activation by *FRI* (*FRIGIDA*) (Poduska et al., 2003) and *HUA2* (Doyle et al., 2005).

Studies by Wang *et al.* indicated that overexpression of *FLC* caused late flowering in primary and axillary meristems and that this late flowering causes the distinctive Sy-0 morphology (Wang et al., 2007). The observation of aerial rosettes in *ubp12* mutants suggests analogy to the Sy-0 phenotype whilst the observed early flowering phenotype is the reverse of that seen in Sy-0 plants. It remains a possibility that AtUBP12 functions in the leaf to regulate *FLC* expression to control flowering time and the axillary meristem to perceive an *FLC* induced signal that influences lateral shoot morphology. The local and meristematic function of *FLC* signalling has been established (Searle et al., 2006) but the possible involvement of AtUBP12 requires further investigation.

Genetic approaches to link AtUBP12 to known flowering pathways may also form the basis of future studies. The generation of crosses between *ubp12* and known late flowering mutants from the autonomous, gibberellin, vernalisation and light dependent pathways (Turck et al., 2008) would allow phenotypic analysis of alterations in *ubp12* associated early flowering.

### 3.8.5 Potential targets of AtUBP12 and AtUBP13

Phenotypes seen in UBP\_RNAi and proposed *ubp12-1 ubp13-1* double mutant lines indicate that both *AtUBP12* and *AtUBP13* proteins can recognise and deubiquitinate common targets which regulate plant development. Conversely, the induction of early flowering seen only in *ubp12* mutants suggests the existence of a specific additional target (or targets) for AtUBP12 which, when stabilised, promote the transition to flowering. Induction data also indicates a coordinated response of *AtUBP12* and *AtUBP13* to pathogen and SA signals implying a further possible target (or targets) that is stabilised during disease resistance signalling.

The simplest interpretation of these results suggests that *AtUBP12* and *AtUBP13* function redundantly to regulate plant development and potentially disease resistance by stabilising target substrates that are presumably distinct. Functional overlap between *AtUBP12* and *AtUBP13* gene products presumably occurs due to the conservation of signal responsive elements in their promoters following gene duplication and the extent of retained amino acid similarity between the proteins. The high level of amino acid identity between *AtUBP12* and *AtUBP13* presumably facilitates deubiquitination of common target proteins giving rise to functional redundancy. As one member of a partially redundant pair of UBP enzymes, *AtUBP12* has gained additional substrate specificity to stabilise a floral suppressor.

Given that thousands of distinct target proteins can potentially be ubiquitinated by the *Arabidopsis* ubiquitination machinery (Vierstra, 2003), the promiscuity of deubiquitinating enzymes (45 identified in this study)

for multiple target substrates is entirely plausible. Specificity of DUBs for multiple targets has been previously reported for HAUSP (Herpesvirus Associated Ubiquitin Specific Protease) (Hu et al., 2006), which is the human ortholog of AtUBP12/AtUBP13 and is proposed to stabilise different substrates in response to specific stimuli (Li et al., 2004).

How *AtUBP12* and *AtUBP13* are potentially regulated to stabilise distinct substrates in response to different signalling cues remains unclear. Previous studies have reported that the conformational activation of UBPs prevents inappropriate stabilisation of targets suggesting a role for interacting partners to modulate enzyme activity (Amerik and Hochstrasser, 2004). The presented data suggests that transcriptional activation of *AtUBP12* and *AtUBP13* may confer a degree of regulation on their function and raises the possibility that regulation of flowering time by *AtUBP12* could also be controlled by tissue specific expression.

Alternatively, the distinction between different substrates of AtUBP12 and AtUBP13 may be based on the post-translational modification of function specific target proteins. In the case of the human UBP HAUSP, Hu *et al.* (Hu et al., 2006) suggest that substrate recognition may be analogous to the required phosphorylation of F-box substrates prior to their ubiquitination (Cardozo and Pagano, 2004). Hu *et al.* suggest that conserved serine residues found in the binding motifs of all currently characterised HAUSP substrates may actually be phosphorylated and that their stabilisation by HAUSP is modulated by dephosphorylation (Hu et al., 2006).

The results presented in this chapter indicate that AtUBP12 and AtUBP13 proteins have redundant and non-redundant roles serving key functions in distinct plant signalling pathways. Presumably, AtUBP12 and AtUBP13 function to stabilise multiple (and in some cases distinct) targets. The observed seedling lethality of *ubp12-1 ubp13-1* double knockouts indicates that a subset of these targets are essential for plant development.

## Chapter 4 – Solanaceous UBP12 orthologs

### 4.1 Introduction

Results reported in Chapter 3 suggest that genetic redundancy between *AtUBP12* and *AtUBP13* in *Arabidopsis* may be obscuring potential disease signalling phenotypes. The finding that *ubp12 ubp13* double mutants are developmentally impaired indicated that alternative approaches to study the potential functions of UBP12 in disease resistance signalling would be required.

Investigations were conducted to identify solanaceous orthologs of *AtUBP12* and *AtUBP13* which would facilitate UBP12 loss of function studies in *N. benthamiana* using Virus Induced Gene Silencing (VIGS). There have been no previous reports which identify or characterise Solanaceous deubiquitinating enzymes and this chapter describes experiments leading to the identification of a novel full length cDNA encoding *NtUBP12*, the tobacco ortholog of *AtUBP12*.

As discussed previously in Chapter 3.6, plant perception of non-host dsRNAs causes initiation of homology dependent mRNA degradation termed post transcriptional gene silencing (PTGS). VIGS is the principle method for loss of function studies in *N. benthamiana* and utilises viral expression of cloned host cDNA fragments to trigger transient PTGS against corresponding endogenous host mRNAs (Ratcliff et al., 2001). VIGS is commonly used to investigate plant disease resistance signalling and has previously been applied successfully to characterise defence regulators such as SGT1 (Peart et al., 2002b) and EDS1 (Peart et al., 2002a).

This chapter reports the application of VIGS to perform reverse genetic studies of *NbUBP12* function in *N. benthamiana* during disease resistance signalling. Solanaceous EST data and various PCR approaches were used to determine the full length cDNA sequence of *UBP12* from tobacco. Using derived *NtUBP12* sequence data, VIGS silencing vectors were generated and the efficiency of gene silencing was established.

Having generated constructs for efficient gene silencing of *NbUBP12*, experiments were performed to investigate its potential role in disease resistance signalling. Cell death assays were conducted during *NbUBP12* silencing to examine its role in HR signalling mediated by *R* genes associated with fungal (*Cf-9*) and bacterial (*Pto*) disease resistance. Alterations to basal resistance by *NbUBP12* silencing was investigated by bacterial growth assays following infection with virulent *Pseudomonas syringae* pv. *tabaci*. This chapter also reports data from our collaborators who have utilised these *NbUBP12* silencing constructs to examine its role in viral resistance against Tobacco Mosaic Virus (TMV).

## 4.2 Identification of solanaceous *UBP12* orthologs

### 4.2.1 Solanaceous EST analysis

To investigate the function of *NbUBP12* using VIGS, sequence data for solanaceous orthologs of *Arabidopsis AtUBP12* was required. The existence of at least a single *AtUBP12* ortholog was confirmed in a recent microarray study comparing transcript changes during HR and PCD in *N. benthamiana* (Kim et al., 2006). The putative *UBP12* EST KS01043A12 was recovered from the hot pepper EST database at the Korea Research Institute of Bioscience and Biotechnology (<http://genepool.kribb.re.kr>). This EST and the *AtUBP12* cDNA sequence were used to query various solanaceous plant EST databases at The Institute for Genome Research (TIGR) (<http://www.tigr.org>).

Detected EST matches to *AtUBP12* cDNA are presented in Table 4.1, only high-scoring ESTs (probability score  $< 1e^{-10}$ ) were included for further analysis. Due to the current absence of a completely sequenced solanaceous genome, genomic approaches instead rely on the availability of EST database resources such as TIGR. The gene indices at TIGR report groups of GenBank published ESTs that correlate to single genes described with comparative annotation as Tentative Consensus (TC) entries (Quackenbush et al., 2001). EST libraries from tobacco (*N. tabacum*), *N. benthamiana* and potato (*S. tuberosum*) were queried with *AtUBP12* cDNA

which detected 13, 5 and 8 high scoring EST matches respectively (Table 4.1).

Within the EST matches, ORF regions were identified by alignment against *AtUBP12* and corresponding DNA regions were excised from the respective EST sequence. Plausible sequence regions obtained using this approach (Figure 4.1 A) were used for subsequent alignment analysis and primer design. Extracted sequence regions from recovered ESTs were aligned to investigate the possibility that two copies of *UBP12* also exist in solanaceous plants (data not shown). Alignment of 7 tobacco ESTs indicated no consistent sequence variations indicating that each cDNA originated from the same genomic template. This result supports the prior conclusion that an ancestral *UBP12* gene underwent duplication after the divergence of the Solanaceae (Chapter 3.3).

Sequence coverage from the recovered *UBP12* ESTs was insufficient to reconstruct full length cDNA so primer sequences were instead derived for 5' and 3' termini to amplify the complete 3.3 kb *NtUBP12* coding sequence from tobacco cDNA. A schematic alignment of the extracted solanaceous EST regions against *AtUBP12* cDNA is presented in Figure 4.1. For the 3' termini of *NtUBP12*, a consensus sequence was derived from three tobacco and *N. benthamiana* ESTs (Figure 4.1 A) from which a 21 bp primer (*NtUbp12\_TAG*) was designed. Sequence coverage of the 5' start codon region was provided by a single potato EST (Figure 4.1 A) from which a 21 bp primer was designed (*StUbp12\_ATG*). The use of a potato cDNA as a template for primers to amplify tobacco cDNA was considered appropriate based on sufficiently close phylogenetic relationship between these species which typically allows DNA hybridisation to occur (Brigneti et al., 2004).

Attempts to PCR amplify *NtUBP12* from tobacco cDNA using the designed primers generated limited quantities of full length 3.3 kb product. Instead, an alternative cloning strategy was adopted whereby overlapping fragments from 5' and 3' region of *NtUBP12* (Figure 4.1 B) were cloned and sequenced. Using EST sequence data, internal *NtUBP12* primers were designed (*NtU12\_2176\_3* and *NtU12\_1677\_5*) and used in combination with *NtUBP12* 5' and 3' termini primers to PCR amplify 5' (*NtUbp12\_5PF*) and 3'

Species	TIGR TC Number	Genbank Associated ESTs	Tissue of Origin
<i>N. tabacum</i>	TC8160	EB682588 EB426207 DV160278 CV021553	Seedling Flower Seedling Mixed
<i>N. tabacum</i>	TC35889	EB428655	Flower
<i>N. tabacum</i>	TC13270	EB450063 DW002122	Leaf Root
<i>N. tabacum</i>	TC9908	DW002622 BP130546 AM824168 EB445701	Root BY-2 Cells Seedling Root
<i>N. tabacum</i>	Singleton	EB430524	Leaf
<i>N. benthamiana</i>	TC9007	CK280687 CK280688 CK280689 CK280686	Mixed Mixed Mixed Mixed
<i>S. tuberosum</i>	TC160358	BQ117852 BG890341 BF052779 BM113079	Mixed Tuber Leaf Root
<i>S. tuberosum</i>	Singleton	CK640776	Leaf

**Table 4.1** Solanaceous *UBP12* ESTs recovered from TIGR gene indices.

TIGR gene indices for *Nicotiana tabacum*, *Nicotiana benthamiana* and *Solanum tuberosum* were queried with the *AtUBP12* cDNA sequence and high scoring TC entries were recovered.

(NtUbp12\_3PF) cDNA fragments (Figure 4.1 B). Amplified *NtUBP12* fragments were cloned and sequenced in duplicate to obtain a final consensus cDNA sequence for *NtUBP12*.

#### **4.2.2 RACE PCR to determine *NtUBP12* 5' terminus sequence**

The final cDNA sequence obtained for *NtUBP12* was derived entirely from tobacco cDNA amplified products with the exception of the 5' terminal primer region which was designed using sequence data from a potato EST (CK640776 - Figure 4.2 A). Rapid Amplification of cDNA Ends (RACE) PCR was performed using tobacco cDNA to verify the *NtUBP12* cDNA sequence in the 5' terminal primer region. Using the established *NtUBP12* sequence, internal primers were designed for sequential SP1, SP2 and SP3 RACE PCR reactions (Figure 4.2 A). RACE primers were designed to hybridize against *NtUBP12* cDNA at 903 bp (NtUbp12\_903RC), 742 bp (NtUbp12\_742RC) and 554 bp (NtUbp12\_554RC) relative to the established start codon (Figure 4.2 A). Using tobacco total RNA, *NtUBP12* specific cDNA was synthesised and used as a template for sequential RACE PCR reactions to obtain a final 554 bp product (Figure 4.2 A). The final RACE PCR product was cloned and two individual clones were sequenced to confirm the *NtUBP12* cDNA sequence in the 5' terminal region. The final verified cDNA sequence of *NtUBP12* was deposited into GenBank under the accession number FJ264198.

Based on an alignment of the catalytic domains of AtUBP1, AtUBP2, AtUBP3, AtUBP4, AtUBP5, AtUBP6, AtUBP12, AtUBP13 and NtUBP12 a phylogeny was inferred using MEGA (Figure 4.2 B). The phylogeny demonstrated significant clustering (bootstrap confidence 100%) of AtUBP12 and AtUBP13 with NtUBP12 conforming that these genes are orthologous (Figure 4.2 B). Sequence analysis of NtUBP12 indicated it shared 83% amino acid identity with AtUBP12 and Pfam analysis confirmed the presence of an N-terminal MATH/TRAF domain (PF00917) as detected in the *Arabidopsis* orthologs (Figure 4.2 B).

**Figure 4.1** *NtUBP12* EST summary and full length cDNA determination.

(A) Summary of sequence regions extracted from Solanaceae EST matches (reported in Table 4.1) based on alignment to *AtUBP12*. (B) *NtUBP12* full length cDNA amplicons, relating to the 5' end (Nt Ubp12\_5PF) and 3' end (Nt Ubp12\_3PF) of *NtUBP12*.

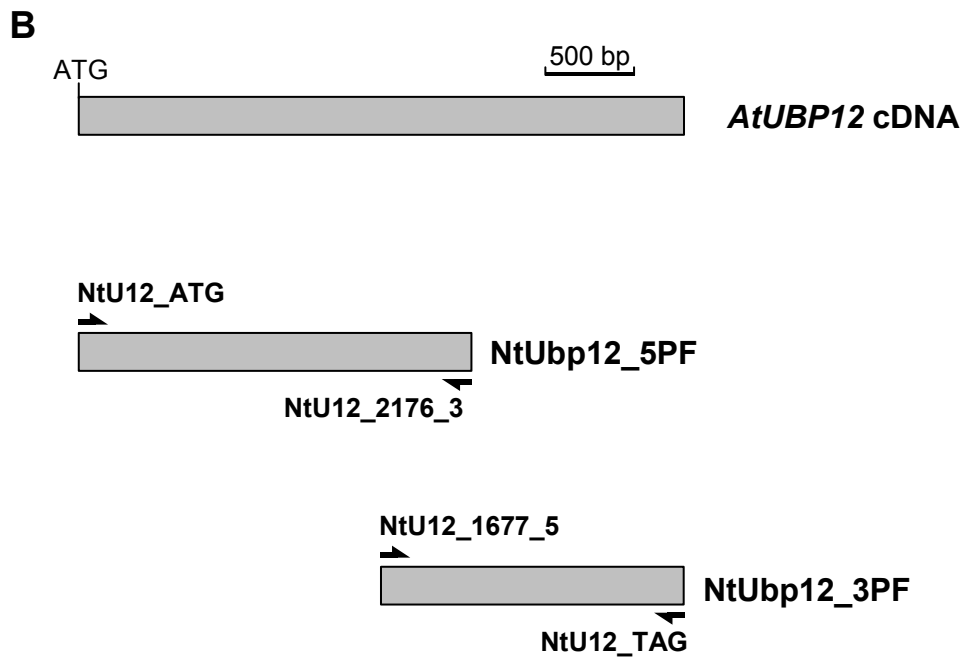
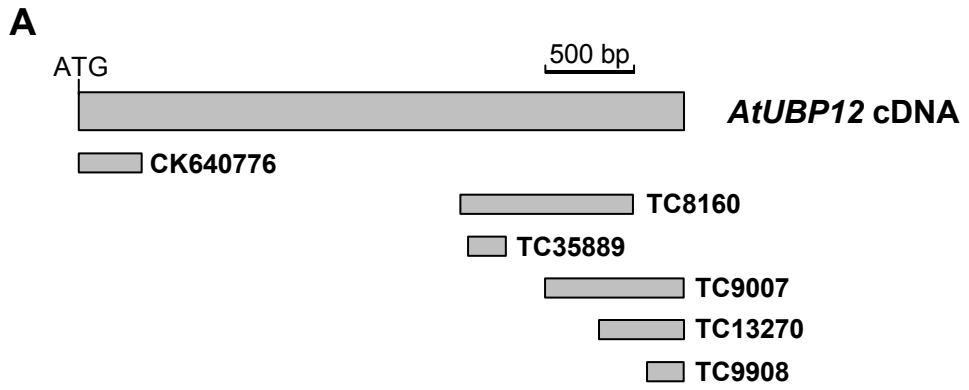
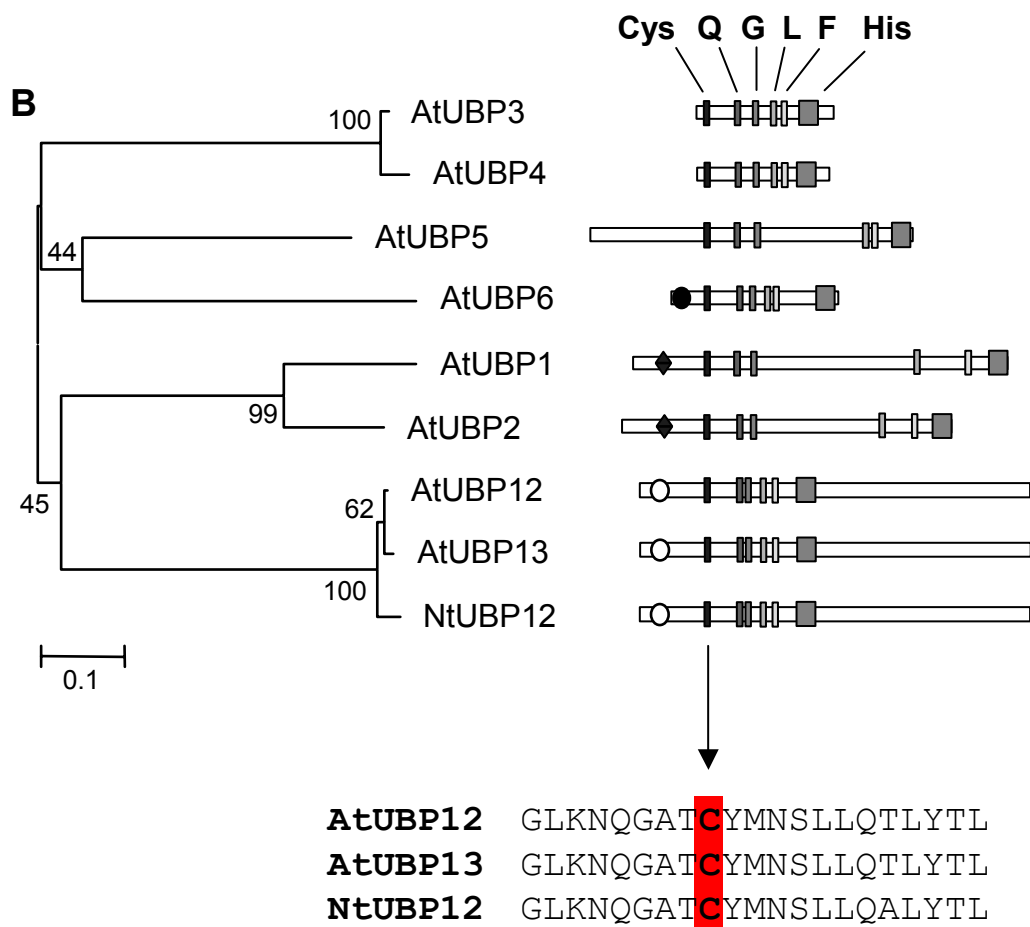
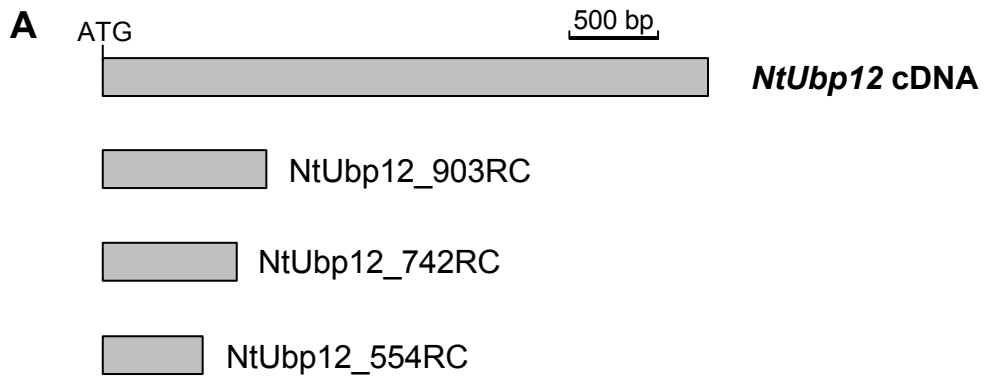


**Figure 4.2** RACE PCR strategy to establish 5' region of *NtUBP12*.

(A) *NtUBP12* amplicon locations for 5' RACE. NtUbp12\_903, NtUbp12\_742 and NtUbp12\_554 fragments were amplified in RACE SP1, SP2 and SP3 reactions respectively. (B) Phylogeny of *NtUBP12* with a subset of *Arabidopsis* UBP enzymes. Phylogeny inferred by neighbor joining from an alignment of UBP Cys and His box catalytic regions. Phylogenetic tree accuracy was tested with 10,000 bootstrap replicates represented by percentage values at respective nodes. Tree scale bar represents substitutions per site. UBP protein domain diagrams indicate catalytic regions. Additional domains as confirmed by Pfam analysis: Ubiquitin-like domain (black circle), Potential zinc finger (black diamond) and MATH/TRAF domain (white circle). Corresponding alignment of Cys box region from AtUBP12, AtUBP13 and *NtUBP12* with active site cysteine (highlighted in red) is indicated.



### 4.3 *NtUBP12* transcript analysis during *Cf-9/Avr9* elicited HR

To investigate the potential involvement of *NtUBP12* in plant disease resistance signalling, the *Cf-9/Avr9* elicitor system was used to elicit hypersensitive cell death in tobacco. As previously described, the protein expressed from *C. fulvum* avirulence gene *Avr9* triggers disease resistance in host tomato (*L. esculentum*) plants mediated by the product of host *R* gene *Cf-9*. The cloning of *Cf-9* and *Avr9* genes has allowed the development of non-host systems to facilitate convenient study of the plant hypersensitive response (HR) (Hammond-Kosack et al., 1998). In this study, transgenic tobacco lines overexpressing the *C. fulvum Avr9* gene were used to obtain *Avr9* peptide in solution (recovered by vacuum extraction) (Hammond-Kosack et al., 1998). Various dilutions of extracted *Avr9* peptide were infiltrated into transgenic tobacco overexpressing the tomato *Cf-9* gene to elicit the hypersensitive response.

To examine changes in *NtUBP12* transcription during the hypersensitive response, *NtUBP12* mRNA levels were measured by RT-PCR during *Avr9* elicited hypersensitive cell death in *Cf-9* tobacco. The HR was elicited in *Cf-9* tobacco using a titrated stock of *Avr9* peptide solution to cause complete tissue necrosis in 8 - 10 hours following infiltration. A parallel wounding control experiment was conducted using *Avr4* peptide solution to infiltrate *Cf-9* tobacco where no HR was induced (Thomas et al., 2000). Leaf tissue samples were taken at 0, 30, 60, 120 and 240 minutes after infiltration and corresponding cDNA samples were normalised using primers for tobacco *ACTIN2* primers as constitutively expressed control gene (Figure 4.3). Transcript levels of the tobacco cell death marker gene *hsr203J* (Pontier et al., 1998) during cell death were measured as a positive experimental control using specific primers (*Hsr203J\_5* and *Hsr203J\_3*). The *hsr203J* marker underwent a marked induction following *Avr9* treatment (maximal at 240 minutes) and lesser induction following *Avr4* treatment (Figure 4.3). The sensitivity of *hsr203j* to both wounding and cell death signals has been established (Durrant et al., 2000) and demonstrated the expected positive induction pattern in this study. *NtUbp12* mRNA levels were measured using specific primers (*NtU12\_742\_KD\_5* and *NtU12\_742\_KD\_3*) and displayed differential

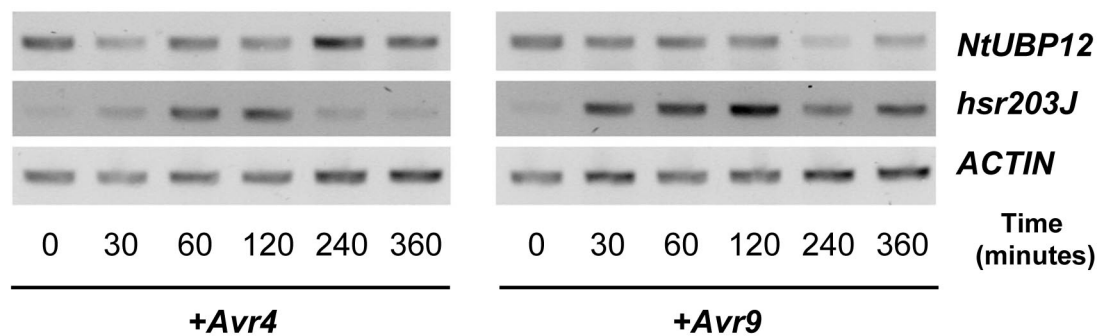


**Figure 4.3** *NtUBP12* is suppressed during Avr9 HR elicitation.

Cf9 tobacco plants were infiltrated with solution containing either Avr4 or Avr9, and leaf samples were harvested at the time points indicated. Total RNA was isolated and used for RT-PCR with specific primers for *NtUBP12* (28 cycles), *hsr203J* (28 cycles) and *ACTIN* (24 cycles).

expression in response to wounding and cell death signals. *NtUbp12* transcript levels were unaltered during the Avr4 elicited wounding response but demonstrated a marked suppression in the latter stages of the Avr9 induced cell death timecourse (Figure 4.3). Densitometry analysis indicated an Avr9 induced 6.5 and 2 fold decrease in *NtUbp12* transcript levels at 240 and 360 minutes respectively after Avr9 elicitor relative to the wounding control (Figure 4.3).

The reported data indicates that *NtUBP12* transcript levels are suppressed in the latter stages (240 minutes post infiltration) of Avr9/Cf9 elicited HR suggesting that the transcriptional control of *NtUBP12* does not contribute to cell death initiation occurring in the 0 - 120 minute stage of the timecourse.

#### **4.4 VIGS based silencing of *NbUbp12***

Having established the cDNA sequence of *NtUBP12*, this data was used to design constructs for VIGS that would facilitate transient reduction of *UBP12* mRNA levels in the close tobacco relative *N. benthamiana*. VIGS exploits an inherent plant anti-viral defence mechanism which leads to the sequence specific post-transcriptional gene silencing (PTGS) based on recognition of 'foreign' RNA molecules (Wang and Metzlaff, 2005). In this study the Tobacco Rattle Virus (TRV) based system was used to initiate gene silencing through *Agrobacterium* mediated delivery of TRV vectors RNA1 and RNA2 into the plant cell (Ratcliff et al., 2001). Following TRV culture inoculation, expressed viral progeny then spread into systemic emerging leaves. The pTV00 vector encoding TRV RNA2 contains a cloned cDNA fragment from the silencing target gene and 21 - 24 days after virus culture inoculation PTGS causes depletion of target gene mRNA levels in new systemic leaves.

When using the VIGS system, the progress and efficiency of silencing is typically monitored using positive control genes which cause a visible phenotype upon transcript depletion. In this study, a 409 bp cDNA fragment of the Phytoene Desaturase (PDS) gene from *N. benthamiana* was cloned into pTV00 for use as a gene silencing positive control (Ratcliff et

al., 2001). Silencing of *PDS* causes a photobleaching phenotype (Kumagai et al., 1995) as demonstrated in *N. benthamiana* plants 21 days after virus culture inoculation (Figure 4.4). *PDS* gene silencing was used as a positive control for every VIGS experiment in this study and based on the development of photobleaching after 21 days the 4<sup>th</sup>, 5<sup>th</sup> and 6<sup>th</sup> emerging leaves were considered to be efficiently silenced (Figure 4.4).

VIGS based gene silencing is typically initiated using sense cDNA fragments sized 200 - 800 bp from the target gene (Liu and Page, 2008). To use the VIGS method, allowances should be made for potential silencing of related genes which may have homology to the target gene, causing so called 'off target' silencing. Gene silencing of *NbUBP12* was initiated using two non-overlapping cDNA fragments (Figures 4.5 A and 4.6 A) which were selected from outside the protease catalytic region that is conserved in all UBP enzymes.

Two pTV00 constructs were made, each containing a distinct *NtUBP12* cDNA fragment. Constructs were named based on insert size with TRV:U12\_562 containing a 562 bp fragment (product amplified using NtUbp12\_562\_5 and NtUbp12\_562\_3 primers) and TRV:U12\_742 containing a 742 bp fragment (product amplified using NtUbp12\_742\_5 and NtUbp12\_742\_3 primers) (Figures 4.5 A and 4.6 A). The potential for off target silencing from each *NtUBP12* cDNA fragment was assessed by BLAST analysis against TIGR tobacco and *N. benthamiana* gene indices. Querying the TIGR EST databases with the *NtUBP12* 562 bp and 742 bp fragments retrieved only high scoring TC entries previously identified in the initial solanaceous EST screen (Chapter 4.2). *NtUBP12* VIGS fragments were also BLAST queried against the *Arabidopsis* genome as a further screen for off target matches from a complete plant genome. In this case *AtUbp12* and *AtUbp13* were recovered as top scoring matches (E values  $\sim 1e^{-25}$ ) with the third match having insignificant homology to the query sequence (E value  $\sim 0.1$ ). No matches with significant homology to sequences other than *Ubp12* were detected in this analysis, indicating that *NtUBP12* VIGS constructs designed for this study should not induce off target gene silencing.

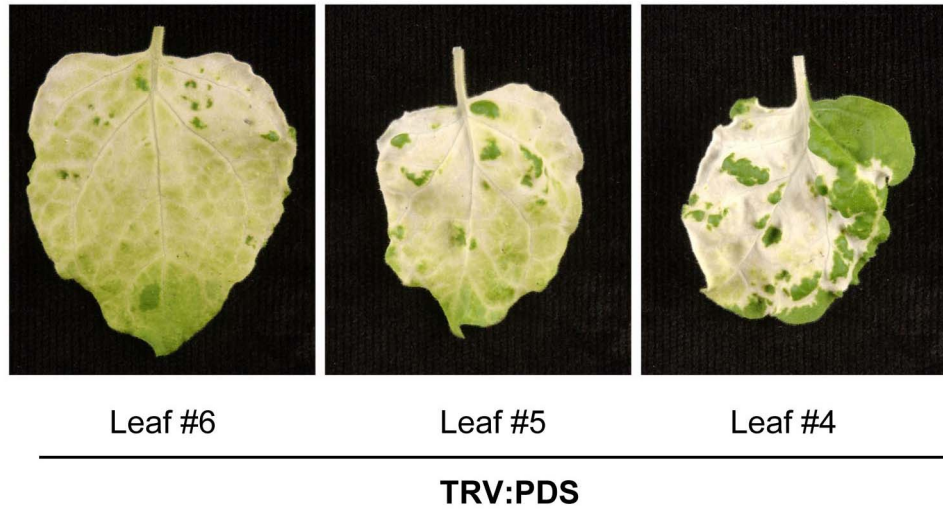


**Figure 4.4** Development of photobleaching in *PDS* silenced *N. benthamiana*

*N. benthamiana* plants were inoculated with *Agrobacterium* carrying TRV:PDS silencing constructs and photographed following 21 days of growth under standard conditions. Photographs represent 4<sup>th</sup>, 5<sup>th</sup> and 6<sup>th</sup> new emerging leaves as indicated.

The efficiency of *NbUBP12* silencing by TRV:U12\_562 and TRV:U12\_742 constructs was assessed by RT-PCR using specific primers to amplify an *NbUBP12* product upstream of the TRV expressed fragment (Figures 4.5 A and 4.6 A). RT-PCR was performed to compare *NbUBP12* mRNA levels in leaves from three independent plants infected with empty pTV00 (TRV:00 control) against leaves from three independent plants infected with TRV\_U12 silencing constructs at 24 days after TRV culture inoculation (Figures 4.5 B and 4.6 B).

Independent cDNA samples for RT-PCR were normalised using primers for the constitutively expressed *ACTIN2* gene (NtActin2\_5 and NtActin2\_3) and specific *NtUBP12* primers were used to quantify silencing caused by TRV:U12\_562 (NtUBP12\_562KD\_5 and NtUBP12\_562KD\_3) (Figure 4.5 A) and TRV:U12\_742 (NtUBP12\_742KD\_5 and NtUBP12\_742KD\_3) (Figure 4.6 A). Gene silencing using both TRV:U12\_562 and TRV:U12\_742 constructs caused a significant decrease in *NbUBP12* mRNA levels relative to TRV:00 control (Figures 4.5 B and 4.6 B). Densitometry analysis indicated that *NbUBP12* mRNA levels were reduced by approximately 69% using TRV\_U12\_562 and 74% using TRV\_U12\_742 relative to TRV:00 infected controls. Characterisation of the gene silencing by *NbUBP12* TRV constructs confirmed that they were suitable for loss of function studies in *N. benthamiana*.

After the requisite growth period to allow the systemic silencing development, *NbUBP12* silenced plants (TRV:U12\_562 or TRV:U12\_742 infected) appeared morphologically indistinct from control plants (TRV:00 infected).

**Figure 4.5** VIGS based silencing of *NbUBP12* using TRV:U12\_562.

(A) Schematic alignment against full length *NtUBP12* cDNA indicating location of *NtUBP12* fragment cloned into TRV:U12\_562 and location of RT-PCR primers used to examine gene silencing by TRV:U12\_562. (B) RT-PCR demonstrating reduction in *NbUBP12* mRNA levels 24 days after introduction of TRV:U12\_562. Total RNA was isolated and from three independent plants infected with either TRV:00 or TRV:U12\_562 and used for RT-PCR with specific primers for *NtUBP12* (NtUBP12\_562KD, 28 cycles) and *ACTIN* (24 cycles).

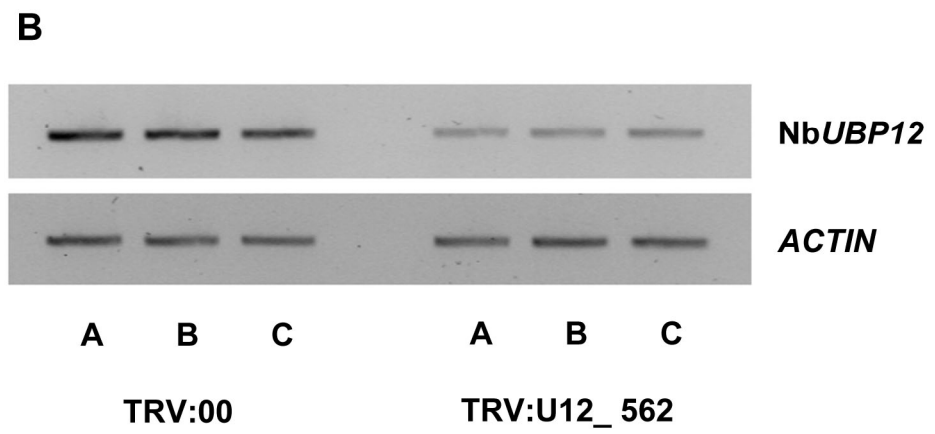
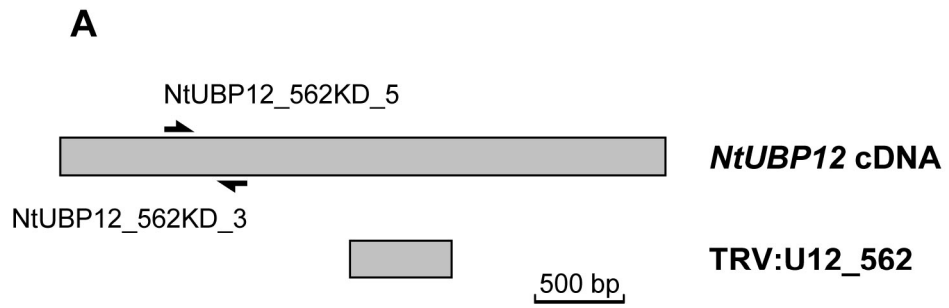
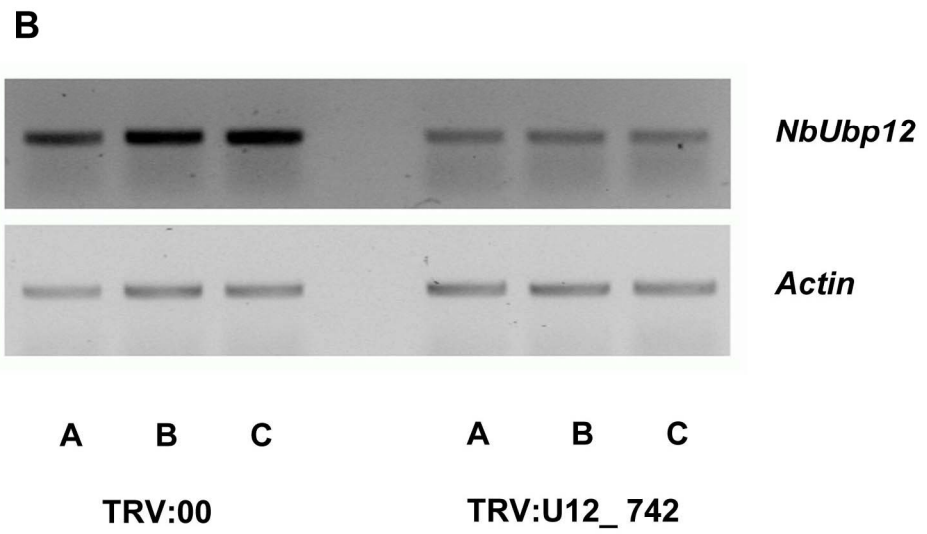
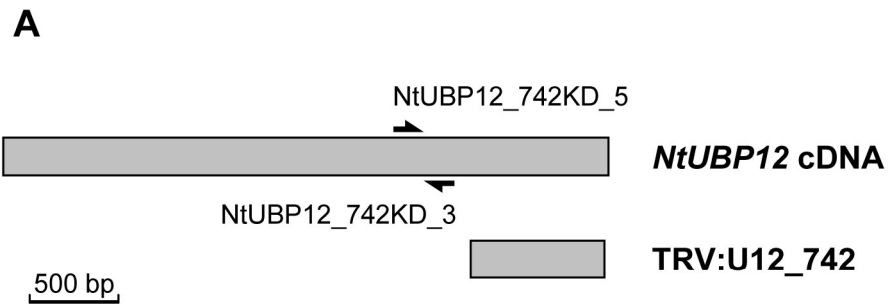


**Figure 4.6** VIGS based silencing of *NbUBP12* using TRV:U12\_742.

(A) Schematic alignment against full length *NtUBP12* cDNA indicating location of *NtUBP12* fragment cloned into TRV:U12\_742 and location of RT-PCR primers used to examine gene silencing by TRV:U12\_742. (B) RT-PCR demonstrating reduction in *NbUBP12* mRNA levels 24 days after introduction of TRV:U12\_742. Total RNA was isolated and from three independent plants infected with either TRV:00 or TRV:U12\_742 and used for RT-PCR with specific primers for *NtUBP12* (NtUBP12\_742KD, 28 cycles) and *ACTIN* (24 cycles).



#### 4.5 Avr9 elicited cell death assay during VIGS silencing of *NbUbp12*

The potential involvement of NbUBP12 in *Cf-9/Avr9* triggered HR was assessed using *Agrobacterium* mediated transient expression of *Cf-9* and *Avr9* genes during VIGS based silencing of *NbUBP12* in *N. benthamiana*.

Phenotypic assessment of the hypersensitive response (HR) is often estimated by the extent of tissue necrosis within a leaf patch infiltrated with the appropriate cell death elicitors (Peart et al., 2002b). To study *Cf-9/Avr9* elicited HR in *N. benthamiana*, individual constructs expressing either *Cf-9* or *Avr9* genes under the 35S Cauliflower Mosaic Virus promoter (Thomas et al., 2000) were transformed into *Agrobacterium* and equalised culture inoculums were mixed and infiltrated into *N. benthamiana* leaves. Following agroinoculation, *Cf-9* R gene and *Avr9* elicitor gene products were expressed and targeted to the plasma membrane (*Cf-9* protein) or secreted (*Avr9* peptide) before triggering the HR (Thomas et al., 2000).

Typically, agroinoculation of *Cf-9/Avr9* constructs results in a visible cell death patch developing 3 - 4 days post infiltration. The HR signalling response to an inoculated titre of elicitor can be measured in accordance with the development of hypersensitive cell death. In this study, HR responses were estimated as a percentage coverage of necrotic cell death area within the total infiltration patch. Cell death scores were classified into three categories of either: No HR (no visible cell death), Weak HR (limited cell death development, typically upto 40% of the infiltration area) or Confluent HR (confluent cell death development, typically in 70 - 100% of the infiltration area).

To elicit the HR, *Cf-9/Avr9* constructs were agroinoculated into *N. benthamiana* at final OD<sub>600</sub> titres of 0.4 and 0.2. Agroinoculation of *N. benthamiana* plants aged 5 - 6 weeks at these titres typically elicited a weak HR response with cell death scores ranging between No HR and Weak HR categories (Figures 4.8 and 4.10). Having established an appropriate sensitivity range for *Cf-9/Avr9* agroinoculation, the HR assay was performed on *N. benthamiana* plants undergoing VIGS based *NbUbp12* silencing.

HR cell death assays were performed on *N. benthamiana* plants 22 days after TRV infection. Experiments included negative control plants infected with TRV:00 (empty pTV00 vector), positive control plants infected with TRV:SGT1 to silence *NbSGT1* and plants infected with TRV:U12\_742 and TRV:U12\_562 to silence *NbUbp12*. As previously described, SGT1 is a positive HR regulator, the silencing of which compromises HR and disease resistance in a broad range of host and non-host plant-pathogen interactions (Peart et al., 2002b).

The HR was triggered in TRV infected plants by agroinoculation of *Cf-9/Avr9* constructs and the resulting hypersensitive cell death was recorded at 5 days post infiltration. Independent VIGS experiments were conducted to silence *NbUbp12* using TRV:U12\_562 (Figures 4.7 and 4.8) and TRV:U12\_742 constructs (Figures 4.9 and 4.10).

**Figure 4.7** Cf-9/Avr9 elicited HR is increased during *NbUBP12* silencing by TRV:U12\_562.

(A) Cf-9/Avr9 construct agroinoculation scheme indicating final *Agrobacterium* titres in patch infiltration sites on silenced *N. benthamiana* leaves. Cf-9/Avr9 constructs were patch inoculated on TRV silenced *N. benthamiana* leaves at final OD<sub>600</sub> of 0.4 (upper patch) or 0.2 (lower patch).

(B) Cf-9/Avr9 elicited HR cell death development in VIGS silenced *N. benthamiana* infected with TRV:00, TRV:U12\_562 or TRV:SGT1. Images taken at 5 days post elicitor infiltration.

**A**

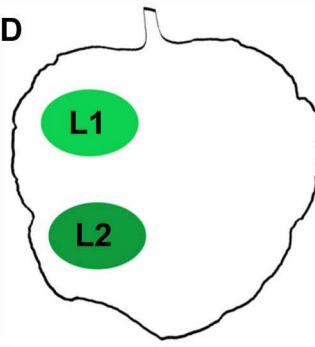
Avr9/Cf-9 OD

0.4

L1

0.2

L2



TRV-silenced leaf

**B**



TRV:U12\_562



TRV:00



TRV:SGT1

**Figure 4.8** Scoring of the increased Cf-9/Avr9 elicited HR during *NbUBP12* silencing by TRV:U12\_562.

Cf-9/Avr9 elicited HR cell death development in VIGS silenced *N. benthamiana* infected with TRV:SGT1, TRV:00 or TRV:U12\_562. HR elicited by agroinoculation of Cf-9/Avr9 constructs at final OD<sub>600</sub> of 0.4 (**A**) or 0.2 (**B**). HR development scored at 5 days post elicitor infiltration.

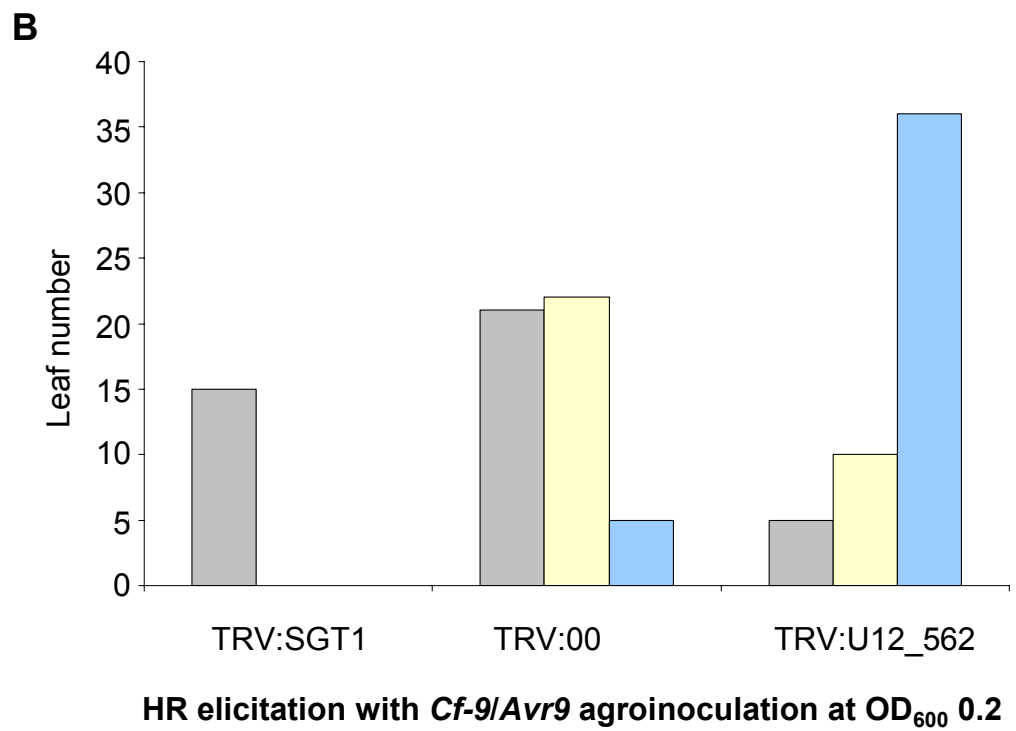
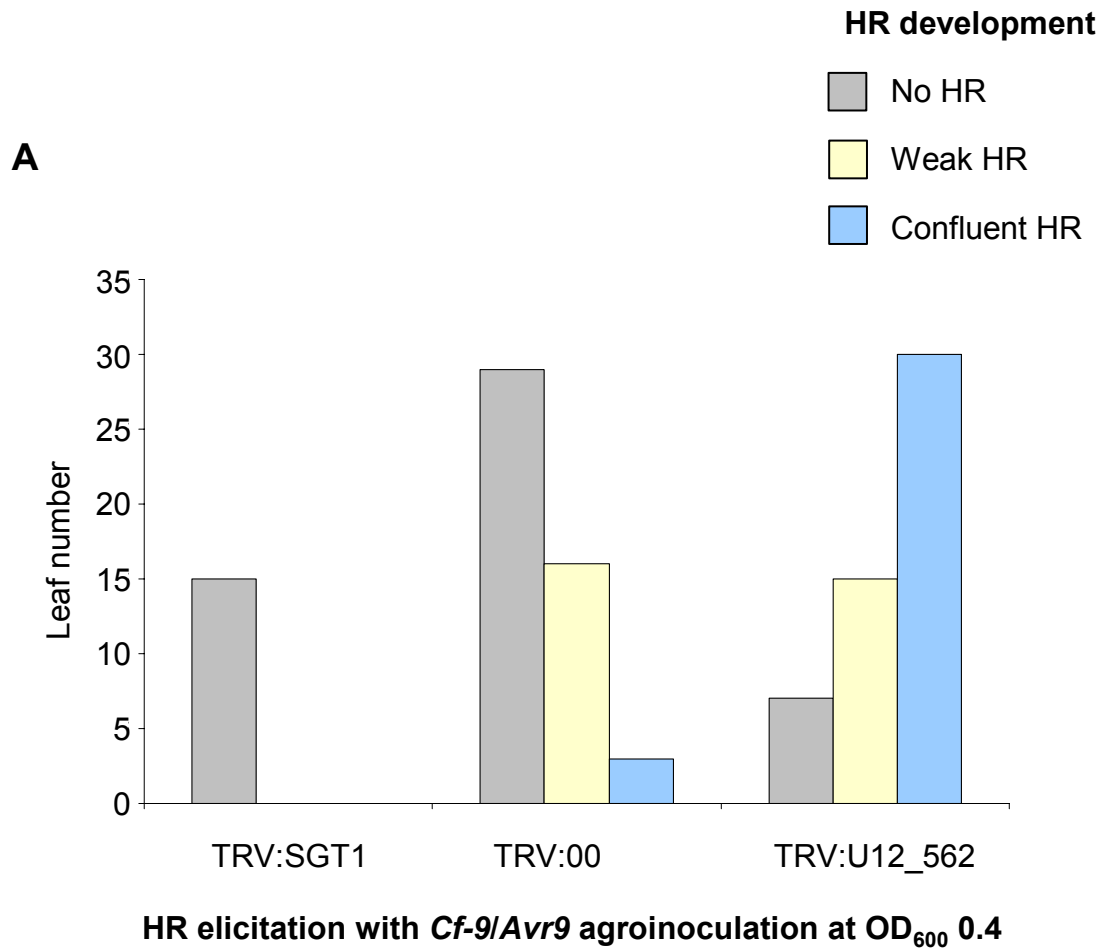


**Figure 4.9** Cf-9/Avr9 elicited HR is increased during *NbUBP12* silencing by TRV:U12\_742.

(A) Cf-9/Avr9 construct agroinoculation scheme indicating final *Agrobacterium* titres in patch infiltration sites on silenced *N. benthamiana* leaves. Cf-9/Avr9 constructs were patch inoculated on TRV silenced *N. benthamiana* leaves at final OD<sub>600</sub> of 0.4 (upper patch - L1) or 0.2 (lower patch - L2).

(B) Cf-9/Avr9 elicited HR cell death development in VIGS silenced *N. benthamiana* infected with TRV:00, TRV:U12\_742 or TRV:SGT1. Images taken at 5 days post elicitor infiltration.

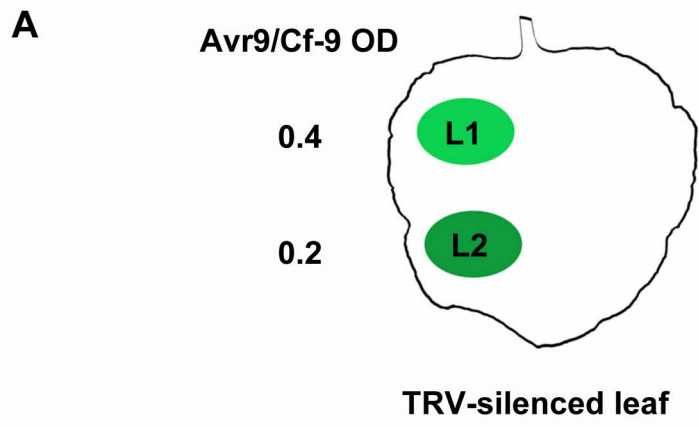
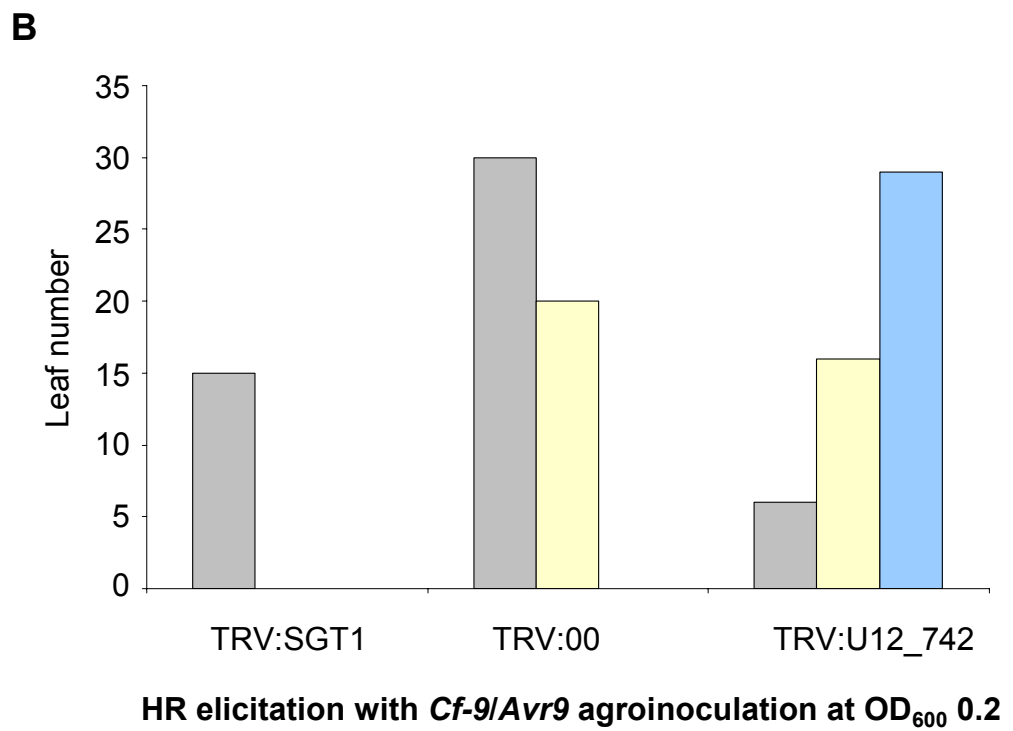
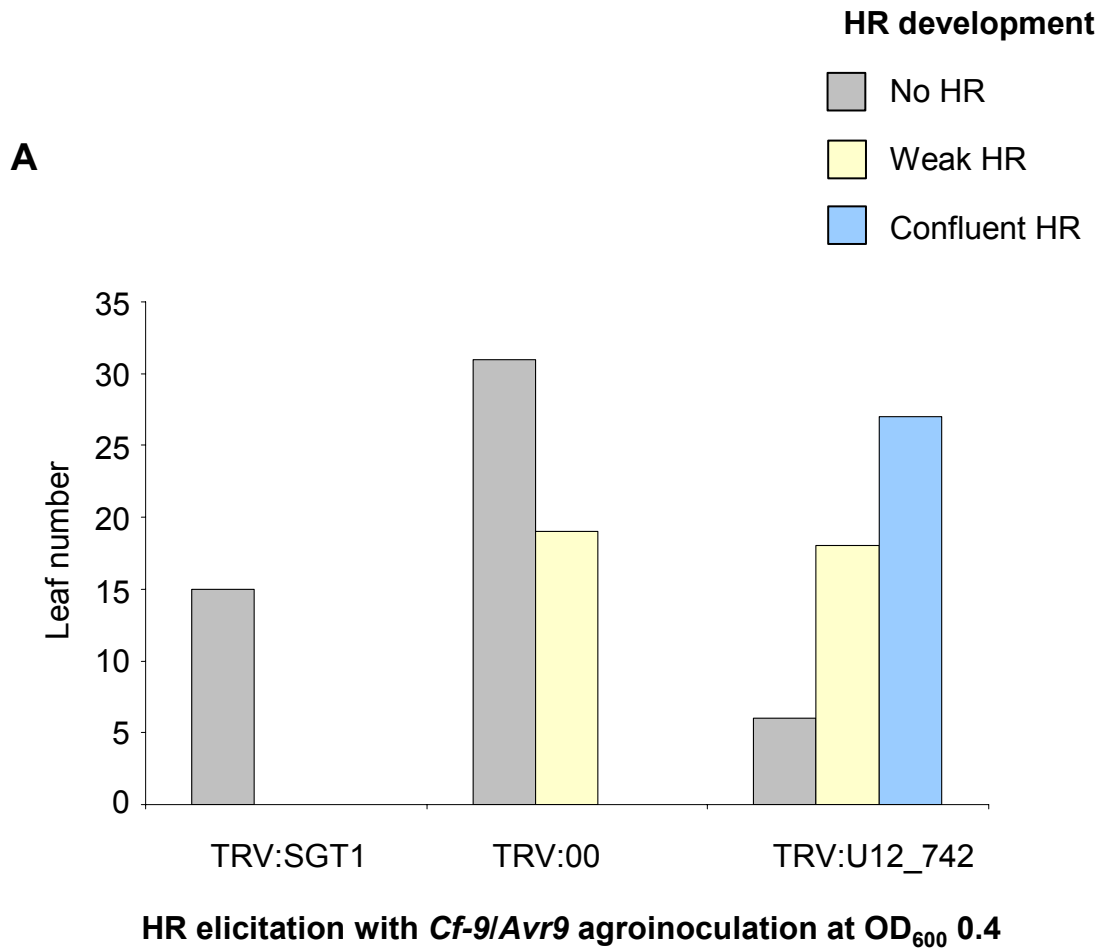


**Figure 4.10** Scoring of the increased Cf-9/Avr9 elicited HR during *NbUBP12* silencing by TRV:U12\_742.

Cf-9/Avr9 elicited HR cell death development in VIGS silenced *N. benthamiana* infected with TRV:SGT1, TRV:00 or TRV:U12\_742. HR elicited by agroinoculation of Cf-9/Avr9 constructs at final OD<sub>600</sub> of 0.4 (**A**) or 0.2 (**B**). HR development scored at 5 days post elicitor infiltration.



In all experiments, negative and positive controls exhibited the expected phenotypes with the development of either no HR or limited HR symptoms in TRV:00 infected plants and no visible HR development in TRV:NbSGT1 infected plants (Figures 4.8 and 4.10).

Increased sensitivity to the Cf-9/Avr9 elicited HR signal was observed in *NbUbp12* silenced plants. Following agroinoculation of *Cf-9/Avr9* constructs at OD<sub>600</sub> 0.4 on TRV:NtU12\_562 infected plants, 58% of leaves tested demonstrated confluent HR compared to 6% of leaves in TRV:00 infected controls (Figures 4.7 and 4.8). Similar results were observed in TRV:NtU12\_742 infected plants where 53% of leaves tested demonstrated confluent HR compared to 0% of leaves in TRV:00 infected controls (Figures 4.9 and 4.10). Equivalent HR development trends were observed in each silencing experiment using lower *Cf-9/Avr9* construct titres at OD<sub>600</sub> 0.2 (Figures 4.8 and 4.10).

Reduced accumulation of *NbUbp12* transcript in three phenotypic leaves was confirmed by RT-PCR for TRV:U12\_562 and TRV:U12\_742 silencing constructs compared with TRV:00 control (Figures 4.5 and 4.6). The increased HR phenotype was observed almost exclusively in *NbUbp12* silenced plants suggesting its role as a negative regulator of Cf-9/Avr9 mediated HR in *N. benthamiana*

#### 4.6 *avrPto/Pto* mediated HR cell death assay during *NbUbp12* silencing

The potential involvement of NtUBP12 in *R* gene mediated bacterial resistance was assessed using the *avrPto/Pto* interaction. Breeding studies established that resistance to *Pseudomonas syringae* pv. *tomato*, the causative agent of tomato bacterial speck disease, was mediated by the tomato *R* gene *Pto* (Pedley and Martin, 2003). Comparison of *P. s. pv. tomato* strains with differential virulence on tomato expressing *Pto* led to the identification of the *avrPto* gene and the subsequent definition of a gene-for-gene interaction between *avrPto* and *Pto* (Ronald et al., 1992). *Pto*-mediated resistance to *avrPto* expressing *P. s. pv. tomato* is associated with a typical localised HR response and reduced bacterial growth (Ronald et al., 1992).

In this study *avrPto/Pto*-mediated HR was elicited in transgenic *N. benthamiana* expressing *Pto* under a 35S promoter following infection with *P. s. pv. tabaci* expressing the *avrPto* gene (Rommens et al., 1995). HR cell death assays were conducted by patch infiltration of *P. s. pv. tabaci avrPto* at intermediate and low titres (Figure 4.11 A). Bacterial inoculation titres were adjusted to cause an intermediate HR with limited cell death (intermediate titre -  $6 \times 10^6$  cfu/ml) or a minimal HR response (low titre -  $3 \times 10^6$  cfu/ml). These intermediate and low bacterial titres defined a sensitivity range for the development of hypersensitive cell death to allow analysis of how silencing *NbUbp12* may suppress or promote the *avrPto/Pto*-mediated HR.

*NbUbp12* was silenced by infection of 35S *Pto N. benthamiana* plants using the TRV:U12\_562 construct. After 22 days the upper leaves (emerging leaves 4, 5 and 6) were patch infiltrated with intermediate and low *P. s. pv. tabaci avrPto* titres and scored for HR development compared to TRV:00 infected controls after 4 days (Figure 4.11 B). HR scoring criteria was based on percentage development of necrotic cell death within the infiltrated patch (as described in Section 4.2).

**Figure 4.11** *avrPto/Pto* elicited HR is unchanged during *NbUBP12* silencing by TRV:U12\_562.

(A) *P. s. pv. tabaci avrPto* infiltration scheme indicating final pathogen titres in patch infiltration sites on silenced *N. benthamiana* leaves. *P. s. pv. tabaci avrPto* was patch infiltrated into TRV-silenced leaves at  $3 \times 10^6$  cfu/ml (upper patch – L1) and  $6 \times 10^6$  cfu/ml (lower patch – L2). (B) *avrPto/Pto* elicited HR cell death development in VIGS silenced *N. benthamiana* infected with TRV:00 or TRV:U12\_562. Images taken at 4 days post *P. s. pv. tabaci avrPto* ( $6 \times 10^6$  cfu/ml) infiltration.

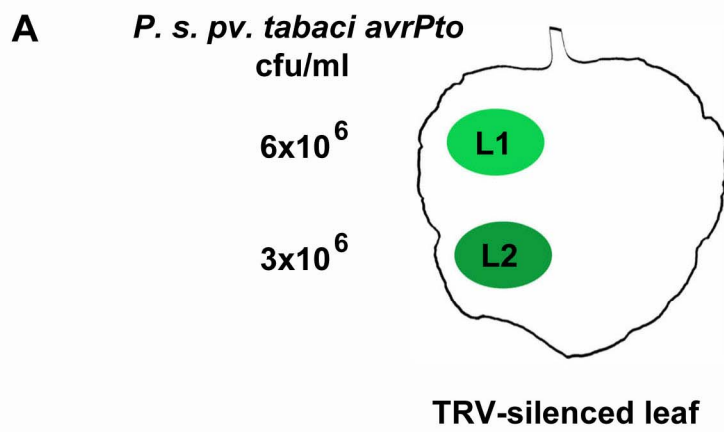
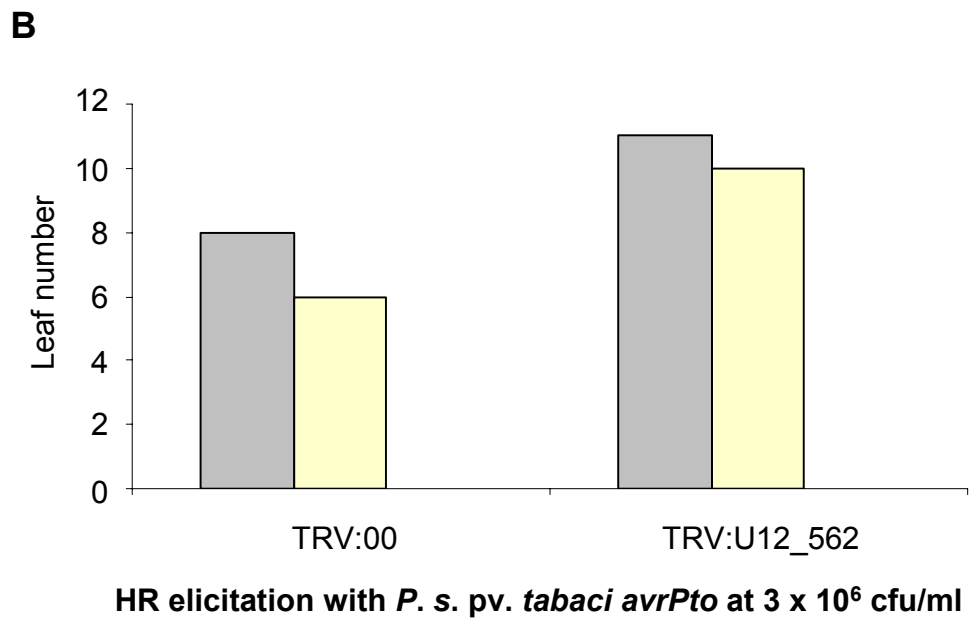
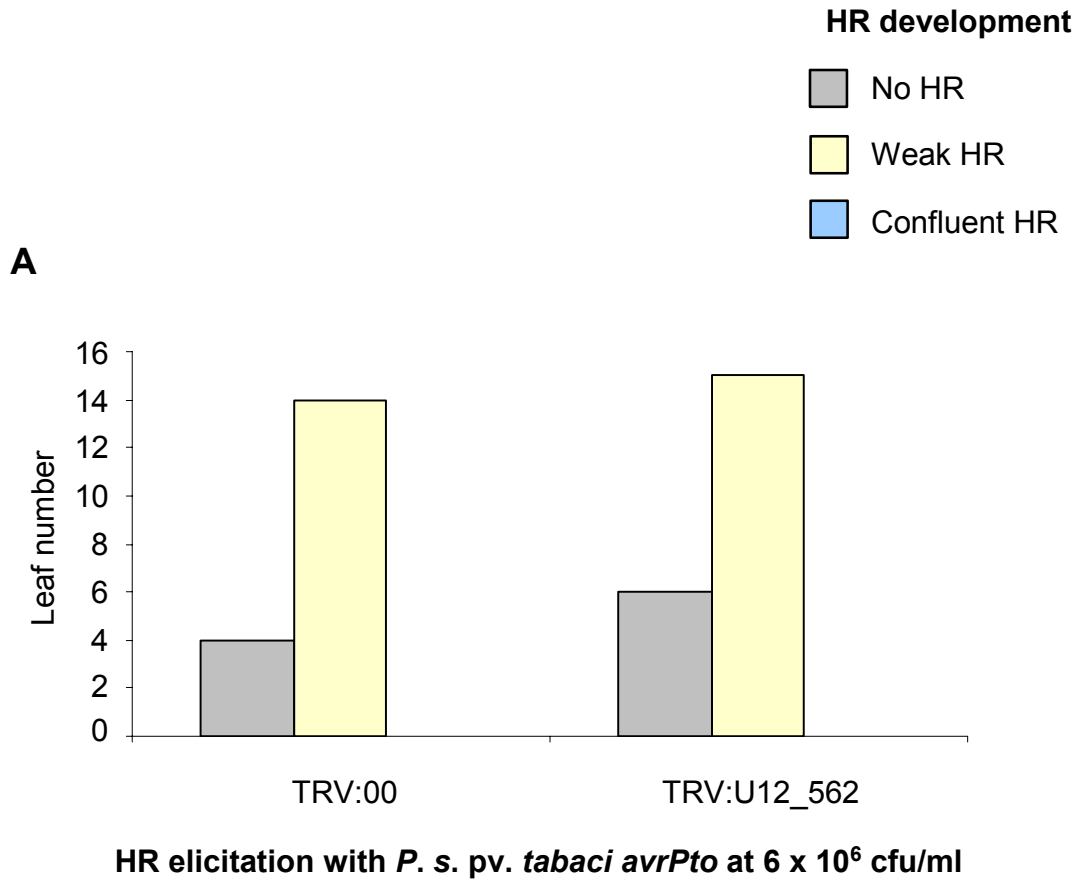


**Figure 4.12** *avrPto/Pto* elicited HR is unchanged during *NbUBP12* silencing by TRV:U12\_562.

*avrPto/Pto* elicited HR cell death development in VIGS silenced *N. benthamiana* infected with TRV:00 or TRV:U12\_562. HR elicited by infiltration of *P. s. pv. tabaci avrPto* at  $6 \times 10^6$  (A) or  $3 \times 10^6$  (B) cfu/ml. HR development scored at 4 days post *P. s. pv tabaci avrPto* infiltration.



Following inoculation of *P. s. pv tabaci avrPto* there was no discernable alteration in hypersensitive cell death development between *NbUbp12* silenced and control plants (Figures 4.11 B and 4.12).

HR scoring data was similar at each bacterial titre for *NbUbp12* silenced and control plants with the expected decrease in overall HR development scores for the low titre inoculated patches relative to intermediate titres (Figure 4.12).

#### **4.7 Induction of basal disease resistance during *NbUBP12* silencing**

As has been previously discussed, the plant defence response can be broadly divided into basal and gene for gene resistance. A major component of basal defence responses relates to the broad host recognition of pathogen associated ligands termed PAMPs (Pathogen Associated Molecular Patterns) (Zipfel and Felix, 2005). PAMP perception induces numerous defence signalling pathways many of which overlap with 'gene for gene' resistance (Navarro et al., 2004) but is thought to function primarily through early events that function to halt microbe colonisation (Chisholm et al., 2006).

To investigate the potential involvement of *NbUBP12* in basal disease resistance, the growth of virulent *Pseudomonas syringae* pv. *tabaci* was measured in *N. benthamiana* plants undergoing VIGS based *NbUBP12* silencing. *N. benthamiana* plants were infected with TRV:00, TRV:U12\_562 or TRV:U12\_742 VIGS constructs and after the development of systemic silencing, new leaves were infected with a low titre of *P. s. pv. tabaci* ( $1 \times 10^4$  cfu/ml). Bacterial growth was measured at 1 and 3 days post infection based on colony counts from serially diluted plant tissue extracts (Figure 4.13).

Silencing *NbUBP12* did not significantly alter growth of *P. s. pv. tabaci* after 3 days (Figure 4.13). Control and *NbUBP12* silenced plants all demonstrated 7 logs cfu/cm<sup>2</sup> of bacterial growth with no significant difference in mean growth based on paired t-test analysis (Figure 4.13).

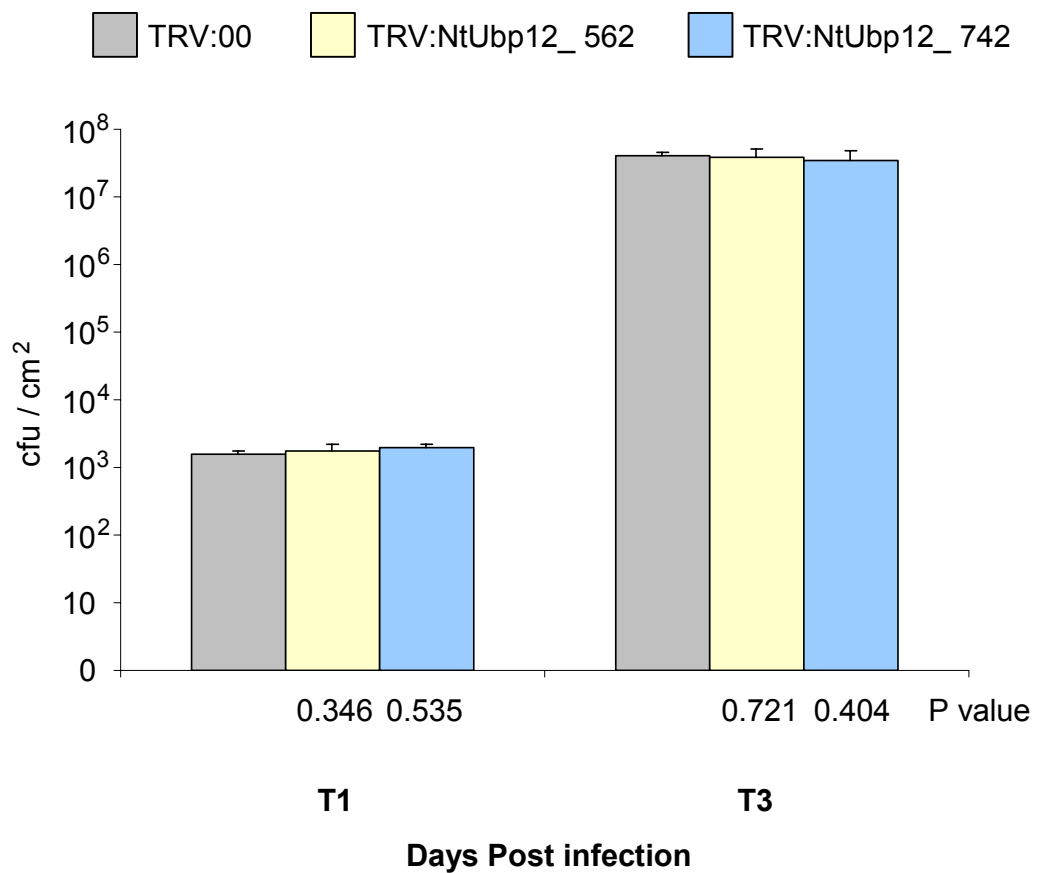


**Figure 4.13** Growth of virulent *P. s. pv. tabaci* is unaltered in *NbUBP12* silenced *N. benthamiana*.

Growth of *P. s. pv. tabaci* was measured in *N. benthamiana* undergoing *NbUBP12* silencing after infection with either TRV:00, TRV:U12\_562 or TRV:U12\_742. Gene silencing was allowed to develop for 22 days then silenced leaves (emerging leaf #5) were infected with *P. s. pv. tabaci* at  $1 \times 10^4$  cfu/ml. Growth was measured by bacterial colony counts at 24 (T1) and 72 (T3) hours post infection. Data points represent the mean of six replicates and error bars represent one standard deviation. Statistical significance of observed growth differences were assessed by two sided t-test where a P value equal to or less than 0.05 was considered significant.

#### 4.8 *NbUBP12* silencing increases resistance against TMV

The potential role of *NbUBP12* in anti-viral resistance was investigated using the model tobamovirus Tobacco Mosaic Virus (TMV) (Scholthof, 2004). The tobacco TIR-NBS-LRR class *R* gene *N* confers resistance to TMV and the genetic interaction between TMV and *N* confers resistance in accordance with the gene-for-gene principle (Whitham et al., 1994).

TMV spreads systemically in tobacco cultivars lacking the *N* gene, causing mosaic disease symptoms characterised by intermingled areas of light and dark green leaf tissue (Erickson et al., 1999). Conversely, TMV infection of *N*-containing tobacco cultivars typically induces HR within 48 hours which restricts virus particles to the region immediately surrounding induced necrotic lesions and is accompanied by systemic acquired resistance (SAR) (Erickson et al., 1999).

The tobacco *N* gene has been introduced into *N. benthamiana* (transgenic A310 line) to facilitate VIGS based reverse genetic studies during *N* mediated TMV resistance (Bendahmane et al., 1999). Whilst the fundamental activation of TMV induced HR and SAR is observed in *N* transgenic *N. benthamiana*, absolute resistance levels to the TMV U1 isolate are reduced (Peart et al., 2002a). Consequently the development of TMV induced lesions is typically reduced in A310 *N. benthamiana* compared to resistant tobacco cultivars and after initial infection events TMV U1 moves systemically in A310 plants (Peart et al., 2002a). HR development against systemic TMV in A310 lines results in systemic necrosis during the latter stages of infection (Peart et al., 2002a).

Using TRV:U12\_742 and TRV:U12\_562 VIGS silencing constructs, collaborators from the laboratory of Dr. M. Taliansky (SCRI, Dundee) examined TMV induced symptom development and virus replication during *NbUBP12* silencing in A310 and wildtype *N. benthamiana* plants. *N* mediated HR symptoms were elicited by rub inoculation of purified TMV U1 virus onto control and *NbUBP12* silenced A310 plants 12 days after the agroinoculation of VIGS constructs (Figure 4.14). At 6 dpi (days post

**Figure 4.14** Silencing of *NbUBP12* reduces TMV induced HR symptoms in A310 *N* transgenic *N. benthamiana*.

(A) TMV induced local lesions on A310 *N* transgenic *N. benthamiana* during silencing with either TRV:00 or TRV:U12\_742. Plants were rub inoculated with 10  $\mu$ l of purified TMV U1 at 0.2  $\mu$ g/ $\mu$ l 12 days after the agroinoculation of TRV:00 or TRV:U12\_742 silencing constructs. Pictures taken at 6 days after TMV U1 infection.

(B) TMV induced systemic necrosis on A310 *N* transgenic *N. benthamiana* during silencing with either TRV:00 or TRV:U12\_742. Plants were rub inoculated with 10  $\mu$ l of purified TMV U1 at 0.2  $\mu$ g/ $\mu$ l 12 days after the agroinoculation of TRV:00 or TRV:U12\_742 silencing constructs. Pictures taken at 10 days after TMV U1 infection.

**Figure reproduced with consent of Dr M. Taliany**

**A**



**TRV:00**



**TRV:U12\_562**

**TMV U1 infected A310 *N. benthamiana* at 6 dpi**

**B**



**TRV:00**



**TRV:U12\_562**

**TMV U1 infected A310 *N. benthamiana* at 10 dpi**

infection), the development of TMV induced local lesions was markedly reduced in A310 plants undergoing *NbUBP12* silencing (Figure 4.14 A). Reduced lesion formation was consistently observed in multiple plants silenced with TRV\_U12\_742 (data not shown) and the phenotype was clearly distinct from light necrosis/damage symptoms caused by rub inoculation of the virus (Figure 4.14 A). The reduction in TMV induced local lesion development was robust and remained apparent during the latter stages of infection at 10 dpi (data not shown).

The development of TMV induced systemic necrosis was largely abolished in *NbUBP12* silenced A310 plants at 10 dpi (Figure 4.14 B). The reduction in systemic necrosis symptoms was clear in comparison to TRV:00 controls and was consistently observed in multiple plants silenced with TRV:U12\_742 (Figure 4.15 B). Mild TMV induced wilting symptoms were seen in systemic tissues of *NbUBP12* silenced plants at 10 dpi (Figure 4.14 B) but an equivalent degree of systemic tissue collapse was not observed until at least 15 dpi (data not shown). The reduction in local and systemic HR related symptoms indicated that silencing *NbUBP12* increased resistance against TMV U1 infection.

Alterations in resistance to TMV during *NbUBP12* silencing were assessed by measuring TMV accumulation following infection. TMV accumulation was monitored in A310 and wildtype plants during *NbUBP12* silencing using a GFP tagged TMV vector (Ryabov et al., 1999) (Figure 4.15). TMV:GFP was rub inoculated onto control and *NbUBP12* silenced A310 plants (12 days after VIGS construct agroinoculation) and virus accumulation was assessed by GFP fluorescence at 6 dpi (Figure 4.15 A). In accordance with the reported reduction in HR symptoms (Figure 4.14), accumulation of TMV:GFP was also markedly reduced in *NbUBP12* silenced A310 plants (Figure 4.15 A). At 6 dpi, most of the detectable GFP foci were of a lower size and intensity in *NbUBP12* silenced A310 plants compared to equivalent TRV:00 controls (Figure 4.15 A). Reduced TMV:GFP accumulation was consistently observed in multiple A310 plants following silencing of *NbUBP12* with TRV:U12\_742

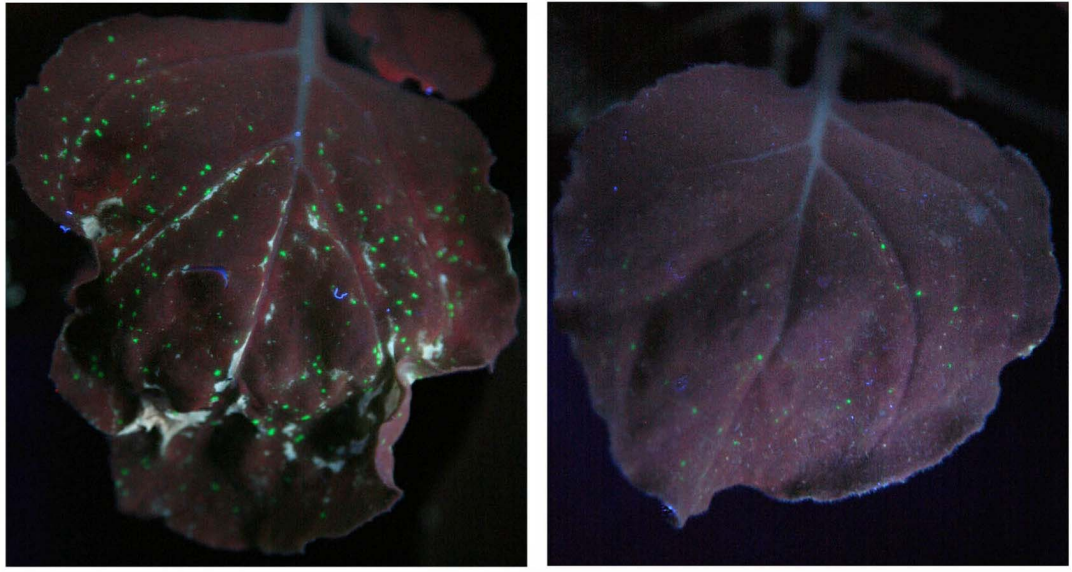
**Figure 4.15** Silencing *NbUBP12* reduces TMV:GFP virus accumulation independent of *N* triggered TMV resistance.

(A) TMV:GFP accumulation on A310 *N* transgenic *N. benthamiana* during silencing with either TRV:00 or TRV:U12\_742. Plants were rub inoculated with 5  $\mu$ l of reconstituted TMV:GFP virion 12 days after the agroinoculation of TRV:00 or TRV:U12\_742 silencing constructs. Pictures taken at 6 days after TMV:GFP infection.

(B) TMV:GFP accumulation on wildtype *N. benthamiana* during silencing with either TRV:00 or TRV:U12\_742. Plants were rub inoculated with 5  $\mu$ l of reconstituted TMV:GFP virion 2 days after the agroinoculation of TRV:00 or TRV:U12\_742 silencing constructs. Pictures taken at 4 days after TMV:GFP infection.

**Figure reproduced with consent of Dr M. Taliansky**

**A**

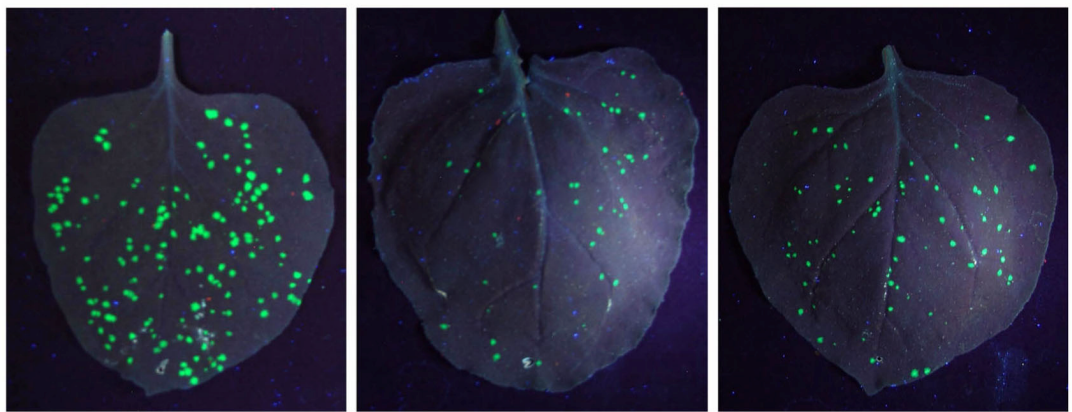


TRV:00

TRV:U12\_742

TMV:GFP infected A310 *N. benthamiana* at 6 dpi

**B**



TRV:00

TRV:U12\_742

TRV:U12\_562

TMV:GFP infected wildtype *N. benthamiana* at 4 dpi

TMV:GFP accumulation assays were also conducted in *NbUBP12* silenced wild type *N. benthamiana* plants to clarify the contribution of *N* triggered HR to the observed TMV resistance phenotype (Figure 4.15 B). At 4 dpi, wild type *N. benthamiana* undergoing *NbUBP12* silencing also demonstrated a marked reduction in TMV:GFP accumulation based on the development of GFP foci compared to TRV:00 controls (Figure 4.15 B). Silencing of *NbUBP12* in wild type *N. benthamiana* with TRV:U12\_742 and TRV:U12\_562 resulted in TMV:GFP foci of reduced size and intensity at 4 dpi compared to TRV:00 controls (Figure 4.15 B). This phenotype was observed in multiple *NbUBP12* silenced plants (data not shown) and suggested that reduced TMV infection was independent of *N* triggered gene-for-gene resistance.

The reported results suggest that reduced HR symptoms seen in *NbUBP12* silenced A310 plants during TMV infection are a secondary consequence of increased resistance mediated by an uncharacterised response to TMV. These results indicate that *NbUBP12* contributes to the uncharacterised TMV resistance mechanism without (and presumably also with) the occurrence of *N* triggered gene-for-gene resistance. In A310 plants, the marked reduction in TMV accumulation resulting from *NbUBP12* silencing results in weaker induction of local lesions and a significant delay in systemic viral movement. Further characterisation of TMV infection during *NbUBP12* silencing is currently being undertaken by collaborators in the laboratory of Dr. M. Taliansky (SCRI, Dundee).

#### **4.9 Discussion**

Results presented in this chapter report the application of VIGS to achieve transient but robust silencing of *N. benthamiana* gene *NbUBP12*, allowing assessment of its potential role in disease resistance signalling. Data from HR assays indicate that silencing *NbUBP12* increases hypersensitive cell death elicited by the fungal avirulence factor Avr9 but not by the bacterial avirulence factor avrPto. Data reported by our collaborators indicates that silencing *NbUBP12* either increases *N* independent resistance to TMV infection or reduces the movement potential of TMV.

EST database analysis and cloning approaches established the full length cDNA sequence of *NbUBP12* allowing the selection of VIGS silencing regions that were unlikely to cause 'off target' cross-silencing effects.

Similar experimental results were observed during *NbUBP12* silencing initiated using two distinct cDNA regions, confirming that specific gene silencing of endogenous *NbUBP12* is the probable cause of the respective HR promotion and viral resistance phenotypes. The lack of a complete *N. benthamiana* genome sequence precludes absolute identification of other potential *NbUBP12* homologs but tobacco EST analysis suggests that *UBP12* is a single copy gene in the Solanaceae.

Silencing *NbUBP12* promotes Cf-9 triggered hypersensitive cell death suggesting the enzyme functions as a negative regulator of cell death. Based on the demonstration of *in vitro* activity of NtUBP12 against K48 linked ubiquitin (Chapter 5), it is likely that NbUBP12 stabilises, through deubiquitination, a target substrate (or substrates) that suppresses the cell death signal during Cf-9 mediated HR.

As has been discussed previously, ubiquitination has been implicated in diverse plant signalling pathways including responses to pathogen perception (Devoto et al., 2003). Various E3 ligases that regulate the HR and disease resistance have been described including SPL11 (Zeng et al., 2004), CMPG1 (Gonzalez-Lamothe et al., 2006) and ACRE276 (Yang et al., 2006). That such proteins confer either positive or negative control over the HR is analogous to the involvement of ubiquitin signalling in animal apoptosis where regulated protein degradation of pro- and anti-apoptotic factors is essential for the execution of programmed cell death (Lee and Peter, 2003).

*CMPG1* and *ACRE276* were identified as genes upregulated rapidly during Avr9/Cf-9 triggered HR (Durrant et al., 2000). Subsequent studies established that *CMPG1* and *ACRE276* both function as positive regulators of the Cf-9 mediated HR, presumably by the specific degradation of substrates that are negative HR regulators (Gonzalez-Lamothe et al., 2006). It is possible that NbUBP12 confers negative HR regulation by

directly stabilising substrates of CMPG1 or ACRE276. In this model of function, UBP12 could serve to attenuate the early pro-HR signal provided by CMPG1 or ACRE276 as one of the negative feedback mechanisms that prevent runaway cell death (Rusterucci et al., 2001).

Two recent studies have reported transcript profiling analysis in solanaceous plants following HR induction. As described in Chapter 3, a comparative transcript analysis of avirulent *Pseudomonas* induced HR and programmed cell death induced by proteasome disruption in *N. benthamiana* (Kim et al., 2006) reported a significant suppression of *NbUBP12* only during pathogen induced cell death. The suppression of *NbUBP12* mRNA reported by Kim *et al.* correlates with the *NtUBP12* expression pattern observed in this study during Cf-9 mediated HR. The fact that Kim *et al.* report transcript changes based on a single timepoint at 24 hours post HR induction limits the value of further comparison between these experiments but provides additional preliminary data supporting the involvement of *NbUBP12* in HR signalling by non-fungal pathogens.

Durrant *et al.* report transcript analysis focussed on early transcript changes after 30 minutes during Cf-9/Avr9 mediated HR in tobacco cell cultures (Durrant et al., 2000). This screen reported the induction of numerous ubiquitin E3 ligases but no deubiquitinating enzymes. The non-induction of *NtUBP12* at early time points following Avr9 elicited HR observed in this study correlates with the ACRE expression data published by Durrant *et al.*.

Data presented in Chapter 3 reports the transcriptional induction of *NtUBP12* orthologs in *Arabidopsis* by avirulent bacterial pathogens and salicylic acid whilst transcript analysis of *NtUBP12* demonstrates its late suppression in a fungus associated HR. Each experimental induction trend is supported by the expected expression of an appropriate marker gene suggesting a genuine induction of *AtUBP12/AtUBP13* but suppression of *NtUBP12* during HR. Given that salicylic acid accumulation is one of the primary signalling cues in plant disease resistance (Alvarez, 2000) it would

be informative to test the transcriptional response of *NtUBP12* to exogenously applied salicylic acid.

#### **4.9.1 NbUBP12 - links to known resistance signalling pathways**

Plant disease resistance is activated through numerous interacting signalling pathways involving the ROI perception, hormone signalling, ionic fluxes and induction of defence genes (Thomma et al., 2001). Classical studies of plant lesion mimic mutants with deregulated cell death have established distinct classes of gene function that regulate cell death initiation and propagation (Lorrain et al., 2003). The discovery that NbUBP12 is a negative regulator of Avr9 elicited HR suggests its function is associated with the propagation class of the HR signalling components. Further analysis to establish which disease resistance signalling pathways are perturbed by *NbUBP12* silencing could be assessed by induction studies of known marker genes specific to various aspects of the HR.

The presented data indicates that silencing *NbUBP12* promotes hypersensitive cell death mediated by the transmembrane LRR *R* gene product Cf-9 but not protein kinase *R* gene product Pto and influences TMV infection independent of *N* triggered resistance. It is possible that NbUBP12 also regulates HR signalling from Pto but that the extent of *NbUBP12* silencing was insufficient to see an alteration in the development of cell death. Silencing of *NbUBP12* using either of the generated VIGS constructs typically yielded an approximate 70% mRNA knockdown so residual NbUBP12 protein expressed from remaining endogenous *NbUBP12* transcript will be present in the cell and provide wild type signalling capacity. Alternative VIGS approaches based on the expression of hpRNA to improve silencing efficiency have been described (Lacomme et al., 2003) and may be applicable in future loss of function studies of NbUBP12.

The presented data does indicate a specific role for NbUBP12 in Cf-9 mediated HR and invites speculation on where it might function in the currently established order of disease resistance signalling pathways. The point at which distinct *R* gene mediated pathways converge to initiate disease resistance requires clarification, but signalling by mitogen

activated protein kinases (MAPK) has been identified as a key regulatory component (Pedley and Martin, 2005). Previous studies have established that Cf-9 mediated HR signalling activates MAPK proteins NtSIPK and NtWIPK (Romeis et al., 1999) which are regulated by the upstream MAPKK NtMEK2 (Yang et al., 2001). The finding that tomato orthologs of NtMEK2, NtSIPK and NtWIPK are essential components of the Pto mediated disease resistance (del Pozo et al., 2004) suggests convergence of Cf-9 and Pto signals at this MAPK cascade. That *NbUBP12* silencing does not alter Pto mediated HR suggests that Cf-9 specific signalling by *NbUBP12* may occur upstream of MEK2 and maybe proximal to the transduction of Avr9 perception rather than conserved between different *R* gene classes. Such hypothesis could be tested both by examining perturbations in early Cf-9 mediated signalling events which are becoming increasingly well characterised (Nekrasov et al., 2006) and analysing HR induction using *Avr/R* gene products from different pathogens and *R* gene classes using methodologies described in Peart *et al.* (Peart et al., 2002b).

The NtMEK2-SIPK/WIPK pathway has also been implicated in *N* mediated resistance against TMV (Pedley and Martin, 2005) but data reported by our collaborators suggests that elevated TMV resistance due to *NbUBP12* silencing is independent of the *N* triggered HR. These findings invite further investigation into the contribution of *NbUBP12* to increased TMV resistance during compatible infection.

One possibility is that *NbUBP12* negatively regulates resistance triggered by perception of a TMV associated PAMP type molecule. In this case, silencing of *NbUBP12* may deregulate TMV associated PAMP defence signalling to cause increased resistance. TMV associated PAMP type responses have been reported (Allan et al., 2001) and PAMP triggered immune responses also lead to the activation of the NtMEK2-SIPK/WIPK pathway (Pedley and Martin, 2005). This raises the possibility that silencing *NbUBP12* activates the MEK2-SIPK/WIPK pathway to increase the Cf-9 triggered HR and TMV associated PAMP triggered resistance.

Based on the resistance assay performed in this study using *P. s. pv. tabaci*, *NbUBP12* does not appear to influence PAMP triggered resistance

against bacteria, however data reported by our collaborators suggests the potential involvement of NbUBP12 in early events associated with TMV perception.

The implication of NbUBP12 in Cf-9 triggered HR and *N* independent TMV responses may be coincidental, suggesting instead its distinct roles in regulating HR execution and the TMV life cycle. NbUBP12 may be directly modulated during TMV infection to permit virus replication, trafficking or movement between cells such that silencing of *NbUBP12* reduces viral pathogenicity.

Previous studies have implicated the ubiquitin 26S proteasome system directly and indirectly in TMV resistance. Initial studies established that perturbation of ubiquitin ligation by competitive titration of a mutant ubiquitin variant led to reduced TMV infection (Bachmair et al., 1993). Further evidence was provided by the characterisation of SGT1 which is a key regulator of non-host and R gene mediated resistance including *N* triggered resistance against TMV (Peart et al., 2002b). The proven interaction between SGT1 and the SCF complex subunit SKP1 indicates its role in degradative processes and broadly implicates ubiquitination in disease resistance signalling (Azevedo et al., 2002). Ubiquitination has also been directly linked to the TMV lifecycle by Reichel *et al.* who reported that the TMV encoded movement protein (MP) was ubiquitinated and degraded at a specific stage of TMV infection (Reichel and Beachy, 2000). Regulated ubiquitination of the TMV MP is proposed to promote viral pathogenicity by minimising post-replicative disruption to the host cell (Reichel and Beachy, 2000). It is possible that NbUBP12 may function as a regulatory factor to oppose TMV associated ubiquitination events to influence defence signalling. The TMV resistance phenotypes reported in this study are apparently independent from *N* triggered HR defences and future studies aim to clarify how *NbUBP12* silencing compromises compatible infection by TMV.

#### 4.9.2 Does NbUBP12 regulate the HR and disease resistance?

Previous studies have highlighted the fact that many HR regulators identified by reverse genetic approaches do not necessarily influence disease resistance against the HR inducing pathogen (Lu et al., 2003). These observations reflect the fact that disease resistance activation depends on the distinct signalling events that are coordinated by a hierarchy of signals (Thomma et al., 2001). Whilst cross-talk and feedback regulation between signalling pathways has been established, (Kunkel and Brooks, 2002) the identification of plant mutants that can initiate disease resistance but not HR (Yu et al., 1998) highlights the fact that hypersensitive cell death is not a definitive outcome of the plant defence response. It is entirely plausible, based on such observations, that NbUBP12 functions specifically within the HR signalling pathway and does not regulate other branches of disease resistance.

To assess the potential involvement of UBP12 in Cf-9 mediated disease resistance requires infection assay experiments using *C. fulvum* on host tomato plants. Tomato is also a suitable host for VIGS based gene silencing studies using the adapted tobacco rattle virus vector pYL156 (Liu et al., 2002a). Having identified a tomato EST exhibiting 83% amino acid identity to NtUBP12 (data not shown), a 200 bp region was cloned into pYL156 to facilitate gene silencing of *LeUBP12* in tomato. To establish if *LeUBP12* regulates Cf-9 mediated disease resistance as well as the HR, *C. fulvum* resistance assays in *LeUBP12* silenced tomato are currently being performed in collaboration with the lab of Prof. J.D.G Jones (Sainsbury Laboratory, Norwich). The generated *NbUBP12* VIGS could be applied in future studies to examine its role in HR and resistance against different classes of pathogen and *Avr/R* gene combinations using *Agrobacterium* based transient expression as described by Peart *et al.* (Peart et al., 2002b).

## Chapter 5 - *In vitro* DUB activity assays of plant UBP12 proteins

### 5.1 Introduction

The majority of known deubiquitinating enzymes are cysteine proteases with specificity for the isopeptide bond made either between ubiquitin and a substrate protein or two linked ubiquitin moieties. DUB enzymes are classified into several subfamilies most of which exhibit catalytic core structures that match closely to the classical cysteine proteases such as papain (Amerik and Hochstrasser, 2004). The active site is composed of a catalytic triad made up of cysteine, histidine and aspartate residues. During catalysis the aspartate polarises the histidine which in turn deprotonates the cysteine, this cysteine can then perform a nucleophilic attack on the scissile isopeptide bond to release the linked target substrate or ubiquitin moiety (Nijman et al., 2005).

Whilst active site geometries are conserved between each DUB family, their catalytic core sequences are not. Despite having largely conserved catalytic triad residues, the individual DUB families have distinct catalytic motifs (Amerik and Hochstrasser, 2004). In the case of the UBP family, the catalytic residues are all found in two short motifs termed the Cys and His boxes (Figure 5.1) present in all UBP enzymes (Yan et al., 2000a).

This chapter reports the *in vitro* demonstration of DUB activity of UBP12 proteins from *Arabidopsis* and tobacco. In each case constructs were made to express full length wild type UBP12 and the corresponding active site cysteine mutant proteins. Numerous assay systems are available to test DUB activity (Kang et al., 2005), the majority of these exploit cleavage of ubiquitin linked to a reporter substrate protein via an isopeptide linkage. Cleavage can then typically be monitored by spectroscopy (Dang et al., 1998) or western blot (Yan et al., 2000a).

To demonstrate the DUB activity of AtUBP12 and NtUBP12 proteins, two different assay systems were used in this study. Both DUB assay systems rely on the digestion of isopeptide linked Ub oligomers with subsequent

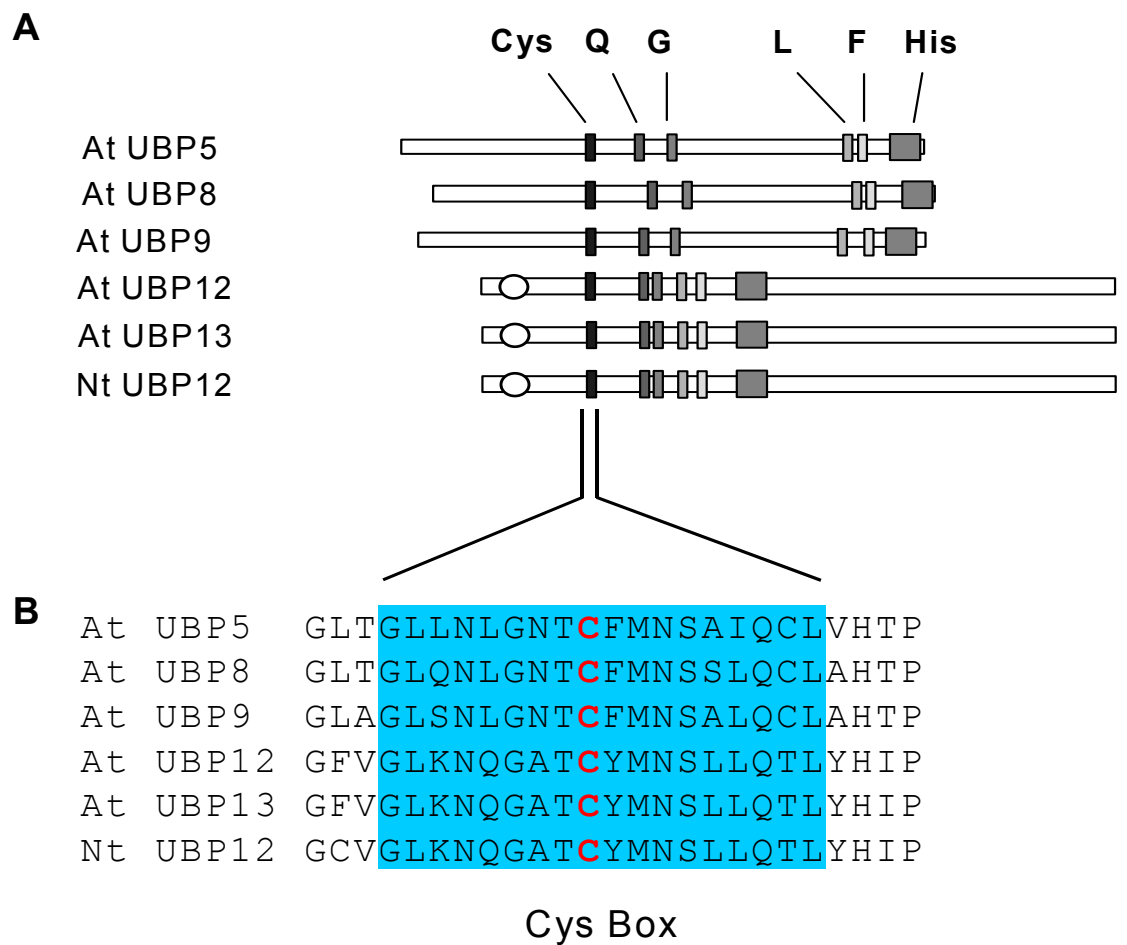


**Figure 5.1** Active site cysteine conservation in UBP enzymes

(A) Domain diagram illustrating conserved catalytic motif regions of UBP enzymes. (B) Alignment of catalytic Cys box region of UBP enzymes, active site cysteine shown in red.

analysis by western blot using anti-ubiquitin antibodies. Different substrates were used in each assay where the Ub chain method used a mixture of varying length Ub oligomers and the DiUb method used only diubiquitin substrate.

## **5.2 *In vitro* activity assay of *E. coli* expressed AtUBP12**

### **5.2.1 Generation of Histidine tagged AtUBP12 proteins for *E. coli* based expression**

To demonstrate the specific activity of AtUBP12, Histidine tagged fusion constructs corresponding to wild type and active site mutant versions of *Arabidopsis AtUBP12* cDNA were generated. AtUBP12 fusion proteins were expressed and purified from *E. coli* then incubated with Ub-chain oligomer substrate. Assay reactions were analysed by western blot to confirm chain hydrolysis.

AtUBP12 His tagged fusion proteins were made using the Gateway compatible pDEST17 destination vector. Full length *AtUBP12* was PCR-amplified from *Arabidopsis* cDNA using primers to introduce NotI (AtUBP12\_5\_NotI) and Asp718I (AtUBP12\_3\_Asp718I) restriction sites at the respective 5' and 3' termini. The amplified product was cloned into pGEMT-Easy and subcloned into pENTR4 at NotI and Asp718I restriction sites to generate the *AtUBP12* WT entry clone. Site-directed mutagenesis was used to generate *AtUBP12* C208S active site mutant entry clone. Mutagenesis was completed using the QuikChange method with pENTR4 *AtUBP12* WT template DNA and specific primers (AtUBP12\_5\_C208S and AtUBP12\_3\_C208S).

Full length cDNA from each respective entry clone was transferred into the pDEST17 destination vector by Gateway LR based recombination to generate N-terminal Histidine tagged *AtUBP12* WT and *AtUBP12* C208S fusion constructs.

## 5.2.2 Expression and purification of AtUBP12 proteins from *E. coli*

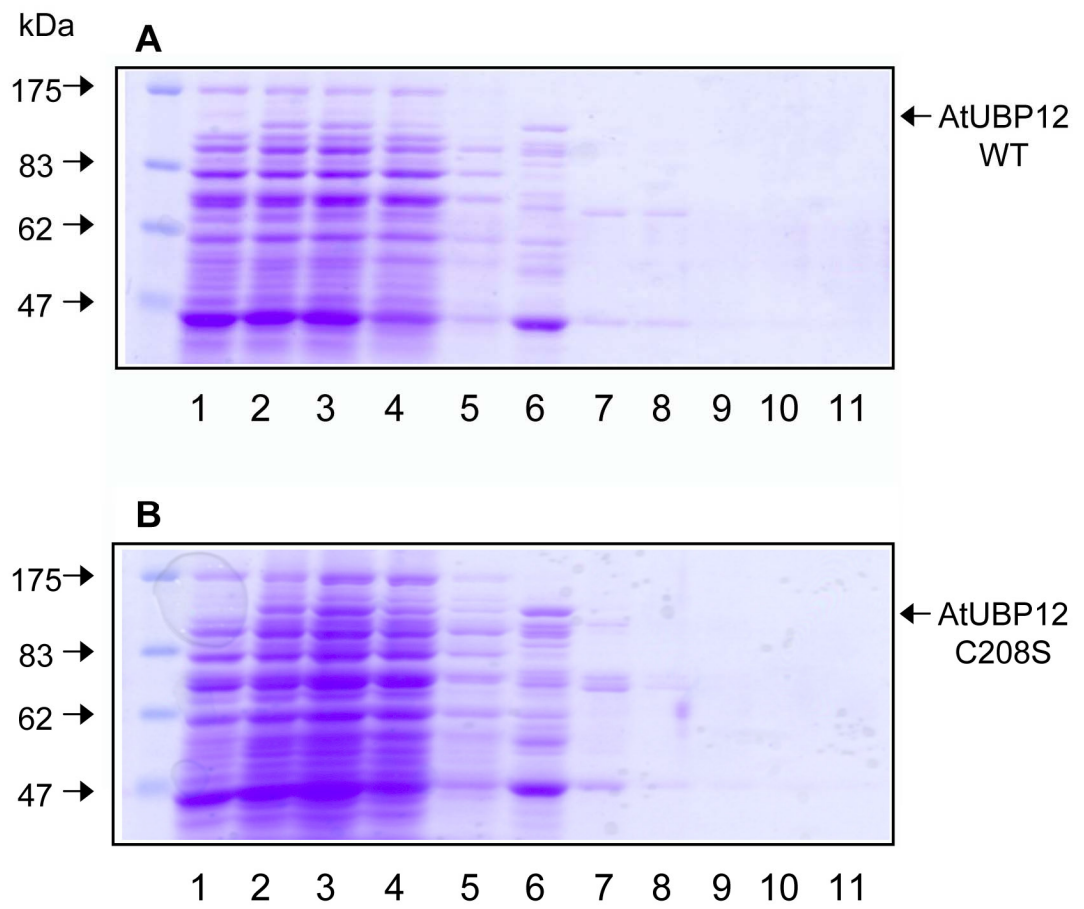
His-*AtUBP12* constructs were transformed into BL21(DE3) *E. coli* and protein expression was induced in 50 ml growth cultures with IPTG. Aliquots of induced *E. coli* culture were analysed by SDS-PAGE to confirm the expression of the ~133 kDa AtUBP12 WT and C208S fusion proteins (Figure 5.2 A and B). After a three hour expression period at 37°C, cells were recovered by centrifugation and soluble extracts were prepared using BugBuster cell lysis solution.

His-AtUBP12 WT and His-AtUBP12 C208S proteins were affinity purified from crude cell lysate using nickel affinity resin (Figure 5.2 A and B). Comparison of the recovered nickel purification fractions (Figure 5.2 A and B) indicated that both fusion proteins had bound to the affinity column but had been eluted in the low imidazole wash rather than final elution fractions.

The premature elution of each respective fusion protein suggested a relatively low binding efficiency to the affinity column. Poor binding efficiency usually requires empirical optimisation and is influenced by buffer conditions, fusion protein size and the size of the histidine tag (hexa-histidine in the case of pDEST17). Despite the early elution, both AtUBP12 fusion proteins were considerably enriched in comparison to crude cell lysate (Figure 5.2 A and B) and were dialysed into Ub-chain assay reaction buffer. Previously published data suggests that recombinant DUB proteins expressed in *E. coli* do not necessarily need to be purified to demonstrate activity (Evans et al., 2003) and that there is no genuine DUB activity in *E. coli* (Iyer et al., 2006) therefore semi-purified AtUBP12 fusion protein extracts were analysed for DUB activity *in vitro*.

**Figure 5.2** Expression and purification of His-AtUBP12 WT and His-AtUBP12 C208S proteins from *E. coli*

Coomassie stained PAGE gel lanes indicate: Pre-induction (1), 3 hours Post-induction (2), Soluble cell lysate (3), Column loading FT (4), Column wash #1 (5), Column wash #2 (6), Elution #1 (7), Elution #2 (8), Elution #3 (9), Elution #4 (10), Elution #5 (11) for His-AtUBP12 WT (**A**) and His-AtUBP12 C208S (**B**) respectively.



### 5.2.3 *In vitro* Ub-chain cleavage assay of *E. coli* expressed AtUBP12 proteins

AtUBP12 WT and C208S fusion protein extracts (10  $\mu$ l) were incubated with 2  $\mu$ g of Ub-chain oligomers for 20 hours at 37°C, assay reactions were analysed by western blot (Figure 5.3). Recombinant Isopeptidase T (Reyes-Turcu et al., 2008) was used as a positive control for DUB activity and demonstrated clear cleavage of oligomeric Ub-chains down to monoubiquitin (Figure 5.3). There was no discernable difference in Ub-chain cleavage between AtUBP12 WT and C208S DUB assay reactions (Figure 5.3), indicating that either the purified AtUBP12 WT had no DUB activity or the activity present was insufficiently high to be detected using the Ub-chain assay protocol. Domain analysis of AtUBP12 using Pfam (Finn et al., 2006) indicates its authenticity as a deubiquitinating enzyme, suggesting that technical issues with either the *E. coli* based expression or the Ub-chain assay conditions/sensitivity were causing the lack of detectable activity.

The viability of *E. coli* as a host for the expression of functional recombinant eukaryotic proteins is often limited by the lack of appropriate chaperones, cofactors and post-translational modification enzymes required to ensure solubility and correct folding (Baneyx and Mujacic, 2004). Whilst a wide variety of modified *E. coli* based expression systems are available to address some of these limitations (Baneyx, 1999), optimisation of recombinant protein expression conditions usually requires empirical adjustment.

The use of oligomeric Ub-chains as a DUB enzyme substrate presented some technical issues during the assay experiments. Ub-chain loading was highly inconsistent for a given volume, where two lanes loaded with 2  $\mu$ g of substrate might differ twenty fold in apparent chain content when analysed by western blot (data not shown).

The diagnostic principle of the assay is based on cleavage of the isopeptide linkages in oligomeric Ub-chains, the consequent decrease in Ub oligomer content is detectable by western blot. In the case of Isopeptidase T

(positive control Figure 5.3) the high specific activity of the enzyme clearly hydrolyses all of the Ub-chain substrate. In testing the purified AtUBP12 fusion proteins it became apparent that limited substrate cleavage (10-20%) in comparison to controls would be difficult to demonstrate on a western blot. Further to this, variability in absolute substrate loading would further complicate attempts to quantify differences by densitometry analysis.

### **5.3 *In vitro* activity assay of *S. frugiperda* expressed AtUBP12**

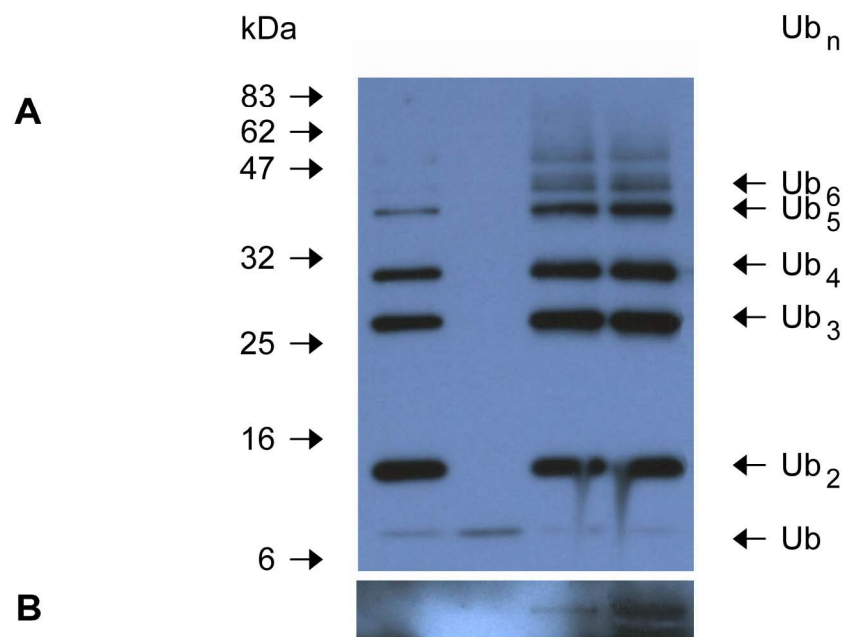
#### **5.3.1 Generation of Histidine tagged AtUBP12 proteins for *S. frugiperda* based expression**

To circumvent the potential limitations of using the prokaryotic *E. coli* based system for protein expression, AtUBP12 proteins were instead expressed using the eukaryotic insect cell - baculovirus system. Recombinant baculovirus encoding AtUBP12 fusion proteins were expressed in *Spodoptera frugiperda* (Sf9) cells which, in comparison to bacterial expression systems, utilise many of the protein modifications and processing present in higher eukaryotic cells (Murphy and Piwnicka-Worms, 2001). To demonstrate the specific activity of AtUBP12, histidine tagged fusion constructs corresponding to wild type and active site mutant versions of *Arabidopsis* *UBP12* cDNA were generated.

Full length *AtUBP12* was PCR amplified from *Arabidopsis* cDNA with primers containing NotI and Asp718I restriction sites (*AtUBP12BAC5\_NotI* and *AtUBP12BAC3\_Asp718I*) then cloned into pGEM T-Easy. Site-directed mutagenesis was used to generate the *AtUBP12* C208S active site mutant construct. Mutagenesis was completed using the QuikChange method with pGEM T-Easy *AtUBP12* WT template DNA and specific primers (*AtUbp12\_5\_C208S* and *AtUbp12\_3\_C208S*). Full length cDNA from each respective *AtUBP12* WT and *AtUBP12* C208S construct was subcloned into pACHLT baculovirus transfer vector at NotI and Asp718I restriction sites (5' and 3' respectively) to generate N-terminal Histidine tagged *AtUBP12* WT and *AtUBP12* C208S fusion constructs.

**Figure 5.3** DUB activity assay of AtUBP12 WT and AtUBP12 C208S proteins.

His-At UB12 WT and His-At UB12 C208S proteins were expressed and partially purified from *E. coli* and assayed for deubiquitinating activity. A mixture of *in vitro* synthesised ubiquitin chains with lengths 1-7 units (Ub-Ub7) (1 µg) were incubated alone (negative control), with Isopeptidase T (positive control), with His-AtUBP12 WT (10 µl) or with His-At UB12 C208S (10 µl) protein extracts in lanes 1, 2, 3 and 4 respectively. The reactions were analysed by Western blot using anti-Ubiquitin antibody (**A**) or anti-Histidine antibody (**B**).



**B**

	1	2	3	4
Ub Chains	+	+	+	+
Isopeptidase T	-	+	-	-
His-At UBP12 WT	-	-	+	-
His-At UBP12 C208S	-	-	-	+

### **5.3.2 Expression and purification of AtUBP12 proteins from *S. frugiperda***

Recombinant baculovirus encoding either *AtUBP12* WT or *AtUBP12* C208S were generated using the BaculoGold transfection kit and *Spodoptera frugiperda* cells (Sf9) were used for expression of each fusion protein. Sf9 cell lysate was obtained by sonication and His-AtUBP12 fusion proteins were recovered by nickel affinity purification. AtUBP12 WT and AtUBP12 C208S purification fractions were analysed by SDS-PAGE and western blot (Figure 5.4) and purified proteins were immediately assayed for activity against diubiquitin substrate.

### **5.3.3 *In vitro* diubiquitin cleavage assay of *S. frugiperda* expressed AtUBP12 proteins**

Purified AtUBP12 WT and C208S fusion proteins were incubated with 2 µg diubiquitin substrate for 20 hours at 37°C then assay reactions were analysed by western blot (Figure 5.5). Recombinant human Isopeptidase T was used as a positive control for DUB activity and demonstrated complete cleavage of diubiquitin to monoubiquitin (Figure 5.5). Purified AtUBP12 WT protein demonstrated DUB activity with a significant fraction of diubiquitin being cleaved to monoubiquitin. Despite being present at a two fold higher concentration (~3.0 µg vs 1.5 µg per reaction) no activity was detected for the AtUBP12 C208S active site mutant protein (Figure 5.5).

**Figure 5.4** Expression and purification of His-AtUBP12 WT and His-AtUBP12 C208S proteins from *S. frugiperda*.

His-AtUBP12 WT (**A**) and His-AtUBP12 C208S (**B**) proteins were expressed and purified from *S. frugiperda*. PAGE gel lanes indicate: Sf9 cell lysate (1), Column loading FT (2), Column wash FT (3) and Column elution (4). PAGE gels were analysed by coomassie staining (**Ai & Bi**) and Western blot using anti-Histidine antibody (**Aii & Bii**).

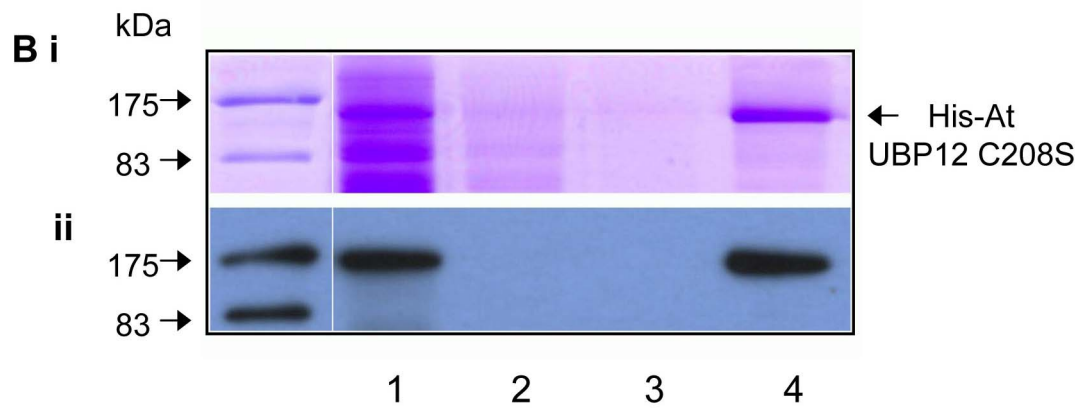
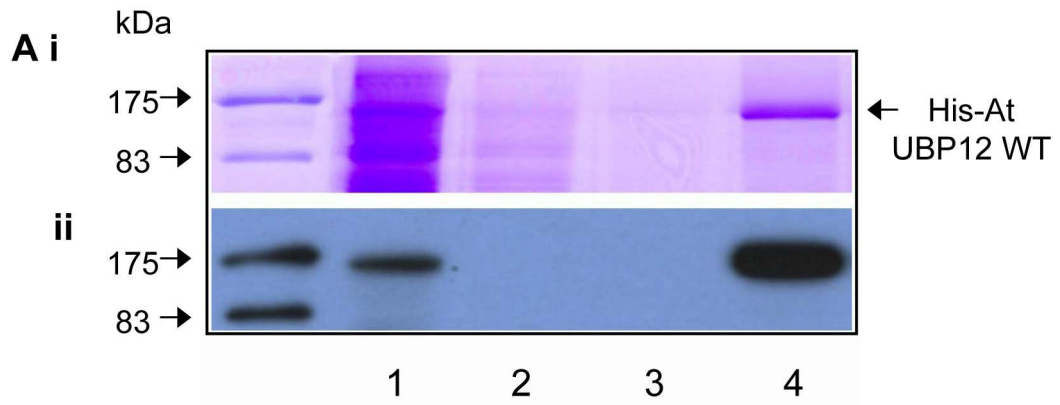
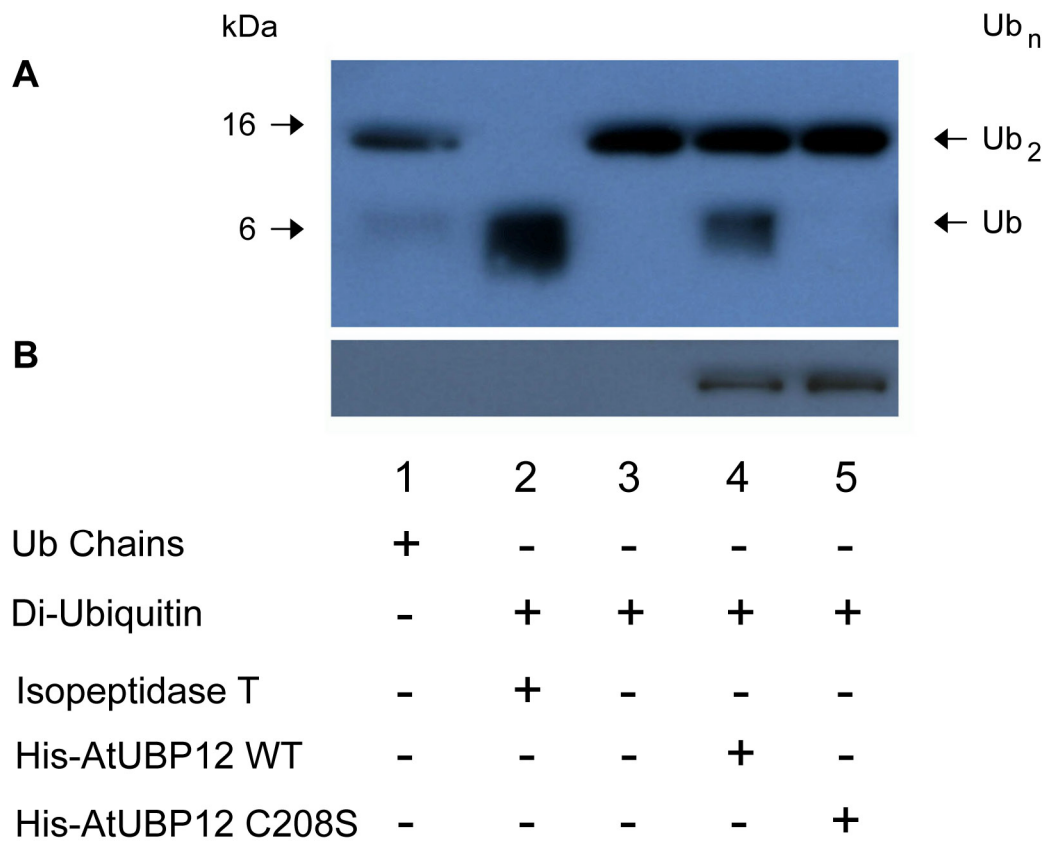


**Figure 5.5** AtUBP12 is a deubiquitinating enzyme and mutations in its active site abolish its activity.

His-AtUBP12 WT and His-AtUBP12 C208S proteins were expressed and purified from *S. frugiperda* and tested for deubiquitinating activity. A mixture of in vitro synthesised ubiquitin chains with lengths 1-7 units (Ub-Ub7) were loaded as a sizing control (lane 1). Di-Ubiquitin substrate (2 µg) was incubated alone (negative control), with Isopeptidase T (positive control), with AtUBP12 WT (~1.5 µg) or with AtUBP12 C208S (~3 µg) in lanes 2, 3, 4 and 5 respectively. The reactions were analysed by Western blot using anti-Ubiquitin antibody (**A**) or anti-Histidine antibody (**B**).



## **5.4 *In vitro* activity assay of *S. frugiperda* expressed NtUBP12**

### **5.4.1 Generation of Histidine tagged NtUBP12 proteins for *S. frugiperda* based expression**

To demonstrate the specific activity of NtUBP12, histidine tagged fusion constructs containing wild type and active site mutant versions of tobacco *NtUBP12* cDNA were generated. Having established the full length cDNA sequence of *NtUBP12* (Chapter 4), primers were made to PCR amplify an *NtUBP12* cDNA containing appropriate restriction sites for directional cloning into the pACHLT baculovirus transfer vector (NtUBP12BAC5\_NotI and NtUBP12BAC3\_Asp718I). Extensive optimisation of the PCR strategy failed to produce sufficient *NtUBP12* product for cloning purposes, so instead full length cDNA was commercially synthesised and cloned by blunt ligation into the pCR2.1TOPO vector.

Site-directed mutagenesis was used to generate *NtUBP12* C206S active site mutant construct. Mutagenesis was completed using the QuikChange method with pCR2.1 TOPO *NtUBP12* WT template DNA and specific primers (NtUBP12\_5\_C206S and NtUBP12\_3\_C206S). Full length cDNA from each respective *NtUBP12* WT and *NtUBP12* C206S cDNA construct was subcloned into pACHLT baculovirus transfer vector at NotI and Asp718I restriction sites (5' and 3' respectively) to generate N-terminal Histidine tagged *NtUBP12* WT and *NtUBP12* C206S fusion constructs.

### **5.4.2 Expression and purification of NtUBP12 proteins from *S. frugiperda***

Recombinant baculovirus encoding either NtUBP12 WT or NtUBP12 C206S were generated using the BaculoGold Transfection kit and *Spodoptera frugiperda* cells (Sf9) were used for expression of each fusion protein. Sf9 cell lysate was obtained by sonication and His-NtUBP12 fusion proteins were recovered by nickel affinity purification. NtUBP12 WT and NtUBP12 C206S purification fractions were analysed by SDS-PAGE and western blot which detected potential His-tagged breakdown products in the case of purified NtUBP12 (Figure 5.6). Despite the observed additional bands,

purified NtUBP12 proteins were immediately assayed for activity against diubiquitin substrate.

#### **5.4.3 *In vitro* diubiquitin cleavage assay of *S. frugiperda* expressed NtUBP12 proteins**

His-NtUBP12 WT and His-NtUBP12 C206 fusion proteins were incubated with 2 µg diubiquitin substrate for 20 hours at 37°C then assay reactions were analysed by western blot (Figure 5.7). Recombinant human Isopeptidase T was used as a positive control for DUB activity and demonstrated complete cleavage of diubiquitin to monoubiquitin (Figure 5.7). Purified NtUBP12 WT protein demonstrated DUB activity with a significant fraction of diubiquitin being cleaved to monoubiquitin, no activity was detected for the NtUBP12 C206S active site mutant protein (Figure 5.7).

Differences in the growth rate of Sf9 cell cultures used for expression of NtUBP12 WT and NtUBP12 C206S resulted in different amounts of purified protein being added to each respective assay (NtUBP12 WT ~ 1.0 µg and NtUBP12 C206S ~ 0.2 µg) (Figure 5.7). To circumvent potential protein stability issues which may compromise protein activity, purified NtUBP12 proteins were immediately assayed for DUB activity rather than after quantification and equalisation. Time constraints precluded further purification experiments to obtain equalised assay samples but nonetheless, active site mutant NtUBP12, which was present at approximately 5 fold lower levels than wildtype NtUBP12 (~0.2 µg vs 1.0 µg) (Figure 5.7), demonstrated no cleavage of diubiquitin substrate. Had the NtUBP12 C206S mutant retained wildtype activity levels then a proportional hydrolysis of diubiquitin would have been expected in the *in vitro* assay. The effect of the DUB UBP12 active site mutant was also confirmed by Sf9 expressed AtUBP12 proteins where variability in Sf9 cell growth resulted in the addition of more AtUBP12 C208S than AtUBP12 WT (~3.0 µg vs 1.5 µg) to the *in vitro* ubiquitin protease assay (Figure 5.5). Despite containing of two fold more AtUBP12 C208S than AtUBP12 WT, assays indicated that AtUBP12 C208S proteins were unable to cleave diubiquitin substrate.

**Figure 5.6** Expression and purification of His-NtUBP12 WT and His-NtUBP12 C206S proteins from *S. frugiperda*.

His-NtUBP12 WT (**A**) and His-NtUBP12 C206S (**B**) proteins were expressed and purified from *S. frugiperda*. PAGE gel lanes indicate: Sf9 cell lysate (1), Column loading FT (2), Column wash FT (3) and Column elution (4). PAGE gels were analysed by coomassie staining (**Ai & Bi**) and Western blot using anti-Histidine antibody (**Aii & Bii**).

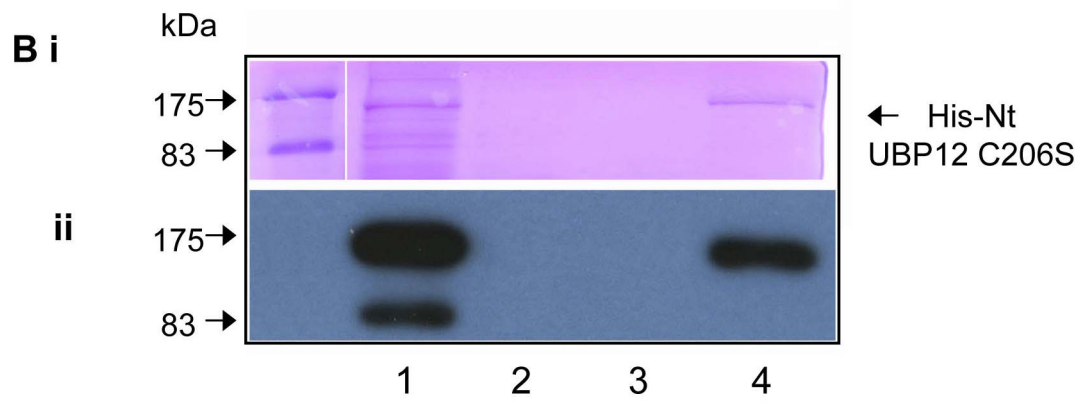
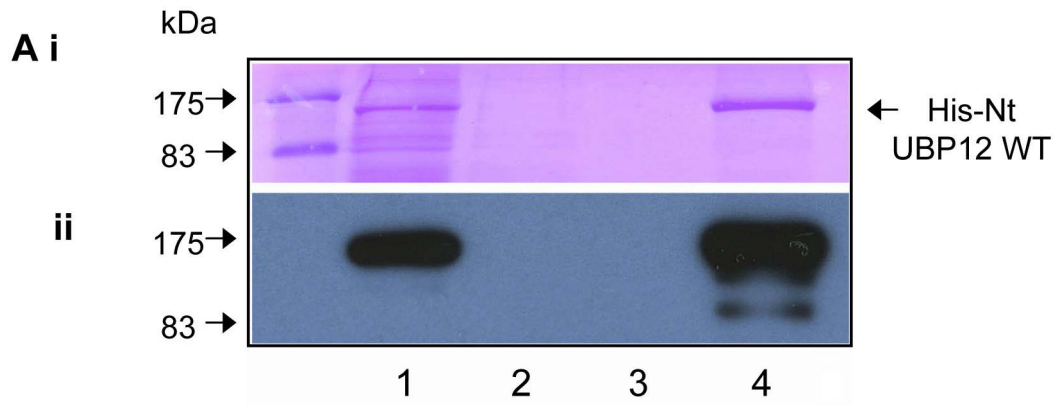
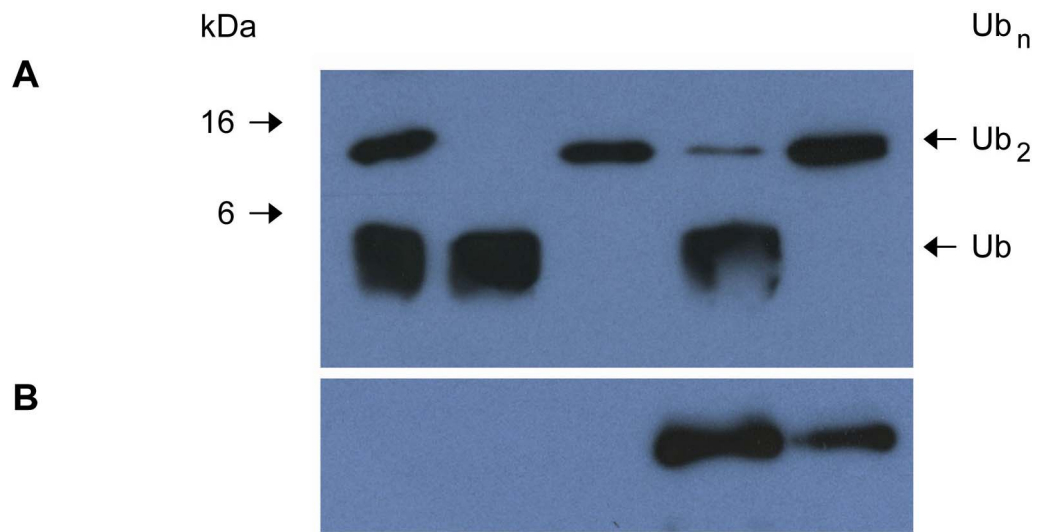


**Figure 5.7** NtUBP12 is a deubiquitinating enzyme and mutations in its active site abolish its activity.

His-NtUBP12 WT and His-NtUBP12 C2086 proteins were expressed and purified from *S. frugiperda* and tested for deubiquitinating activity. A mixture of in vitro synthesised ubiquitin chains with lengths 1-7 units (Ub-Ub7) were loaded as a sizing control (lane 1). Di-Ubiquitin substrate (2 µg) was incubated alone (negative control), with Isopeptidase T (positive control), with NtUBP12 WT (~1 µg) or with AtUBP12 C206S (~0.2 µg) in lanes 2, 3, 4 and 5 respectively. The reactions were analysed by Western blot using anti-Ubiquitin antibody (**A**) or anti-Histidine antibody (**B**).



**B**

	1	2	3	4	5
Ub Chains	+	-	-	-	-
Di-Ubiquitin	-	+	+	+	+
Isopeptidase T	-	+	-	-	-
His-NtUBP12 WT	-	-	-	+	-
His-NtUBP12 C206S	-	-	-	-	+

## 5.5 Phylogenetic analysis of eukaryotic UBP12 proteins

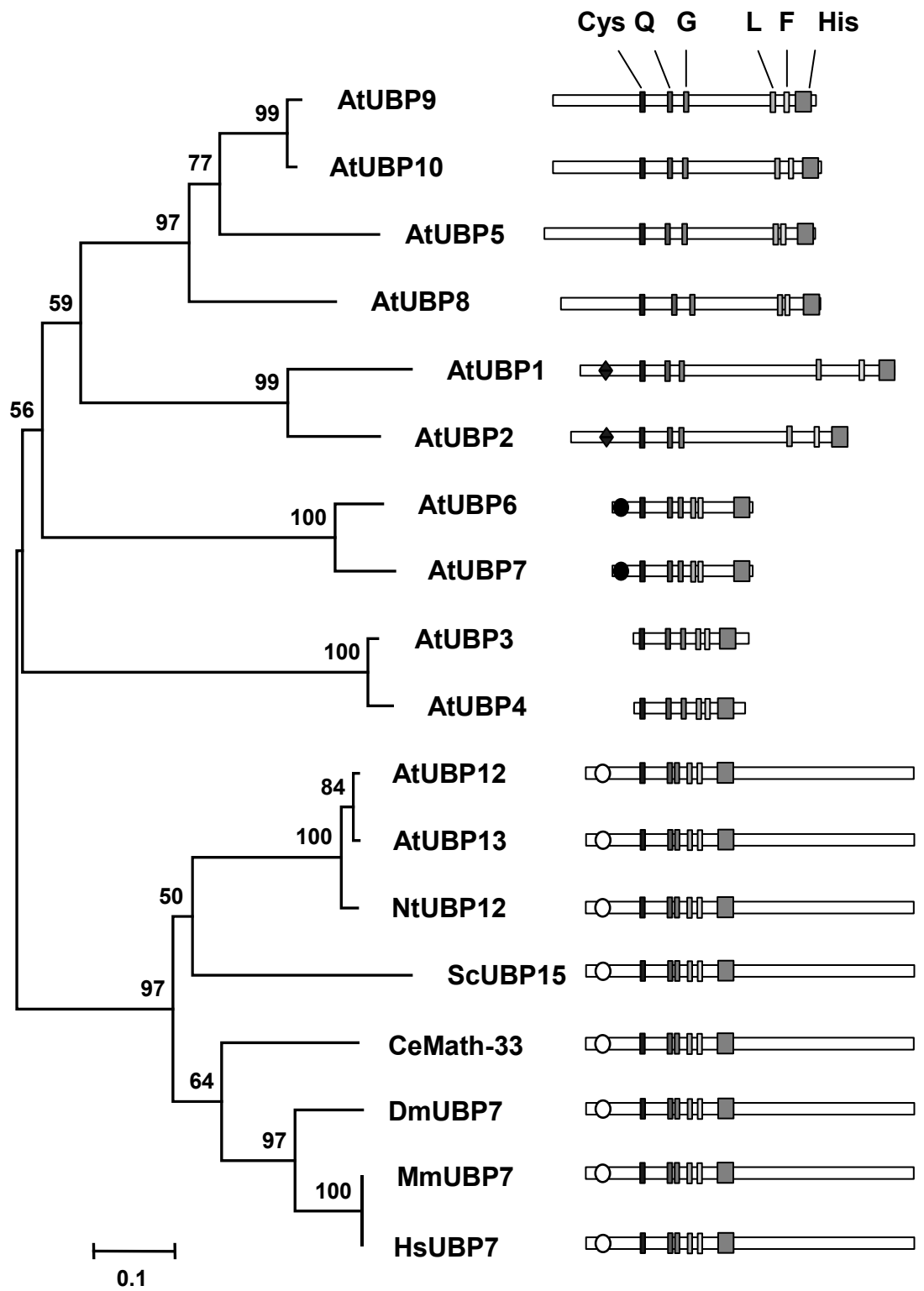
There are several distinct classes of DUB enzyme found in eukaryotes, but in most cases the UBP family is the largest and most diverse (Nijman et al., 2005). Despite this diversity, a core group of archetypal ‘eukaryotic DUBs’ can be detected which are the proposed evolutionary ancestors of the current UBP families (Amerik et al., 2000). To confirm if the plant UBP12 genes in this study were specific to plant or eukaryote lineages, the best scoring BLAST hits to AtUBP12 from various model eukaryotes were subjected to phylogenetic analysis.

High scoring matches to AtUBP12 from yeast (*S. cerevisiae*), worm (*C. elegans*), fly (*D. melanogaster*), mouse (*M. musculus*) and human (*H. sapiens*) were recovered from the UniProt protein database (Bairoch et al., 2005) and their respective His and Cys boxes were extracted from each sequence. Extracted catalytic regions from the recovered sequences, AtUBP12, AtUBP13, NtUBP12 and a subset of other *Arabidopsis* UBP enzymes were aligned using ClustalW. A phylogeny of the aligned UBP sequences was inferred using MEGA with neighbour joining based tree construction (Figure 5.8).

The phylogeny presented in Figure 5.8 indicates that plant UBP12 proteins form a clade with other apparent eukaryotic counterparts. The node values on the tree represent bootstrap confidence percentage (based on 10,000 replicates) which are typically required to be over 70% to provide significant support for a particular phylogenetic relationship (Soltis and Soltis, 2003). Bootstrap analysis provides strong support (bootstrap 97%) for the clustering of plant UBP12 proteins with orthologous eukaryotic proteins. The relative positioning of Yeast UBP15 and Worm Math-33 proteins within this clade is poorly supported (bootstrap 50% and 64% respectively). This observation probably results from the limited amount of sequence data in the alignment (80-100 residues) which is insufficient to place all the sequences in a relevant order. In this case the ordering of sequences in the UBP12 clade is of limited relevance, however the strong overall support for the cluster is indicative of their common ancestry.

**Figure 5.8** Plant UBP12 proteins cluster with their eukaryotic orthologs.

Neighbour Joining phylogeny of plant and model eukaryote UBP proteins. Phylogeny was inferred from an alignment of catalytic regions of UBP proteins (recovered from UniProt) of *Arabidopsis*: AtUBP1 (Q9FPT5), AtUBP2 (Q8W4N3), AtUBP3 (O24454), AtUBP4 (Q8LAM0), AtUBP5 (O22207), AtUBP6 (Q949Y0), AtUBP7 (Q84WC6), AtUBP8 (Q9C585), AtUBP9 (Q93Y01), AtUBP10 (Q9ZSB5), AtUBP12 (Q9FPT1), AtUBP13 (Q84WU2), Tobacco: NtUBP12 (established in this study), Yeast: ScUBP15 (P50101), Fly: DmUBP7 (Q9VYQ8), Worm: CeMath-33 (O45624), Mouse: MmUBP7 (Q6A4J8) and Human: HsUBP7 (Q93009). Phylogenetic tree accuracy was tested with 10,000 bootstrap replicates represented as percentage values at respective nodes. Tree scale bar represents substitutions per site. UBP protein domain diagrams indicate catalytic regions and additional domains as confirmed by Pfam analysis.



Recovered eukaryotic UBP12 orthologs were also analysed using Pfam which confirmed the presence of an N-terminal MATH domain (accession PF00917) in all cases (Figure 5.8).

The inferred phylogeny confirms that UBP12/13 proteins investigated in this study are not specific only to plants and that they form a significant clade with other eukaryotic orthologs rather than other plant UBPs (Figure 5.8). The eukaryotic conservation of UBP12 type DUB proteins suggests a potentially fundamental role for this enzyme in the cell. Functional characterisation of orthologous eukaryotic proteins may yield insights that are applicable or at least relevant to the study of the plant UBP12 proteins.

## **5.6 Discussion**

### **5.6.1 *In vitro* activity assay of AtUBP12 and NtUBP12 proteins**

The current chapter focused on the demonstration of genuine *in vitro* ubiquitin protease activity for *Arabidopsis* and tobacco orthologs of UBP12. Proof of this activity correlates with the loss of function data observed during VIGS based *NtUBP12* gene silencing in *N. benthamiana* (Chapter 4) and gain of function during transient *AtUBP12* overexpression in tobacco (Chapter 6). Purified AtUBP12 and NtUBP12 fusion proteins exhibit ubiquitin protease activity against K48 linked diubiquitin substrate, whereas active site mutant versions of each respective protein do not. Expression of recombinant AtUBP12 proteins in *E. coli* yielded a soluble but apparently inactive product. This is a frequently encountered problem when expressing eukaryotic proteins in prokaryotic hosts which lack many of post-translational processing enzymes typically required to guide protein modification and folding (Baneyx and Mujacic, 2004). Active UBP12 proteins were instead obtained by using eukaryotic insect Sf9 cell based expression.

### 5.6.2 UBP12 linkage specificity

Both *Arabidopsis* and tobacco UBP12 proteins demonstrated cleavage activity against K48 linked diubiquitin. This substrate is composed of two ubiquitin monomers linked by an isopeptide linkage from the terminal glycine (G76) of one Ub moiety to an internal lysine (K48) of the other. In the cell, substrate proteins that are tagged with K48 linked ubiquitin chains are targeted for degradation by the 26S proteasome (Chau et al., 1989). Whilst classical studies established that post-translational modification by ubiquitin dramatically alters a proteins stability, recent data indicate that variation in ubiquitin chain length and structure correspond to differing signalling outcomes (Pickart and Fushman, 2004).

Proteomic approaches to dissect ubiquitination in yeast (Peng et al., 2003) have reported distinct ubiquitin chains linked through all seven available lysine residues (K6, K11, K27, K29, K33, K48 and K63). Biochemical and structural data suggest that distinct ubiquitin chain topologies adopt markedly different three-dimensional conformations and discrimination between these various chain structures is presumed to confer distinct signalling outcomes (Pickart and Fushman, 2004). In addition to the canonical K48 linkage, the best characterised alternative ubiquitin chain topologies are linked through lysines K63 and K29. In mammalian cells, K63 linked ubiquitin has been implicated in numerous signalling processes that include DNA damage tolerance and protein trafficking (Zapata et al., 2001). Recent data indicates that K29 linked ubiquitin chains function in lysosomal protein degradation where K29 tagged substrates are targeted to lysosomes via the Ubiquitin Fusion Degradation (UFD) pathway (Chastagner et al., 2006). In addition to chain based signalling, ligation of a single ubiquitin moiety (monoubiquitination) can influence protein activity or localisation (Hicke, 2001a).

Further to the regulatory aspects of ubiquitin chain linkage, unbranched ubiquitin fusions are generated as translation products from their respective genes. Translated ubiquitin gene products are linear fusion proteins (poly-Ub or Ub-protein) linked by peptide bonds (Finley and Chau, 1991). In the cell, these fusion proteins are cleaved by deubiquitinating

enzymes to generate mature ubiquitin moieties (Amerik and Hochstrasser, 2004).

The emerging variety of peptide and isopeptide linked ubiquitin fusions made *in vivo* reflects the diversity of signalling pathways in which ubiquitination is involved. Accordingly, numerous different cellular DUB activities hydrolyse the various ubiquitin linkages and it is now becoming clear that many DUB enzymes cleave specific linkage types whilst others have promiscuous activities (Nijman et al., 2005).

Ubiquitin binding sequence motifs have been identified within most DUB enzymes but the determinants of branch mode preference are unclear. Current research suggests that both active site architecture and the regulatory influence of non-catalytic domains may influence branch mode selection and efficiency (Nijman et al., 2005) (Komander et al., 2008). In the case of the UBP enzyme family, no generic determinants of chain linkage specificity have been determined and current insights into enzyme function are being determined experimentally on a case by case basis (Komander et al., 2008) (Hu et al., 2002b).

Sequence analysis indicates that UBP12 belongs to a subset of plant UBP genes which are conserved in other eukaryotic genomes. Phylogenetic analysis confirms that AtUBP12 forms a significant cluster with eukaryotic orthologs including yeast USP7 and human USP7/HAUSP. The human ortholog HAUSP is one of the most extensively characterised UBP proteins and *in vitro* activity assays indicate its specificity for K48 linked ubiquitin isopeptide bonds (Hu et al., 2002b).

Based on the genetic conservation of UBP12 in various model eukaryotes (Figure 5.7), it is likely that orthologs also share core structural features and some aspects of function. The established activity of human HAUSP against K48 linked ubiquitin was suggestive that plant UBP12 may exhibit a similar specificity. This prediction was borne out in assay experiments on AtUBP12 and NtUBP12 with K48 linked diubiquitin and is indicative that UBP12 functions *in vivo* to stabilise its biological substrates against proteasomal degradation.

*In vitro* assays indicate that HAUSP has no detectable activity against K63 linked ubiquitin chains (Hu et al., 2002b) and this linkage specificity is probably conserved in plant UBP12 orthologs. This prediction could be tested by *in vitro* assay experiments using K63 linked diubiquitin which is commercially available.

Ultimately, the use of ubiquitin oligomer substrates provides a suitable tool to demonstrate DUB enzyme activity and linkage specificity. However, assays of *in vitro* activity provide only approximate insight into *in vivo* enzyme function when considering the role of conformational changes and interacting partners in enzymatic regulation. Further consideration should also be made for the potential *in vivo* preference of DUB enzymes for isopeptide bonds that are proximal to ubiquitinated substrates or distal within poly-Ub chains.

### **5.6.3 Structural aspects of HAUSP and plant UBP12 function**

Extensive biochemical characterisation of HAUSP has identified three biological substrates, established the crystal structure of the core protease and substrate binding TRAF-like domains (Hu et al., 2006) and that the active site undergoes significant conformational rearrangement to bind and then hydrolyse linked ubiquitin moieties (Hu et al., 2002b). Phylogenetic analysis indicates that HAUSP and plant UBP12 proteins share a common evolutionary ancestor (Figure 5.7) and it is plausible that aspects of enzymatic function have been retained. Current research suggests that HAUSP adjusts from inactive to active conformations to become a functional protease against K48 linked ubiquitin (Hu et al., 2002b). HAUSP activation is likely to be concerted and mediated by the perception of signalling events but the role of the C-terminal domain (which has not been crystallised) or the role of interacting regulatory proteins in this activation is unclear.

In this study, active plant UBP12 proteins were purified from Sf9 cells suggesting a constitutive activity which maybe suppressed or regulated through the influence of interacting proteins that are not present in Sf9 host cells. An alternative explanation is based on the possibility that Sf9

expressed plant UBP12 proteins were constitutively inactive but that basal activity from non-specifically activated enzyme was sufficient to cleave the available diubiquitin substrate. The regulatory role of conformational activation for deubiquitinating enzymes is an active research topic (Amerik and Hochstrasser, 2004) typically requiring structural data from NMR and crystallography studies (Hu et al., 2005). In the case of plant UBP12 proteins, it is plausible that conformational activation may contribute some degree of regulation based on studies of the orthologous human protein HAUSP.

## Chapter 6 - Transient overexpression of AtUBP12 proteins

### 6.1 Introduction

During loss of function studies reported in Chapter 4, *N. benthamiana* plants undergoing *NbUBP12* silencing demonstrated an increased Cf-9 triggered HR phenotype. This chapter reports gain of function experiments to investigate the effect of increased *in vivo* UBP12 activity during disease resistance signalling in tobacco and *N. benthamiana*. Gain of function studies were conducted using *Agrobacterium* based transient overexpression of full length N-terminal GFP-AtUBP12 fusion proteins. Transient expression systems exploit the ability of *Agrobacterium tumefaciens* to efficiently transfer DNA constructs from the bacterial Ti plasmid into the plant cell (Cazzonelli and Velten, 2006). Following infiltration of *Agrobacterium* carrying DNA constructs, expression of the corresponding proteins typically occurs within 2 - 4 days in the majority of plant cells within the infusion area (Sparkes et al., 2006). Transient expression is compatible with a range of host plant species but is typically conducted in Solanaceous plants where it has been previously applied to study gene silencing, promoter structure and disease resistance (Cazzonelli and Velten, 2006). This approach can circumvent the requirement for stable transgenics and allows rapid assessment of gene function during biotic and abiotic treatments.

Based on the *in vitro* activity of AtUBP12 proteins reported in Chapter 5, wildtype and active site mutant GFP-AtUBP12 fusion proteins were transiently expressed from a 35S promoter in tobacco and *N. benthamiana*. The timing of GFP-AtUBP12 transient expression was established and cell death responses during Cf-9 and Pto triggered HR were characterised.

Results reported in this chapter establish that elevations of *in vivo* UBP12 activity resulting from transient overexpression of GFP-AtUBP12 suppress the cell death component of Cf-9 triggered HR in tobacco but do not alter Pto triggered HR in *N. benthamiana*.

## 6.2 Transient overexpression of AtUBP12 proteins in tobacco

Having established that VIGS based silencing of *NbUBP12* caused an increased HR response following elicitation by Cf-9/Avr9, transient overexpression was used to investigate possible gain of function phenotypes associated with UB12 activity during Cf-9 triggered HR.

At the initiation of overexpression experiments, the full length *NtUBP12* cDNA sequence was not determined. To circumvent this issue, the cDNA sequence of *AtUBP12*, the *Arabidopsis* ortholog of *NtUBP12* was cloned for overexpression studies. The validity of this transgenomic approach was based on two assumptions. First, that *AtUBP12* is transcriptionally induced by *Pseudomonas syringae* and SA and may have a general role in disease resistance signalling. Second, that based on the high degree of amino acid conservation between *AtUBP12* and *NtUBP12* (86% identity), *AtUBP12* could respond to *in vivo* stimuli and stabilise the same target substrates as *NtUBP12* during Cf-9 triggered HR.

### 6.2.1 Generation and expression of GFP-AtUBP12 fusion proteins

For overexpression studies, the Gateway compatible pGWB6 vector (Nakagawa et al., 2007) was used to generate an N-terminal GFP-AtUBP12 fusion construct expressed under a CaMV 35S promoter. Results presented in Chapter 5 confirm that the active site mutant protein *AtUBP12* C208S lacks ubiquitin protease activity. The corresponding GFP-AtUBP12 C208S fusion construct was generated for use as a negative control in transient overexpression experiments. Subcloning of cDNA fragments corresponding to *AtUBP12* and *AtUBP12* C208S into the Gateway entry vector pENTR4 was described in Chapter 5 (Section 5.2.1). Full length cDNA from each respective *AtUBP12* entry clone was transferred into the pGWB6 destination vector by Gateway LR based recombination to generate N-terminal GFP tagged *AtUBP12* WT and *AtUBP12* C208S fusion constructs.

Transgenic tobacco lines overexpressing the tomato R gene *Cf-9* (as described in Chapter 4 - Section 4.3) (Hammond-Kosack et al., 1998) were used for transient overexpression of *AtUBP12* proteins. Protocols for

transient overexpression of proteins using *Agrobacterium* in tobacco are established (Sparkes et al., 2006) and the utilisation of transgenic *Cf-9* lines allows efficient triggering of the HR following infiltration of extracted Avr9 peptide solution (Hammond-Kosack et al., 1998).

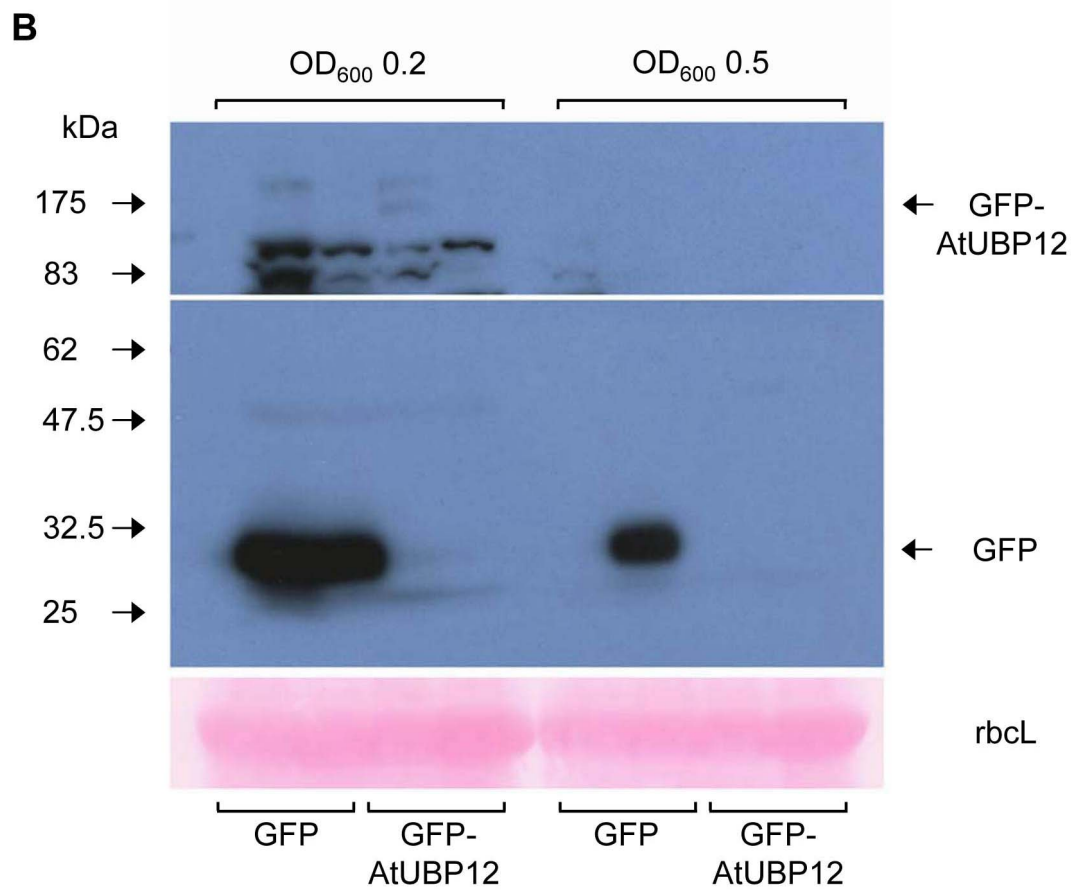
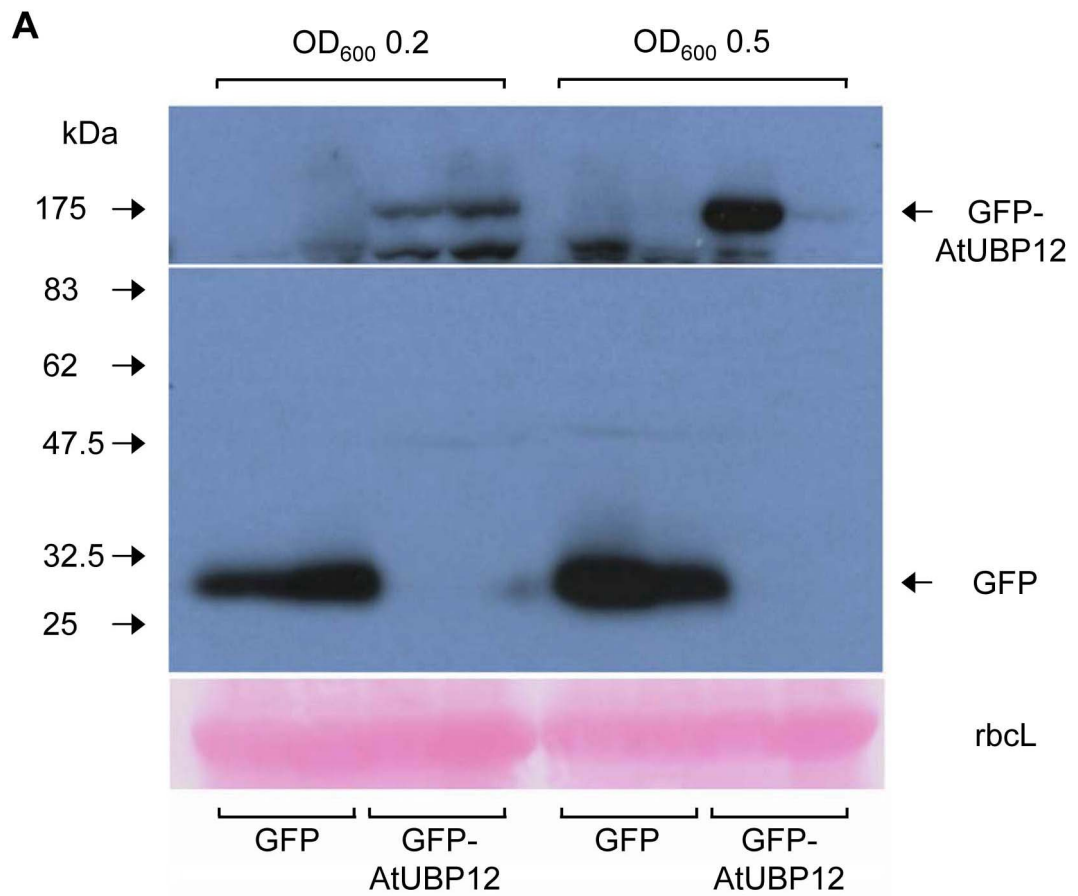
*Agrobacterium* mediated transient gene expression in *Nicotiana* species typically results in the accumulation of corresponding protein from two days until upto five days after construct inoculation (Sparkes et al., 2006). To establish the peak of transgene expression for GFP-AtUBP12 fusion constructs, a timecourse analysis of GFP-AtUBP12 protein expression in tobacco was conducted (Figure 6.1). Tobacco leaf sections were inoculated with *Agrobacterium* containing GFP-AtUBP12 constructs at either OD<sub>600</sub> 0.2 or 0.5 (Figure 6.1). Protein expression was analysed in duplicate using anti-GFP antibodies on leaf samples taken either two (Figure 6.1 A) or three (Figure 6.1 B) days after agroinoculation of GFP-AtUBP12 constructs.

The calculated molecular weight of AtUBP12 is ~133 kDa which when fused to the 27 kDa GFP tag (Niwa, 2002) in pGWB6 produces a ~160 kDa fusion protein. In day two samples, anti-GFP analysis indicated the expected GFP-AtUBP12 band migrating slightly faster than the 175 kDa marker in GFP-AtUBP12 extracts which was not present in GFP (empty pGWB6) controls (Figure 6.1 A). In all cases 100 µg of total protein extract was resolved on SDS-PAGE gels and western blot analysis indicated that GFP-AtUBP12 fusion protein expression levels were highest two days after *Agrobacterium* infiltration (Figure 6.1). GFP-AtUBP12 expression was not detectable in 75% of leaf samples taken three days after *Agrobacterium* infiltration and where detected, was markedly reduced compared to the majority of day two expression samples (Figure 6.1 B).

Western blotting results indicated higher expression of GFP-AtUBP12 at day two compared to day three but also that the absolute level of expression was highly variable between individual replicates (Figure 6.1 A). An approximate 20 fold difference in GFP-AtUBP12 expression was seen between duplicate day two samples infiltrated at OD<sub>600</sub> 0.5 (Figure 6.1 A). Despite the variability in expression, GFP-AtUBP12 was detectable in all

**Figure 6.1** GFP-AtUBP12 fusion protein accumulation peaks on day 2 during transient overexpression in tobacco.

Western blot analysis of total protein extract (100 µg) from tobacco leaves either two (**A**) or three (**B**) days after agroinoculation of 35S GFP-AtUBP12 or 35S GFP at OD<sub>600</sub> 0.2 and OD<sub>600</sub> 0.5. Samples were analysed in duplicate and western blots were probed with anti-GFP antibody. Upper and lower panels of film images represent different exposure times of a single western blot. Upper panel represents long exposure (10 minutes) and lower panel represents short exposure (5 seconds). Ponceau stain of rubisco large subunit (rbcl) was used as a loading control.



day two samples and this timepoint was considered the peak of expression. For transient overexpression studies, *Agrobacterium* cultures containing GFP-AtUBP12 fusion constructs were infiltrated into *Cf-9* tobacco at OD<sub>600</sub> 0.5 and HR cell death assays were conducted two days later at the established peak of transgene expression.

### **6.2.2 *Cf-9*/Avr9 triggered HR assay during transient overexpression of AtUBP12 proteins**

Using transgenic *Cf-9* tobacco lines, an efficient HR response can be triggered following infiltration of extracted Avr9 peptide as described by Hammond-Kosack *et al* (Hammond-Kosack *et al.*, 1998).

Extracted Avr9 peptide stock was adjusted by titration to elicit HR in *Cf-9* tobacco leaves such that confluent cell death and severe tissue necrosis were established approximately 12-16 hours after infiltration. Using Avr9 peptide diluted to either 2 or 4 fold from a stock solution elicited an appropriate HR response in the majority of *Agrobacterium* treated *Cf-9* tobacco leaf sections tested (data not shown). The oldest (first 4-5) and youngest (last 3-4) leaves in 6 week old *Cf-9* tobacco plants were not used for transient expression based on the respective hypersensitivity and hyposensitivity to established Avr9 peptide titres typically observed in these leaves (data not shown).

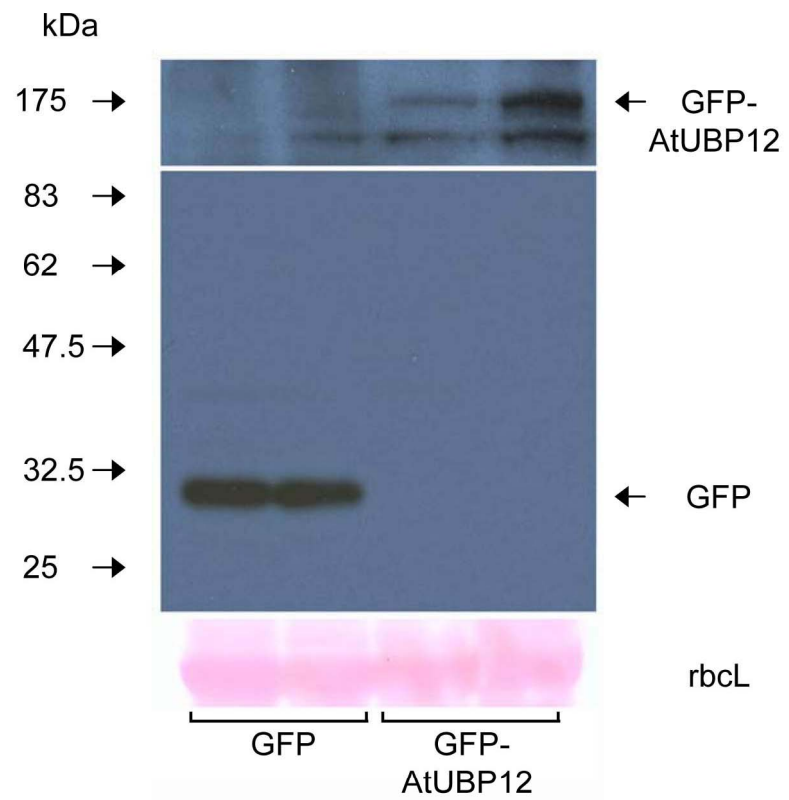
Overexpression of GFP-AtUBP12 and GFP-AtUBP12 C208S fusion constructs was conducted in *Cf-9* tobacco plants and accumulation of corresponding GFP-AtUBP12 and GFP-AtUBP12 C208S proteins on day two was confirmed by western blotting with anti-GFP antibodies (Figure 6.2).

GFP-AtUBP12 fusion GFP control constructs were infiltrated into appropriate *Cf-9* tobacco leaf segments as indicated (Figure 6.3 A). Two adjacent segments left of the main vein were infiltrated with the GFP-AtUBP12 construct (L1 and L2 Figure 6.3 A) whilst corresponding segments right of the main vein were infiltrated with GFP only (R1 and R2 Figure 6.3 A). Two days after infiltration, during the peak of transgene expression,

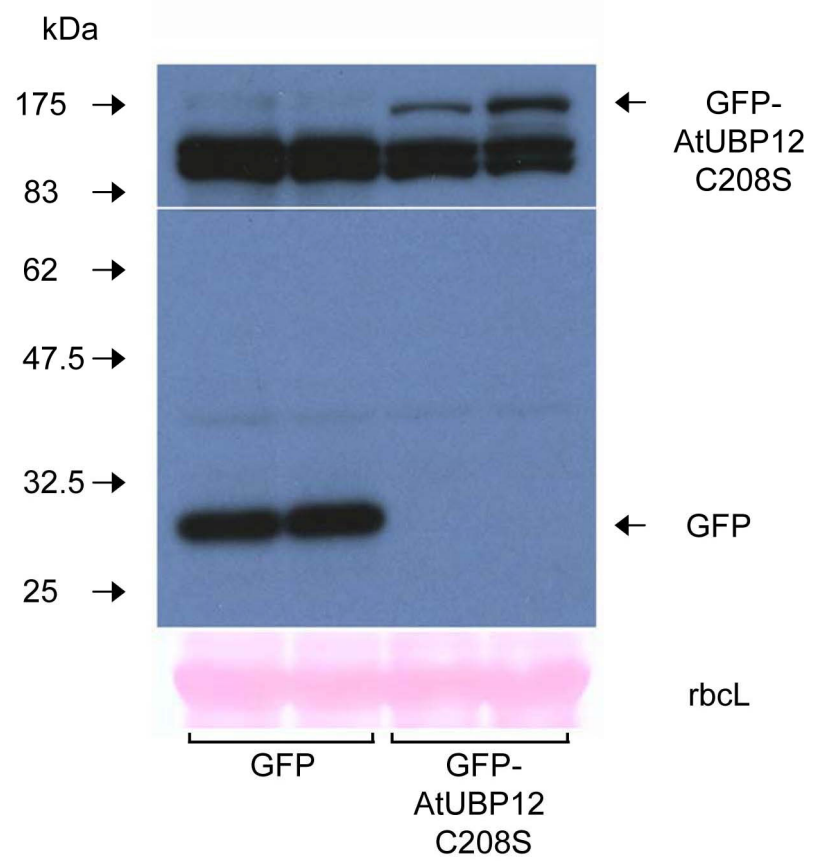
**Figure 6.2** Expression GFP-AtUBP12 WT and GFP-AtUBP12 C208S in tobacco.

Western blot analysis of total protein extract (100 µg) from tobacco leaves two days after agro-inoculation of 35S GFP-AtUBP12 WT (**A**) or 35S GFP-AtUBP12 C208S (**B**). Samples were analysed in duplicate and western blots were probed with anti-GFP antibody. Upper and lower panels of film images represent different exposure times of a single western blot. Upper panel represents long exposure (5 minutes) and lower panel represents short exposure (5 seconds). Ponceau stain of rubisco large subunit (rbcl) was used as a loading control.

**A**



**B**



*Cf-9* tobacco leaf segments were infiltrated with Avr9 peptide at 2 and 4 fold dilutions in upper and lower respective leaf segments to elicit the HR (Figure 6.3 A and B). After Avr9 peptide infiltration, a clear reduction in the development of hypersensitive cell death was observed in numerous GFP-AtUBP12 expressing leaf segments relative to GFP expressing controls (Figure 6.3 B).

HR assays were conducted in 28 independent leaves expressing GFP-AtUBP12 and GFP (as indicated in Figure 6.3 A) and the development of cell death in GFP-AtUBP12 overexpressing segments was scored relative to the corresponding GFP control (Figure 6.3 C). Based on hypersensitive cell death coverage in the infiltrated leaf segment, HR was scored as: suppressed (at least 50% less cell death compared to corresponding GFP control), unchanged (no clear difference in cell death compared to corresponding GFP control) or increased (at least 50% more cell death compared to corresponding GFP control).

During GFP-AtUBP12 overexpression experiments in 28 leaves, HR elicitation by 2 fold diluted Avr9 peptide was suppressed in 39%, unchanged in 57% and increased in 4% of leaves (Figure 6.3 C). A similar trend following HR elicitation with 4 fold diluted Avr9 peptide was observed where HR was suppressed in 43%, unchanged in 53% and increased in 4% of leaves (Figure 6.3 C).

Equivalent transient overexpression assays were conducted using the GFP-AtUBP12 C208S active site mutant construct (Figure 6.4). In 21 independent leaves, no HR suppression was observed during overexpression of GFP-AtUBP12 C208S (Figure 6.4 B and C). Scoring indicated that following elicitation by 2 fold diluted Avr9 peptide, the HR was suppressed in 0%, unchanged in 95% and increased in 5% of leaves (Figure 6.4 C). A similar scoring trend was observed following HR elicitation with 4 fold diluted Avr9 peptide where the HR was suppressed in 0%, unchanged in 90% and increased in 10% of leaves (Figure 6.4 C).

**Figure 6.3** Transient overexpression of AtUBP12 in *Cf-9* tobacco suppresses Avr9 elicited HR.

(A) Agroinoculation and Avr9 peptide infiltration scheme in *Cf-9* tobacco leaf sections. 35S GFP-AtUBP12 and 35S GFP constructs were agroinoculated at OD<sub>600</sub> 0.5 into left (L1 and L2) and right (R1 and R2) tobacco leaf segments respectively. Two days after agroinoculation, upper leaf segments (L1 and R1) and lower leaf segments (L2 and R2) were infiltrated with Avr9 elicitor at x 0.5 and x 0.25 dilutions respectively.

(B) HR development in *Cf-9* tobacco leaf segments overexpressing GFP-AtUBP12 (left segments) and GFP (right segments) following Avr9 elicitor infiltration. Pictures taken five days after Avr9 elicitor infiltration.

(C) Avr9 elicited HR cell death assay during GFP-AtUBP12 overexpression. Extent of cell death in GFP-AtUBP12 overexpressing segments was scored against the corresponding GFP overexpressing control segment five days after infiltration of Avr9 elicitor at x 0.5 and x 0.25 dilutions.

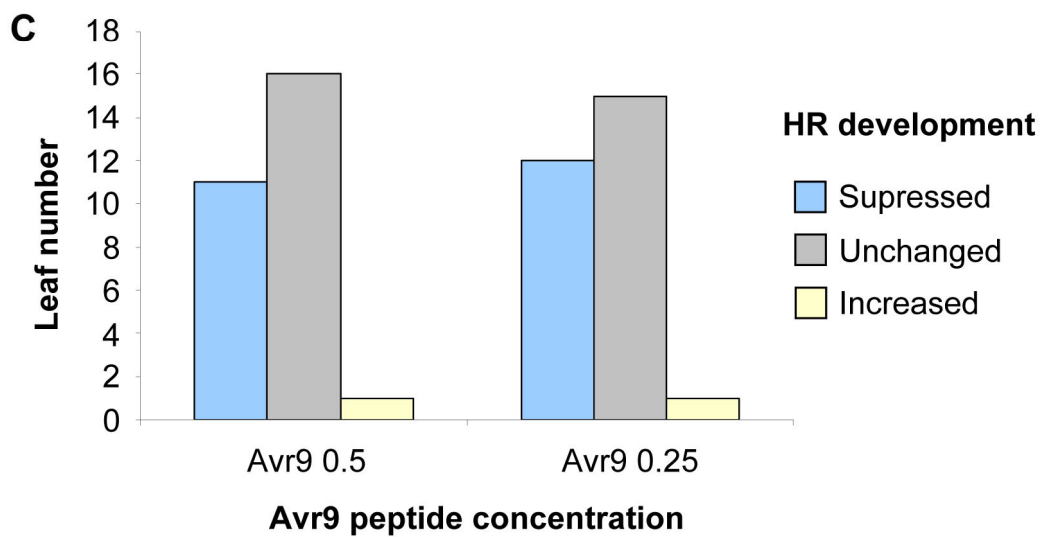
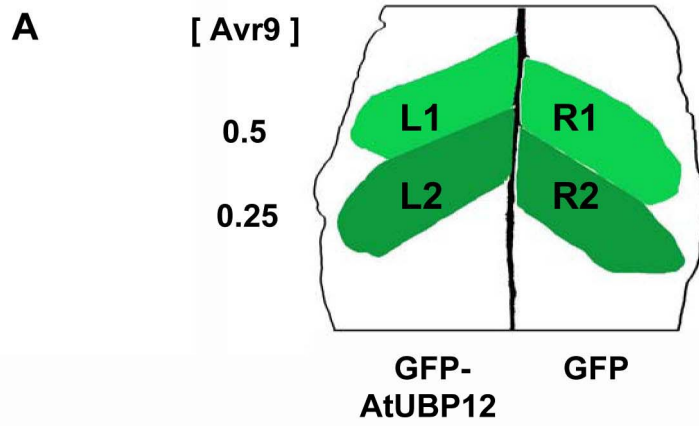
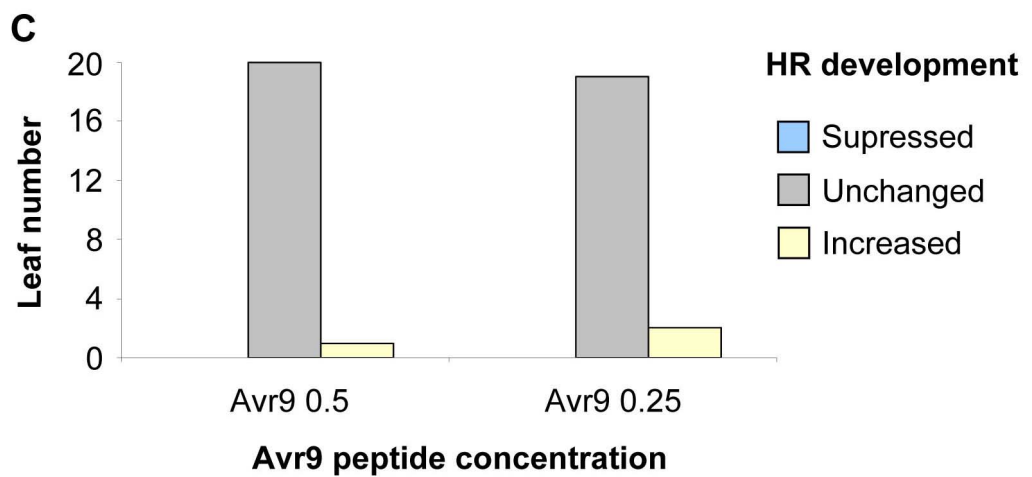
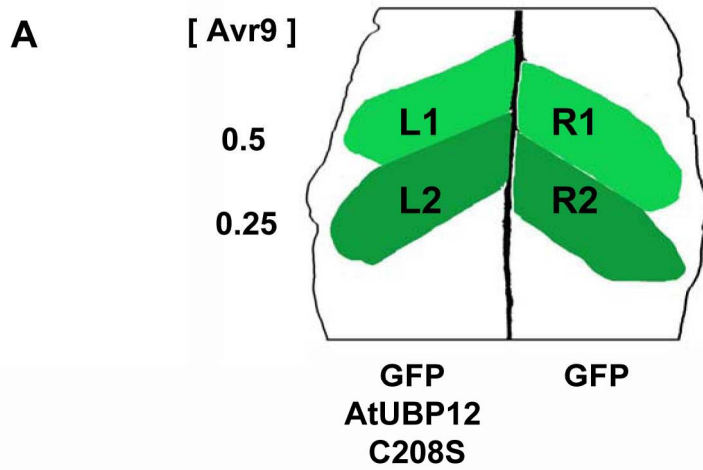


**Figure 6.4** Transient overexpression of the non-catalytic mutant AtUBP12 C208S in *Cf-9* tobacco fails to suppress Avr9 elicited HR.

**(A)** Agroinoculation and Avr9 peptide infiltration scheme in *Cf-9* tobacco leaf sections. 35S GFP-AtUBP12 C208S and 35S GFP constructs were agroinoculated at OD<sub>600</sub> 0.5 into left (L1 and L2) and right (R1 and R2) tobacco leaf segments respectively. Two days after agroinoculation, upper leaf segments (L1 and R1) and lower leaf segments (L2 and R2) were infiltrated with Avr9 elicitor at x 0.5 and x 0.25 dilutions respectively.

**(B)** HR development in *Cf-9* tobacco leaf segments overexpressing GFP-AtUBP12 C208S (left segments) and GFP (right segments) following Avr9 elicitor infiltration. Pictures taken five days after Avr9 elicitor infiltration.

**(C)** Avr9 elicited HR cell death assay during GFP-AtUBP12 C208S overexpression. Extent of cell death in GFP-AtUBP12 C208S overexpressing segments was scored against the corresponding GFP overexpressing control segment five days after infiltration of Avr9 elicitor at x 0.5 and x 0.25 dilutions.



Having confirmed that overexpression of mutant AtUBP12 C208S failed to suppress the Cf-9 triggered HR, further experiments were conducted to investigate possible competitive substrate binding effects of the mutant protein. Avr9 peptide levels were titrated to establish if overexpression of AtUBP12 C208S resulted in increased sensitivity to the HR elicitor. Equivalent transient overexpression assays were conducted with the GFP-AtUBP12 C208S active site mutant construct but HR was elicited using 12 fold and 20 fold diluted Avr9 peptide in upper and lower respective leaf segments (Figure 6.5 A).

Transient assays were conducted in 18 independent leaves and an increased HR phenotype was observed in leaf segments overexpressing the GFP-AtUBP12 C208S protein (Figure 6.5 B and C). Scoring indicated that following elicitation by 12 fold diluted Avr9 peptide, the HR was suppressed in 0%, unchanged in 67% and increased in 33% of leaves (Figure 6.5 C). A similar scoring trend was observed following elicitation with 20 fold diluted Avr9 peptide where the HR was suppressed in 0%, unchanged in 55% and increased in 45% of leaves (Figure 6.5 C). These findings indicate that overexpression of an active site mutant AtUBP12 C208S protein confers a dominant negative effect to promote the development of Cf-9 triggered HR.

The suppression of Cf-9 triggered HR during AtUBP12 overexpression correlates with loss of function data presented in Chapter 4 where VIGS based silencing of *NbUBP12* causes an increase in Cf-9 triggered HR. The presented results indicate that AtUBP12 overexpression can enhance the function of its solanaceous ortholog in *N. tabacum* to regulate Cf-9 triggered disease resistance signalling. Overexpression of an inactive AtUBP12 mutant fails to suppress the Cf-9 triggered HR, confirming that the elevated levels of UBP12 activity are responsible for the observed HR suppression phenotype.

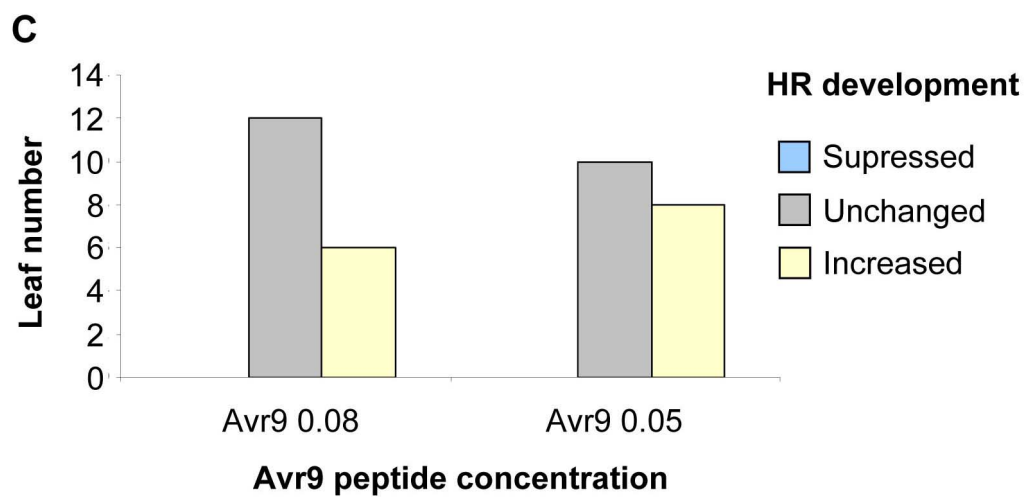
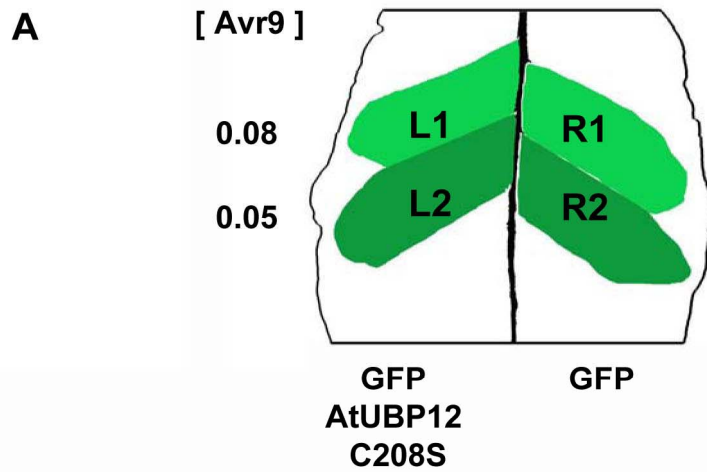
Based on loss and gain of function approaches, solanaceous UBP12 proteins apparently function to deubiquitinate and stabilise a negative HR regulator. Overexpression of AtUBP12 in tobacco presumably leads to a 'hyper-stabilisation' of target substrates with increased levels of negative

**Figure 6.5** Transient overexpression of AtUBP12 C208S in *Cf-9* tobacco promotes Avr9 elicited HR through a dominant negative effect.

**(A)** Agroinoculation and Avr9 peptide infiltration scheme in *Cf-9* tobacco leaf sections. 35S GFP-AtUBP12 C208S and 35S GFP constructs were agroinoculated at OD<sub>600</sub> 0.5 into left (L1 and L2) and right (R1 and R2) tobacco leaf segments respectively. Two days after agroinoculation, upper leaf segments (L1 and R1) and lower leaf segments (L2 and R2) were infiltrated with Avr9 elicitor at x 0.08 and x 0.05 dilutions respectively.

**(B)** HR development in *Cf-9* tobacco leaf segments overexpressing GFP-AtUBP12 C208S (left segments) and GFP (right segments) following Avr9 elicitor infiltration. Pictures taken five days after Avr9 elicitor infiltration.

**(C)** Avr9 elicited HR cell death assay during GFP-AtUBP12 C208S overexpression. Extent of cell death in GFP-AtUBP12 C208S overexpressing segments was scored against the corresponding GFP overexpressing control segment five days after infiltration of Avr9 elicitor at x 0.08 and x 0.05 dilutions.



regulators leading to the observed HR suppression phenotype. The dominant negative effect (Veitia, 2007) seen during overexpression of AtUBP12 C208S indicates that the mutant protein competes with endogenous NtUBP12 to bind a ubiquitinated negative HR regulator (or regulators). As the mutant AtUBP12 C208S protein lacks ubiquitin protease activity, it presumably fails to stabilise its ubiquitinated substrate. By competitively binding NtUBP12 substrates AtUBP12 C208S effectively maintains the ubiquitination status of negative HR regulators thereby promoting their proteasomal degradation to cause the reported increased HR phenotype.

### **6.3 Transient overexpression of AtUBP12 proteins in *N. benthamiana* during Pto/avrPto triggered HR**

Loss of function results reported in Chapter 4 indicated that silencing of *NbUBP12* did not alter the development of HR triggered mediated by the *Pto R* gene. To investigate possible gain of function phenotypes during *avrPto/Pto* triggered HR, AtUBP12 fusion proteins were transiently overexpressed in transgenic 35S *Pto N. benthamiana* plants. The HR was elicited in transgenic *N. benthamiana* expressing the *Pto R* gene under a CaMV 35S promoter as described in Chapter 4 (Section 4.6) by high titre inoculation of *Pseudomonas* expressing the *avrPto* avirulence gene.

The efficiency of *Agrobacterium* based transient gene expression is normally reduced by the induction of RNA mediated anti-viral plant defence mechanisms which act to silence the transgene (Johansen and Carrington, 2001). Many viral genomes encode silencing suppressors which overcome gene silencing effects by inhibiting different aspects the gene silencing process (Silhavy and Burgyan, 2004). Disruption of siRNA binding to silencing effector complexes prevents the initiation of gene silencing and increases virus pathogenicity. Numerous silencing suppressors have been identified (Silhavy and Burgyan, 2004), some of which have been employed to yield considerable improvements during transient gene expression (Voinnet et al., 2003). In this study, the tomato bushy stunt virus silencing suppressor P19 (Voinnet et al., 2003) was utilised to increase transient expression levels of GFP-AtUBP12 constructs in *N. benthamiana*.

#### **6.3.1 Transient overexpression of AtUBP12 proteins in *N. benthamiana***

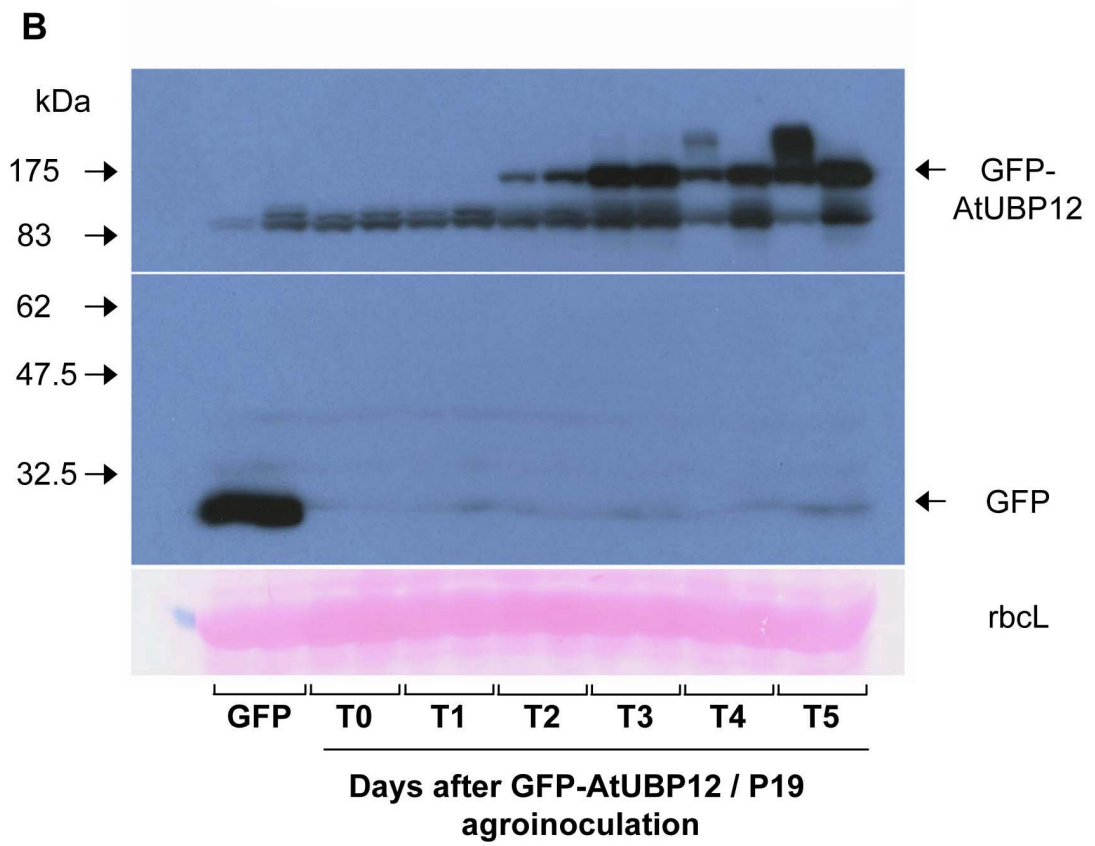
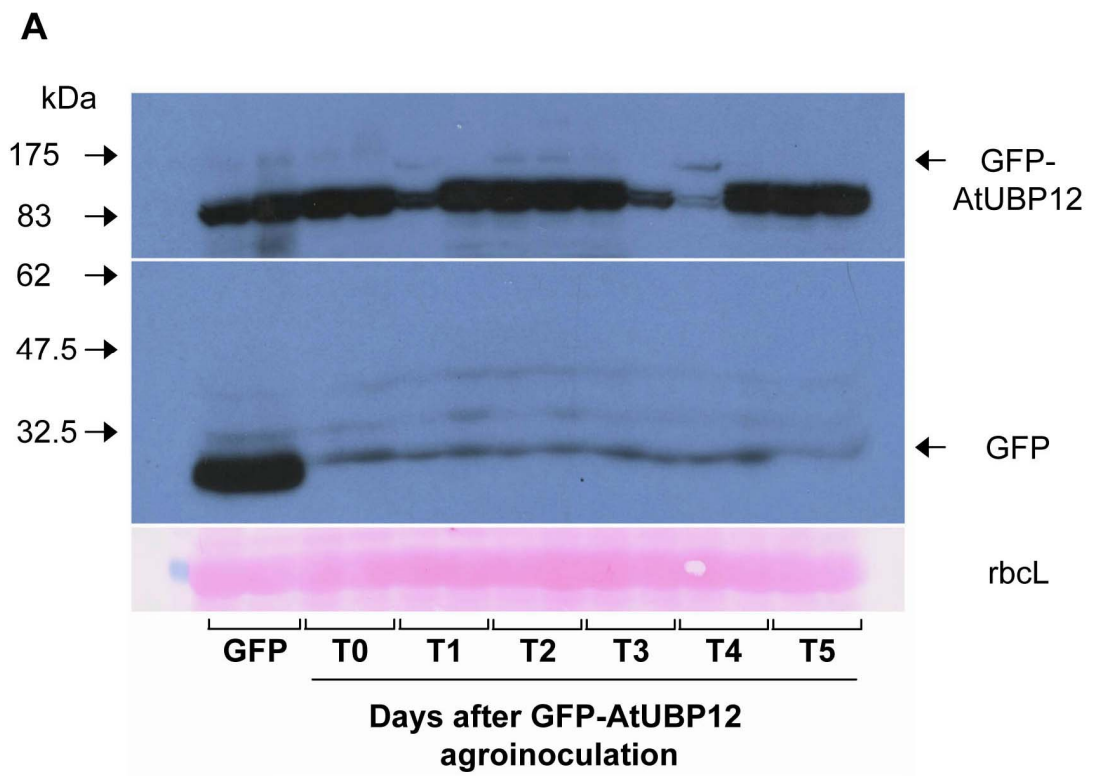
To examine the effect of P19 on GFP-AtUBP12 transgene expression in *N. benthamiana*, a timecourse protein expression analysis was conducted (Figure 6.6). GFP-AtUBP12 fusion protein constructs (described in Section 6.2.1) were agroinoculated into *N. benthamiana* leaves at a final OD<sub>600</sub> of 0.5. *Agrobacterium* containing the P19 silencing suppressor construct was coinfiltrated with GFP-AtUBP12 constructs at a final OD<sub>600</sub> of 0.2.

Timecourse studies of GFP-AtUBP12 fusion protein accumulation were conducted both with and without P19 for five days after agroinoculation (Figure 6.6). Timecourse expression samples were analysed in duplicate where in all cases, 100 µg of total protein extract were resolved on SDS-PAGE gels and analysed by western blotting using anti-GFP antibodies (Figure 6.6). As expected, coinfiltration of the P19 silencing suppressor caused a major improvement in GFP-AtUBP12 protein expression (Figure 6.6). In accordance with prior tobacco overexpression experiments (Section 6.2.2), without P19 coinfiltration accumulation of GFP-AtUBP12 fusion protein peaked at two days after construct infiltration (Figure 6.6 B). Coinfiltration of the P19 silencing suppressor led to increased GFP-AtUBP12 expression at two days after infiltration (approximately 10 fold higher) and a further elevation in fusion protein accumulation expression during subsequent timepoints upto five days after infiltration (Figure 6.6 A).

Coinfiltration of P19 during transient overexpression caused an approximate 50 fold increase in GFP-AtUBP12 accumulation at day 3 compared to the day 2 peak of expression observed without P19 (Figure 6.6). The observed approximate 50 fold increase in protein accumulation was maintained at days four and five and appeared to be slightly increased in some samples (Figure 6.6 A). As there was no major difference in P19 associated fusion protein accumulation at three, four and five days after construct agroinoculation the peak of GFP-AtUBP12 expression was considered to be during day three (Figure 6.6 A).

**Figure 6.6** Coinfiltration of the P19 silencing suppressor enhances transient overexpression of GFP-AtUBP12 in *N. benthamiana*.

Western blot analysis of total protein extract (100 µg) from *N. benthamiana* leaves sampled for five days (T0-T5) after agroinoculation of 35S GFP-AtUBP12 or 35S GFP constructs at OD<sub>600</sub> 0.5 either without (A) or with (B) coinfiltration of P19 silencing suppressor. Samples were analysed in duplicate and western blots were probed with anti-GFP antibody. Upper and lower panels of film images represent different exposure times of a single western blot. Upper panel represents a longer exposure (20 seconds in A and 10 seconds in B) and lower panel represents short exposure (2 seconds in A and B). Ponceau stain of rubisco large subunit (rbcL) was used as a loading control.



### 6.3.2 *avrPto/Pto* triggered HR during overexpression of AtUBP12 proteins in *N. benthamiana*

Results reported in Section 6.2 indicated that transient ectopic expression of AtUBP12 can functionally enhance NtUBP12 activity to confer a gain of function HR suppression phenotype during Cf-9 triggered HR. An equivalent approach was taken to overexpress GFP-AtUBP12 fusion proteins during *avrPto/Pto* triggered HR in *N. benthamiana*.

To investigate the potential involvement of UBP12 activity in *Pto* mediated HR, various titres of avirulent *Pseudomonas syringae* pv. *tabaci avrPto* were inoculated onto 35S *Pto N. Benthamiana* during transient overexpression of GFP-AtUBP12 proteins.

Inoculation of high titre *P. s. pv. tabaci avrPto* at  $4 \times 10^7$  cfu/ml on 35S *Pto N. benthamiana* typically elicits a strong HR response with confluent cell death between 14 - 18 hours after infiltration. In this study, *P. s. pv. tabaci avrPto* inoculations were conducted at three different titres to examine potential AtUBP12 associated suppression or promotion of the *Pto* triggered HR (Figure 6.8 A).

High *P. s. pv. tabaci avrPto* titres of  $4 \times 10^7$  cfu/ml were used to elicit a strong HR response, HR suppression by GFP-AtUBP12 overexpression would cause a corresponding decrease in visible cell death at this titre. Low *P. s. pv. tabaci avrPto* titres of  $6 \times 10^6$  cfu/ml were used to elicit a weak HR response, HR promotion by GFP-AtUBP12 overexpression would cause a corresponding increase in visible cell death at this titre. An intermediate *P. s. pv. tabaci avrPto* titre of  $1 \times 10^7$  cfu/ml was included for comparative purposes during HR elicitation (Figure 6.8 A). This range of *P. s. pv. tabaci avrPto* titres defined a suitable sensitivity range for HR cell death assays during transient overexpression of GFP-AtUBP12 fusion proteins.

Transient overexpression assays were conducted in individual *N. benthamiana* leaves with agroinoculation of entire half leaves to express GFP-AtUBP12 fusion proteins left of the main vein or the GFP control right of main vein (Figure 6.8 A).

Data is reported for *avrPto/Pto* triggered HR development during transient overexpression assays of GFP-AtUBP12 vs GFP (Figure 6.8) and the corresponding control experiment with active site mutant GFP-AtUBP12 C208S vs GFP (Figure 6.9). Equivalent transient overexpression assays were also conducted with coinfiltration of the P19 silencing suppressor to achieve increased expression during GFP-AtUBP12 vs GFP (Figure 6.11) and GFP-AtUBP12 C208S vs GFP experiments (Figure 6.12).

Transient overexpression of GFP-AtUBP12 and GFP-AtUBP12 C208S fusion proteins without P19 was conducted in 13 and 14 independent leaves of 35S *Pto N. benthamiana* respectively (Figures 6.8 and 6.9). Fusion protein accumulation at day 2 was confirmed by western blot analysis of duplicate samples with anti-GFP antibodies (Figure 6.7). As previously described, transient expression of GFP-AtUBP12 fusion proteins demonstrated marked variability between samples. Even though 100 µg of total protein extract was resolved for western blot analysis, relatively low amounts of fusion protein accumulation were observed (Figure 6.7) with one GFP-AtUBP12 C208S sample demonstrating no detectable expression (Figure 6.7 B).

During the second day of transient GFP-AtUBP12 expression without P19 coinfiltration, avirulent *P. s. pv tabaci avrPto* was patch inoculated onto 35S *Pto N. benthamiana* leaves expressing GFP-AtUBP12 and GFP at three titres to elicit a weak ( $6 \times 10^6$  cfu/ml), intermediate ( $1 \times 10^7$  cfu/ml) or strong ( $4 \times 10^7$  cfu/ml) HR response (Figures 6.8 A). Analysis of the resultant HR in 13 leaf replicates indicated no clear trend of cell death promotion or suppression relative to GFP controls at any of the inoculated bacterial titres (Figure 6.8 B and C). Equivalent transient assays were conducted with active site mutant GFP-AtUBP C208S and GFP in 14 leaves (Figure 6.9). Analysis of the resultant HR indicated no alteration in the development of cell death relative to GFP controls (Figure 6.9 B and C).

**Figure 6.7** Transient overexpression GFP-AtUBP12 and GFP-AtUBP12 C208S in *N. benthamiana*.

Western blot analysis of total protein extract (100 µg) from *N. benthamiana* leaves two days after agroinoculation of 35S GFP-AtUBP12 (**A**) or 35S GFP-AtUBP12 C208S (**B**) constructs with corresponding 35S GFP controls at OD<sub>600</sub> 0.5. Samples were analysed in duplicate and western blots were probed with anti-GFP antibody. Upper and lower panels of film images represent different exposure times of a single western blot. Upper panel represents long exposure (8 minutes) and lower panel represents short exposure (10 seconds). Ponceau stain of rubisco large subunit (rbcl) was used as a loading control.

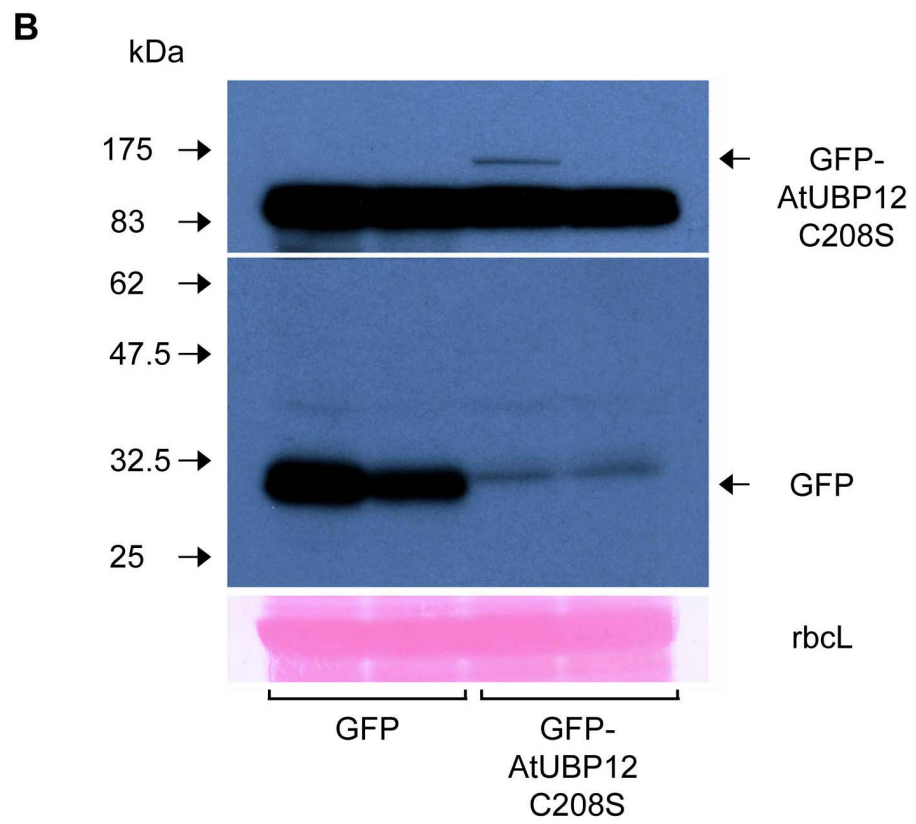
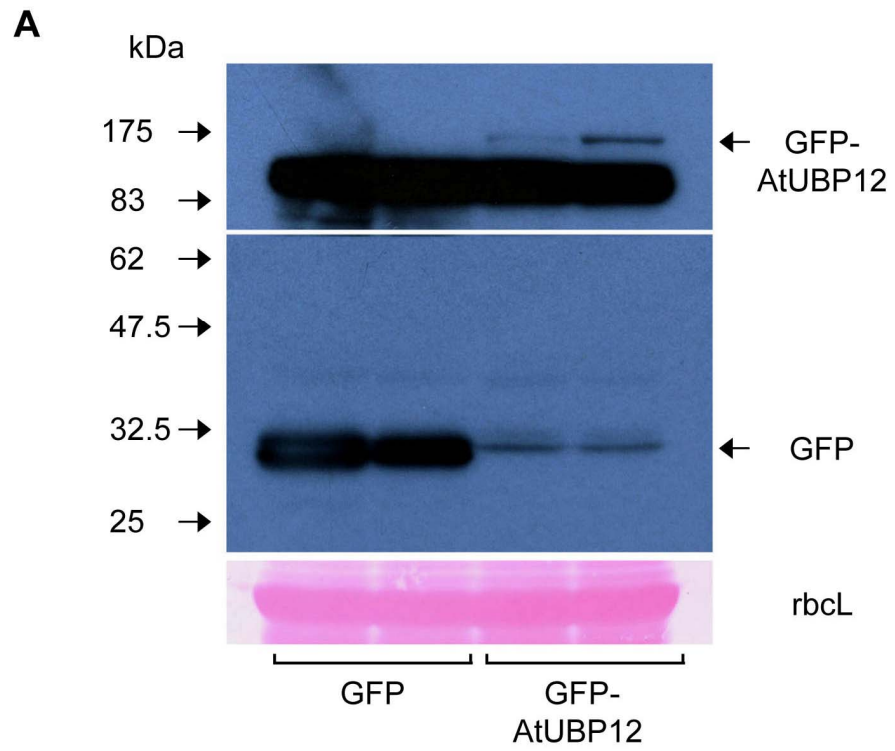


**Figure 6.8** Overexpression of AtUBP12 in *N. benthamiana* does not effect *avrPto/Pto* elicited HR.

(A) Agroinoculation and *P. s. pv. tabaci avrPto* infiltration scheme in 35S *Pto N. benthamiana* leaves. 35S GFP-AtUBP12 and 35S GFP constructs were agroinoculated at OD<sub>600</sub> 0.5 into left and right leaf halves respectively. Two days after agroinoculation, *P. s. pv. tabaci avrPto* infiltration patches were made on each leaf half at  $4 \times 10^7$  (L1 and R1),  $1 \times 10^7$  (L2 and R2) and  $6 \times 10^6$  (L3 and R3) cfu/ml respectively.

(B) HR development in 35S *Pto N. benthamiana* leaves overexpressing GFP-AtUBP12 (upper panels) and GFP (lower panels) following infiltration of *P. s. pv. tabaci avrPto* at  $1 \times 10^7$  cfu/ml. Pictures taken four days after *P. s. pv. tabaci avrPto* infiltration.

(C) *avrPto* elicited HR cell death assay during GFP-AtUBP12 overexpression. Extent of cell death in GFP-AtUBP12 overexpressing sections was scored against the corresponding GFP overexpressing control sections four days after infiltration of *P. s. pv. tabaci avrPto* at  $4 \times 10^7$ ,  $1 \times 10^7$  and  $6 \times 10^6$  cfu/ml respectively.

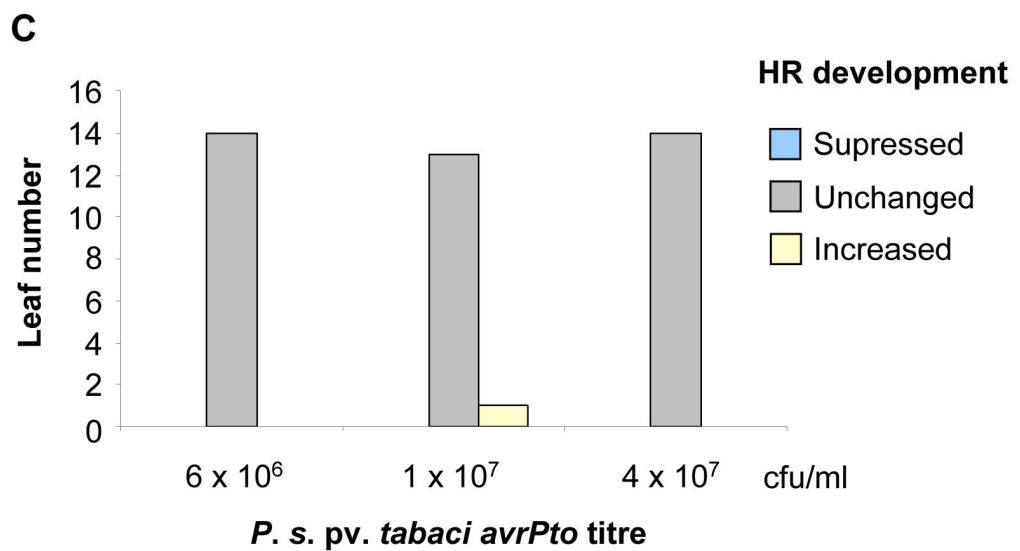
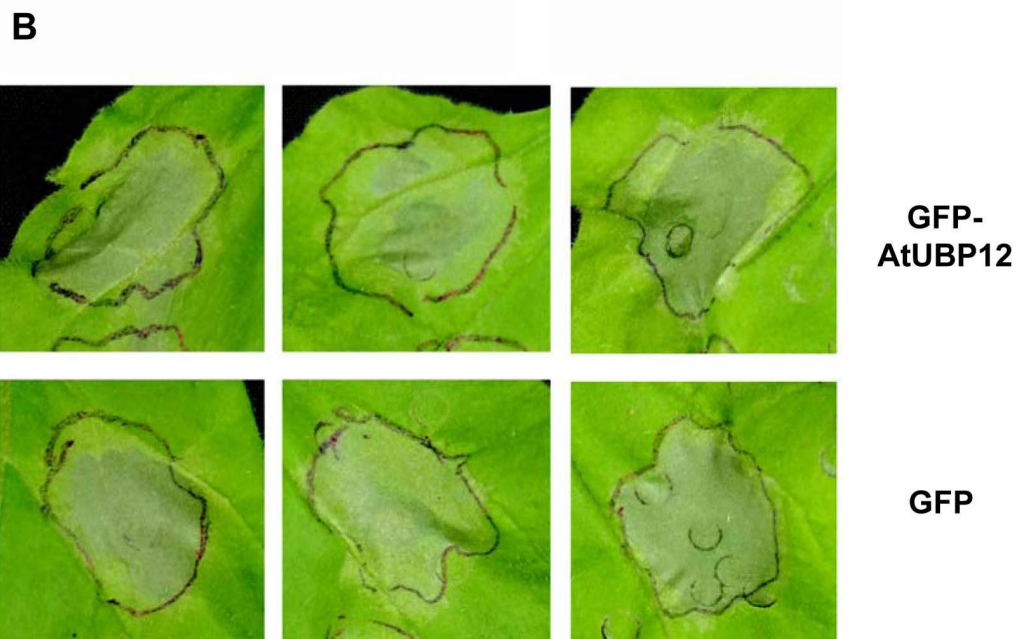
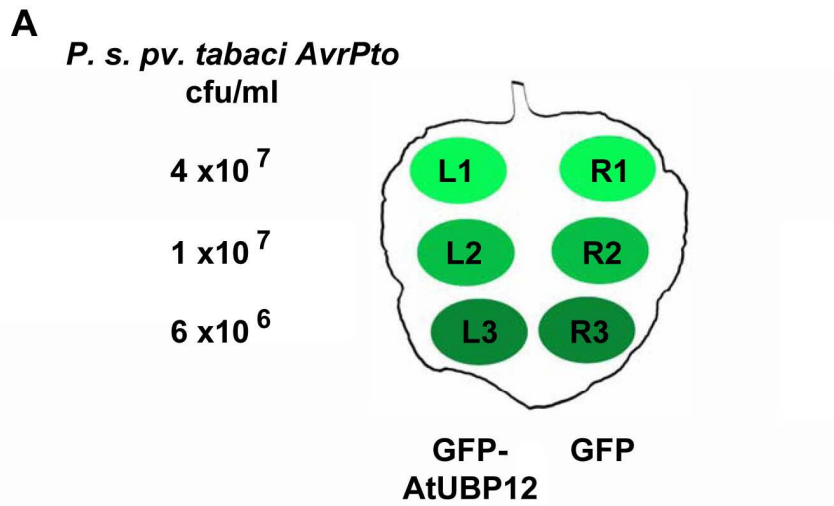
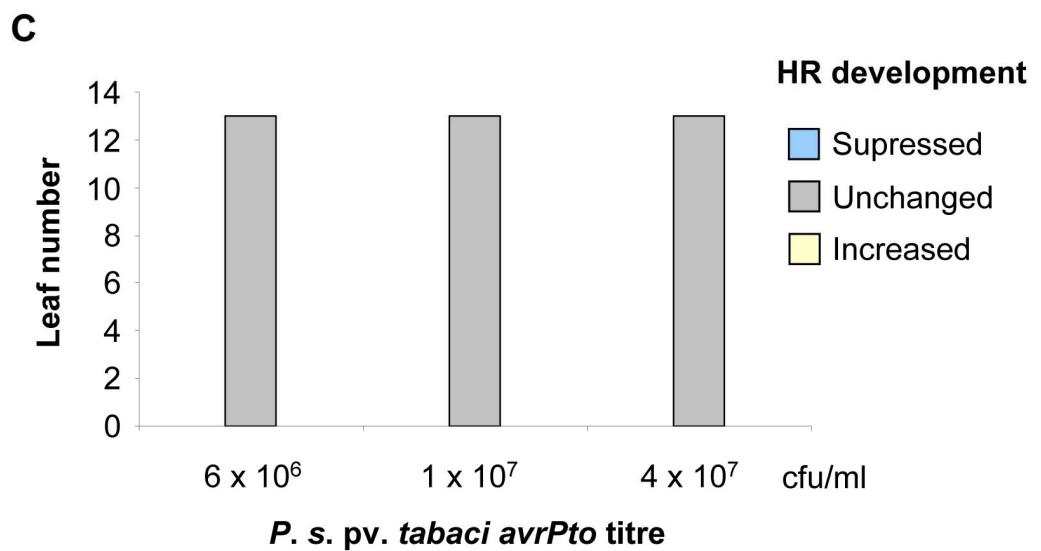
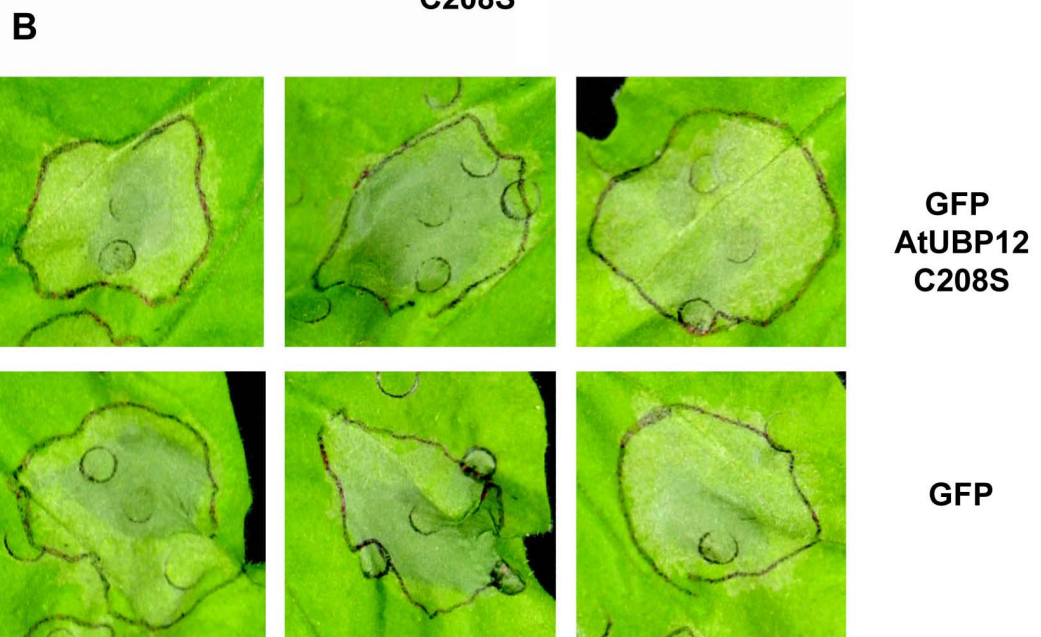
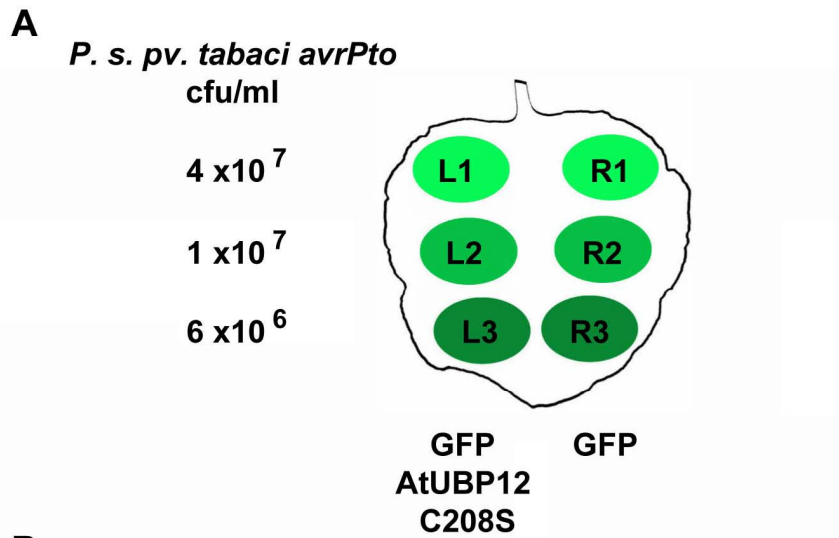


**Figure 6.9** Overexpression of AtUBP12 C208S in 35S *Pto*  
*N. benthamiana* does not effect *avrPto/Pto* elicited HR.

(A) Agroinoculation and *P. s. pv. tabaci avrPto* infiltration scheme in 35S *Pto* *N. benthamiana* leaves. 35S GFP-AtUBP12 C208S and 35S GFP constructs were agroinoculated at OD<sub>600</sub> 0.5 into left and right leaf halves respectively. Two days after agroinoculation, *P. s. pv. tabaci avrPto* infiltration patches were made on each leaf half at  $4 \times 10^7$  (L1 and R1),  $1 \times 10^7$  (L2 and R2) and  $6 \times 10^6$  (L3 and R3) cfu/ml respectively.

(B) HR development in 35S *Pto* *N. benthamiana* leaves overexpressing GFP-AtUBP12 C208S (upper panels) and GFP (lower panels) following infiltration of *P. s. pv. tabaci avrPto* at  $1 \times 10^7$  cfu/ml. Pictures taken four days after *P. s. pv. tabaci avrPto* infiltration.

(C) *avrPto* elicited HR cell death assay during GFP-AtUBP12 C208S overexpression. Extent of cell death in GFP-AtUBP12 C208S overexpressing sections was scored against the corresponding GFP overexpressing control sections four days after infiltration of *P. s. pv. tabaci avrPto* at  $4 \times 10^7$ ,  $1 \times 10^7$  and  $6 \times 10^6$  cfu/ml respectively.



Transient overexpression of GFP-AtUBP12 fusion proteins conferred no detectable alteration in the development *avrPto/Pto* triggered HR. The results of these experiments suggest that UB12 activity is either not required or not rate limiting in the cell death component of *avrPto/Pto* triggered HR.

Initial experiments established that coinfiltration of the P19 silencing suppressor could exert a significant improvement in the transient expression of GFP-AtUBP12 with an approximate 50 fold increase in expression at 3 days post infiltration (Figure 6.6). Transient overexpression of GFP-AtUBP12 and GFP-AtUBP12 C208S fusion proteins with P19 was conducted in 11 and 12 independent leaves of 35S *Pto N. benthamiana* respectively (Figures 6.11 and 6.12). Expression of GFP-AtUBP12 fusion proteins was analysed in duplicate 3 days after P19/GFP-AtUBP construct agroinoculation by western blotting with anti-GFP antibodies (Figure 6.10). As expected, elevated expression of GFP-AtUBP12 (Figure 6.10 A) and GFP-AtUBP12 C208S (Figure 6.10 B) proteins was detected when compared to previous experiments without P19 coinfiltration (Figure 6.7).

Potential side effects of P19 expression on the *Pto* triggered HR were also investigated. HR was induced by inoculation of three *P. s. pv tabaci avrPto* titres (as previously described) on 35S *Pto N. benthamiana* leaves three days after agroinoculation of either GFP alone or GFP and P19 constructs (data not shown). Results indicated that expression of P19 did not alter the development of *Pto* triggered hypersensitive cell death (data not shown). Three days after P19/GFP-AtUBP12 construct agroinoculation, HR was induced by patch inoculation with three *P. s. pv. tabaci avrPto* titres as previously described (Figure 6.11 A) in 11 independent 35S *Pto N. benthamiana* leaves. Analysis of resulting HR indicated no alteration in the development cell death at any of the inoculated bacterial titres relative to GFP controls (Figure 6.11 B and C). Equivalent transient assays were conducted with active site mutant GFP-AtUBP C208S and GFP in 12 leaves (Figure 6.9). Similar results were observed and analysis of resultant the HR indicated no alteration in the development of cell death relative to GFP controls (Figure 6.12 B and C).

**Figure 6.10** Transient overexpression GFP-AtUBP12 and GFP-AtUBP12 C208S with P19 coinfiltration in *N. benthamiana*.

Western blot analysis of total protein extract (50 µg) from *N. benthamiana* leaves two days after agroinoculation of 35S GFP-AtUBP12 (**A**) or 35S GFP-AtUBP12 C208S (**B**) constructs with corresponding 35S GFP controls at OD<sub>600</sub> 0.5 and coinfiltration of P19 silencing suppressor. Samples were analysed in duplicate and western blots were probed with anti-GFP antibody. Upper and lower panels of film images represent different exposure times of a single western blot. Upper panel represents long exposure (2 minutes in **A** and 3 minutes in **B**) and lower panel represents short exposure (10 seconds). Ponceau stain of rubisco large subunit (rbcl) was used as a loading control.

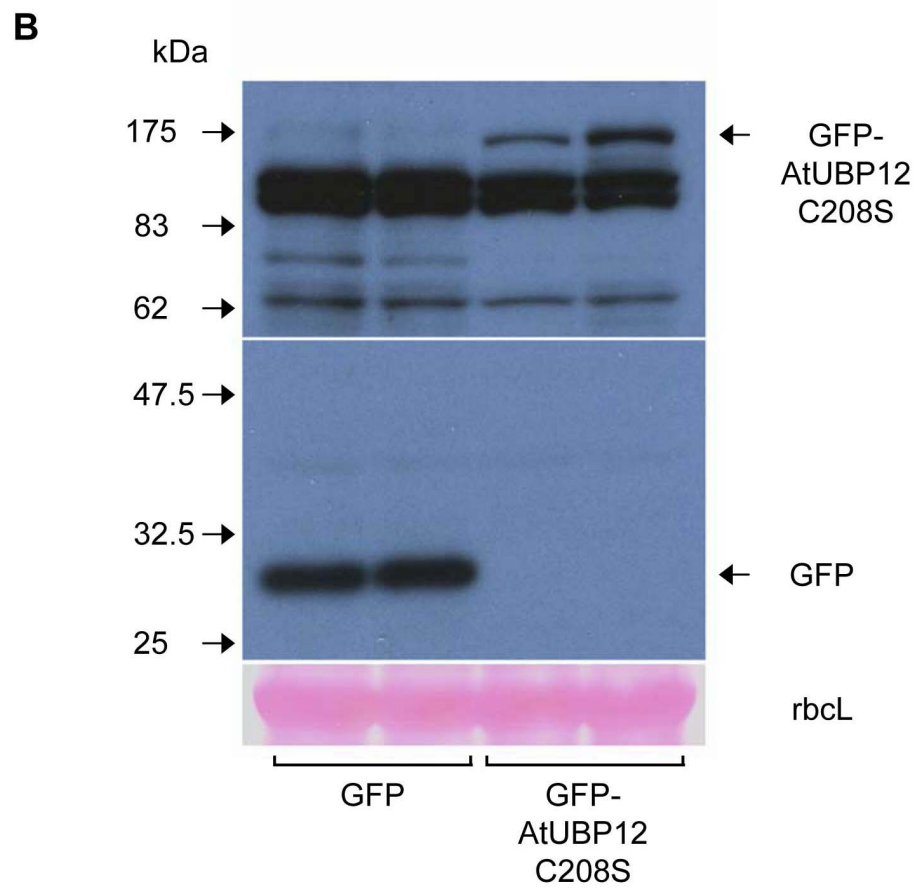
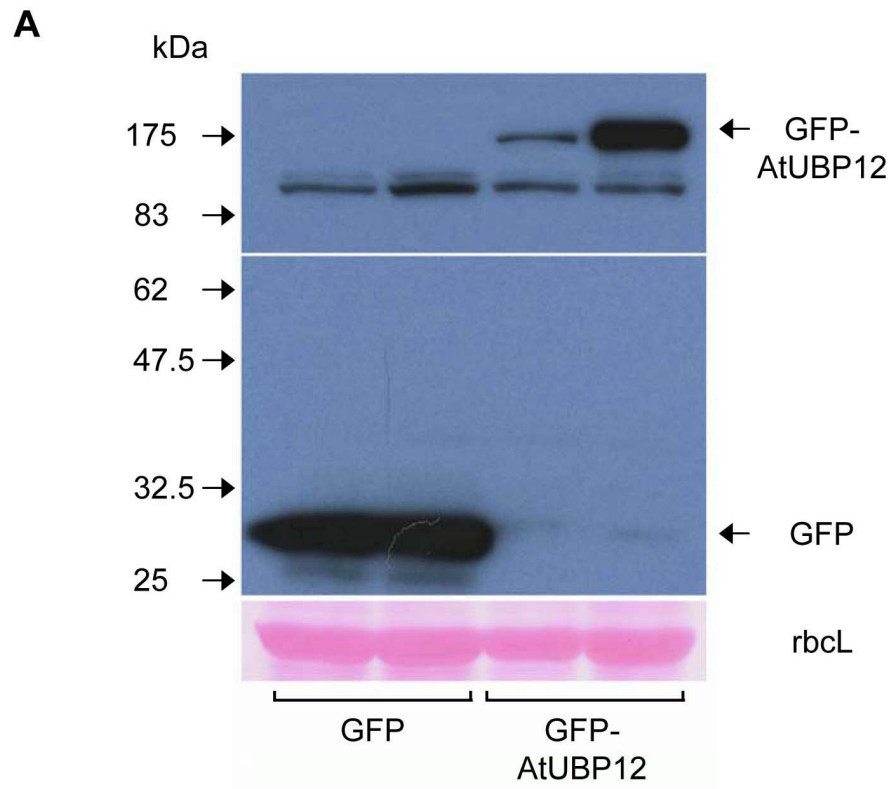


**Figure 6.11** P19 enhanced transient overexpression of AtUBP12 in 35S

*Pto N. benthamiana* does not effect *avrPto/Pto* elicited HR.

(A) Agroinoculation and *P. s. pv. tabaci avrPto* infiltration scheme in 35S *Pto N. benthamiana* leaves. 35S AtUBP12 and 35S GFP constructs were agroinoculated at OD<sub>600</sub> 0.5 into left and right leaf halves respectively with coinfiltration of P19. Two days after agroinoculation, *P. s. pv. tabaci avrPto* infiltration patches were made on each leaf half at  $4 \times 10^7$  (L1 and R1),  $1 \times 10^7$  (L2 and R2) and  $6 \times 10^6$  (L3 and R3) cfu/ml respectively.

(B) HR development in 35S *Pto N. benthamiana* leaves overexpressing GFP-AtUBP12 (upper panels) and GFP (lower panels) following infiltration of *P. s. pv. tabaci avrPto* at  $1 \times 10^7$  cfu/ml. Pictures taken four days after *P. s. pv. tabaci avrPto* infiltration.

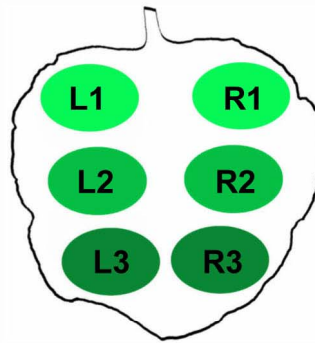
(C) *avrPto* elicited HR cell death assay during GFP-AtUBP12 overexpression. Extent of cell death in GFP-AtUBP12 overexpressing sections was scored against the corresponding GFP overexpressing control sections four days after infiltration of *P. s. pv. tabaci avrPto* at  $4 \times 10^7$ ,  $1 \times 10^7$  and  $6 \times 10^6$  cfu/ml respectively.

**A** *P. s. pv. tabaci avrPto*  
cfu/ml

$4 \times 10^7$

$1 \times 10^7$

$6 \times 10^6$



GFP  
AtUBP12  
+p19

GFP  
+p19

**B**



GFP  
AtUBP12  
+p19



GFP  
+p19

**C**

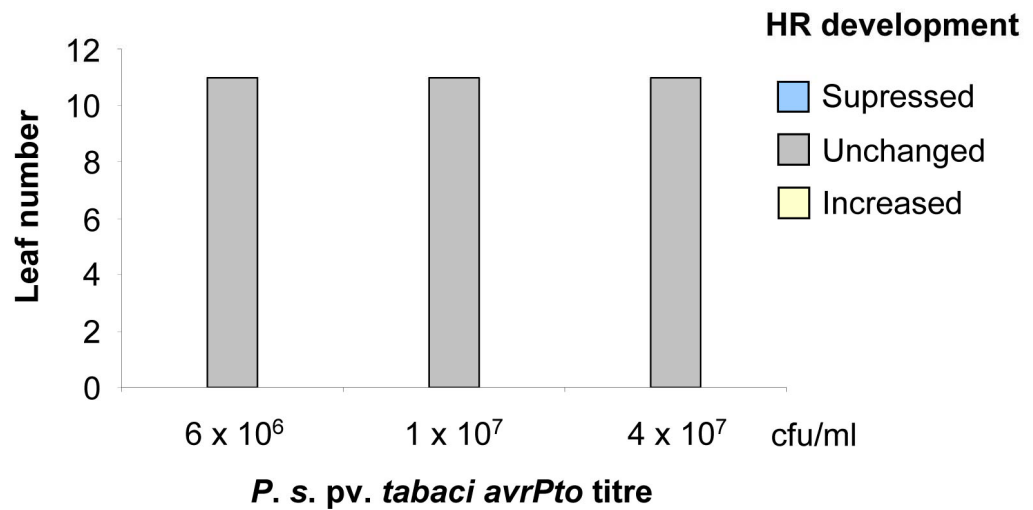
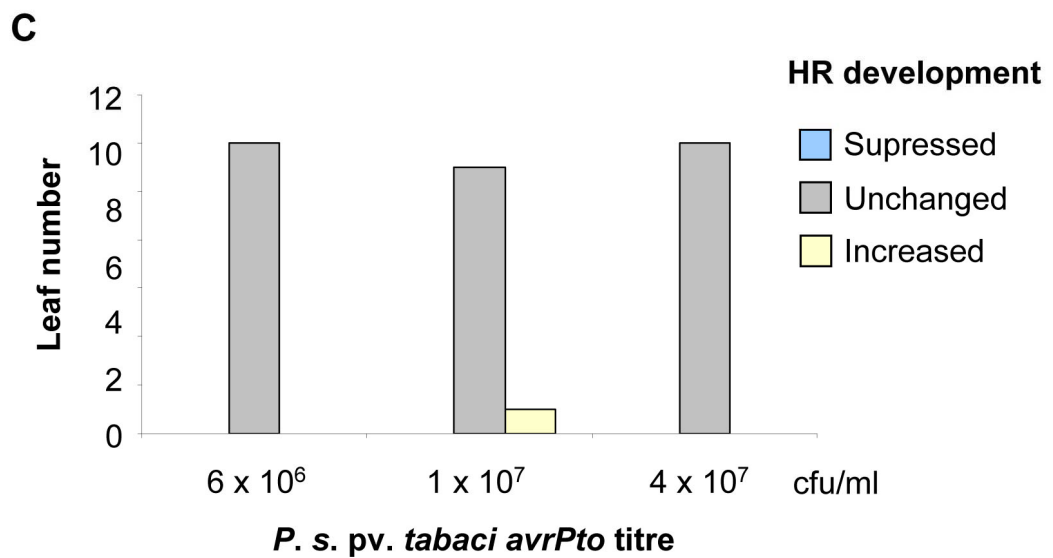
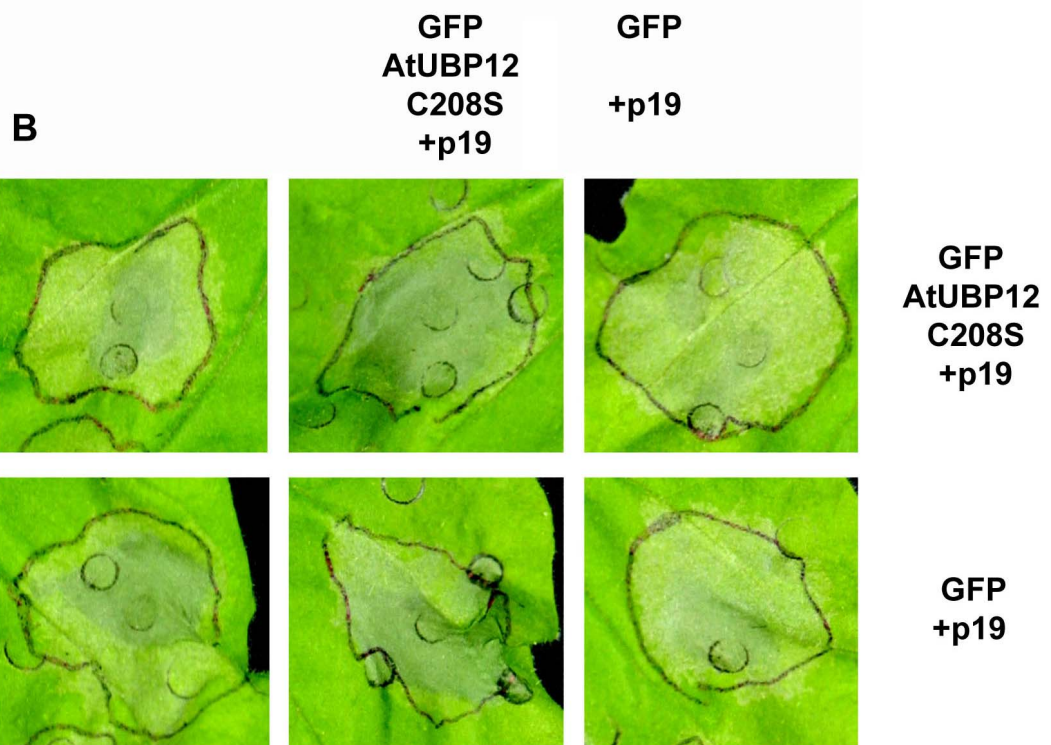
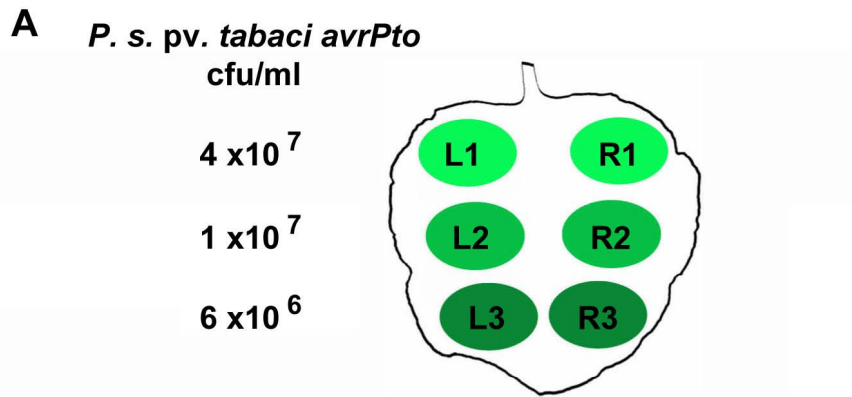


**Figure 6.12** P19 enhanced transient overexpression of AtUBP12 C208S in 35S *Pto N. benthamiana* does not effect *avrPto*/*Pto* elicited HR

(A) Agroinoculation and *P. s. pv. tabaci avrPto* infiltration scheme in 35S *Pto N. benthamiana* leaves. 35S AtUBP12 C208S and 35S GFP constructs were agroinoculated at OD<sub>600</sub> 0.5 into left and right leaf halves respectively with coinfiltration of P19. Two days after agroinoculation, *P. s. pv. tabaci avrPto* infiltration patches were made on each leaf half at  $4 \times 10^7$  (L1 and R1),  $1 \times 10^7$  (L2 and R2) and  $6 \times 10^6$  (L3 and R3) cfu/ml respectively.

(B) HR development in 35S *Pto N. benthamiana* leaves overexpressing GFP-AtUBP12 C208S (upper panels) and GFP (lower panels) following infiltration of *P. s. pv. tabaci avrPto* at  $1 \times 10^7$  cfu/ml. Pictures taken four days after *P. s. pv. tabaci avrPto* infiltration.

(C) *avrPto* elicited HR cell death assay during GFP-AtUBP12 C208S overexpression. Extent of cell death in GFP-AtUBP12 C208S overexpressing sections was scored against the corresponding GFP overexpressing control sections four days after infiltration of *P. s. pv. tabaci avrPto* at  $4 \times 10^7$ ,  $1 \times 10^7$  and  $6 \times 10^6$  cfu/ml respectively.



#### **6.4 Analysis of GFP-AtUBP12 localisation during transient expression by confocal microscopy**

The application of fluorescent proteins as fusion tags allows *in vivo* analysis of many aspects of protein function including: trafficking, turnover, interactions and movement (Sparkes et al., 2006). The subcellular distribution of GFP-AtUBP12 during transient overexpression in *N. benthamiana* was analysed by laser-scanning confocal microscopy to detect GFP fluorescence (Figure 6.13).

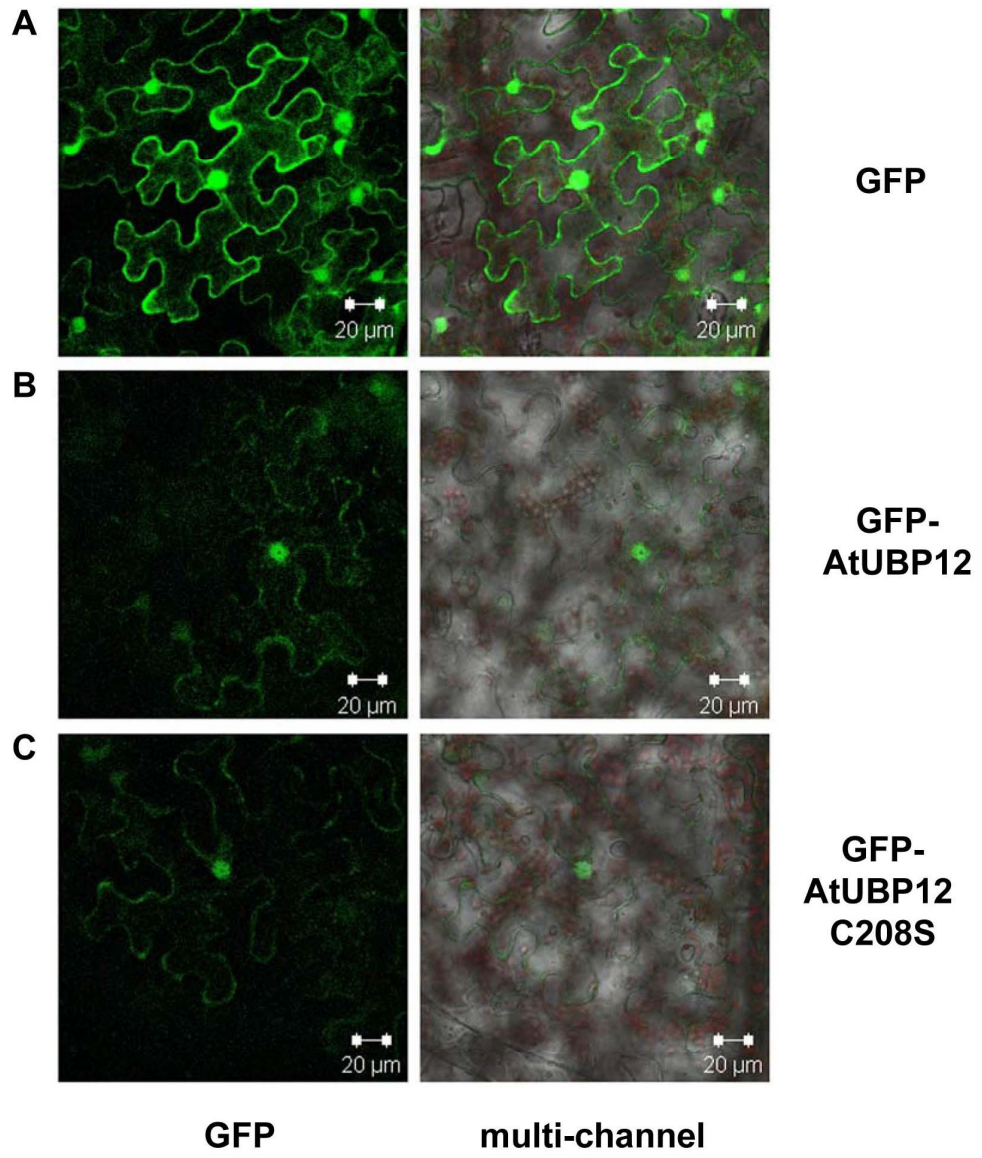
Fusion protein localisation was analysed during the observed peak of transient expression at two days after agroinoculation of GFP-AtUBP12, GFP-AtUBP12 C208S and control GFP constructs without coinfiltration of the P19 silencing suppressor. Confocal analysis detected GFP-AtUBP12 and GFP-AtUBP12 C208S fluorescence in both the nucleus and cytoplasm of all cells examined (Figure 6.13).

The weak transient expression of GFP-AtUBP12 constructs relative to GFP controls seen in western blot analysis (Figure 6.7) was reflected in a correspondingly low GFP signal strength detected during confocal analysis (Figure 6.13). Despite the weak transgene expression, GFP fluorescence was clearly visible in both nuclear and cytoplasmic cell compartments during transient expression of both wildtype and active site mutant GFP-AtUBP12 proteins. Analysis of chloroplast autofluorescence confirmed that weak detection of cytoplasmic GFP signals was genuine and not a cross excitation artefact (Figure 6.13). No difference in distribution was observed by between wildtype and active site mutant GFP-AtUBP12 fusion proteins indicating that ubiquitin protease activity is not required for nuclear localisation (Figure 6.13).

*In silico* analysis of AtUBP12 and NtUBP12 protein sequences using the predictive localisation programs NLSPredict and TargetP indicated no significant likelihood of either sequence being targeted to any specific organelle based on known motifs in the primary sequence.

**Figure 6.14** GFP-AtUBP12 and GFP-AtUBP12 C208S fusion proteins are localised in the cytoplasm and nucleus during transient overexpression in *N. benthamiana*.

Confocal images of GFP fluorescence (left) and composite images of GFP (green) and chloroplast autofluorescence (red) channels (right) during transient overexpression of GFP (**A**), GFP-AtUBP12 (**B**) and GFP-AtUBP12 C208S (**C**). Samples were analysed during the peak of protein expression, two days after agroinoculation of constructs into *N. benthamiana* leaves.



The observed nuclear localisation of 160 kDa GFP-AtUBP12 fusion proteins (Figure 6.13 B and C) is presumably concerted as passive uptake at the nuclear pore complex is typically restricted to proteins smaller than approximately 50 kDa (Poon and Jans, 2005). Conversely, the unfused 27 kDa GFP protein is sufficiently small to enter the nucleus through passive diffusion (Niwa, 2002) and its nucleocytoplasmic localisation pattern reflects this (Figure 6.13 A). During western blot analysis, no GFP-AtUBP12 breakdown products were detected (Figure 6.7) suggesting that the observed nuclear signal results from accumulation of intact full length GFP-AtUBP12 fusions rather than passive diffusion of fragments containing GFP.

Despite lacking clear nuclear localisation signals, GFP-AtUBP12 fusion proteins are detected in the nucleus. This is presumably due to either unmasking/post-translational modification of a cryptic localisation signal (Poon and Jans, 2005) or interaction with nuclear shuttling factors in the cytoplasm (Xu and Massague, 2004). Either of these scenarios imply interaction of the AtUBP12 protein with *N. benthamiana* host components thereby suggesting that AtUBP12 is sufficiently similar to its *N. benthamiana* ortholog to make functional interactions in the cell.

The reported suppression of Cf-9 mediated HR by AtUBP12 overexpression (Section 6.2) provides evidence of the functional conservation between *Arabidopsis* and tobacco UBP12 proteins. The presented localisation data provides further evidence of this conservation, suggesting that AtUBP12 mimics NbUBP12 interactions to be specifically targeted to the nucleus.

The observed localisation data raise further questions regarding the subcellular location of UBP12 proteins in the cell. Transient overexpression of the *Arabidopsis* AtUBP12 protein in the heterologous *N. benthamiana* system from a CaMV 35S promoter represents only an approximation of *in vivo* conditions. Future experiments aim to clarify the subcellular localisation of solanaceous UBP12 proteins using an equivalent GFP tagging and overexpression approach with the *NtUBP12* cDNA sequence determined in this study.

Further issues may arise from the use of the strong CaMV 35S promoter where overexpression of fusion proteins may potentially disrupt their trafficking behaviour (Sparkes et al., 2006). In the case of UBP12 proteins, targeted localisation of NbUBP12 to the nucleus may be constitutive. Elevated levels of introduced GFP-AtUBP12 may saturate the endogenous NbUBP12 cytoplasmic-nuclear trafficking pathway with residual GFP-tagged proteins remaining evident in the cytoplasm. One possible alternative is that UBP12 proteins are targeted to the nucleus at a critical UBP12 concentration threshold in the cytoplasm (providing sensitivity to transcriptional activation of the *UBP12* gene or increased stability of the UBP12 protein), overexpression approaches may potentially obscure such stimuli dependent movements.

Expression of GFP tagged UBP12 fusion proteins from their own promoter may overcome such limitations and provide a potentially more accurate view of their localisation patterns and movements. Identification and cloning of putative promoter elements for solanaceous UBP12 genes will require further RACE PCR based approaches to identify 5' UTR regions owing to the incomplete sequencing of any solanaceous genomes.

Promoter related effects on UBP12 localisation could be investigated more easily in *Arabidopsis* where putative upstream promoter regions have already been identified (Chapter 3 Section 3.3.4). Generation of AtUBP12 GFP fusion constructs containing various truncations of the 5' UTR region could be used for stable transgenic transformation of *Arabidopsis* as a starting point to define the functional *AtUBP12* promoter region. Despite the potential limitations of 35S mediated overexpression, the reported data does indicate that AtUBP12 proteins are specifically rather than passively targeted to the nucleus. The lack of obvious localisation signals suggests that AtUBP12 (and by inference, NbUBP12) interact with other cytoplasmic trafficking regulators to undergo nuclear localisation.

Western blotting experiments confirmed that coinfiltration of the P19 silencing suppressor significantly enhanced transient overexpression of GFP-AtUBP12, indicating that post transcriptional gene silencing was reducing transgene expression efficiency in the absence of P19. Whilst P19

coinfiltration clearly improved transient expression efficiency of GFP-AtUBP12, the correct subcellular localisation of fusion proteins may be disrupted or masked at high overexpression levels (Joelle Mesmar - unpublished data). For this reason, P19 coinfiltration was not used for localisation studies during transient overexpression.

Collectively, silencing and overexpression based approaches report UBP12 associated gain and loss of function phenotypes during Cf-9 triggered HR signalling. Future experiments to investigate changes in the localisation of NtUBP12 or AtUBP12 and AtUBP13 during disease resistance signalling in tobacco and *Arabidopsis* respectively may provide further insight into the regulatory function of these proteins.

## **6.5 Discussion**

### **6.5.1 Overexpression of AtUBP12 suppresses the Cf-9 triggered HR in tobacco**

Results presented in this chapter confirm that solanaceous UBP12 proteins function to stabilise a negative regulator (or regulators) of the Cf-9 triggered HR. Transient overexpression of AtUBP12 proteins in tobacco demonstrates a gain of function HR suppression phenotype that correlates with the loss of function HR promotion phenotype reported during Cf-9 triggered HR in *NbUBP12* silenced plants (Chapter 4).

The reported results indicate a conservation of substrate binding between NtUBP12 and its *Arabidopsis* ortholog AtUBP12 and suggest that overexpression of AtUBP12 leads to hyper-stabilisation of NtUBP12 targets to suppress the Cf-9 triggered HR. Overexpression of the AtUBP12 C208S active site mutant fails to suppress Cf-9 triggered HR, confirming that increased *in vivo* UBP12 activity is the specific cause of suppression. Having subsequently established the full length cDNA sequence of *NtUBP12* (Chapter 4), equivalent wildtype and active site mutant GFP fusion constructs are currently being generated. Future studies aim to recapitulate the observed HR suppression phenotype by overexpressing tobacco rather than *Arabidopsis* UBP12 proteins.

Technical issues relating to the reproducibility of transient assays are frequently caused by environmental variables and differences in the developmental stage of infiltrated leaves (Cazzonelli and Velten, 2006). Issues pertaining to hypo- and hypersensitivity of different aged tobacco leaves to standardised Avr9 peptide concentrations were encountered in this study. Despite the selection of developmentally equivalent leaves, Avr9 elicitor sensitivity issues probably masked the AtUBP12 induced HR suppression in a significant fraction of assays where an unchanged HR result was recorded.

The complementary dominant and dominant negative effects associated with respective overexpression of wildtype and active site mutant GFP-AtUBP12 proteins indicate that steady state levels of its substrate directly regulate Cf-9 triggered HR. Identification of NtUBP12 substrates will be essential to clarify the role of this UBP enzyme during disease resistance signalling. The application of GFP-AtUBP12 overexpression approaches may benefit future attempts to identify such substrates, the quantities of which are presumably elevated by increased *in vivo* UBP12 activity. Biologically relevant substrates of NtUBP12 could potentially be identified using co-immunoprecipitation against the GFP epitope of GFP-AtUBP12 during its transient or stable overexpression in tobacco.

### **6.5.2 Overexpression of AtUBP12 does not alter Pto triggered HR development**

Transient overexpression of AtUBP12 caused no detectable alteration in HR elicited by *avrPto/Pto*. Transient overexpression experiments were conducted both with and without coinfiltration of P19 which is a silencing suppressor that is compatible with *N. benthamiana* (Voinnet et al., 2003).

Whilst absolute levels of GFP-AtUBP12 fusion protein expression showed marked variation between leaves in tobacco, a clear overexpression effect was observed during Cf-9 triggered HR. Phenotypic results seen in tobacco during GFP-AtUBP12 transient overexpression without P19 were considered sufficient evidence to conduct equivalent overexpression assays without P19 during *avrPto/Pto* triggered HR in *N. benthamiana*. The reported data

indicates that AtUBP12 overexpression does not alter *avrPto/Pto* triggered HR following inoculation with weak, intermediate and high strength HR inducing bacterial titres.

P19 was used to achieve significant improvements in AtUBP12 fusion protein expression where coinfiltration of the silencing suppressor caused an approximate 50 fold increase in expression. Whilst the use of P19 to improve transient expression is an established protocol (Voinnet et al., 2003), silencing suppressors may also have unwanted side effects either as avirulence factors (Scholthof et al., 1995) or through binding to endogenous micro RNAs (miRNAs) which regulate gene expression (Silhavy and Burgyan, 2004). Expression of P19 in tobacco is reported to cause HR symptoms (Scholthof et al., 1995) and potentially activates other associated defence pathways. For these reasons, potential effects of P19 alone on *Pto* mediated HR development were investigated and transient overexpression assays were conducted both with and without the P19 silencing suppressor. Despite the marked improvement in GFP-AtUBP12 expression resulting from P19 coinfiltration, no gain of function phenotype was seen during *avrPto/Pto* triggered HR in 35S *PtoN. Benthamiana*.

Collectively, these results are in agreement with those reported for *NbUBP12* loss of function experiments during *avrPto/Pto* triggered HR (Chapter 4) which indicated no clear *avrPto/Pto* induced HR phenotype associated with *NbUBP12* silencing. The reported data suggests that either solanaceous UBP12 proteins are not involved in *avrPto/Pto* triggered defence, or are not rate limiting for the development of *avrPto/Pto* triggered cell death. Alternatively, the level of amino acid similarity between AtUBP12 and NbUBP12 may be insufficient to bind and stabilise relevant *N. benthamiana* substrates during *avrPto/Pto* triggered cell death. As discussed previously in Chapter 4, the reported results support the possibility that solanaceous UBP12 proteins function within selected *R* gene signalling pathways to regulate the HR rather than as downstream mediators of the integrated HR signal.

### **6.5.3 AtUBP12 overexpression approaches prove that solanaceous UBP12 functions as a negative HR regulator**

The transient overexpression approach has successfully demonstrated a GFP-AtUBP12 associated gain of function phenotype in Cf-9 triggered HR. This finding confirms that solanaceous UBP12 proteins stabilise a negative HR regulator (or regulators) and that increased *in vivo* UBP12 activity by GFP-AtUBP12 overexpression can directly influence regulated stability of substrates to alter HR signalling. Similar results would be expected during overexpression of solanaceous UBP12.

Despite post transcriptional silencing effects reducing the efficiency of transgene expression, transiently expressed GFP-AtUBP12 proteins demonstrated a clear nucleocytoplasmic localisation pattern. The large size of GFP-AtUBP12 fusion proteins precludes their passive accumulation in the nucleus suggesting instead that their nuclear targeting is concerted. As neither AtUBP12 or NtUBP12 contain known nuclear localisation signals, the nuclear targeting of GFP-AtUBP12 presumably requires interaction with host trafficking machinery. This predicted interaction suggests functional conservation between AtUBP12 and NtUBP12 proteins and that NtUBP12 may also undergo nuclear targeting.

The most plausible interpretation of reported localisation data is that during overexpression, GFP-AtUBP12 is able to functionally mimic solanaceous host UBP12 proteins to stabilise negative HR regulators in the nucleus thus causing the observed suppression of Cf-9 triggered HR. The functional relevance of UBP12 nuclear localisation could be investigated using an engineered nuclear export signal (NES) (Stacey et al., 1999) within the GFP-AtUBP12 fusion protein. By using a GFP-AtUBP12-NES fusion protein in the described transient overexpression system, the functional consequences of nuclear exclusion on the Cf-9 triggered HR suppression phenotype could be investigated.

## Chapter 7 – Final Discussion

### 7.1 Introduction

Signalling by ubiquitination is implicated in diverse aspects of plant physiology and enzymes of ubiquitin metabolism are overrepresented in the *Arabidopsis* genome compared to other model eukaryotes (Vierstra, 2003). It is now established that deubiquitinating (DUB) enzymes, which reverse the process of ubiquitination, can potentially confer regulatory outcomes in many signalling pathways with which ubiquitination has been associated (Nijman et al., 2005). This primary aim of this study was to contribute to existing knowledge of plant DUB enzymes using molecular genetic approaches.

Data reported in this study updates the existing knowledge of plant DUB enzyme families having identified several novel putative plant DUBS using sequence data from animal genomes. Preliminary pathogen associated gene induction data invited the further characterisation of two closely related *Arabidopsis* DUB enzymes: AtUBP12 and AtUBP13. Various loss of function approaches were taken to study AtUBP12 and AtUBP13 which established that AtUBP12 specifically regulates the transition to flowering but that AtUBP12 and AtUBP13 also function redundantly to regulate plant development.

The solanaceous AtUBP12 ortholog NtUBP12 was identified and transient loss and gain of function approaches were employed to examine its role in disease resistance signalling. Using gene silencing and transient overexpression demonstrated that solanaceous UBPs function as negative regulators of the Cf-9 triggered HR and also influence TMV resistance.

In this final discussion, consideration is given as to how the plant UBPs may function in distinct signalling pathways, what the key results of this study contribute to existing knowledge of regulatory deubiquitination and how existing knowledge of eukaryotic UBPs may be of relevance to future studies.

## 7.2 AtUBP12 and AtUBP13 regulate multiple pathways

Results presented in this study indicate that AtUBP12 has orthologs in other model eukaryotes and belongs to a subset of UBP enzymes that are eukaryotic rather than plant specific deubiquitinating enzymes (Yan et al., 2000a). Phylogenetic analysis confirmed paralogy between AtUBP12 and AtUBP13 and synteny analysis conducted by Blanc *et al.* suggests that *AtUBP13* was part of a larger DNA region that arose from segmental chromosome duplication in a recent *Arabidopsis* ancestor (Blanc et al., 2003).

Gene induction experiments conducted in this study indicated that both *AtUBP12* and *AtUBP13* are transcriptionally activated by avirulent *Pseudomonas* expressing *avrB* and exogenously applied SA. The pathogen inducibility of *AtUBP12* and *AtUBP13* is contrary to the reported suppression of their *N. benthamiana* ortholog *NbUBP12* during HR induced by avirulent *Pseudomonas* (Kim et al., 2006). However, the lack of multiple time point samples in HR induction experiments described by Kim *et al.* (Kim et al., 2006) may limit the value of such comparisons. Tobacco *NtUBP12* transcript levels were also suppressed in the later stages of the Avr9 elicited HR.

The apparent inconsistency between defence associated induction of *Arabidopsis AtUBP12/AtUBP13* and suppression of tobacco *NtUBP12* may be a result of different signalling requirements between *avrB* and Cf-9 mediated HR or the timing and extent of the induced HR. The principle difference between the experimental HR induction systems in *Arabidopsis* and tobacco was the use of an intact pathogen (*Pseudomonas syringae*) versus a purified HR elicitor (Avr9 from *Cladisporium fulvum*). One possible explanation may be that additional *Pst* effectors actually activate *AtUBP12/AtUBP13* induction to promote HR suppression and pathogen virulence. On this basis, *NtUBP12* suppression may reflect the reduced requirement for negative HR regulation by *NtUBP12* during cell death development. Whilst the respective timecourse studies examined similar timepoints during HR induction, differences in the actual timing

and magnitude of HR may explain the observed differences in transcriptional behaviour between *AtUBP12/AtUBP13* and *NtUBP12*.

Based on their close evolutionary relationship, similar patterns of induction and conserved 5' UTR regions it appears that *AtUBP13* has retained the stimuli response characteristics of *AtUBP12*. Despite this, no significant enrichment of known transcription factor binding sites was detected either upstream of or between each respective gene. These findings do not preclude the possibility that *AtUBP12* and *AtUBP13* are coordinately regulated by uncharacterised transcription factor or chromatin modification effects which may be amenable to future analysis using chromatin immunoprecipitation methods.

Bacterial resistance assays in *ubp12* and *ubp13* mutant lines indicated no alteration in susceptibility to virulent and avirulent *Pseudomonas* strains. This outcome may indicate that neither *AtUBP12* or *AtUBP13* regulate bacterial resistance or that functional redundancy between the two proteins is obscuring potential loss of function phenotypes. The latter possibility is supported by the finding that transient overexpression of *AtUBP12* in the heterologous tobacco system suppresses the HR induced by the *C. fulvum* avirulence factor Avr9. The ability of *AtUBP12* to function in a transgenomic functional assay suggests that is a conserved signalling component of plant disease resistance and that overexpression of either *AtUBP12* or *AtUBP13* in *Arabidopsis* may also yield novel HR associated phenotypes. Corresponding transgenic *Arabidopsis AtUBP12* overexpression lines are currently being isolated for this purpose.

The developmental phenotypes observed in *Arabidopsis AtUBP12* and *AtUBP13* T<sub>1</sub> co-silencing and *ubp12 ubp13* T<sub>4</sub> double mutant lines clearly indicate that both proteins stabilise common targets and sets a precedent for their potential redundancy in other signalling pathways. Chromosome duplication events have shaped the *Arabidopsis* genome extensively (Blanc et al., 2003) and frequently result in masking of potential phenotypes due to genetic redundancy between closely related genes such as *AtUBP12* and *AtUBP13* (Pickett and Meeks-Wagner, 1995).

Attempts to circumvent functional redundancy using stable transgenic *AtUBP12/AtUBP13* RNAi cosuppression lines were compromised by apparent transgene silencing effects in the T<sub>3</sub> generation whereas homozygous *ubp12 ubp13* double mutants exhibit a seedling lethal phenotype. As constitutive abolition of *AtUBP12* and *AtUBP13* results in early developmental arrest, an alternative approach based on inducible RNAi may be applicable to conduct loss of function studies in mature *Arabidopsis* plants. Such studies could be conducted using the dexamethsone inducible HELLSGATE RNAi vector described by Wielopolska *et al.* (Wielopolska *et al.*, 2005) to induce silencing of *AtUBP13* in a *ubp12* mutant background. The generation of such stable lines may be essential to clarify the association of *AtUBP12/AtUBP13* with disease resistance signalling, providing a robust alternative system to the Solanaceae based transient gain and loss of function approaches described in this study.

Robust depletion of *AtUBP12* and *AtUBP13* transcript levels in mature *Arabidopsis* plants may be required to cause altered resistance against *Pseudomonas* and associated disease signalling events may also be subject to redundant regulation by both *AtUBP12* and *AtUBP13*. Based on the SA responsiveness of both *AtUBP12* and *AtUBP13*, future studies aim to investigate alterations in established SA dependent downstream marker gene induction in *ubp12* and *ubp13* mutant lines. Functional redundancy between *AtUBP12* and *AtUBP13* could also potentially obscure such alterations in SA dependent marker gene behaviour thus the described inducible RNAi lines would be beneficial in this application.

### **7.3 *AtUBP12* regulates the floral transition**

Results reported in this study have shown that *ubp12* mutants demonstrate early flowering under long and short days indicating that functional redundancy between *AtUBP12* and *AtUBP13* is not complete. This finding suggests that *AtUBP12* has acquired additional substrate specificity over *AtUBP13* and functions in this context to stabilise a floral suppressor.

As the Vernalisation, Autonomous, Gibberellin and Light-dependent flowering pathways that integrate biological and environmental signals are

well characterised (Mouradov et al., 2002), future studies aim to clarify within which pathway AtUBP12 may function to promote flowering. The prominent effect of *ubp12* mutants on flowering time under short days may be caused by deregulation of photoperiod perception, the gibberellin pathway or reduced activation of the floral repressor FLC (FLOWERING LOCUS C) (Mouradov et al., 2002). The association of AtUBP12 function with established short day early flowering mutants would be a viable line of investigation for future studies. Prevalent short day early flowering phenotypes have previously been described in *elf4* (*early flowering 4*) (McWatters et al., 2007), *esd4* (*early flowering in short days 4*) (Murtas et al., 2003) and *ebs1* (*early bolting in short days 1*) (Pineiro et al., 2003) mutants and approaches described in these studies may also be applicable in the characterisation of *ubp12* mutants.

The association of AtUBP12 function with FLC regulation seems plausible based on the observation of aerial rosettes in *ubp12* mutants. The development of aerial rosettes is observed to occur naturally in the *Arabidopsis* Sy-0 ecotype and has previously been associated with late flowering due to the synergistic activation of FLC by functional *FRI* and *HUA2* alleles in the Sy-0 background (Poduska et al., 2003) (Wang et al., 2007). The possibility that AtUBP12 interacts with FLC based repression of flowering is intriguing as *ubp12* mutants exhibit an FLC gain of function aerial rosette phenotype and an FLC loss of function early flowering phenotype (Wang et al., 2007). The association of AtUBP12 with flowering time established in this study is a novel finding as is the decoupling of late flowering from aerial rosette development seen in short day grown *ubp12* mutants.

#### **7.4 Solanaceous UBP12 proteins regulate the Cf-9 triggered HR and TMV infection**

Virus induced gene silencing (VIGS) was used to circumvent the issues of functional redundancy encountered between AtUBP12 and AtUBP13 to allow reverse genetic study of NbUBP12 function in mature *N. benthamiana*.

Analysis of tobacco EST data suggested the existence of a single copy *NtUBP12* gene, supporting the conclusions of Blanc *et al.* that large scale gene duplication events led to the generation of ancestral *AtUBP12* and *AtUBP13* genes at a point subsequent to the divergence of Solanaceae within the Brassicaceae (Blanc *et al.*, 2003). InParanoid genome analysis indicates that orthologs of *NtUBP12* are also present in other sequenced eukaryotes as single copy genes. This study reports the identification of the novel full length tobacco *NtUBP12* cDNA sequence and the application of VIGS to investigate *NbUBP12* loss of function phenotypes in *N. benthamiana* during disease resistance signalling.

Silencing of *NbUBP12* by VIGS initiated from two distinct *NbUBP12* TRV silencing constructs resulted in the promotion of cell death during Cf-9/Avr9 triggered HR. This novel finding suggests that *NbUBP12* is a negative regulator of the Cf-9 triggered HR which functions to stabilise target proteins that suppress cell death. Complementary gain of function studies based on transient overexpression of *AtUBP12* in tobacco demonstrated a corresponding suppression of cell death during Cf-9 triggered HR indicating that *AtUBP12* and *NtUBP12* activities were interchangeable in this context and may function in a conserved signalling pathway.

*In vitro* biochemical assays demonstrated the genuine ubiquitin protease activity of *S. frugiperda* expressed *AtUBP12* and *NtUBP12* proteins and that corresponding active site mutant proteins were catalytically null. Transient overexpression of the corresponding *AtUBP12* C208S null mutant in tobacco failed to suppress cell death development during Cf-9 triggered HR and conferred a dominant negative effect at reduced Avr9 titres to promote cell death. These observations confirm that increased *in vivo* *UBP12* activity specifically suppresses the Cf-9 triggered HR and that alterations in the steady state level of Solanaceous *UBP12* targets can directly regulate hypersensitive cell death suppression or promotion.

Investigations by our collaborators have established novel results indicating that *NbUBP12* silenced *N. benthamiana* plants exhibit increased TMV

resistance which is independent of the established gene-for-gene resistance conferred by the *N* resistance gene.

Elevated resistance against TMV during *NbUBP12* silencing in wildtype *N. benthamiana* plants lacking the *N* resistance gene suggests that *NbUBP12* may regulate basal defence responses elicited by TMV or directly influence virus movement. Early defence responses due to the perception of the TMV coat protein (CP) have been reported (Allan et al., 2001) and future work aims to determine if the reported phenotypes reflect the perturbation of a single disease resistance pathway or if *NbUBP12* functions to stabilise multiple targets in discrete pathogen signalling responses.

As is the case for the majority of deubiquitinating enzymes, target substrates of the plant UBP12 proteins are currently unknown. The reported data raises the question of whether the Cf-9 and TMV associated phenotypes seen during *NbUBP12* silencing result from the reduced deubiquitination of single or multiple target proteins. The reported data implicates *NbUBP12* in Cf-9 triggered HR but also a HR independent resistance mechanism against TMV, suggesting the possibility that *NbUBP12* regulates distinct pathways to achieve this outcome. However, as discussed previously, it may also be possible that *NbUBP12* functions at a point of overlap between gene-for-gene and basal defence to regulate Cf-9 and TMV associated signalling through a single deubiquitination event.

The presented data reports a novel association between deubiquitination and the plant HR and emphasises the established regulatory involvement of ubiquitination in disease resistance signalling (Dreher and Callis, 2007). Negative HR regulation by UBP12 may oppose positive HR regulation conferred by E3 ubiquitin ligases such as CMPG1 (Gonzalez-Lamothe et al., 2006) and ACRE276 (Yang et al., 2006) to prevent runaway activation of disease resistance.

## **7.5 *NbUBP12* orthologs and their substrates**

The reported phenotypes of *Arabidopsis ubp12* mutants and *ubp12 ubp13* double mutants do suggest stabilisation of distinct substrates that regulate

different signalling pathways. By analogy, the solanaceous UBP12 proteins may also have multiple specificities which regulate distinct signalling events.

As has been previously discussed, UBP12 orthologs have been detected in other eukaryotic genomes including the human protein HAUSP (Herpesvirus-associated Ubiquitin Specific Protease) also termed HsUSP7 (Ubiquitin Specific Protease 7) (Everett et al., 1997). Established functions of the HAUSP protein may have relevance to its plant orthologs in regard to its affinity for multiple biological substrates and its mode of substrate interaction. HAUSP has been extensively characterised and is reported to promote apoptosis through the stabilisation of the major tumour suppressor protein p53 and its cognate E3 ubiquitin ligase MDM2 (Li et al., 2004), binding to substrates through its N-terminal TRAF/MATH domain (Hu et al., 2006). HAUSP is also targeted by Herpes simplex virus and Epstein barr virus (EBV) proteins ICP90 and EBNA1 (Everett et al., 1997) (Holowaty et al., 2003). Stabilisation of the ICP90 transcription factor by HAUSP promotes Herpes genome transcription and is proposed to promote virus infection (Sheng et al., 2006). High affinity binding of EBNA1 to HAUSP outcompetes binding of p53 protein leading to reduced apoptosis and is proposed to promote latent EBV infection by indirectly reducing p53 stability (Saridakis et al., 2005).

Studies of HAUSP set a precedent for the direct functional manipulation of deubiquitinating enzymes during virus infection (Sheng et al., 2006) and establish that NbUBP12 orthologs stabilise multiple targets. By analogy, TMV may directly target NbUBP12 to promote replication or movement between plant cells and the reported resistance phenotype during NbUBP12 silencing may be a consequence of such cooperative interactions rather than a specific increase in viral resistance. The TMV movement protein (MP) has been shown to undergo multiple post-translational modifications including ubiquitination which promotes its proteasomal degradation at a post-replicative stage during virus infection (Reichel and Beachy, 2000). It is possible that NbUBP12 functions to directly oppose ubiquitination of TMV-MP during the early stages of TMV infection and that reduced TMV-MP stability caused by silencing *NbUBP12* causes the reported

reduction of TMV accumulation. Future studies aim to investigate the possible role of NbUBP12 in stabilising the TMV-MP.

Based on the eukaryotic conservation of UBP12 orthologs and the fundamental involvement of HAUSP in apoptosis regulation, it is tempting to speculate that plant UBP12 proteins perform an evolutionarily conserved function to regulate PCD during the Cf-9 triggered HR. The programmed cell death that occurs during the induced plant HR response is thought to be mechanistically similar to apoptosis (Hofius et al., 2007) and numerous plant HR regulators have been identified on the basis of animal orthologs that function to control apoptotic cell death including cathepsin B and the caspase-like vacuolar processing enzymes (Gilroy et al., 2007) (Chichkova et al., 2004).

However, the conservation of UBP12 function between animal and plant kingdoms is not clear based on *in silico* analysis as plant orthologs of the HAUSP substrates p53 and MDM2 are not detected in the *Arabidopsis* genome or solanaceous EST resources. If there is a trans-kingdom conservation of UBP12 substrates then functional equivalence may be retained at the protein structural rather than sequence level. It is also possible that UBP12 proteins may regulate other conserved eukaryotic pathways through the stabilisation of orthologous substrates that have yet to be identified.

Structural analyses of HAUSP conducted by Hu *et al.* established that its MATH/TRAF domain forms a typical eight stranded beta sheet TRAF domain structure but lacks canonical TRAF domain residues in its peptide binding cleft (Hu et al., 2006). On this basis, Hu *et al.* accurately described the HAUSP TRAF domain as TRAF-like and previous studies have established that TRAF-like domains are protein-protein interaction domains of ancient eukaryotic origin which are the likely evolutionary precursors of the classical TRAF domain (Zapata et al., 2001).

Hu *et al.* reported crystal structures of the TRAF-like and ubiquitin protease domains of HAUSP (Figure 7.1) and demonstrated that its substrates: p53, MDM2 and EBNA1 all bind to HAUSP via a substrate binding

groove in the TRAF-like domain (Figure 7.1 B) (Hu et al., 2006). All three HAUSP substrates contain four residue binding motifs of (X/E)-G-(X/G)-S (where X is a polar residue) which were found to make critical hydrogen bond and van der Waals contacts with HAUSP residues DWGF<sup>164-167</sup> in the substrate binding groove (Figure 7.1 B) (Hu et al., 2006).

Whilst sequence analysis does not detect plant orthologs of the HAUSP substrates p53 and MDM2, alignment of the TRAF-like domains from of NbUBP12 and its eukaryotic orthologs (Figure 7.1 C) suggests that the substrate binding mechanism has been conserved. Despite limited overall amino acid conservation in this domain, the HAUSP substrate binding residues DWGF<sup>164-167</sup> are conserved in orthologs from mouse, worm, yeast, *Arabidopsis*, potato, tobacco and rice (Figure 7.1 C). Hu *et al.* propose a functional mechanism for HAUSP whereby four residue motifs in ubiquitinated substrates are coordinated by interactions with DWGF<sup>164-167</sup> in the substrate binding groove of the TRAF-like domain, this coordination allows substrate deubiquitination to occur at the ubiquitin protease domain leading to the stabilisation of HAUSP substrates.

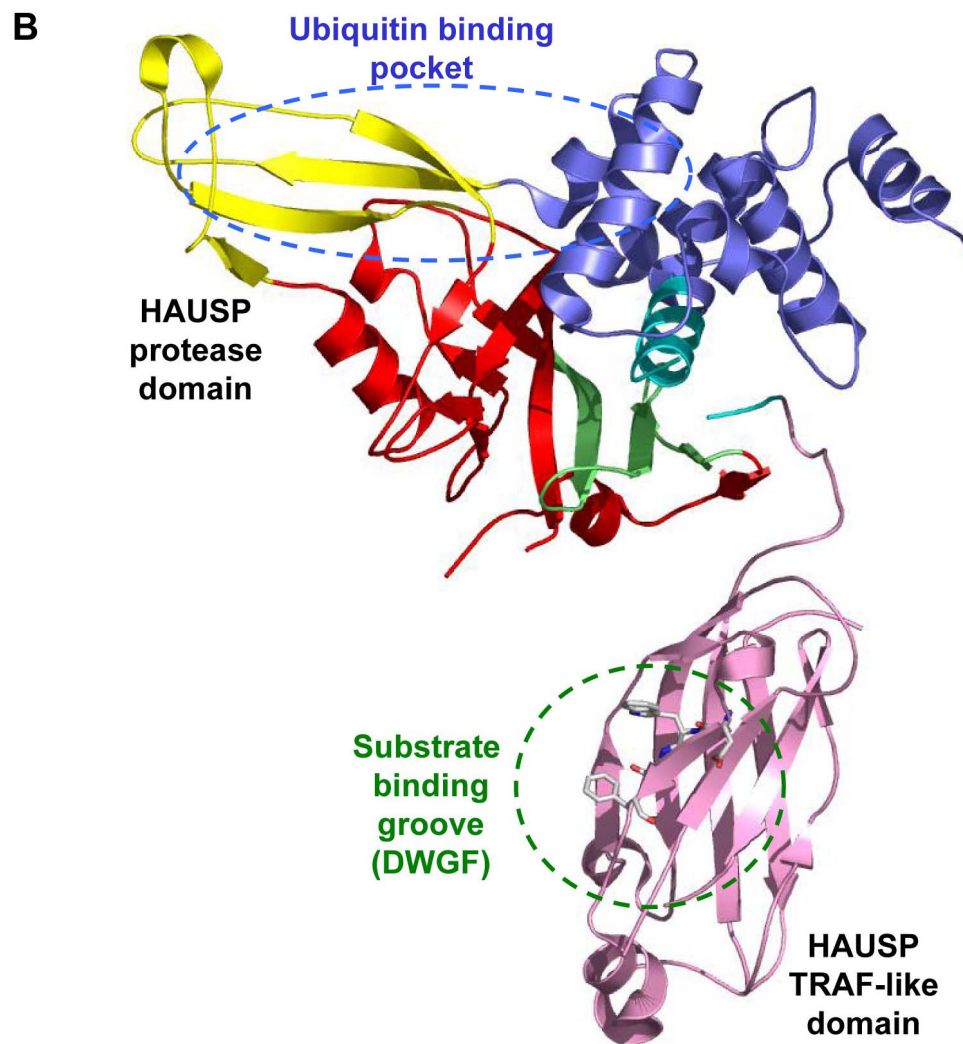
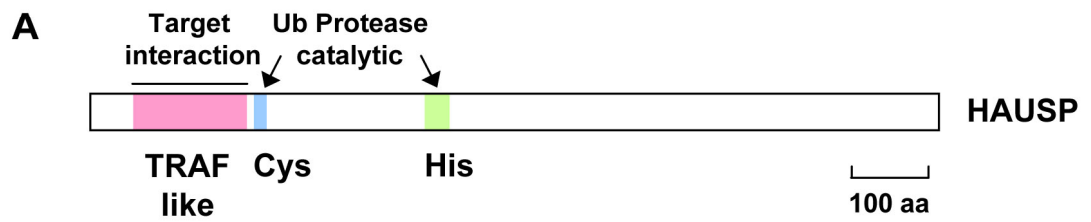
This knowledge may be applicable in future structure-function studies of the plant UBP12 proteins and also benefit attempts to identify their *in vivo* substrates. Mutations in the DWGF motif of plant UBP12 TRAF-like domains would presumably disrupt substrate interactions. Such interaction-null mutant proteins could be examined using *in vivo* transient overexpression gain of function assays during Cf-9 triggered HR in tobacco and *in vitro* deubiquitination assays as described in this study. The reported structure of HAUSP suggests that TRAF-like domain mutations are unlikely to affect the enzymatic activity of ubiquitin protease domain. On this basis, *in vitro* expressed plant UBP12 interaction-null proteins would be expected to retain ubiquitin protease activity against model diubiquitin substrates but fail to reproduce the *in vivo* Cf-9 triggered HR suppression phenotype seen during transient overexpression of wildtype UBP12 proteins. UBP12 interaction-null proteins may also be utilised as a negative control in coimmunoprecipitation experiments to identify the genuine biological targets of plant UBP12 proteins.

**Figure 7.1** Substrate interaction determinants in the TRAF-like domain of HAUSP are conserved in its eukaryotic orthologs.

(A) Domain structure of HAUSP (Herpesvirus-associated Ubiquitin Specific Protease). HAUSP TRAF-like domain and catalytic Cys and His boxes are indicated by pink, blue and green boxes respectively.

(B) Structural model of HAUSP TRAF-like and ubiquitin protease domains produced from 2f1z.pdb and rendered with PyMOL. TRAF-like and ubiquitin protease domains are labelled with respective substrate binding groove and ubiquitin binding pocket and circled in green and blue. TRAF-like domain interacting peptide from HAUSP substrate p53 is represented by grey stick model.

(C) Alignment of TRAF-like domain from eukaryotic HAUSP orthologs. Corresponding protein regions from human HAUSP (GI:1545951) and its orthologs in mouse (MmUSP7 - GI:33334630), worm (CeUSP7 - GI:2414214), yeast (ScUSP15 - GI:798940), *Arabidopsis* (AtUBP12 - AT5G06600), potato (St\_CK6407 - TIGR:CK6407), tobacco (NtUBP12 - GI:FJ264198) and rice (Os\_TC3040 - TIGR:TC3040) were aligned using ClustalX and HAUSP substrate interacting motif DWGF<sup>164-167</sup> is highlighted by coloured residues.



**C**

Hs_HAUSP	DEKSFSSRRISHLFFHKENDWGFSNFMWSEVTDPEK	182
Mm_USP7	DDKSFSSRRISHLFFHEENDWGFSNFMWSEVTDPEK	182
Ce_USP7	--PSIQKKIHHSFHNTQVWGFSDNYDQYDTLCNPKDG	180
Sc_UCH15	DTINL INKSHRFNALDTDWGFANLIDLNNLKHPSRG	193
At_UBP12	TRYTVRKETQHQFNARESDWGFTSFMPPLSELYDPSRG	183
St_CK6407	NKLTVKKDTQHQFNARESDWGFTSFMPPLGELYDPGK	183
Nt_UBP12	NKFTVRKDTQHQFNARESDWGFTSFMPPLSELYDPIRG	183
Os_TC3040	PKYTIKDKDTQHQFNARESDWGFTSFMPPLSDLYDPSRG	183

**TRAF domain**

The conservation of substrate binding residues may also be relevant to future localisation studies of plant UBP12 proteins. A previous study by Zapata *et al.* using HAUSP deletion mutants indicated that the TRAF-like domain of HAUSP was necessary and sufficient for nuclear localisation in human COS7 cells (Zapata et al., 2001). This raises the possibility that HAUSP binds a substrate through its N-terminal TRAF-like domain which facilitates nuclear targeting. Based on these findings, mutation of the substrate binding DWGF motif in the TRAF-like domain would presumably prevent such interactions causing a loss of nuclear localisation. In this study, transiently overexpressed GFP-AtUBP12 showed a nucleocytoplasmic localisation pattern in tobacco epidermal cells despite its lack of canonical nuclear localisation signals. The functional requirement of an intact DWGF motif for nuclear targeting in plant UBP12 proteins could also be tested using the transient assay approach with the GFP tagged UBP12 interaction-null fusion protein.

## 7.6 Conclusions

By undertaking functional characterisation of the *Arabidopsis* UBPs *AtUBP12/AtUBP13* and their solanaceous orthologs, this study has established several novel findings that contribute to existing knowledge of the plant deubiquitinating enzymes.

*AtUBP12* and *AtUBP13* are closely related paralogs that function redundantly to regulate plant development with simultaneous abolition of their respective transcripts causing seedling lethality. Gene induction data suggests that *AtUBP12* and *AtUBP13* may also function to regulate disease resistance. Resistance to bacterial pathogens was not compromised in single *ubp12* and *ubp13* mutant alleles but the reported data suggests that functional redundancy may obscure genuine loss of function phenotypes for these genes.

The reported functional redundancy between *AtUBP12* and *AtUBP13* is not complete with *ubp12* mutants demonstrating an early flowering phenotype. The early flowering of *ubp12* mutants is most prevalent under a short day photoperiod where it is accompanied by the development of

aerial rosettes. The development of aerial rosettes has been previously reported in the *Arabidopsis* Sy-0 ecotype and suggests a potential involvement of AtUBP12 in FLC based floral repression.

Having cloned the novel tobacco *AtUBP12* ortholog *NtUBP12*, UBP12 gain and loss of function studies were conducted in tobacco and *N. benthamiana* respectively during HR cell death assays using VIGS and transient overexpression. These experiments established that UBP12 proteins negatively regulate the HR elicited by the *C. fulvum* fungal elicitor Avr9. Similar studies indicated no alteration to the HR elicited by the bacterial avirulence factor *avrPto*. *NbUBP12* loss of function studies also indicated no alteration in PAMP triggered basal resistance during *P. s. pv tabaci* bacterial growth assays. Our collaborators have established that *NbUBP12* silencing results in reduced TMV accumulation through a mechanism independent of *N* triggered gene-for-gene resistance.

## 7.7 Future work

Future studies aim to recapitulate HR suppression reported during transient *Arabidopsis* AtUBP12 overexpression with the corresponding tobacco NtUBP12 protein. Stable transgenic *Arabidopsis* AtUBP12/AtUBP13 gain of function lines will also be utilised for further analysis of their functions in disease resistance signalling.

Transgenic approaches could also investigate proposed UBP12 interaction-null proteins in localisation and overexpression studies to examine if mutations in the TRAF-like domain disrupt nuclear targeting or disease signalling events. Corresponding AtUBP13 gain of function lines may also be required for future studies as the extent of functional redundancy between AtUBP12 and AtUBP13 is not clear.

Ultimately, transgenic *Arabidopsis* AtUBP12/AtUBP13 loss and gain of function lines could be applied to investigate the role of these genes in a broad range of model plant-pathogen interactions. Established model *Arabidopsis* pathogens include: *Peronospora parasitica* and *Erysiphe cruciferarum* (fungal), Cauliflower Mosaic Virus and Tobacco Mosaic Virus

(viral) and *Pseudomonas syringae* and *Xanthomonas campestris* (bacterial) (Kunkel, 1996). Use of these pathogen systems would allow investigation into whether AtUBP12/AtUBP13 have broad or specific roles in the disease resistance.

Transgenic *AtUBP12* overexpression lines are also being generated in the *ubp12* mutant background to allow complementation of the reported early flowering and aerial rosette phenotypes. Future attempts to characterise the molecular basis of early flowering in *ubp12* mutants will initially focus on deregulation in the behaviour of key floral integrators such as FLC and CO at the transcript and protein level respectively.

Future work aims to more fully characterise the role of NbUBP12 in TMV infection using TMV:GFP resistance assays to quantify the observed phenotypes. The possibility that the reported TMV resistance phenotype results from a direct interaction between the TMV movement protein and NbUBP12 will also be investigated using coimmunoprecipitation approaches.

Putative interactors of AtUBP12 have been identified by yeast two-hybrid analysis (by commercial screening - data not shown) but these interactions have yet to be experimentally verified. Future attempts to identify biological UB12 substrates may utilise knowledge of proposed TRAF-like domain substrate binding residues in combination with immunoprecipitation and yeast two-hybrid approaches to identify interactions that occur specifically during disease resistance signalling events.

## References

- Aarts, N., Metz, M., Holub, E., Staskawicz, B.J., Daniels, M.J., and Parker, J.E. (1998). Different requirements for EDS1 and NDR1 by disease resistance genes define at least two R gene-mediated signaling pathways in Arabidopsis. *Proc Natl Acad Sci U S A* **95**, 10306-10311.
- Abramovitch, R.B., Kim, Y.J., Chen, S., Dickman, M.B., and Martin, G.B. (2003). Pseudomonas type III effector AvrPtoB induces plant disease susceptibility by inhibition of host programmed cell death. *Embo J* **22**, 60-69.
- Alfano, J.R., and Collmer, A. (1996). Bacterial Pathogens in Plants: Life up against the Wall. *Plant Cell* **8**, 1683-1698.
- Allan, A.C., Lapidot, M., Culver, J.N., and Fluhr, R. (2001). An early tobacco mosaic virus-induced oxidative burst in tobacco indicates extracellular perception of the virus coat protein. *Plant Physiol* **126**, 97-108.
- Altenbach, D., and Robatzek, S. (2007). Pattern recognition receptors: from the cell surface to intracellular dynamics. *Mol Plant Microbe Interact* **20**, 1031-1039.
- Altschul, S.F., Madden, T.L., Schaffer, A.A., Zhang, J., Zhang, Z., Miller, W., and Lipman, D.J. (1997). Gapped BLAST and PSI-BLAST: a new generation of protein database search programs. *Nucleic Acids Res* **25**, 3389-3402.
- Alvarez, M.E. (2000). Salicylic acid in the machinery of hypersensitive cell death and disease resistance. *Plant Mol Biol* **44**, 429-442.
- Ambroggio, X., Rees, D., and Deshaies, R. (2004a). JAMM: A metalloprotease-like Zinc Site in the Proteasome and Signalosome. *PLoS Biology* **2**, 113-120.
- Ambroggio, X.I., Rees, D.C., and Deshaies, R.J. (2004b). JAMM: a metalloprotease-like zinc site in the proteasome and signalosome. *PLoS Biol* **2**, E2.
- Amerik, A.Y., and Hochstrasser, M. (2004). Mechanism and function of deubiquitinating enzymes. *Biochim Biophys Acta* **1695**, 189-207.
- Amerik, A.Y., Li, S.J., and Hochstrasser, M. (2000). Analysis of the deubiquitinating enzymes of the yeast *Saccharomyces cerevisiae*. *Biol Chem* **381**, 981-992.
- Asai, T., Tena, G., Plotnikova, J., Willmann, M.R., Chiu, W.L., Gomez-Gomez, L., Boller, T., Ausubel, F.M., and Sheen, J. (2002). MAP kinase signalling cascade in Arabidopsis innate immunity. *Nature* **415**, 977-983.
- Azevedo, C., Sadanandom, A., Kitagawa, K., Freialdenhoven, A., Shirasu, K., and Schulze-Lefert, P. (2002). The RAR1 interactor SGT1, an essential component of R gene-triggered disease resistance. *Science* **295**, 2073-2076.
- Bachmair, A., Becker, F., and Schell, J. (1993). Use of a reporter transgene to generate arabidopsis mutants in ubiquitin-dependent protein degradation. *Proc Natl Acad Sci U S A* **90**, 418-421.
- Bairoch, A., Apweiler, R., Wu, C.H., Barker, W.C., Boeckmann, B., Ferro, S., Gasteiger, E., Huang, H., Lopez, R., Magrane, M., Martin, M.J., Natale, D.A., O'Donovan, C., Redaschi, N., and Yeh, L.S. (2005). The Universal Protein Resource (UniProt). *Nucleic Acids Res* **33**, D154-159.
- Balakirev, M.Y., Tcherniuk, S.O., Jaquinod, M., and Chroboczek, J. (2003). Otubains: a new family of cysteine proteases in the ubiquitin pathway. *EMBO Reports* **4**, 517-525.

- Baneyx, F.** (1999). Recombinant protein expression in *Escherichia coli*. *Curr Opin Biotechnol* **10**, 411-421.
- Baneyx, F., and Mujacic, M.** (2004). Recombinant protein folding and misfolding in *Escherichia coli*. *Nat Biotechnol* **22**, 1399-1408.
- Bastow, R., Mylne, J.S., Lister, C., Lippman, Z., Martienssen, R.A., and Dean, C.** (2004). Vernalization requires epigenetic silencing of FLC by histone methylation. *Nature* **427**, 164-167.
- Baulcombe, D.** (2005). RNA silencing. *Trends Biochem Sci* **30**, 290-293.
- Bendahmane, A., Kanyuka, K., and Baulcombe, D.C.** (1999). The Rx gene from potato controls separate virus resistance and cell death responses. *Plant Cell* **11**, 781-792.
- Bent, A.F., Kunkel, B.N., Dahlbeck, D., Brown, K.L., Schmidt, R., Giraudat, J., Leung, J., and Staskawicz, B.J.** (1994). RPS2 of *Arabidopsis thaliana*: a leucine-rich repeat class of plant disease resistance genes. *Science* **265**, 1856-1860.
- Berger, S.L.** (2001). An embarrassment of niches: the many covalent modifications of histones in transcriptional regulation. *Oncogene* **20**, 3007-3013.
- Blanc, G., Hokamp, K., and Wolfe, K.H.** (2003). A recent polyploidy superimposed on older large-scale duplications in the *Arabidopsis* genome. *Genome Res* **13**, 137-144.
- Blanco, F., Garreton, V., Frey, N., Dominguez, C., Perez-Acle, T., Van der Straeten, D., Jordana, X., and Holuigue, L.** (2005). Identification of NPR1-dependent and independent genes early induced by salicylic acid treatment in *Arabidopsis*. *Plant Mol Biol* **59**, 927-944.
- Bostock, R.M.** (2005). Signal crosstalk and induced resistance: straddling the line between cost and benefit. *Annu Rev Phytopathol* **43**, 545-580.
- Boyes, D.C., Nam, J., and Dangl, J.L.** (1998). The *Arabidopsis thaliana* RPM1 disease resistance gene product is a peripheral plasma membrane protein that is degraded coincident with the hypersensitive response. *Proc Natl Acad Sci U S A* **95**, 15849-15854.
- Brigneti, G., Martin-Hernandez, A.M., Jin, H., Chen, J., Baulcombe, D.C., Baker, B., and Jones, J.D.** (2004). Virus-induced gene silencing in *Solanum* species. *Plant J* **39**, 264-272.
- Burnett, B., Li, F., and Pittman, R.N.** (2003). The polyglutamine neurodegenerative protein ataxin-3 binds polyubiquitinated proteins and has ubiquitin protease activity. *Human Molecular Genetics* **12**, 3195-3205.
- Callis, J., Raasch, J.A., and Vierstra, R.D.** (1990). Ubiquitin extension proteins of *Arabidopsis thaliana*. Structure, localization, and expression of their promoters in transgenic tobacco. *Journal of Biological Chemistry* **265**, 12486-12493.
- Callis, J., Carpenter, T., Sun, C.W., and Vierstra, R.D.** (1995). Structure and evolution of genes encoding polyubiquitin and ubiquitin-like proteins in *Arabidopsis thaliana* ecotype Columbia. *Genetics* **139**, 921-939.
- Capron, A., Okresz, L., and Genschik, P.** (2003). First glance at the plant APC/C, a highly conserved ubiquitin-protein ligase. *Trends in plant science* **8**, 83-90.
- Cardozo, T., and Pagano, M.** (2004). The SCF ubiquitin ligase: insights into a molecular machine. *Nat Rev Mol Cell Biol* **5**, 739-751.
- Cazzonelli, C.I., and Velten, J.** (2006). An in vivo, luciferase-based, *Agrobacterium*-infiltration assay system: implications for post-transcriptional gene silencing. *Planta* **224**, 582-597.

- Chastagner, P., Israel, A., and Brou, C. (2006). Itch/AIP4 mediates Deltex degradation through the formation of K29-linked polyubiquitin chains. *EMBO Rep* **7**, 1147-1153.
- Chau, V., Tobias, J.W., Bachmair, A., Marriott, D., Ecker, D.J., Gonda, D.K., and Varshavsky, A. (1989). A multiubiquitin chain is confined to specific lysine in a targeted short-lived protein. *Science* **243**, 1576-1583.
- Chenna, R., Sugawara, H., Koike, T., Lopez, R., Gibson, T.J., Higgins, D.G., and Thompson, J.D. (2003). Multiple sequence alignment with the Clustal series of programs. *Nucleic Acids Res* **31**, 3497-3500.
- Chichkova, N.V., Kim, S.H., Titova, E.S., Kalkum, M., Morozov, V.S., Rubtsov, Y.P., Kalinina, N.O., Taliansky, M.E., and Vartapetian, A.B. (2004). A plant caspase-like protease activated during the hypersensitive response. *Plant Cell* **16**, 157-171.
- Chisholm, S.T., Coaker, G., Day, B., and Staskawicz, B.J. (2006). Host-microbe interactions: shaping the evolution of the plant immune response. *Cell* **124**, 803-814.
- Cokol, M., Nair, R., and Rost, B. (2000). Finding nuclear localization signals. *EMBO Rep* **1**, 411-415.
- Cope, G.A., Suh, G.S., Aravind, L., Schwarz, S.E., Zipursky, S.L., Koonin, E.V., and Deshaies, R. (2002). Role of Predicted Metalloprotease Motif of Jab1/Csn5 in Cleavage of NEDD8 from CUL1. *Science* **298**.
- Dang, L.C., Melandri, F.D., and Stein, R.L. (1998). Kinetic and mechanistic studies on the hydrolysis of ubiquitin C-terminal 7-amido-4-methylcoumarin by deubiquitinating enzymes. *Biochemistry* **37**, 1868-1879.
- Dangl, J.L., and Jones, J.D. (2001). Plant pathogens and integrated defence responses to infection. *Nature* **411**, 826-833.
- Dangl, J.L., and McDowell, J.M. (2006). Two modes of pathogen recognition by plants. *Proc Natl Acad Sci U S A* **103**, 8575-8576.
- del Pozo, O., Pedley, K.F., and Martin, G.B. (2004). MAPKKKalpha is a positive regulator of cell death associated with both plant immunity and disease. *Embo J* **23**, 3072-3082.
- Delauré, S.L., Hemelrijck, W.V., Bolle, M.F.C.D., Cammue, B.P.A., and Coninck, B.M.A.D. (2008). Building up plant defenses by breaking down proteins *Plant Science* **174**, 375-385.
- Deshaies, R. (1999). SCF and Cullin/Ring H2-based ubiquitin ligases. *Annual Review of Cellular Developmental Biology* **15**, 435-467.
- Devoto, A., Muskett, P.R., and Shirasu, K. (2003). Role of ubiquitination in the regulation of plant defence against pathogens. *Curr Opin Plant Biol* **6**, 307-311.
- Doelling, J.H., Yan, N., Kurepa, J., Walker, J., and Vierstra, R.D. (2001). The ubiquitin-specific protease UBP14 is essential for early embryo development in *Arabidopsis thaliana*. *Plant J* **27**, 393-405.
- Doelling, J.H., Phillips, A.R., Soyler-Ogretim, G., Wise, J., Chandler, J., Callis, J., Otegui, M.S., and Vierstra, R.D. (2007). The ubiquitin-specific protease subfamily UBP3/UBP4 is essential for pollen development and transmission in *Arabidopsis*. *Plant Physiol* **145**, 801-813.
- Dong, C.H., Agarwal, M., Zhang, Y., Xie, Q., and Zhu, J.K. (2006). The negative regulator of plant cold responses, HOS1, is a RING E3 ligase that mediates the ubiquitination and degradation of ICE1. *Proc Natl Acad Sci U S A* **103**, 8281-8286.
- Dong, X. (2004). NPR1, all things considered. *Curr Opin Plant Biol* **7**, 547-552.

- Dong, X., Mindrinos, M., Davis, K.R., and Ausubel, F.M. (1991). Induction of Arabidopsis defense genes by virulent and avirulent *Pseudomonas syringae* strains and by a cloned avirulence gene. *Plant Cell* **3**, 61-72.
- Downes, B.P., Stupar, R.M., Gingerich, D.J., and Vierstra, R.D. (2003). The HECT ubiquitin-protein ligase (UPL) family in *Arabidopsis*: UPL3 has a specific role in trichome development. *The Plant Journal* **35**, 729-742.
- Doyle, M.R., Bizzell, C.M., Keller, M.R., Michaels, S.D., Song, J., Noh, Y.S., and Amasino, R.M. (2005). HUA2 is required for the expression of floral repressors in *Arabidopsis thaliana*. *Plant J* **41**, 376-385.
- Dreher, K., and Callis, J. (2007). Ubiquitin, hormones and biotic stress in plants. *Ann Bot (Lond)* **99**, 787-822.
- Dunand-Sauthier, I., Walker, C., Wilkinson, C., Gordon, C., and Crane, R. (2002). Sum1, a component of the fission yeast eIF3 translation initiation complex, is rapidly relocalised during environmental stress and interacts with components of the 26S proteasome. *Molecular Biology of the Cell* **13**, 1626-1640.
- Durrant, W.E., and Dong, X. (2004). Systemic acquired resistance. *Annu Rev Phytopathol* **42**, 185-209.
- Durrant, W.E., Rowland, O., Piedras, P., Hammond-Kosack, K.E., and Jones, J.D. (2000). cDNA-AFLP reveals a striking overlap in race-specific resistance and wound response gene expression profiles. *Plant Cell* **12**, 963-977.
- Emanuelsson, O., Brunak, S., von Heijne, G., and Nielsen, H. (2007). Locating proteins in the cell using TargetP, SignalP and related tools. *Nat Protoc* **2**, 953-971.
- Erickson, F.L., Dinesh-Kumar, S.P., Holzberg, S., Ustach, C.V., Dutton, M., Handley, V., Corr, C., and Baker, B.J. (1999). Interactions between tobacco mosaic virus and the tobacco N gene. *Philos Trans R Soc Lond B Biol Sci* **354**, 653-658.
- Evans, P.C., Smith, T.S., Lai, M.J., Williams, M.G., Burke, D.F., Heyninck, K., Kreike, M.M., Beyaert, R., Blundell, T.L., and Kilshaw, P.J. (2003). A novel type of deubiquitinating enzyme. *J Biol Chem* **278**, 23180-23186.
- Everett, R.D., Meredith, M., Orr, A., Cross, A., Katoria, M., and Parkinson, J. (1997). A novel ubiquitin-specific protease is dynamically associated with the PML nuclear domain and binds to a herpesvirus regulatory protein. *Embo J* **16**, 1519-1530.
- Finley, D., and Varshavsky, A. (1985). The ubiquitin system: functions and mechanisms. *Trends in Biochemical Sciences* **10**, 343-346.
- Finley, D., and Chau, V. (1991). Ubiquitination. *Annu Rev Cell Biol* **7**, 25-69.
- Finn, R.D., Mistry, J., Schuster-Bockler, B., Griffiths-Jones, S., Hollich, V., Lassmann, T., Moxon, S., Marshall, M., Khanna, A., Durbin, R., Eddy, S.R., Sonnhammer, E.L., and Bateman, A. (2006). Pfam: clans, web tools and services. *Nucleic Acids Res* **34**, D247-251.
- Freemont, P.S. (2000). Ubiquitination: RING for destruction? *Current Biology* **10**, R84-R87.
- Fu, H., Reis, N., Lee, Y., Glickman, M., and Vierstra, R.D. (2001). Subunit interaction maps for the regulatory particle of the 26S proteasome and the COP9 signalosome. *EMBO Journal* **20**, 7096-7107.
- Fujiwara, S., Wang, L., Han, L., Suh, S.S., Salome, P.A., McClung, C.R., and Somers, D.E. (2008). Post-translational Regulation of the Arabidopsis Circadian Clock through Selective Proteolysis and Phosphorylation of Pseudo-response Regulator Proteins. *J Biol Chem* **283**, 23073-23083.

- Fushman, D., and Pickart, C.M. (2004). Polyubiquitin chains: polymeric protein signals. *Current Opinion in Chemical Biology* **8**, 610-616.
- Gagne, J.M., Downes, B.P., Shiu, S., Durski, A.M., and Vierstra, R.D. (2002). The F-Box subunit of the SCF E3 complex is encoded by a diverse superfamily of genes in *Arabidopsis*. *PNAS* **99**, 11519-11524.
- Gassmann, W., Hinsch, M.E., and Staskawicz, B.J. (1999). The *Arabidopsis* RPS4 bacterial-resistance gene is a member of the TIR-NBS-LRR family of disease-resistance genes. *Plant J* **20**, 265-277.
- Gilroy, E.M., Hein, I., van der Hoorn, R., Boevink, P.C., Venter, E., McLellan, H., Kaffarnik, F., Hrubikova, K., Shaw, J., Holeva, M., Lopez, E.C., Borrás-Hidalgo, O., Pritchard, L., Loake, G.J., Lacomme, C., and Birch, P.R. (2007). Involvement of cathepsin B in the plant disease resistance hypersensitive response. *Plant J* **52**, 1-13.
- Glazebrook, J. (2005). Contrasting mechanisms of defense against biotrophic and necrotrophic pathogens. *Annu Rev Phytopathol* **43**, 205-227.
- Glickman, M., Rubin, D., Coux, O., Wefes, I., Pfeifer, G., Cjeka, Z., Baumeister, W., Fried, V., and Finely, D. (1998). A Subcomplex of the Proteasome Regulatory Particle Required for Ubiquitin-Conjugate Degradation and Related to the COP9-Signalosome and eIF3. *Cell* **94**, 615-623.
- Gonzalez-Lamothe, R., Tsitsigiannis, D.I., Ludwig, A.A., Panicot, M., Shirasu, K., and Jones, J.D. (2006). The U-box protein CMPG1 is required for efficient activation of defense mechanisms triggered by multiple resistance genes in tobacco and tomato. *Plant Cell* **18**, 1067-1083.
- Gooding, G.V., and Herbert, T.T. (1967). A simple technique for purification of TMV in larger quantities. *Phytopathology* **57**, 1285.
- Gottesman, S., and Maurizi, M. (1992). Regulation by proteolysis: energy dependent proteases and their targets. *Microbiology Review* **56**, 592-621.
- Grant, M.R., Godiard, L., Straube, E., Ashfield, T., Lewald, J., Sattler, A., Innes, R.W., and Dangl, J.L. (1995). Structure of the *Arabidopsis* RPM1 gene enabling dual specificity disease resistance. *Science* **269**, 843-846.
- Gray, W.M., Muskett, P.R., Chuang, H.W., and Parker, J.E. (2003). *Arabidopsis* SGT1b is required for SCF(TIR1)-mediated auxin response. *Plant Cell* **15**, 1310-1319.
- Gu, Z., Steinmetz, L.M., Gu, X., Scharfe, C., Davis, R.W., and Li, W.H. (2003). Role of duplicate genes in genetic robustness against null mutations. *Nature* **421**, 63-66.
- Gusmaroli, G., Figueroa, P., Serino, G., and Deng, X.W. (2007). Role of the MPN subunits in COP9 signalosome assembly and activity, and their regulatory interaction with *Arabidopsis* Cullin3-based E3 ligases. *Plant Cell* **19**, 564-581.
- Haas, B.J., Delcher, A.L., Wortman, J.R., and Salzberg, S.L. (2004). DAGchainer: a tool for mining segmental genome duplications and synteny. *Bioinformatics* **20**, 3643-3646.
- Hamilton, K.S., Ellison, M.J., Barber, K.R., Williams, R., and Huzil, J. (2001). Structure of a conjugating enzyme-ubiquitin thiolester intermediate reveals a novel role for the ubiquitin tail. *Structure* **9**.
- Hammond-Kosack, K.E., Tang, S., Harrison, K., and Jones, J.D. (1998). The tomato Cf-9 disease resistance gene functions in tobacco and potato to confer responsiveness to the fungal avirulence gene product avr 9. *Plant Cell* **10**, 1251-1266.
- Hartmann-Petersen, R., and Gordon, C. (2004). Protein Degradation: Recognition of Ubiquitylated Substrates. *Current Biology* **14**, R754-R756.

- Hartmann-Petersen, R., Seeger, M., and Gordon, C. (2003). Transferring substrates to the 26S proteasome. *Trends in Biochemical Sciences* **28**, 26-31.
- Hatfield, P.M., Gosink, M.M., Carptenter, T.B., and Vierstra, R.D. (1997). The ubiquitin activating (E1) gene family in *Arabidopsis thaliana*. *Plant Journal* **11**, 213-226.
- He, Y., and Amasino, R.M. (2005). Role of chromatin modification in flowering-time control. *Trends Plant Sci* **10**, 30-35.
- He, Y., Michaels, S.D., and Amasino, R.M. (2003). Regulation of flowering time by histone acetylation in *Arabidopsis*. *Science* **302**, 1751-1754.
- Hellens, R.P., Edwards, E.A., Leyland, N.R., Bean, S., and Mullineaux, P.M. (2000). pGreen: a versatile and flexible binary Ti vector for *Agrobacterium*-mediated plant transformation. *Plant Mol Biol* **42**, 819-832.
- Helliwell, C., and Waterhouse, P. (2003). Constructs and methods for high-throughput gene silencing in plants. *Methods* **30**, 289-295.
- Helliwell, C.A., and Waterhouse, P.M. (2005). Constructs and methods for hairpin RNA-mediated gene silencing in plants. *Methods Enzymol* **392**, 24-35.
- Hershko, A., and Ciechanover, A. (1998). The ubiquitin system. *Annu Rev Biochem* **67**, 425-479.
- Hicke, L. (2001a). Protein regulation by monoubiquitin. *Nat Rev Mol Cell Biol* **2**, 195-201.
- Hicke, L. (2001b). Protein regulation by monoubiquitin. *Nature Reviews Molecular Cell Biology* **2**, 195-201.
- Hodis, E., Schreiber, G., Rother, K., and Sussman, J.L. (2007). eMovie: a storyboard-based tool for making molecular movies. *Trends Biochem Sci* **32**, 199-204.
- Hofius, D., Tsitsigiannis, D.I., Jones, J.D., and Mundy, J. (2007). Inducible cell death in plant immunity. *Semin Cancer Biol* **17**, 166-187.
- Holowaty, M.N., Sheng, Y., Nguyen, T., Arrowsmith, C., and Frappier, L. (2003). Protein interaction domains of the ubiquitin-specific protease, USP7/HAUSP. *J Biol Chem* **278**, 47753-47761.
- Hough, R., Pratt, G., and Rechsteiner, M. (1987). Purification of two high molecular weight proteases in rabbit reticulocyte lysate. *Journal of Biological Chemistry* **262**, 8303-8313.
- Hu, F., Doelling, J.H., Arendt, C.S., Hochstrasser, M., and Vierstra, R.D. (1998). Molecular organisation of the 20S proteasome gene family from *Arabidopsis thaliana*. *Genetics* **149**.
- Hu, M., Gu, L., Li, M., Jeffrey, P.D., Gu, W., and Shi, Y. (2006). Structural basis of competitive recognition of p53 and MDM2 by HAUSP/USP7: implications for the regulation of the p53-MDM2 pathway. *PLoS Biol* **4**, e27.
- Hu, M., Li, P., Song, L., Jeffrey, P.D., Chenova, T.A., Wilkinson, K.D., Cohen, R.E., and Shi, Y. (2005). Structure and mechanisms of the proteasome-associated deubiquitinating enzyme USP14. *Embo J* **24**, 3747-3756.
- Hu, M., Li, P., Li, M., Li, W., Yao, T., Wu, J., Gu, W., Cohen, R., and Shi, Y. (2002a). Crystal structure of a UBP-Family Deubiquitinating Enzyme in Isolation and in Complex with Ubiquitin Aldehyde. *Cell* **111**, 1054.
- Hu, M., Li, P., Li, M., Li, W., Yao, T., Wu, J.W., Gu, W., Cohen, R.E., and Shi, Y. (2002b). Crystal structure of a UBP-family deubiquitinating enzyme in isolation and in complex with ubiquitin aldehyde. *Cell* **111**, 1041-1054.

- Huibregtse, J.M., Scheffner, M., Beaudenon, S., and Howley, P.M. (1995). A family of proteins structurally and functionally related to the E6-AP ubiquitin-protein ligase. *PNAS* **94**, 3656-3661.
- Iyer, L.M., Burroughs, A.M., and Aravind, L. (2006). The prokaryotic antecedents of the ubiquitin-signaling system and the early evolution of ubiquitin-like beta-grasp domains. *Genome Biol* **7**, R60.
- Janjusevic, R., Abramovitch, R.B., Martin, G.B., and Stebbins, C.E. (2006). A bacterial inhibitor of host programmed cell death defenses is an E3 ubiquitin ligase. *Science* **311**, 222-226.
- Jentsch, S., and Pyrowolakis, G. (2000). Ubiquitin and its kin: how close are the family ties? *Trends in Cell Biology* **10**, 335-342.
- Johansen, L.K., and Carrington, J.C. (2001). Silencing on the spot. Induction and suppression of RNA silencing in the *Agrobacterium*-mediated transient expression system. *Plant Physiol* **126**, 930-938.
- Jones, D.A., and Takemoto, D. (2004). Plant innate immunity - direct and indirect recognition of general and specific pathogen-associated molecules. *Curr Opin Immunol* **16**, 48-62.
- Jones, J.D., and Dangl, J.L. (2006). The plant immune system. *Nature* **444**, 323-329.
- Kajava, A.V. (1998). Structural diversity of leucine-rich repeat proteins. *J Mol Biol* **277**, 519-527.
- Kang, S.H., Park, J.J., Chung, S.S., Bang, O.S., and Chung, C.H. (2005). Strategies for assaying deubiquitinating enzymes. *Methods Enzymol* **398**, 500-508.
- Katagiri, F. (2004). A global view of defense gene expression regulation--a highly interconnected signaling network. *Curr Opin Plant Biol* **7**, 506-511.
- Katagiri, F., Thilmony, R., and He, S.Y. (2002). The *Arabidopsis thaliana*-*Pseudomonas syringae* Interaction. *The Arabidopsis Book*, 1-35.
- Kawasaki, T., Nam, J., Boyes, D.C., Holt, B.F., 3rd, Hubert, D.A., Wiig, A., and Dangl, J.L. (2005). A duplicated pair of *Arabidopsis* RING-finger E3 ligases contribute to the RPM1- and RPS2-mediated hypersensitive response. *Plant J* **44**, 258-270.
- Kawchuk, L.M., Hachey, J., Lynch, D.R., Kulcsar, F., van Rooijen, G., Waterer, D.R., Robertson, A., Kokko, E., Byers, R., Howard, R.J., Fischer, R., and Pruffer, D. (2001). Tomato Ve disease resistance genes encode cell surface-like receptors. *Proc Natl Acad Sci U S A* **98**, 6511-6515.
- Kim, H.S., and Delaney, T.P. (2002). *Arabidopsis* SON1 is an F-box protein that regulates a novel induced defense response independent of both salicylic acid and systemic acquired resistance. *Plant Cell* **14**, 1469-1482.
- Kim, M., Lee, S., Park, K., Jeong, E.J., Ryu, C.M., Choi, D., and Pai, H.S. (2006). Comparative microarray analysis of programmed cell death induced by proteasome malfunction and hypersensitive response in plants. *Biochem Biophys Res Commun* **342**, 514-521.
- Kitagawa, K., Skowyra, D., Elledge, S.J., Harper, J.W., and Hieter, P. (1999). SGT1 encodes an essential component of the yeast kinetochore assembly pathway and a novel subunit of the SCF ubiquitin ligase complex. *Mol Cell* **4**, 21-33.
- Komander, D., Lord, C.J., Scheel, H., Swift, S., Hofmann, K., Ashworth, A., and Barford, D. (2008). The structure of the CYLD USP domain explains its specificity for Lys63-linked polyubiquitin and reveals a B box module. *Mol Cell* **29**, 451-464.

- Komeda, Y. (2004). Genetic regulation of time to flower in *Arabidopsis thaliana*. *Annu Rev Plant Biol* **55**, 521-535.
- Kosarev, P., Mayer, K., and Hardtke, C.S. (2002). Evaluation and classification of RING-finger domains encoded by the *Arabidopsis* genome. *Genome Biology* **3**, 0016.0011-0016.0012.
- Krysan, P.J., Young, J.C., and Sussman, M.R. (1999). T-DNA as an insertional mutagen in *Arabidopsis*. *Plant Cell* **11**, 2283-2290.
- Kumagai, M.H., Donson, J., della-Cioppa, G., Harvey, D., Hanley, K., and Grill, L.K. (1995). Cytoplasmic inhibition of carotenoid biosynthesis with virus-derived RNA. *Proc Natl Acad Sci U S A* **92**, 1679-1683.
- Kunkel, B.N. (1996). A useful weed put to work: genetic analysis of disease resistance in *Arabidopsis thaliana*. *Trends Genet* **12**, 63-69.
- Kunkel, B.N., and Brooks, D.M. (2002). Cross talk between signaling pathways in pathogen defense. *Curr Opin Plant Biol* **5**, 325-331.
- Lacomme, C., Hrubikova, K., and Hein, I. (2003). Enhancement of virus-induced gene silencing through viral-based production of inverted-repeats. *Plant J* **34**, 543-553.
- Lam, Y.A., Xu, W., DeMartino, G.N., and Cohen, R.E. (1997). Editing of ubiquitin conjugates by an isopeptidase in the 26S proteasome. *Nature* **385**.
- Larsen, C.N., Krantz, B.A., and Wilkinson, K.D. (1998). Substrate specificity of deubiquitinating enzymes: ubiquitin C-terminal hydrolases. *Biochemistry* **37**, 3358-3368.
- Laval, V., Koroleva, O.A., Murphy, E., Lu, C., Milner, J.J., Hooks, M.A., and Tomos, A.D. (2002). Distribution of actin gene isoforms in the *Arabidopsis* leaf measured in microsamples from intact individual cells. *Planta* **215**, 287-292.
- Lee, J.C., and Peter, M.E. (2003). Regulation of apoptosis by ubiquitination. *Immunol Rev* **193**, 39-47.
- Lee, S.W., Han, S.W., Bartley, L.E., and Ronald, P.C. (2006). Unique characteristics of *Xanthomonas oryzae* pv. *oryzae* AvrXa21 and implications for plant innate immunity. *Proc Natl Acad Sci U S A* **103**, 18395-18400.
- Li, M., Brooks, C.L., Kon, N., and Gu, W. (2004). A dynamic role of HAUSP in the p53-Mdm2 pathway. *Mol Cell* **13**, 879-886.
- Liu, E., and Page, J.E. (2008). Optimized cDNA libraries for virus-induced gene silencing (VIGS) using tobacco rattle virus. *Plant Methods* **4**, 5.
- Liu, Y., Schiff, M., and Dinesh-Kumar, S.P. (2002a). Virus-induced gene silencing in tomato. *Plant J* **31**, 777-786.
- Liu, Y., Schiff, M., Serino, G., Deng, X.W., and Dinesh-Kumar, S.P. (2002b). Role of SCF ubiquitin-ligase and the COP9 signalosome in the N gene-mediated resistance response to Tobacco mosaic virus. *Plant Cell* **14**, 1483-1496.
- Liu, Y., Wang, F., Zhang, H., He, H., Ma, L., and Deng, X.W. (2008). Functional characterization of the *Arabidopsis* ubiquitin-specific protease gene family reveals specific role and redundancy of individual members in development. *Plant J*.
- Lorrain, S., Vaillau, F., Balague, C., and Roby, D. (2003). Lesion mimic mutants: keys for deciphering cell death and defense pathways in plants? *Trends Plant Sci* **8**, 263-271.
- Lu, R., Malcuit, I., Moffett, P., Ruiz, M.T., Peart, J., Wu, A.J., Rathjen, J.P., Bendahmane, A., Day, L., and Baulcombe, D.C. (2003). High throughput virus-induced

- gene silencing implicates heat shock protein 90 in plant disease resistance. *Embo J* **22**, 5690-5699.
- Mackey, D., Belkhadir, Y., Alonso, J.M., Ecker, J.R., and Dangl, J.L.** (2003). Arabidopsis RIN4 is a target of the type III virulence effector AvrRpt2 and modulates RPS2-mediated resistance. *Cell* **112**, 379-389.
- Makarova, K.S., Aravind, L., and Koonin, E.V.** (2000). A novel family of cysteine proteases from eukaryotes, viruses and Chlamydia pneumoniae. *Trends in Biochemical Sciences* **25**, 50-52.
- Martin, G.B., Bogdanove, A.J., and Sessa, G.** (2003). Understanding the functions of plant disease resistance proteins. *Annu Rev Plant Biol* **54**, 23-61.
- Masselink, H., and Bernards, R.** (2000). The adenovirus E1A binding protein BS69 is a corepressor of transcription through recruitment of N-CoR. *Oncogene* **19**, 1538-1546.
- Matzke, A.J., Matzke, A.J.M., and Eggleston, W.B.** (1996). Paramutation and transgene silencing: a common response to invasive DNA? . *Trends in Plant Science* **1**, 382 - 389.
- McCullough, J., Clague, M.J., and Urbe, S.** (2004a). AMSH is an endosome-associated ubiquitin isopeptidase. *J Cell Biol* **166**, 487-492.
- McCullough, J., Clague, M.J., and Urbe, S.** (2004b). AMSH is an endosome-associated ubiquitin isopeptidase. *Journal of Cell Biology* **166**, 487-492.
- McSteen, P., and Leyser, O.** (2005). Shoot branching. *Annu Rev Plant Biol* **56**, 353-374.
- McWatters, H.G., Kolmos, E., Hall, A., Doyle, M.R., Amasino, R.M., Gyula, P., Nagy, F., Millar, A.J., and Davis, S.J.** (2007). ELF4 is required for oscillatory properties of the circadian clock. *Plant Physiol* **144**, 391-401.
- Mouradov, A., Cremer, F., and Coupland, G.** (2002). Control of flowering time: interacting pathways as a basis for diversity. *Plant Cell* **14 Suppl**, S111-130.
- Mudgil, Y., Shiu, S., Stone, S.L., Salt, J.N., and Goring, D.R.** (2004). A Large Complement of the Predicted Arabidopsis ARM Repeat Proteins Are Members of the U-Box E3 Ubiquitin Ligase Family. *Plant Physiology* **134**, 59-66.
- Murphy, C.I., and Piwnica-Worms, H.** (2001). Overview of the baculovirus expression system. *Curr Protoc Protein Sci Chapter 5*, Unit5 4.
- Murtas, G., Reeves, P.H., Fu, Y.F., Bancroft, I., Dean, C., and Coupland, G.** (2003). A nuclear protease required for flowering-time regulation in Arabidopsis reduces the abundance of SMALL UBIQUITIN-RELATED MODIFIER conjugates. *Plant Cell* **15**, 2308-2319.
- Muskett, P., and Parker, J.** (2003). Role of SGT1 in the regulation of plant R gene signalling. *Microbes Infect* **5**, 969-976.
- Nakagawa, T., Kurose, T., Hino, T., Tanaka, K., Kawamukai, M., Niwa, Y., Toyooka, K., Matsuoka, K., Jinbo, T., and Kimura, T.** (2007). Development of series of gateway binary vectors, pGWBs, for realizing efficient construction of fusion genes for plant transformation. *J Biosci Bioeng* **104**, 34-41.
- Nanao, M.H., Tcherniuk, S.O., Chroboczek, J., Dideberg, O., and Dessen, A.** (2004). Crystal structure of human otubain 2. *EMBO Reports* **5**, 783-795.
- Navarro, L., Zipfel, C., Rowland, O., Keller, I., Robatzek, S., Boller, T., and Jones, J.D.** (2004). The transcriptional innate immune response to flg22. Interplay and overlap with Avr gene-dependent defense responses and bacterial pathogenesis. *Plant Physiol* **135**, 1113-1128.

- Nekrasov, V., Ludwig, A.A., and Jones, J.D. (2006). CITRX thioredoxin is a putative adaptor protein connecting Cf-9 and the ACIK1 protein kinase during the Cf-9/Avr9-induced defence response. *FEBS Lett* **580**, 4236-4241.
- Nijman, S.M., Luna-Vargas, M.P., Velds, A., Brummelkamp, T.R., Dirac, A.M., Sixma, T.K., and Bernards, R. (2005). A genomic and functional inventory of deubiquitinating enzymes. *Cell* **123**, 773-786.
- Nimchuk, Z., Eulgem, T., Holt, B.F., 3rd, and Dangl, J.L. (2003). Recognition and response in the plant immune system. *Annu Rev Genet* **37**, 579-609.
- Niwa, Y. (2002). A Synthetic Green Fluorescent Protein Gene for Plant Biotechnology. *Plant Biotechnology* **20**, 1-11.
- Nurnberger, T., Brunner, F., Kemmerling, B., and Piater, L. (2004). Innate immunity in plants and animals: striking similarities and obvious differences. *Immunol Rev* **198**, 249-266.
- O'Connor, T.R., Dyreson, C., and Wyrick, J.J. (2005). Athena: a resource for rapid visualization and systematic analysis of Arabidopsis promoter sequences. *Bioinformatics* **21**, 4411-4413.
- Ohi, M.D., Kooi, C.W.V., Rosenberg, J.A., and Chazin, W.J. (2003). Structural insights into the U-box, a domain associated with multi-ubiquitination. *Nature Structural Biology* **10**, 250-255.
- Osterlund, M.T., Hardtke, C.S., Wei, N., and Deng, X.W. (2000). Targeted destabilization of HY5 during light-regulated development of *Arabidopsis*. *Nature* **405**.
- Peart, J.R., Cook, G., Feys, B.J., Parker, J.E., and Baulcombe, D.C. (2002a). An EDS1 orthologue is required for N-mediated resistance against tobacco mosaic virus. *Plant J* **29**, 569-579.
- Peart, J.R., Lu, R., Sadanandom, A., Malcuit, I., Moffett, P., Brice, D.C., Schausser, L., Jaggard, D.A., Xiao, S., Coleman, M.J., Dow, M., Jones, J.D., Shirasu, K., and Baulcombe, D.C. (2002b). Ubiquitin ligase-associated protein SGT1 is required for host and nonhost disease resistance in plants. *Proc Natl Acad Sci U S A* **99**, 10865-10869.
- Pedley, K.F., and Martin, G.B. (2003). Molecular basis of Pto-mediated resistance to bacterial speck disease in tomato. *Annu Rev Phytopathol* **41**, 215-243.
- Pedley, K.F., and Martin, G.B. (2005). Role of mitogen-activated protein kinases in plant immunity. *Curr Opin Plant Biol* **8**, 541-547.
- Peng, J., Schwartz, D., Elias, J.E., Thoreen, C.C., Cheng, D., Marsischky, G., Roelofs, J., Finley, D., and Gygi, S.P. (2003). A proteomics approach to understanding protein ubiquitination. *Nat Biotechnol* **21**, 921-926.
- Pickart, C.M. (2001). Mechanisms underlying ubiquitination. *Annual Review of Biochemistry* **70**, 503-533.
- Pickart, C.M., and Fushman, D. (2004). Polyubiquitin chains: polymeric protein signals. *Curr Opin Chem Biol* **8**, 610-616.
- Pickett, F.B., and Meeks-Wagner, D.R. (1995). Seeing double: appreciating genetic redundancy. *Plant Cell* **7**, 1347-1356.
- Pieterse, C.M., and Van Loon, L.C. (2004). NPR1: the spider in the web of induced resistance signaling pathways. *Curr Opin Plant Biol* **7**, 456-464.
- Pineiro, M., Gomez-Mena, C., Schaffer, R., Martinez-Zapater, J.M., and Coupland, G. (2003). EARLY BOLTING IN SHORT DAYS is related to chromatin remodeling factors and regulates flowering in Arabidopsis by repressing FT. *Plant Cell* **15**, 1552-1562.

- Poduska, B., Humphrey, T., Redweik, A., and Grbic, V. (2003). The synergistic activation of FLOWERING LOCUS C by FRIGIDA and a new flowering gene AERIAL ROSETTE 1 underlies a novel morphology in Arabidopsis. *Genetics* **163**, 1457-1465.
- Pontier, D., Tronchet, M., Rogowsky, P., Lam, E., and Roby, D. (1998). Activation of *hsr203*, a plant gene expressed during incompatible plant-pathogen interactions, is correlated with programmed cell death. *Mol Plant Microbe Interact* **11**, 544-554.
- Poon, I.K., and Jans, D.A. (2005). Regulation of nuclear transport: central role in development and transformation? *Traffic* **6**, 173-186.
- Potuschak, T., Stary, S., Schlogelhofer, P., Becker, F., Nejinskaia, V., and Bachmir, A. (1998). PRT1 of *Arabidopsis thaliana* encodes a component of the pant N-end rule pathway. *PNAS* **95**, 7904-7908.
- Quackenbush, J., Cho, J., Lee, D., Liang, F., Holt, I., Karamycheva, S., Parvizi, B., Pertea, G., Sultana, R., and White, J. (2001). The TIGR Gene Indices: analysis of gene transcript sequences in highly sampled eukaryotic species. *Nucleic Acids Res* **29**, 159-164.
- Ratcliff, F., Harrison, B.D., and Baulcombe, D.C. (1997). A similarity between viral defense and gene silencing in plants. *Science* **276**, 1558-1560.
- Ratcliff, F., Martin-Hernandez, A.M., and Baulcombe, D.C. (2001). Technical Advance. Tobacco rattle virus as a vector for analysis of gene function by silencing. *Plant J* **25**, 237-245.
- Reichel, C., and Beachy, R.N. (2000). Degradation of tobacco mosaic virus movement protein by the 26S proteasome. *J Virol* **74**, 3330-3337.
- Remm, M., Storm, C.E., and Sonnhammer, E.L. (2001). Automatic clustering of orthologs and in-paralogs from pairwise species comparisons. *J Mol Biol* **314**, 1041-1052.
- Reyes-Turcu, F.E., Shanks, J.R., Komander, D., and Wilkinson, K.D. (2008). Recognition of polyubiquitin isoforms by the multiple ubiquitin binding modules of isopeptidase T. *J Biol Chem*.
- Rivas, S., and Thomas, C.M. (2005). Molecular interactions between tomato and the leaf mold pathogen *Cladosporium fulvum*. *Annu Rev Phytopathol* **43**, 395-436.
- Romeis, T., Piedras, P., Zhang, S., Klessig, D.F., Hirt, H., and Jones, J.D. (1999). Rapid Avr9- and Cf-9 -dependent activation of MAP kinases in tobacco cell cultures and leaves: convergence of resistance gene, elicitor, wound, and salicylate responses. *Plant Cell* **11**, 273-287.
- Rommens, C.M., Salmeron, J.M., Oldroyd, G.E., and Staskawicz, B.J. (1995). Intergeneric transfer and functional expression of the tomato disease resistance gene *Pto*. *Plant Cell* **7**, 1537-1544.
- Ronald, P.C., Salmeron, J.M., Carland, F.M., and Staskawicz, B.J. (1992). The cloned avirulence gene *avrPto* induces disease resistance in tomato cultivars containing the *Pto* resistance gene. *J Bacteriol* **174**, 1604-1611.
- Rosebrock, T.R., Zeng, L., Brady, J.J., Abramovitch, R.B., Xiao, F., and Martin, G.B. (2007). A bacterial E3 ubiquitin ligase targets a host protein kinase to disrupt plant immunity. *Nature* **448**, 370-374.
- Rouse, D.T., Sheldon, C.C., Bagnall, D.J., Peacock, W.J., and Dennis, E.S. (2002). *FLC*, a repressor of flowering, is regulated by genes in different inductive pathways. *Plant J* **29**, 183-191.
- Rowland, O., and Jones, J.D. (2001). Unraveling regulatory networks in plant defense using microarrays. *Genome Biol* **2**, REVIEWS1001.

- Rozen, S., and Skaletsky, H. (2000).** Primer3 on the WWW for general users and for biologist programmers. *Methods Mol Biol* **132**, 365-386.
- Rusterucci, C., Aviv, D.H., Holt, B.F., 3rd, Dangl, J.L., and Parker, J.E. (2001).** The disease resistance signaling components EDS1 and PAD4 are essential regulators of the cell death pathway controlled by LSD1 in Arabidopsis. *Plant Cell* **13**, 2211-2224.
- Ryabov, E.V., Robinson, D.J., and Taliansky, M.E. (1999).** A plant virus-encoded protein facilitates long-distance movement of heterologous viral RNA. *Proc Natl Acad Sci U S A* **96**, 1212-1217.
- Sambrook, J., and Russel, D. (2001).** *Molecular Cloning: A Laboratory Manual* Cold Spring Harbour Laboratory Press.
- Saridakis, V., Sheng, Y., Sarkari, F., Holowaty, M.N., Shire, K., Nguyen, T., Zhang, R.G., Liao, J., Lee, W., Edwards, A.M., Arrowsmith, C.H., and Frappier, L. (2005).** Structure of the p53 binding domain of HAUSP/USP7 bound to Epstein-Barr nuclear antigen 1 implications for EBV-mediated immortalization. *Mol Cell* **18**, 25-36.
- Schadick, K., Fourcade, H.M., Boumenot, P., Seitz, J.J., Morrell, J.L., Chang, L., Gould, K.L., Partridge, J.F., Allshire, R.C., Kitagawa, K., Hieter, P., and Hoffman, C.S. (2002).** Schizosaccharomyces pombe Git7p, a member of the Saccharomyces cerevisiae Sgtp family, is required for glucose and cyclic AMP signaling, cell wall integrity, and septation. *Eukaryot Cell* **1**, 558-567.
- Scheel, H., Tomiuk, S., and Hofmann, K. (2003).** Elucidation of ataxin-3 and ataxin-7 function by integrative bioinformatics. *Human Molecular Genetics* **12**, 2845-2852.
- Schimke, R.T. (1973).** Control of enzyme levels in mammalian tissues. *Advances in enzymology & related areas of molecular biology* **37**, 135-187.
- Scholthof, H.B., Scholthof, K.B., and Jackson, A.O. (1995).** Identification of tomato bushy stunt virus host-specific symptom determinants by expression of individual genes from a potato virus X vector. *Plant Cell* **7**, 1157-1172.
- Scholthof, K.B. (2004).** Tobacco mosaic virus: a model system for plant biology. *Annu Rev Phytopathol* **42**, 13-34.
- Schrammeijer, B., Risseuw, E., Pansegrau, W., Regensburg-Tuink, T.J., Crosby, W.L., and Hooykaas, P.J. (2001).** Interaction of the virulence protein VirF of Agrobacterium tumefaciens with plant homologs of the yeast Skp1 protein. *Curr Biol* **11**, 258-262.
- Schultz, E.A., and Haughn, G.W. (1991).** LEAFY, a Homeotic Gene That Regulates Inflorescence Development in Arabidopsis. *Plant Cell* **3**, 771-781.
- Schwechheimer, C., and Villalobos, L.I. (2004).** Cullin-containing E3 ubiquitin ligases in plant development. *Current Opinion in Plant Biology* **7**, 677-686.
- Schwessinger, B., and Zipfel, C. (2008).** News from the frontline: recent insights into PAMP-triggered immunity in plants. *Curr Opin Plant Biol* **11**, 389-395.
- Searle, I., He, Y., Turck, F., Vincent, C., Fornara, F., Krober, S., Amasino, R.A., and Coupland, G. (2006).** The transcription factor FLC confers a flowering response to vernalization by repressing meristem competence and systemic signaling in Arabidopsis. *Genes Dev* **20**, 898-912.
- Sheng, Y., Saridakis, V., Sarkari, F., Duan, S., Wu, T., Arrowsmith, C.H., and Frappier, L. (2006).** Molecular recognition of p53 and MDM2 by USP7/HAUSP. *Nat Struct Mol Biol* **13**, 285-291.
- Shirasu, K., and Schulze-Lefert, P. (2003).** Complex formation, promiscuity and multi-functionality: protein interactions in disease-resistance pathways. *Trends Plant Sci* **8**, 252-258.

- Shirasu, K., Lahaye, T., Tan, M.W., Zhou, F., Azevedo, C., and Schulze-Lefert, P. (1999). A novel class of eukaryotic zinc-binding proteins is required for disease resistance signaling in barley and development in *C. elegans*. *Cell* **99**, 355-366.
- Shiu, S.H., and Bleecker, A.B. (2003). Expansion of the receptor-like kinase/Pelle gene family and receptor-like proteins in *Arabidopsis*. *Plant Physiol* **132**, 530-543.
- Silhavy, D., and Burgyan, J. (2004). Effects and side-effects of viral RNA silencing suppressors on short RNAs. *Trends Plant Sci* **9**, 76-83.
- Soltis, D.E., and Soltis, P.S. (2003). Applying the Bootstrap in Phylogeny Reconstruction. *Statistical Science* **18**, 256-267.
- Sparkes, I.A., Runions, J., Kearns, A., and Hawes, C. (2006). Rapid, transient expression of fluorescent fusion proteins in tobacco plants and generation of stably transformed plants. *Nat Protoc* **1**, 2019-2025.
- Stacey, M.G., Hicks, S.N., and von Arnim, A.G. (1999). Discrete domains mediate the light-responsive nuclear and cytoplasmic localization of *Arabidopsis* COP1. *Plant Cell* **11**, 349-364.
- Staub, E., Fiziev, P., Rosenthal, A., and Hinzmann, B. (2004). Insights into the evolution of the nucleolus by an analysis of its protein domain repertoire. *Bioessays* **26**, 567-581.
- Stone, S.L., Anderson, E.M., Mullen, R.T., and Goring, D.R. (2003). ARC1 is an E3 ubiquitin ligase and promotes the ubiquitination of proteins during the rejection of self-incompatible *Brassica* pollen. *Plant Cell* **15**.
- Sullivan, M.L., Callis, J., and Vierstra, R.D. (1990). High Performance Liquid Chromatography Resolution of Ubiquitin Pathway Enzymes from Wheat Germ. *Plant Physiol* **94**, 710-716.
- Swain, S.M., and Singh, D.P. (2005). Tall tales from sly dwarves: novel functions of gibberellins in plant development. *Trends Plant Sci* **10**, 123-129.
- Swarbreck, D., Wilks, C., Lamesch, P., Berardini, T.Z., Garcia-Hernandez, M., Foerster, H., Li, D., Meyer, T., Muller, R., Ploetz, L., Radenbaugh, A., Singh, S., Swing, V., Tissier, C., Zhang, P., and Huala, E. (2008). The *Arabidopsis* Information Resource (TAIR): gene structure and function annotation. *Nucleic Acids Res* **36**, D1009-1014.
- Takahashi, A., Casais, C., Ichimura, K., and Shirasu, K. (2003). HSP90 interacts with RAR1 and SGT1 and is essential for RPS2-mediated disease resistance in *Arabidopsis*. *Proc Natl Acad Sci U S A* **100**, 11777-11782.
- Takken, F.L., Albrecht, M., and Tameling, W.I. (2006). Resistance proteins: molecular switches of plant defence. *Curr Opin Plant Biol* **9**, 383-390.
- Tamura, K., Dudley, J., Nei, M., and Kumar, S. (2007). MEGA4: Molecular Evolutionary Genetics Analysis (MEGA) software version 4.0. *Mol Biol Evol* **24**, 1596-1599.
- Thomas, C.M., Tang, S., Hammond-Kosack, K., and Jones, J.D. (2000). Comparison of the hypersensitive response induced by the tomato Cf-4 and Cf-9 genes in *Nicotiana* spp. *Mol Plant Microbe Interact* **13**, 465-469.
- Thomma, B.P., Penninckx, I.A., Broekaert, W.F., and Cammue, B.P. (2001). The complexity of disease signaling in *Arabidopsis*. *Curr Opin Immunol* **13**, 63-68.
- Thrower, J.S., Hoffman, L., Rechsteiner, M., and Pickart, C.M. (2000). Recognition of the polyubiquitin proteolytic signal. *EMBO Journal* **19**, 94-102.

- Trujillo, M., Ichimura, K., Casais, C., and Shirasu, K. (2008). Negative regulation of PAMP-triggered immunity by an E3 ubiquitin ligase triplet in Arabidopsis. *Curr Biol* **18**, 1396-1401.
- Tsuda, K., Sato, M., Glazebrook, J., Cohen, J.D., and Katagiri, F. (2008). Interplay between MAMP-triggered and SA-mediated defense responses. *Plant J* **53**, 763-775.
- Turck, F., Fornara, F., and Coupland, G. (2008). Regulation and identity of florigen: FLOWERING LOCUS T moves center stage. *Annu Rev Plant Biol* **59**, 573-594.
- Turner, J.G., Ellis, C., and Devoto, A. (2002). The jasmonate signal pathway. *Plant Cell* **14 Suppl**, S153-164.
- Tzfira, T., Vaidya, M., and Citovsky, V. (2004). Involvement of targeted proteolysis in plant genetic transformation by *Agrobacterium*. *Nature* **431**, 87-92.
- Uren, A.G., and Vaux, D.L. (1996). TRAF proteins and meprins share a conserved domain. *Trends Biochem Sci* **21**, 244-245.
- van den Burg, H.A., Tsitsigiannis, D.I., Rowland, O., Lo, J., Rallapalli, G., Maclean, D., Takken, F.L., and Jones, J.D. (2008). The F-box protein ACRE189/ACIF1 regulates cell death and defense responses activated during pathogen recognition in tobacco and tomato. *Plant Cell* **20**, 697-719.
- van der Biezen, E.A., and Jones, J.D. (1998). The NB-ARC domain: a novel signalling motif shared by plant resistance gene products and regulators of cell death in animals. *Curr Biol* **8**, R226-227.
- Van der Hoorn, R.A., Laurent, F., Roth, R., and De Wit, P.J. (2000). Agroinfiltration is a versatile tool that facilitates comparative analyses of Avr9/Cf-9-induced and Avr4/Cf-4-induced necrosis. *Mol Plant Microbe Interact* **13**, 439-446.
- Varshavsky, A. (1996). The N-end rule: Functions, mysteries and uses. *PNAS* **93**, 12142-12149.
- Veitia, R.A. (2007). Exploring the molecular etiology of dominant-negative mutations. *Plant Cell* **19**, 3843-3851.
- Verma, R., Aravind, L., Oania, R., McDonald, W.H., Yates, J.R., 3rd, Koonin, E.V., and Deshaies, R.J. (2002a). Role of Rpn11 metalloprotease in deubiquitination and degradation by the 26S proteasome. *Science* **298**, 611-615.
- Verma, R., Aravind, L., Oania, R., MacDonald, W.H., Yates, Y.R., Koonin, E.V., and Deshaies, R. (2002b). Role of Rpn11 metalloprotease in deubiquitination and degradation by the 26S proteasome. *Science* **298**.
- Vierstra, R.D. (1996). Proteolysis in plants: mechanisms and functions. *Plant and Molecular Biology* **32**, 275-302.
- Vierstra, R.D. (2003). The ubiquitin/26S proteasome pathway, the complex last chapter in the life of many plant proteins. *Trends Plant Sci* **8**, 135-142.
- Vierstra, R.D. (2004). The Ubiquitin 26S Proteasome Proteolytic Pathway. *Annual Review of Plant Biology* **55**, 555-590.
- Vodermaier, H.C. (2001). Cell cycle: waiters serving the destruction machinery. *Current Biology* **11**, R834-R837.
- Voinnet, O., Rivas, S., Mestre, P., and Baulcombe, D. (2003). An enhanced transient expression system in plants based on suppression of gene silencing by the p19 protein of tomato bushy stunt virus. *Plant J* **33**, 949-956.

- Volko, S.M., Boller, T., and Ausubel, F.M.** (1998). Isolation of new *Arabidopsis* mutants with enhanced disease susceptibility to *Pseudomonas syringae* by direct screening. *Genetics* **149**, 537-548.
- Wang, M.B., and Metzloff, M.** (2005). RNA silencing and antiviral defense in plants. *Curr Opin Plant Biol* **8**, 216-222.
- Wang, Q., Sajja, U., Rosloski, S., Humphrey, T., Kim, M.C., Bomblies, K., Weigel, D., and Grbic, V.** (2007). HUA2 caused natural variation in shoot morphology of *A. thaliana*. *Curr Biol* **17**, 1513-1519.
- Wasch, R., and Cross, F.R.** (2002). APC-dependent proteolysis of the mitotic cyclin Clb2 is essential for mitotic exit. *Nature* **418**, 495-496.
- Waterhouse, P.M., and Helliwell, C.A.** (2003). Exploring plant genomes by RNA-induced gene silencing. *Nat Rev Genet* **4**, 29-38.
- Weake, V.M., and Workman, J.L.** (2008). Histone ubiquitination: triggering gene activity. *Mol Cell* **29**, 653-663.
- Wei, N., Tsuge, T., Serino, G., Dohmae, N., Takio, K., Matsui, M., and Deng, X.** (1998). The COP9 complex is conserved between plants and mammals and is related to the 26S proteasome regulatory complex. *Current Biology* **8**, 919-922.
- Welchman, R.L., Gordon, C., and Mayer, R.J.** (2005). Ubiquitin and ubiquitin-like proteins as multifunctional signals. *Nat Rev Mol Cell Biol* **6**, 599-609.
- Whitham, S., Dinesh-Kumar, S.P., Choi, D., Hehl, R., Corr, C., and Baker, B.** (1994). The product of the tobacco mosaic virus resistance gene N: similarity to toll and the interleukin-1 receptor. *Cell* **78**, 1101-1115.
- Wielopolska, A., Townley, H., Moore, I., Waterhouse, P., and Helliwell, C.** (2005). A high-throughput inducible RNAi vector for plants. *Plant Biotechnol J* **3**, 583-590.
- Wiermer, M., Feys, B.J., and Parker, J.E.** (2005). Plant immunity: the EDS1 regulatory node. *Curr Opin Plant Biol* **8**, 383-389.
- Wolf, D.H., and Hilt, W.** (2004). The proteasome: a proteolytic nanomachine of cell regulation and waste disposal. *Biochimica et Biophysica Acta* **1695**, 19-31.
- Xiao, S., Ellwood, S., Calis, O., Patrick, E., Li, T., Coleman, M., and Turner, J.G.** (2001). Broad-spectrum mildew resistance in *Arabidopsis thaliana* mediated by RPW8. *Science* **291**, 118-120.
- Xiao, S., Calis, O., Patrick, E., Zhang, G., Charoenwattana, P., Muskett, P., Parker, J.E., and Turner, J.G.** (2005). The atypical resistance gene, RPW8, recruits components of basal defence for powdery mildew resistance in *Arabidopsis*. *Plant J* **42**, 95-110.
- Xu, L., and Massague, J.** (2004). Nucleocytoplasmic shuttling of signal transducers. *Nat Rev Mol Cell Biol* **5**, 209-219.
- Xu, L., Menard, R., Berr, A., Fuchs, J., Cognat, V., Meyer, D., and Shen, W.H.** (2008). The E2 ubiquitin-conjugating enzymes, AtUBC1 and AtUBC2, play redundant roles and are involved in activation of FLC expression and repression of flowering in *Arabidopsis thaliana*. *Plant J*.
- Yan, J., Wang, J., Li, Q., Hwang, J.R., Patterson, C., and Zhang, H.** (2003). AtCHIP a U-box E3 ligase plays a critical role in temperature stress tolerance in *Arabidopsis*. *Plant Physiology* **132**, 1-9.
- Yan, N., Doelling, J.H., Falbel, T.G., Durski, A.M., and Vierstra, R.D.** (2000a). The ubiquitin-specific protease family from *Arabidopsis*. AtUBP1 and 2 are required for the resistance to the amino acid analog canavanine. *Plant Physiol* **124**, 1828-1843.

- Yan, N., Doelling, J.H., Falbel, T.G., Durski, A.M., and Vierstra, R.D. (2000b). The Ubiquitin-Specific Protease Family from Arabidopsis. AtUBP1 and 2 are required for the resistance to the amino acid analog canavanine. *Plant Physiology* **124**.
- Yang, C.W., Gonzalez-Lamothe, R., Ewan, R.A., Rowland, O., Yoshioka, H., Shenton, M., Ye, H., O'Donnell, E., Jones, J.D., and Sadanandom, A. (2006). The E3 ubiquitin ligase activity of arabidopsis PLANT U-BOX17 and its functional tobacco homolog ACRE276 are required for cell death and defense. *Plant Cell* **18**, 1084-1098.
- Yang, K.Y., Liu, Y., and Zhang, S. (2001). Activation of a mitogen-activated protein kinase pathway is involved in disease resistance in tobacco. *Proc Natl Acad Sci U S A* **98**, 741-746.
- Yang, P., Smalle, J., Lee, S., Yan, N., Emborg, T.J., and Vierstra, R.D. (2007). Ubiquitin C-terminal hydrolases 1 and 2 affect shoot architecture in Arabidopsis. *Plant J* **51**, 441-457.
- Yin, Z., Chen, J., Zeng, L., Goh, M., Leung, H., Khush, G.S., and Wang, G.L. (2000). Characterizing rice lesion mimic mutants and identifying a mutant with broad-spectrum resistance to rice blast and bacterial blight. *Mol Plant Microbe Interact* **13**, 869-876.
- Yu, I.C., Parker, J., and Bent, A.F. (1998). Gene-for-gene disease resistance without the hypersensitive response in Arabidopsis dnd1 mutant. *Proc Natl Acad Sci U S A* **95**, 7819-7824.
- Zapata, J.M., Pawlowski, K., Haas, E., Ware, C.F., Godzik, A., and Reed, J.C. (2001). A diverse family of proteins containing tumor necrosis factor receptor-associated factor domains. *J Biol Chem* **276**, 24242-24252.
- Zeng, L.R., Qu, S., Bordeos, A., Yang, C., Baraoidan, M., Yan, H., Xie, Q., Nahm, B.H., Leung, H., and Wang, G.L. (2004). Spotted leaf11, a negative regulator of plant cell death and defense, encodes a U-box/armadillo repeat protein endowed with E3 ubiquitin ligase activity. *Plant Cell* **16**, 2795-2808.
- Zhang, J.Z., and Somerville, C.R. (1997). Suspensor-derived polyembryony caused by altered expression of valyl-tRNA synthetase in the twn2 mutant of Arabidopsis. *Proc Natl Acad Sci U S A* **94**, 7349-7355.
- Zipfel, C., and Felix, G. (2005). Plants and animals: a different taste for microbes? *Curr Opin Plant Biol* **8**, 353-360.
- Zipfel, C., Robatzek, S., Navarro, L., Oakeley, E.J., Jones, J.D., Felix, G., and Boller, T. (2004). Bacterial disease resistance in Arabidopsis through flagellin perception. *Nature* **428**, 764-767.
- Zipfel, C., Kunze, G., Chinchilla, D., Caniard, A., Jones, J.D., Boller, T., and Felix, G. (2006). Perception of the bacterial PAMP EF-Tu by the receptor EFR restricts Agrobacterium-mediated transformation. *Cell* **125**, 749-760.

## Appendices

**Table A1** Initial DUB protein sequences used to query the *Arabidopsis* proteome.

DUB	Organism	Swissprot code	UBP Class
YUH1	<i>S. Cerevisiae</i>	P35127	UCH
UBP1	<i>A. thaliana</i>	Q9FPT5	UBP
USP14	<i>H. sapiens</i>	P54578	UBP
Ataxin-3	<i>H. sapiens</i>	P54252	Ataxin
RPN11	<i>S. Cerevisiae</i>	P43588	JAMM

**Table A2** PCR primers used for RT-PCR and cloning.

Primer	Primer Sequence
AtActin2_5	CTTACAATTTCCCGCTCTGC
AtActin2_3	GTTGGGATGAACCAGAAGGA
AtPR-1_5	TTCTTCCCTCGAAAGCTCAA
AtPR-1_3	ACTTTGGCACATCCGAGTCT
AtUBP12_RT5	CCAGAAACAGACACCATTTC
AtUBP12_RT3	GTGTTTCGCACATAACACAAGGT
AtUBP13_RT5	GATGCACCTACCGCTAGTATCC
AtUBP13_RT3	TCCTTCTGCATGGTATTTGTTG
AtActin2_REAL5	CTAAGCTCTCAAGATCAAAGGCTTA
AtActin2_REAL3	ACTAAAACGCAAACGAAAGCGGTT
AtPR1_REAL5	TCAGTGAGACTCGGATGTG
AtPR1_REAL3	CCTGCATATGATGCTCCTT
UBP12_REAL5	GACCCCGAGAAGGCAGTATT
UBP12_REAL3	TCGCACATAACACAAGGTTCA
UBP13_REAL5	GGCAAAGCGTCAAACCATTA
UBP13_REAL3	TCTGGGGGAGGAATAGGAAG
SALK_Lba1	TGGTTCACGTAGTGGGCCATCG
GK_T-DNA	ATATTGACCATCATACTCATTGC
ubp8-1_FLK5	TTCTGTGACAGGTGGTTTTGG
ubp8-1_FLK3	GCAAGTCAGACGCACAAAAAG
ubp11-1_FLK5	TCCATTAGAAGCGGAECTCAAG
ubp11-1_FLK3	ACTAGGAAACCAGTGCCTTCG
ubp12-1_FLK5	ATTTTGACAGGTGAGGCTAAAGAA
ubp12-1_FLK3	AACTCGCATATCCAGAAGAAAGAG
ubp12-2_FLK5	TAGGCTGCACCTTGTATTTTCTT
ubp12-2_FLK3	GCCCTCTTAGGAGTAGTGTCAGC
ubp13-1_FLK5	TTGTTCCCTCCACAACAGTTC
ubp13-1_FLK3	GGAATGGAGTCAAGTTACCGC
ubp13-2_FLK5	CAAGGACTGTATTTGCATAAGCC
ubp13-2_FLK3	AGCCACCCTTTCCACTACATC
ubp25-1_FLK5	TTTCATGTAAGAGAACTTGGAAAGC
ubp25-1_FLK3	GTGCGGAGTCTAATAAAGCCG

U12-1_FL_5	AACCCGAGACTGCTGCGAGTA
U12-1_FL_3	GCATGCTCCAACCCGAGGTAC
U12-1_5P_3	TAAATCCAGGTGCTCTACTTC
U12-1_3P_5	CTACCTAAACAAAGCACGGTC
U12-2_3P_5	CCAAGTGGAAAGTTTGC GTTCA
U13-1_FL_5	ATGACTATGATGACTCCGCCCGCTAG
U13-1_FL_3	ATTGTATATTTTCACCGGCTTCTCGTA
U13-1_5P_5	AAACTGATCCTGCTGCTACCG
U13-1_5P_3	CCTCGAGTGGGTTTCATAGAGC
U13-1_3P_5	GATGTACAAGAACTCAACAGA
U13-1_3P_3	TAGGAAGGTCATCCGGTCCAC
U13-2_5P_5	TTGGTCGAGGGACCTCAGCCT
U13-2_3P_5	TATGATGATGTAGTGAAAGG
U13-2_3P_3	CTTTTAGGAGCATTATCAATG
UBP_RNAi_5	CACCGGACCGGATGACCTTCTAT
UBP_RNAi_3	TCAGCCACCTTTTCCACTAC
HG12_35S	ATCCCACTATCCTTCGCAAGA
HG12_int	CTTCGTCTTACACATCACTTGTC
AtUBP12_KD5	ATGACTATGATGACTCCGCCTCCC
AtUBP12_KD3	CCAAGGTGCAACAAGCTACATGAATT
AtUBP13_KD5	GATGCACCTACCGCTAGTATCC
AtUBP13_KD3	TCCTTCTGCATGGTATTTGTTG
NtUbp12_TAG	AAGCCTGTTCCGGATCTACAACACTAG
StUbp12_ATG	ATGACTATGATGACTCCTCCCCC
NtU12_2176_3	CAGGAGCAAATCCAGCCAATTCA
NtU12_1677_5	AGAGGCTCACCTTTATAACAATAATCAAG
NtUbp12_903RC	GATGAAGGGAACCGTTGTAGAG
NtUbp12_742RC	CCTTTGGCTCTTCAGAGTTTGT
NtUbp12_554RC	CTGTGCGTAGGGTCATTGATTA
NtACTIN2_5	CTATTCTCCGCTTTGGACTTGCA
NtACTIN2_3	ACCTGCTGGAAGGTGCTGAGGGAA
Hsr203J_5	TCCCGTCATTCTTCACTTCC
Hsr203J_3	ATCTTTCTCCGCCACACAGT
NtUbp12_562_5	GCGTGGAAGCTTACATAGCAGAGCATCTCAGGGTA
NtUbp12_562_3	GCCTACGGTACCGTTAATATCTCCATCGGCTTGC
NtUbp12_742_5	GCGTGGAAGCTTGATGCCAATAAAGTATCAAGG
NtUbp12_742_3	GCCTACGGTACCATGTCCGTTCTGGTTGCTAGC
NtUBP12_562KD_5	AAGAAGGAGACGGGTTGTGTT
NtUBP12_562KD_3	ATCACGACACCCTTTGACATC
NtUBP12_742KD_5	GAATTGGCTGGATTTGCTCCTG
NtUBP12_742KD_3	CGCCACTCTCTCCACTACATC
AtUBP12_5_NotI	TATACTGCGGCCGGAATTGTATATTTTTACCGGCTT
AtUBP12_3_Asp718I	GTAAGAGGTACCGAATGACTATGATGACTCCGCCT
AtUBP12_5_C208S	CTCAAGAACCAAGGTGCAACAAGCTACATGAATTCTCTCCTACAG
AtUBP12_3_C208S	CTGTAGGAGAGAATTCATGTAGCTTGTTGCACCTTGGTTCTTGAG
AtUBP12BAC5_NotI	GTAAGAGCGGCCGCGATGACTATGATGACTCCGCCTCCCC
AtUBP12BAC3_Asp718I	TATACTGGTACCGAATTGTATATTTTTACCGGCTT
NtUBP12BAC5_NotI	GTAAGAGCGGCCGCGATGACTATGATGACTCCTCCCCC
NtUBP12BAC3_Asp718I	TATACTGGTACCGAGTTGTAGATCCGAACAGGCTTCT
NtUBP12_5_C206S	GCCTTAAGAATCAGGGAGCTACTAGTTATATGAACTCTCTCCTCC
NtUBP12_3_C206S	GGAGGAGAGAGTTCATATAACTAGTAGCTCCTGATTCTTAAGGC

**Figure A1** Alignment of *AtUBP12*, *AtUBP13* and *NtUBP12* cDNA sequences.

```

AtUBP12    1  ATGACTATGATGACTCCGCCTCCCGTTGATCAGCCAGAAGATGAGGAGATGCTTGTGCCG
AtUBP13    1  ATGACTATGATGACTCCGCCGCCGCTAGATCAGCAGGAAGACGAGGAGATGCTTGTTCGG
NtUBP12    1  ATGACTATGATGACTCCTCCCCCGTAGATC---CAGAAGAGGACGAGATGCTCGTTCTCT

AtUBP12    61  AATTCAGATTTGGTCGACGGTCTCTGCTCAGCCCATGGAAGTTACCCAACCCGAGACTGCT
AtUBP13    61  AATCCGGATTTGGTCGAGGGACCT---CAGCCTATGGAAGTTGCCCAAACCTGATCCTGCT
NtUBP12    58  AATTCAGATTTTCCCGTTGAAGTCTCTCAGCCAATGGAAGTTGC---GACTGCGGATACA

AtUBP12   121  GCGAGTACTGTGGAGAACCAGCCAGCTGAGGATCCTCCTACTCTGAAATTCACGTGGACT
AtUBP13   118  GCTACCGCTGTGGAGAATCCACCACCCGAGGATCCTCCAAGTCTGAAATTCACGTGGACC
NtUBP12   115  GCTAGTACGGTGGATGGACCGCAGTGGATGATCCGCCATCTGCTCGGTTACATGGACA

AtUBP12   181  ATCCCTAATTTCTCTAGGCCAAAACACCAGGAAGCATTACTCCGATGTATTTGTGCGTTGGA
AtUBP13   178  ATCCCAATGTTCACTAGGCTCAATACCAGGAAGCATTACTCTGACGTATTTGTTGTAGGC
NtUBP12   175  ATAGAGAACTTTTCAAGGTTGAATCAAAGAAGCTATACTCGGATGTTTTCCATGTGGGA

AtUBP12   241  GGTTACAAATGGCGCATATTAATTTTCCCGAAAGGGAACAATGTTGATCATTTGTCCATG
AtUBP13   238  GGTTATAAGTGGCGTATATTGATTTTTCCCAAAGGAAACAATGTCGACCATTTGTCAATG
NtUBP12   235  GGATATAAATGGAGGATATTGATATTTCCCTAAAGGGAACAACGTGGACCATTTGTCTATG

AtUBP12   301  TACTTGGATGTTTCTGATGCTGCGAGTTTGCCGTACGGTTGGAGCAGATATGCTCAGTTC
AtUBP13   298  TACTTGGATGTTGCTGATGCTGCGAATTTGCCGTACGGTGGAGCAGATATTCACAGTTC
NtUBP12   295  TATTTAGATGTTGCAGATTCGCCGGCATTGCCTTACGGTGGAGTAGACATGCTCAGTTC

AtUBP12   361  AGTCTGGCTGTAGTCAATCAAATCCACACCAGATATACCGTTAGAAAAGAGACGCAACAT
AtUBP13   358  AGTCTGGCTGTAGTGAATCAAGTCAACAACCGATATTCATCAGAAAAGGAGACGCAACAT
NtUBP12   355  AGCTTAGCTGTTCTCAACCGAGTCCATAACAAGTTTACAGTGAGAAAAGATACTCAACAC

AtUBP12   421  CAATTCAATGCTAGAGAAAGCGATTGGGGATTTACATCATTTCATGCCACTTAGCGAACTT
AtUBP13   418  CAATTCAATGCAAGAGAAAGCGACTGGGGGTTTACATCATTTCATGCCTCTCAGCGAGCTC
NtUBP12   415  CAGTTTAAATGCAAGAGAGAGTACTGGGGTTTACAGTCTTTCATGCCTCTTAGTGAATTA

AtUBP12   481  TATGATCCTAGTAGAGGATATTTAGTGAATGATACTGTTTTGGTTGAAGCTGAAGTCGCT
AtUBP13   478  TATGAACCCACTCGAGGATATTTAGTGAATGACACTGTTCTGATTGAAGCTGAAGTTGCT
NtUBP12   475  TATGATCCTATCAGAGGTTATCTTGTGGATGATACAGTAATAGTTGAAGCTGATGTTGCT

AtUBP12   541  GTACGTAAGGTTCTTGATTACTGGTCATATGACTCTAAAAAAGAGACTGGTTTTGTTGGA
AtUBP13   538  GTGCGTAAAGTTCTTGATTATTGGTCATATGACTCAAAAAAAGAGACAGGTTTTGTTGGA
NtUBP12   535  GTGCGTAGGGTCATTGATTACTGGTCTCACGACTCGAAGAAGGAGACGGGTTGTGTTGCG

AtUBP12   601  CTCAAGAACCAAGGTGCAACATGCTACATGAATTCCTCCTACAGACACTATAACCACATA
AtUBP13   598  CTAAAAAACCAAGGTGCTACCTGTTACATGAATTCCTCCTGCAGACTTTATAACCACATA
NtUBP12   595  CTTAAGAATCAGGGAGCTACTTGTATATGAATTCCTCCTCCAAACATTGTACCATATT

AtUBP12   661  CCTTACTTCAGAAAGGCTGTATACCACATGCCAACAACTGAGAATGATGCACCCACAGCA
AtUBP13   658  CCTTACTTTAGAAAGGCTGTTTACCACATGCCAACGACTGAAAATGATGCACCTACCCTG
NtUBP12   655  CCTTACTTTAGAAAGGCTGTGTATCATATGCCAACAACTGAGAATGACAATCCATCCGGG

AtUBP12   721  AGTATACCGTTGGCTCTCCAAAGTTGTTTTACAAGCTCCAATACAATGACACTAGTGTT
AtUBP13   718  AGTATCCCATTGGCGCTCCAGAGTTTATTTTACAAGCTTCAGTATAATGATACCAGTGTA
NtUBP12   715  AGCATCCCTTTGGCTCTCAGAGTTTGTGTTTATAAGCTACAATACAGTGACACTAGTGTA

AtUBP12   781  GCAACAAAAGAGCTGACAAAGTCGTTTGGTTGGGATACATATGATTCTTTCATGCAGCAT
AtUBP13   778  GCGACAAAGGAGCTGACAAAGTCGTTTGGTTGGGATACATATGATTCTTTTATGCAACAT
NtUBP12   775  GCAACAAAAGAATTGACAAAGTCCTTTGGATGGGATACCTATGATTCTTTCATGCAGCAT

AtUBP12   841  GATGTGCAAGAACTCAATCGGGTCTCTGCGAAAAGCTTGAGGACAAAATGAAGGGAAC
AtUBP13   838  GATGTACAAGAACTCAACAGAGTTCCTGTGAAAAGCTTGAGGACAAGATGAAGGGAAC
NtUBP12   835  GATGTACAAGAACTTAACAGGGTCTTTTGTGAAAAGCTTGAAAGATAAGATGAAGGGAACC

AtUBP12   901  GTTGTGGAGGGAACAATACAACAACCTTTTTGAGGGCCACCATATGAATTACATTGAGTGC
AtUBP13   898  GTTGTGGAGGGAACAATACAACAACCTTTTTGAAGGTCACCACATGAATTACATTGAGTGC
NtUBP12   895  GTTGTAGAGGGCACAATACAACAACCTTTTCGAGGGGCATCATATGAATTATATTGAATGT

AtUBP12   961  ATAAATGTAGATTTTAAATCTACACGGAAAAGAATCATTTTACGACCTTCAGCTGGATGTT
AtUBP13   958  ATTAATGTAGATTACAAATCTACACGGAAAAGAGTCATTTTATGACCTCCAGCTTGATGTT
NtUBP12   955  ATCAATGTGGACTATAAATCAACAAGAAAAGAATCTTTTTATGATTTGCAGCTTGATGTC

```

AtUBP12 1021 AAAGGCTGCAAGGATGTTTATGCTTCTTTTGACAAGTATGTTGAAGTTGAACGCTTTGAA  
 AtUBP13 1018 AAAGGCTGCAAAGATGTATATGCTTCTTTTGACAAGTATGTTGAAGTTGAACGCCTTGAA  
 NtUBP12 1015 AAAGGGTGTCGTGATGTCTATGCTTCTTTTGACAAGTATGTTGAAGTTAGAACGCCTTGAG  
  
 AtUBP12 1081 GGAGACAACAAATATCATGCAGAAGGACATGGTTTACAGGATGCAAAAAAGGTGTTCTT  
 AtUBP13 1078 GGAGACAACAAATACCATGCAGAAGGACATGATTTGCAGGATGCAAAAAAGGTGTTCTA  
 NtUBP12 1075 GGTGATAATAAGTACCATGCAGAAAAGTATGGTTTACAGGATGCTCGAAAAGGTGTGCTT  
  
 AtUBP12 1141 TTCATTGACTTTCCACCGGTTCTTCAACTCCAGCTCAAGAGGTTTGAATATGACTTTTATG  
 AtUBP13 1138 TTCATAGACTTTCCACCAGTTCTTCAACTCCAGCTCAAGAGGTTTGAATACGATTTTATG  
 NtUBP12 1135 TTCATTGATTTCCCCCTGTTCTTCCAGCTTCCAGTTAAAACGATTTGAATATGATTTTGT  
  
 AtUBP12 1201 AGGGACACCATGGTGAAGATAAATGATCGGTATGAGTTTCCGCTTGAACCTGGATCTTGAT  
 AtUBP13 1198 AGGGACACAATGGTGAAGATTAATGATCGGTATGAGTTTCTCTCCAACCTGGATCTCGAC  
 NtUBP12 1195 CGGGATACTATGGTCAAGATAAACGCACAGATATGAGTTTCTTTTAGAACTCGATCTTGAT  
  
 AtUBP12 1261 AGAGAAGATGGAAAGTATCTGTGCCTGATGCTGACAGGAGTGTCCGCAACCTTTATACT  
 AtUBP13 1258 AGAGAAGATGGAAAGATATTTATCCCTGATGCAGACAAGAGTGTCCGCAATCTCTACACC  
 NtUBP12 1255 AGAGAGAATGGCAAATACTTATCTCTGATGCAGATCGAAGTGTTCGCAATCTCTATACC  
  
 AtUBP12 1321 CTTACAGTGTTTTAGTTTCATAGTGGAGGAGTACATGGTGGGCACTATTATGCTTTTATA  
 AtUBP13 1318 CTCCACAGTGTCTTGGTTCACAGTGGAGGAGTGCATGGAGGGCATTATTATGCTTTTATF  
 NtUBP12 1315 CTTACAGTGTTTTGGTTCATAGTGGTGGGGTCCACGGGGGACACTATTATGCTTTATAC  
  
 AtUBP12 1381 AGGCCTACGCTCTCAGATCAGTGGTATAAATTTGATGATGAACGAGTAACCAAGGAAGAT  
 AtUBP13 1378 AGGCCAACACTTTTTCAGATCAGTGGTATAAATTTGACGATGAACGGGTCACGAAAGAAGAT  
 NtUBP12 1375 AGGCCAACACTCTCTGATCAATGGTTTAAATTTGATGATGAGCGTGTGACAAAAGAAGAT  
  
 AtUBP12 1441 TTGAAAAGGGCTTTGGAGGAGCAATATGGTGGTGAAGAAGAGCTACCACAGACTAATCCT  
 AtUBP13 1438 GTCAAAAAGAGCACTGGAAGAGCAATATGGTGGTGAAGAAGAGTTACCCGAGAATAATCCT  
 NtUBP12 1435 TCGAAGAGGGCTTTGGAAGAACAATATGGTGGTGAAGAAGAGTTACCTCATGCAAACCTT  
  
 AtUBP12 1501 GGTTTCAATAATAACCCCTCCTTTCAAATTCACAAAGTACTCGAATGCTTACATGCTTGTA  
 AtUBP13 1498 GGTTTCAATAAT---CCACCTTTCAAATTCACAAAATACTCGAATGCATACATGCTTGT  
 NtUBP12 1495 GGGTTCAACAAT---TCACCGTTCAAATTTACAAAATATTCAAATGCATATATGCTTGT  
  
 AtUBP12 1561 TATATCCGAGAAAGTGACAAAGATAAAAATAATCTGCAACGTTGATGAGAAAGACATAGCA  
 AtUBP13 1555 TATATTCGGGAAAGTGACAAGGATAAGATAATCTGCAACGTTGATGAGAAAGACATTGCG  
 NtUBP12 1552 TATATACGTGAAAGTGACAAAGAAAAGATTATATGCAATGTGGATGAAAAGGACATAGCA  
  
 AtUBP12 1621 GAACATTTAAGGGTGAAGCTAAAGAAAAGAGCAAGAAGAAAAGGAAGATAAAAAGAAGATAC  
 AtUBP13 1615 GAACATTTGCGGGTGAAGCTGAAAAAAGAACAAGAAGAAAAGGAAGATAAAAAGAAAATAC  
 NtUBP12 1612 GAGCATCTCAGGGTAAGGCTGAAGAAAAGAGCAAGATGAAAAGGAGCAAAAAGAGAAAAGGAA  
  
 AtUBP12 1681 AAGGCACAAGCTCACTTATATACCATAATTAAGGTTGCAAGAGATGAAGACCTTAAGGAA  
 AtUBP13 1675 AAGGCTCAAGCTCACCTTTTACAGCAATCAAGGTCGCAAGAGATGATGACATCACTGAG  
 NtUBP12 1672 AAAGCAGAGGCTCACCTTTATACAATAATCAAGGTTGCTCGCGATGAAGACCTTGGTGAA  
  
 AtUBP12 1741 CAAATTGGAAGGATATATATTTTTGATCTTGTGGATCATGACAAAGTTCGAGTTTCCGT  
 AtUBP13 1735 CAAATTGGAAGAATATATATTTTTGATCTTGTGGATCATGAAAAGTGAGGAGTTTTCGA  
 NtUBP12 1732 CAAATTGGAAGGATATTTATTTTTGATCTCGTAGATCATGACAAAGTCCGTAGTTTCCGT  
  
 AtUBP12 1801 ATCCAGAAACAGACACCATTTCAACAGTTTAAAGGAGGAGGTAGCAAAAAGAAATTTGGTGTA  
 AtUBP13 1795 ATCCAGAAACAGACCCCTTTCAACAATTTAAGGAAGAGGTAGCCAAAAGAGTTTGGTGTC  
 NtUBP12 1792 ATCCAGAAACAGATGGCATTACACAATTCAGGAGGAAGTTGCTAAGGAATTTGGGTATA  
  
 AtUBP12 1861 CCTGTTCAAGTACAGAGGTTCTGGATTTGGGCAAAGAGACAAAACCATACCTATCGTCCC  
 AtUBP13 1855 CCGTTCAACTACAGCGGTTCTGGATCTGGGCAAAGCGTCAAACCATACTTACCGCCCC  
 NtUBP12 1852 CCGGTGCAATTTACAGGTTATTGGCTATGGGCAAACGCACAAAACCACACTTATCGGCCCT  
  
 AtUBP12 1921 AATCGCCCCCTTACGCCTCAAGAGGAATTAACAACCGTTGGACAAATAAGGGAAGCATCT  
 AtUBP13 1915 AATCGTCCCCTATCACCTAATGAAGAATTACAGACGTTGGACAAATACGAGAGGCATCT  
 NtUBP12 1912 AATCGGCCATTGACACCTCAAGAGGAACTCAATCTGTTGGACAACTGAGAGAGGTCCT  
  
 AtUBP12 1981 AATAAGGCAAACACTGCAGAACTCAAGCTTTTTTTGGAAAGTAGAGCAC---CTGGATTTA  
 AtUBP13 1975 AACAAGGCAAACAATGCTGAGCTAAAGCTGTTTTTTGGAAATAGAGCGTGGACCGGATGAC  
 NtUBP12 1972 AATAAAGCAAATAACGCTGAGCTAAAACCTTTATTTGGAAAGTTGAATTTGGCCTGGATTTG  
  
 AtUBP12 2038 CGTCTATTCTCTCTCTGAAAAATCAAAAAGAAGATATCTTCTTTTCTTCAAGCTTTAT  
 AtUBP13 2035 CTTCCTATTCTCTCCCCAGAAAAACTTCTGAGGATATCCTTCTTTTCTTTAAACTCTAT  
 NtUBP12 2032 CGACCTTGTCCTCCACTGAGAAGACCAAAGAAGATATCTTCTATTTTCAAACTGTAT

AtUBP12 2098 GACCCCGAGAAGGCAGTATTAAGCTATGCTGGCAGGCTGATGGTGAAAAGTTCCAGTAAG  
 AtUBP13 2095 GACCTGAGAACGCAGTACTAAGATATGTTGGCAGGCTAATGGTGAAAAGTTCCAGTAAG  
 NtUBP12 2092 GACCTCTGAAAGAGGAGATGAGGTATGTTGGCGGCTCTTTGTAAAAGGTAGTGCCAAAG

AtUBP12 2158 CCTATGGATATAACTGGAAAACCTGAATGAAATGGTTGGCTTTGCTCCTGATGAAGAAATA  
 AtUBP13 2155 CCCATGGATATAGTAGGGCAATTGAATAAAAATGGCTGGTTTTGCTCCTGATGAGGAAATA  
 NtUBP12 2152 CCATTGGAGATATTGACCAAGCTAAATGAGCTGGCTGGCTTTTCGCTGACGAAGAGATT

AtUBP12 2218 GAACTTTTTGAGGAAATCAAGTTTTGAACCTTGTGTTATGTGCGAACCTTGATAAAGAAA  
 AtUBP13 2215 GAACTTTTTGAGGAAATAAAGTTTTGAACCTTGCCTAATGTGTGAACAGATTGATAAAGAA  
 NtUBP12 2212 GAACTCTTTGAGGAAATAAAACTTGTATCCCAACGTGATGTGTGAACCCATTGACTGGAAG

AtUBP12 2278 ACTTCATTCAGATTGTGTCAAATTTGAAGATGGAGATATCATTGCTTTCAGAAAACCTCTT  
 AtUBP13 2275 ACTTCTTTTCAGGCTGTGTCAAATTTGAAGATGGAGATATCATTGTTTATCAGAAAACCTCTT  
 NtUBP12 2272 CTAAACATTTTCGCGGAGTCAAGCTTGAAGATGGGACATTTATTTGCATTCAGAAAACCTCTT

AtUBP12 2338 GTTAAACAAGGAGATTGAA---TGCCTTACCCAGCTGTGCCCTTCGTTTTCTGAATATGTC  
 AtUBP13 2335 TCTATCGAGGAGAGTGAA---TTTCGATACCCAGATGTGCCATCATTTTTGGAGTATGTA  
 NtUBP12 2332 CGAAGTCAAACCTAGTGAACAATATCGATTTCTGACGTTCTTTCATTTTTAGAGTACGTC

AtUBP12 2395 CAGAATAGACAGCTGGTCCGGTTTTCGTGCTCTGGAAAAACCTAAAGAAGATGAGTTTTGTT  
 AtUBP13 2392 CAGAATCGAGAGCTGGTGCCTTTTTTCGCACACTGGAAAAACCAAAGAGGATGAGTTTTACT  
 NtUBP12 2392 CACAATCGCCAGGTTGTTTCGCTTCCGCTCATTGGAGAAAACCAAAGAGGATGATTTTCAGT

AtUBP12 2455 CTGGAGTTGTGCGAAGCAGCACACTTATGACGATGTTGTGGAGAAAGTGGCTGAGAAGCTT  
 AtUBP13 2452 ATGGAGCTGTCAAAGCTGCACACTTATGATGATGTAGTGGAAAGGTTGGCTGAGAAGCTT  
 NtUBP12 2452 CTTGAGTTGTGCGAAGCAGGATACATATGATGATGTAGTGGAGAGAGTGGCGCAACGGCTT

AtUBP12 2515 GGTCTTGACGATCCATCCAAAACCTTAGGCTTACATCTCACAATTGCTATTTCCAGCAACCC  
 AtUBP13 2512 GGCCTTGACGATCCATCCAAAACCTTAGGCTTACATCTCACAATTGCTACTCTCAGCAACCC  
 NtUBP12 2512 GGTGTGGATGATCCCTCCAAAATTTAGGCTTACTCCACACAACCTGCTACTCACAGCAGCCA

AtUBP12 2575 AAGCCTCAGCCTATCAAAGTACCGTGGAGTAGACCATTTGTGAGATATGTTAGTTCATTAC  
 AtUBP13 2572 AAGCCTCAGCCAATCAAATACCGTGGAGTAGATCATCTTTTCAGATATGTTAGTTCACTAT  
 NtUBP12 2572 AAACCTCAGCCAATAAAGTATCAAGGAGTGGACCGTCTTACAGAAATGCTTGTTCACTAT

AtUBP12 2635 AATCAGACGTCTGACATTTTGTATTATGAAGTTCTGGACATCCCTCTTCCAGAATTACAA  
 AtUBP13 2632 AATCAGACGTCTGACATATTGTATTATGAAGTTTTGGATATTCCTCTTCCAGAATTGCAA  
 NtUBP12 2632 AATCAGACTTCAGACATTTTGTATTATGAAGTCTCGATATTCCTTACCAGAGCTGCAG

AtUBP12 2695 GGTCTTAAAACCTTAAAAGTTGCTTTCCATCATGCCACGAAGGAAGAAGTGGTAATCCAC  
 AtUBP13 2692 GGTCTTAAAGACTCTAAAAGTAGCTTTCCATAGTGCCACAAAGGATGAAGTGATAATCCAC  
 NtUBP12 2692 TGCTTAAAACCTCTCAAAGTGCCTTCTATAATTTGCAAAAAGATGAAGTGACAATCCAT

AtUBP12 2755 AATATCAGACTACCTAAACAAAGCAGGTCGGAGATGTTATTAATGAACTTAAAACAAG  
 AtUBP13 2752 AATATCAGACTACCTAAGCAGAGTACTGTTGGAGATGTTATTAACGAACTGAAAACAAG  
 NtUBP12 2752 ACTATTAGATTGCCGAAACAAAGTACTGTAGATGATGTCCTTAATCATCTCAAGACAAG

AtUBP12 2815 GTGGAGCTTTTCGCATCCAGATGCAGAAGTGAAGTTGCTCGAGGTGTTTTACCACAAGATC  
 AtUBP13 2812 GTGGAGCTTTTCGCATCAAGATGCAGAAGTGAAGTTGCTCGAGGTGTTTTACCACAAGATC  
 NtUBP12 2812 GTTGAGTTGTACATCCAGATGCTGAACTGAGATTGCTGGAAGTTTTCTACCACAAAATA

AtUBP12 2875 TACAAGATTTTCCCATCAACTGAAAGAATTGAGAATATAAATGACCAGTACTGGACTTTA  
 AtUBP13 2872 TACAAGATCTTTCCATCTACTGAACGAATTGAAAACATCAATGACCAGTACTGGACTTTA  
 NtUBP12 2872 TATAAGATTTTCCCAACTGAGAGAATTGAGGACATAAATGATCAATACTGGACCTTG

AtUBP12 2935 CGAGCTGAGGAGATTCCGGAAGAAGAGAAGAATATTGGTCCAAATGATCGCTTAATTCTT  
 AtUBP13 2932 CGAGCAGAGGAGATACCTGAAGAAGAGAAGAATATTGGTCCCAATGATAGGTTAATTAC  
 NtUBP12 2932 CGTGCAGAGGAGATCCCCGAAGAGGAGAAAAACCTGGGTCTCATGATCGCTTGATTCAAT

AtUBP12 2995 GTGTACCATTTTGCACAAGGAGACTGGACAAAACCTG---CAAGTGCAAAACCTTTGGCGAG  
 AtUBP13 2992 GTATATCATTTTTACTTAAAGAGGCGGACAAAATCAG---CAAGTGCAAAACCTTTGGGGAA  
 NtUBP12 2992 GTTTACCATTTTATGAAGGACACGACTCAAATCAAGCACACGTACAAAACCTTTGGGGAG

AtUBP12 3052 CCCTTCTTCTTGGTAATCCATGAAGGTGAAACTCTTGAAGAAATCAAGAACCCTATCCAA  
 AtUBP13 3049 CCCTTCTTTTTTGGTAATCCACGAAGGTGAAACTTTAGAAGAAATCAAGACCCCTATCCAA  
 NtUBP12 3052 CCCTTCTTCTTGGTTATTTCATGAGGGTGAAGACTGACTGAAGTTAAAGCGCGCATCCAG

AtUBP12 3112 AAGAAGCTTTCATGTATCTGATGAAGATTTTGCACAAGTGAAGTTTGCCTTCATGTCAATG  
 AtUBP13 3109 AAGAAACTCCATGTCCCTGATGAGGACTTTGCACAAGTGAAGTTTGCATCGTTTTTCAATG  
 NtUBP12 3112 AAAAAATTGCAGGTTCCAGATGAGGAGTTTTTGCACAAGTGAAGTTTGCCTTTTTTGTCCATG

AtUBP12 3172 GGGCGTCCAGAGTACTTGCAGGACACAGATGTTGTTTATAATCGCTTCCAGAGAAGAGAT  
 AtUBP13 3169 GGACGTCCTGATTACTTGCTGGACACAGATGTTGTTTATAATCGCTTCCAGAGAAGAGAT  
 NtUBP12 3172 GGCCGTCTGACTACCTCCAGGATTCAGATGTTGTGTCCAATCGCTTTCAGAGGAGAGAT  
  
 AtUBP12 3232 GTCTATGGTGCTTTTGAGCAGTACCTCGGGTTGGAGCATGCTGACACTACTCCTAAGAGG  
 AtUBP13 3229 GTATACGGTGCGTGGGAGCAGTATCTTGGGTTGGAGCACATTGATAATGCTCCTAAAAGG  
 NtUBP12 3232 GTTTATGGTGCTTGGGAGCAGTATCTTGGATTAGAGCATGCTGACAATGCTCCTAAAAGG  
  
 AtUBP12 3292 GCTTATGCTGCAAACCAGAACCGCCATGCTTACGAGAAGCCGGTAAAAATATAACAATTAG  
 AtUBP13 3289 GCTTATGCTGCAAATCAGAACCGACACGCATACGAGAAGCCGGTAAAAATATAACAATTAG  
 NtUBP12 3292 TCATATGCTAGCAAACCAGAACCGACATACTTTTGAGAAGCCTGTTCGGATCTACAACCTAG

**Table A3** *Arabidopsis* T-DNA lines isolated in this study.

Mutant allele	TAIR code	T-DNA identifier	KO origin
ubp8-1	AT5G22030	SALK_149329	SALK
ubp11-1	AT1G32850	SALK_043515	SALK
ubp12-1	AT5G06600	GK_244E11	GABI-Kat
ubp12-2	AT5G06600	GK_742C10	GABI-Kat
ubp13-1	AT3G11910	SALK_128312	SALK
ubp13-2	AT3G11910	SALK_130784	SALK
ubp25-1	AT3G14400	SALK_111336	SALK